Arnout Jozef Ceulemans

Group Theory Applied to Chemistry

ECTN
European Chemistry
Thematic Network Association
EUROMASTER®

European Commission
ERASMUS
MUNDUS

Springer

Theoretical Chemistry and Computational Modelling

Modern Chemistry is unthinkable without the achievements of Theoretical and Computational Chemistry. As a matter of fact, these disciplines are now a mandatory tool for the molecular sciences and they will undoubtedly mark the new era that lies ahead of us. To this end, in 2005, experts from several European universities joined forces under the coordination of the Universidad Autónoma de Madrid, to launch the *European Masters Course on Theoretical Chemistry and Computational Modeling* (TCCM). The aim of this course is to develop scientists who are able to address a wide range of problems in modern chemical, physical, and biological sciences via a combination of theoretical and computational tools. The book series, *Theoretical Chemistry and Computational Modeling*, has been designed by the editorial board to further facilitate the training and formation of new generations of computational and theoretical chemists.

Prof. Manuel Alcami
Departamento de Química
Facultad de Ciencias, Módulo 13
Universidad Autónoma de Madrid
28049 Madrid, Spain

Prof. Ria Broer
Theoretical Chemistry
Zernike Institute for Advanced Materials
Rijksuniversiteit Groningen
Nijenborgh 4
9747 AG Groningen, The Netherlands

Dr. Monica Calatayud
Laboratoire de Chimie Théorique
Université Pierre et Marie Curie, Paris 06
4 place Jussieu
75252 Paris Cedex 05, France

Prof. Arnout Ceulemans
Departement Scheikunde
Katholieke Universiteit Leuven
Celestijnenlaan 200F
3001 Leuven, Belgium

Prof. Antonio Laganà
Dipartimento di Chimica
Università degli Studi di Perugia
via Elce di Sotto 8
06123 Perugia, Italy

Prof. Colin Marsden
Laboratoire de Chimie
et Physique Quantiques
Université Paul Sabatier, Toulouse 3
118 route de Narbonne
31062 Toulouse Cedex 09, France

Prof. Otilia Mo
Departamento de Química
Facultad de Ciencias, Módulo 13
Universidad Autónoma de Madrid
28049 Madrid, Spain

Prof. Ignacio Nebot
Institut de Ciència Molecular
Parc Científic de la Universitat de València
Catedrático José Beltrán Martínez, no. 2
46980 Paterna (Valencia), Spain

Prof. Minh Tho Nguyen
Departement Scheikunde
Katholieke Universiteit Leuven
Celestijnenlaan 200F
3001 Leuven, Belgium

Prof. Maurizio Persico
Dipartimento di Chimica e Chimica
Industriale
Università di Pisa
Via Risorgimento 35
56126 Pisa, Italy

Prof. Maria Joao Ramos
Chemistry Department
Universidade do Porto
Rua do Campo Alegre, 687
4169-007 Porto, Portugal

Prof. Manuel Yáñez
Departamento de Química
Facultad de Ciencias, Módulo 13
Universidad Autónoma de Madrid
28049 Madrid, Spain

Arnout Jozef Ceulemans

Group Theory Applied to Chemistry

Arnout Jozef Ceulemans
Division of Quantum Chemistry
    Department of Chemistry
Katholieke Universiteit Leuven
Leuven, Belgium

To my grandson Louis

"The world is so full of a number of things,
I'm sure we should all be as happy as kings."
Robert Louis Stevenson

Preface

Symmetry is a general principle, which plays an important role in various areas of knowledge and perception, ranging from arts and aesthetics to natural sciences and mathematics. According to Barut,[1] the symmetry of a physical system may be looked at in a number of different ways. We can think of symmetry as representing

- the impossibility of knowing or measuring some quantities, e.g., the impossibility of measuring absolute positions, absolute directions or absolute left or right;
- the impossibility of distinguishing between two situations;
- the independence of physical laws or equations from certain coordinate systems, i.e., the independence of absolute coordinates;
- the invariance of physical laws or equations under certain transformations;
- the existence of constants of motions and quantum numbers;
- the equivalence of different descriptions of the same system.

Chemists are more used to the operational definition of symmetry, which crystallographers have been using long before the advent of quantum chemistry. Their ball-and-stick models of molecules naturally exhibit the symmetry properties of macroscopic objects: they pass into congruent forms upon application of bodily rotations about proper and improper axes of symmetry. Needless to say, the practitioner of quantum chemistry and molecular modeling is not concerned with balls and sticks, but with subatomic particles, nuclei, and electrons. It is hard to see how bodily rotations, which leave all interparticle distances unaltered, could affect in any way the study of molecular phenomena that only depend on these internal distances. Hence, the purpose of the book will be to come to terms with the subtle metaphors that relate our macroscopic intuitive ideas about symmetry to the molecular world. In the end the reader should have acquired the skills to make use of the mathematical tools of group theory for whatever chemical problems he/she will be confronted with in the course of his or her own research.

---

[1] A.O. Barut, Dynamical Groups and Generalized Symmetries in Quantum Theory, Bascands, Christchurch (New Zealand) (1972)

Acknowledgements

Contents

Chapter 1
Operations

Abstract In this chapter we examine the precise meaning of the statement that a symmetry operation *acts* on a point in space, on a function, and on an operator. The difference between active and passive views of symmetry is explained, and a few practical conventions are introduced.

Contents

1.1 Operations and Points

In the usual crystallographic sense, symmetry operations are defined as rotations and reflections that turn a body into a congruent position. This can be realized in two ways. The active view of a rotation is the following. An observer takes a snapshot of a crystal, then the crystal is rotated while the camera is left immobile. A second snapshot is taken. If the two snapshots are identical, then we have performed a symmetry operation. In the passive view, the camera takes a snapshot of the crystal, then the camera is displaced while the crystal is left immobile. From a new perspective a second snapshot is taken. If this is the same as the first one, we have found a symmetry-related position. Both points of view are equivalent as far as the *relative* positions of the observer and the crystal are concerned. However, viewed in the frame of absolute space, there is an important difference: if the rotation of the crystal in the active view is taken to be counterclockwise, the rotation of the observer in the passive alternative will be clockwise. Hence, the transformation from active to passive involves a change of the sign of the rotation angle. In order to avoid annoying sign problems, only one choice of definition should be adhered to. In the present monograph we shall consistently adopt the *active view*, in line with the usual convention in chemistry textbooks. In this script the part of the observer is played by

Fig. 1.1 Stereographic view
of the reflection plane. The
point P_1, indicated by X, is
above the plane of the gray
disc. The reflection operation
in the horizontal plane, $\hat{\sigma}_h$, is
the result of the $\hat{C}_2^z$ rotation
around the center by an angle
of π, followed by inversion
through the center of the
diagram, to reach the position
P_3 below the plane, indicated
by *the small circle*
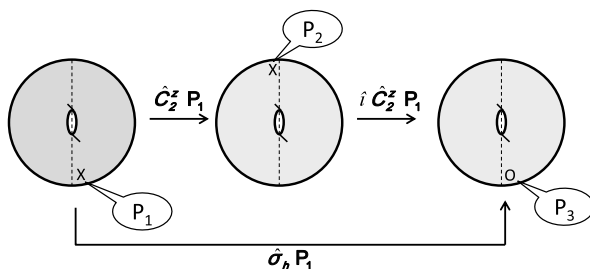
the set of coordinate axes that defines the absolute space in a Cartesian way. They
will stay where they are. On the other hand, the structures, which are operated on,
are moving on the scene. To be precise, a symmetry operation $\hat{R}$ will move a point
P_1 with coordinates[1] (x_1, y_1, z_1) to a new position P_2 with coordinates (x_2, y_2, z_2):

$$\hat{R} P_1 = P_2 \tag{1.1}$$

A pure rotation, $\hat{C}_n$ $(n > 1)$, around a given axis through an angle $2\pi/n$ radians
displaces all the points, except the ones that are lying on the rotation axis itself. A
reflection plane, $\hat{\sigma}_h$, moves all points except the ones lying in the reflection plane
itself. A rotation–reflection, $\hat{S}_n$ $(n > 2)$, is a combination in either order of a $\hat{C}_n$
rotation and a reflection through a plane perpendicular to the rotation axis. As a
result, only the point of intersection of the plane with the axis perpendicular to it is
kept. A special case arises for $n = 2$. The $\hat{S}_2$ operator corresponds to the inversion
and will be denoted as $\hat{\imath}$. It maps every point onto its antipode. A plane of symmetry
can also be expressed as the result of a rotation through an angle π around an axis
perpendicular to the plane, followed by inversion through the intersection point of
the axis and the plane. A convenient way to present these operations is shown in
Fig. 1.1. Operator products are "right-justified," so that $\hat{\imath}\hat{C}_2^z$ means that $\hat{C}_2^z$ is applied
first, and *then* the inversion acts on the intermediate result:

$$\hat{\sigma}_h P_1 = \hat{\imath}\hat{C}_2^z P_1 = \hat{\imath} P_2 = P_3 \tag{1.2}$$

From the mathematical point of view the rotation of a point corresponds to
a transformation of its coordinates. Consider a right-handed Cartesian coordinate
frame and a point P_1 lying in the xy plane. The point is being subjected to a rotation
about the upright z-axis by an angle α. By convention, a positive value of α will
correspond to a counterclockwise direction of rotation. An observer on the pole of
the rotation axis and looking down onto the plane will view this rotation as going

---

[1]The use of upright (roman) symbols for the coordinates is deliberate. Italics will be reserved
for variables, but here $x_1, y_1, \ldots$ refer to fixed values of the coordinates. The importance of this
difference will become clear later (see Eq. (1.15)).

Fig. 1.2 Counterclockwise
rotation of the point P_1 by an
angle α in the xy plane
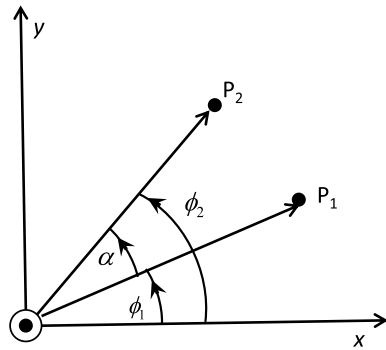
in the opposite sense to that of the rotation of the hands on his watch. A synonym
for counterclockwise here is right-handed. If the reader orients his/her thumb in
the direction of the rotational pole, the palm of his/her right hand will indicate the
counterclockwise direction. The transformation can be obtained as follows. Let r be
the length of the radius-vector, $\mathbf{r}$, from the origin to the point P_1, and let ϕ_1 be the
angular coordinate of the point measured in the horizontal plane starting from the
x-direction, as shown in Fig. 1.2. The coordinates of P_1 are then given by

$$x_1 = r\cos\phi_1$$
$$y_1 = r\sin\phi_1 \tag{1.3}$$
$$z_1 = 0$$

Rotating the point will not change its distance from the origin, but the angular co-
ordinate will increase by α. The angular coordinate of P_2 will thus be given by
$\phi_2 = \phi_1 + \alpha$. The coordinates of the image point in terms of the coordinates of the
original point are thus given by

$$x_2 = r\cos\phi_2 = r\cos(\phi_1 + \alpha)$$
$$= r\cos\phi_1\cos\alpha - r\sin\phi_1\sin\alpha$$
$$= x_1\cos\alpha - y_1\sin\alpha$$
$$y_2 = r\sin\phi_2 = r\sin(\phi_1 + \alpha) \tag{1.4}$$
$$= r\cos\phi_1\sin\alpha + r\sin\phi_1\cos\alpha$$
$$= x_1\sin\alpha + y_1\cos\alpha$$
$$z_2 = 0$$

In this way the coordinates of P_2 are obtained as functions of the coordinates of P_1
and the rotation angle. This derivation depends simply on the trigonometric rela-
tionships for sums and differences of angles. We may also express this result in the
form of a matrix transformation. For this, we put the coordinates in a column vector

and operate on it (on the left) by means of a transformation matrix $\mathbb{D}(R)$:

$$\begin{pmatrix} x_2 \\ y_2 \end{pmatrix} = \mathbb{D}(R) \begin{pmatrix} x_1 \\ y_1 \end{pmatrix} = \begin{pmatrix} \cos\alpha & -\sin\alpha \\ \sin\alpha & \cos\alpha \end{pmatrix} \begin{pmatrix} x_1 \\ y_1 \end{pmatrix} \tag{1.5}$$

Having obtained the algebraic expressions, it is always prudent to consider whether the results make sense. Hence, while the point P_1 is rotated as shown in the picture, its x-coordinate will decrease, while its y-coordinate will increase. This is reflected by the entries in the first row of the matrix which show how x_1 will change: the $\cos\alpha$ factor is smaller than 1 and thus will reduce the x-value as the acute angle increases, and this will be reinforced by the second term, $-y_1\sin\alpha$, which will be negative for a point with y_1 and $\sin\alpha$ both positive. In what follows we also need the inverse operation, $\hat{R}^{-1}$, which will undo the operation itself. In the case of a rotation this is simply the rotation around the same axis by the same angle but in the opposite direction, that is, by an angle $-\alpha$. The combination of clockwise and counterclockwise rotations by the same angle will leave all points unchanged. The resulting nil operation is called the unit operation, $\hat{E}$:

$$\hat{R}\hat{R}^{-1} = \hat{R}^{-1}\hat{R} = \hat{E} \tag{1.6}$$

1.2 Operations and Functions

Chemistry of course goes beyond the structural characteristics of molecules and considers functional properties associated with the structures. This is certainly the case for the quantum-mechanical description of the molecular world. The primary functions which come to mind are the orbitals, which describe the distribution of the electrons in atoms and molecules. A function $f(x, y, z)$ associates a certain property (usually a scalar number) with a particular coordinate position. A displacement of a point will thus induce a change of the function. This can again be defined in several ways. Let us agree on the following: when we displace a point, the property associated with that point will likewise be displaced with it. In this way we create a new property distribution in space and hence a new function. This new function will be denoted by $\hat{R}f$ (or sometimes as f'), i.e., it is viewed as the result of the action of the operation on the original function. In line with our agreement, a property associated with the displaced point will have the same value as that property had when associated with the original point, hence:

$$\hat{R}f(P_2) = f(P_1) \tag{1.7}$$

or, in general,

$$\hat{R}f(\hat{R}P_1) = f(P_1) \tag{1.8}$$

Note that in this expression the same symbol $\hat{R}$ is used in two different meanings, either as transforming coordinates or a function, as is evident from the entity that follows the operator. This rule is sufficient to *plot* the transformed function, as shown

Fig. 1.3 The rotation of the function $f(x, y)$ counterclockwise by an angle α generates a new function, $f'(x, y)$. The value of the new function at P_2 is equal to the value of the old function at P_1. Similarly, to find the value of the new function at P_1, we have to retrieve the value of the old function at a point P_0, which is the point that will be reached by the clockwise rotation of P_1
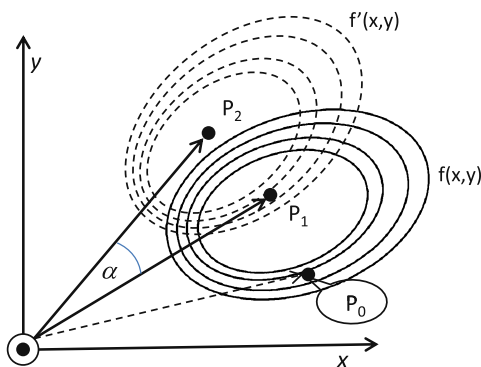
in Fig. 1.3. In order to determine the mathematical form of the new transformed function, we must be able to compare the value of the new function with the original function *at the same point*, i.e., we must be able to see how the property changes at a given point. Thus, we would like to know what would be the value of $\hat{R}f$ in the original point P_1. Equation (1.8) cannot be used to determine this since the transformed function is as yet unknown and we thus do not know the rules for working out the brackets in the left-hand side of the equation. However, this relationship must be true for every point; thus, we may substitute $\hat{R}^{-1}P_1$ for P_1 on both the left- and right-hand sides of Eq. (1.8). The equation thus becomes

$$\hat{R}f\big(\hat{R}\big(\hat{R}^{-1}P_1\big)\big) = \hat{R}f(\hat{E}P_1) = \hat{R}f(P_1) = f\big(\hat{R}^{-1}P_1\big) \tag{1.9}$$

This result reads as follows: the transformed function attributes to the original point P_1 the property that the original function attributed to the point $\hat{R}^{-1}P_1$. In Fig. 1.3 this point from which the function value was retrieved is indicated as P_0. Thus, the function and the coordinates transform in opposite ways.[2] This connection transfers the operation from the function to the coordinates, and, since the original function is a known function, we can also use the toolbox of corresponding rules to work out the bracket on the right-hand side of Eq. (1.9).

As an example, consider the familiar $2p$ orbitals in the xy plane: $2p_x, 2p_y$. These orbitals are usually represented by the iconic dumbell structure.[3] We can easily find out what happens to these upon rotation, simply by inspection of Fig. 1.4, in which we performed the rotation of the $2p_x$ orbital by an angle α around the z-axis. Clearly, when the orbital rotates, the overlap with the $2p_x$ function decreases, and the $2p_y$ orbital gradually appears. Now let us apply the formula to determine $\hat{R}2p_x$. The functional form of the $2p_x$ orbital for a hydrogen atom, in polar coordinates, reads: $R_{2p}(r)\Theta_{2p|1|}(\theta)\Phi_x(\phi)$, where $R_{2p}(r)$ is the radial part, $\Theta_{2p|1|}(\theta)$ is the part

---

[2] A more general expression for the transportation of a quantum state may also involve an additional phase factor, which depends on the path. See, e.g., [1].

[3] The electron distribution corresponding to the square of these orbitals is described by a lemniscate of Bernoulli. The angular parts of the orbitals themselves are describable by osculating spheres.

Fig. 1.4 The dashed orbital
is obtained by rotating the
$2p_x$ orbital, counterclockwise
through an angle α
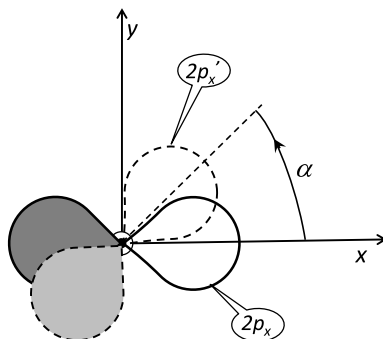
which depends on the azimuthal angle, and $\Phi_x(\phi)$ indicates how the function depends on the angle ϕ in the xy plane, measured from the positive x-direction. One has:

$$\Phi_x(\phi) = \frac{1}{\sqrt{\pi}} \cos\phi$$
$$\Phi_y(\phi) = \frac{1}{\sqrt{\pi}} \sin\phi \tag{1.10}$$

Both r and θ are invariant under a rotation around the z-direction, $\theta_1 = \theta_0$, and $r_1 = r_0$; hence, only the ϕ part will matter when we rotate in the plane. The transformed functions are easily determined starting from the general equation and using the matrix expression for the coordinate rotation, where we replace α by $-\alpha$, since we need the inverse operation here:

$$\hat{R}(\cos\phi_1) = \cos\phi_0 = \cos(\phi_1 - \alpha)$$
$$= \cos\phi_1 \cos\alpha + \sin\phi_1 \sin\alpha$$
$$\hat{R}(\sin\phi_1) = \sin\phi_0 = \sin(\phi_1 - \alpha)$$
$$= \sin\phi_1 \cos\alpha - \cos\phi_1 \sin\alpha \tag{1.11}$$

Multiplying with the radial and azimuthal parts, we obtain the desired functional transformation of the in-plane $2p$-orbitals:

$$\hat{R}2p_x = 2p_x \cos\alpha + 2p_y \sin\alpha$$
$$\hat{R}2p_y = -2p_x \sin\alpha + 2p_y \cos\alpha \tag{1.12}$$

Again we should get accustomed to read these expressions almost visually. For instance, when the angle is 90°, one has $2p_x' = 2p_y$ and $2p_y' = -2p_x$. This simply means: take the $2p_x$ orbital, rotate it over 90° counterclockwise around the z-direction, and it will become $2p_y$. If the same is done with $2p_y$, it will go over into $-2p_x$ since the plus and minus lobes of the dumbell become congruent with the oppositely signed lobes of the $2p_x$ orbital.

Equation (1.12) further reveals an important point. To express the transformation of a function, one almost automatically encounters the concept of a *function space*. To describe the transformation of the cosine function, one really also needs the sine. The two form a two-dimensional space, which we shall call a vector space. This will be explained in greater depth in Chap. 2. For now, we may cast the transformation of the basis components of this space in matrix form. This time we arrange the basis orbitals in a row-vector notation, so that the transformation matrix is written to the right of the basis. Thus,

$$\hat{R}\begin{pmatrix} 2p_x & 2p_y \end{pmatrix} = \begin{pmatrix} 2p_x & 2p_y \end{pmatrix}\begin{pmatrix} \cos\alpha & -\sin\alpha \\ \sin\alpha & \cos\alpha \end{pmatrix} \tag{1.13}$$

The matrix that is used here is precisely the same matrix which we used for the coordinate transformation. How is this possible if functions and points transform in opposite ways? The reason is of course that we also switched from a column vector for points to a row vector for functions. Indeed, transposition, T, of the entire matrix multiplication simultaneously inverts the transformation matrix and interchanges columns and rows:

$$\left[\mathbb{D}^{-1}\begin{pmatrix} x \\ y \end{pmatrix}\right]^{\mathrm{T}} = \begin{pmatrix} x & y \end{pmatrix}\left(\mathbb{D}^{-1}\right)^{\mathrm{T}} = \begin{pmatrix} x & y \end{pmatrix}\mathbb{D} \tag{1.14}$$

where we made use of the property that transposition of the rotation matrix changes α into $-\alpha$ and thus is the same as taking the inverse of $\mathbb{D}$. The final point about functions is somewhat tricky, so attention is required. Just like the value of a field, or the amplitude of an orbital, the values of the coordinates themselves are properties associated with points. As an example, the function that yields the x-coordinate of a point P_1, will be denoted as $x(P_1)$. The value of this function is x_1, where we are using different styles to distinguish the function x, which is a variable, and the coordinate x_1, which is a *number*. We can thus write

$$x(P_1) = x_1 \tag{1.15}$$

A typical quantum-chemical example of the use of these coordinate functions is the dipole operator; e.g., the x-component of the electric dipole is simply given by $\mu_x = -ex$, where $-e$ is the electronic charge. We may thus write in analogy with Eq. (1.5)

$$\hat{R}\begin{pmatrix} x & y \end{pmatrix} = \begin{pmatrix} x & y \end{pmatrix}\begin{pmatrix} \cos\alpha & -\sin\alpha \\ \sin\alpha & \cos\alpha \end{pmatrix} \tag{1.16}$$

In summary, we have learned that when a symmetry operator acts on all the points of a space, it induces a change of the functions defined in that space. The transformed functions are the result of a direct action of the symmetry operator in a corresponding function space. Furthermore, there exists a dual relation between the transformations of coordinate points and of functions. They are mutual inverses. Finally, the active picture also applies to the functions: the symmetry operation sets the function itself into motion as if we were (physically) grasping the orbitals and twisting them.

1.3 Operations and Operators

Besides functions, we must also consider the action of operations on operators. In quantum chemistry, operators, such as the Hamiltonian, $\mathcal{H}$, are usually spatial functions and, as such, are transformed in the same way as ordinary functions, e.g., $\mathcal{H}'(P_1) = \mathcal{H}(\hat{R}^{-1}P_1)$. So why devote a special section to this? Well, operators are different from functions in the sense that they also operate on a subsequent argument, which is itself usually a function. Hence, when symmetry is applied to an operator, it will also affect whatever follows the operator. Symmetry operations act on the entire expression at once. This can be stated for a general operator $\mathcal{O}$ as follows:

$$\hat{R}\mathcal{O}f = \mathcal{O}'\hat{R}f \tag{1.17}$$

From this we can identify the transformed operator $\mathcal{O}'$ by smuggling $\hat{R}^{-1}\hat{R} \, (= \hat{E})$ into the left-hand side of the equation:

$$\hat{R}\mathcal{O}\hat{R}^{-1}\hat{R}f = \mathcal{O}'\hat{R}f \tag{1.18}$$

This equality is true for any function f and thus implies[4] that the operators preceding $\hat{R}f$ on both sides must be the same:

$$\mathcal{O}' = \hat{R}\mathcal{O}\hat{R}^{-1} \tag{1.19}$$

This equation provides the algebraic formalism for the transformation of an operator. In the case where $\mathcal{O}' = \mathcal{O}$, we say that the operator is *invariant* under the symmetry operation. Equation (1.19) then reduces to

$$\hat{R}\mathcal{O} - \mathcal{O}\hat{R} = [\hat{R}, \mathcal{O}] = 0 \tag{1.20}$$

This bracket is know as the *commutator* of $\hat{R}$ and $\mathcal{O}$. If the commutator vanishes, we say that $\hat{R}$ and $\mathcal{O}$ commute. This is typically the case for the Hamiltonian. As an application, we shall study the functional transformations of the differential operators $\frac{\partial}{\partial x}, \frac{\partial}{\partial y}$ under a rotation around the positive z-axis. To find the transformed operators, we have to work out expressions such as $\frac{\partial}{\partial x'}$ where $x' = x(\hat{R}^{-1}P_1)$. Hence, we are confronted with a functional form, viz., the derivative operator, of a transformed argument, x', but this is precisely where classical analysis comes to our rescue because it provides the chain rule needed to work out the coordinate change. We have:

$$\frac{\partial}{\partial x'} = \frac{\partial x}{\partial x'}\frac{\partial}{\partial x} + \frac{\partial y}{\partial x'}\frac{\partial}{\partial y} \tag{1.21}$$

In order to evaluate this equation, we have to determine the partial derivatives in the transformed coordinates. Using the result in Sect. 1.1 but keeping in mind that the

---

[4]The fact that two operators transform a given function in the same way does not automatically imply that those operators are the same. Operators will be the same if this relationship extends over the entire Hilbert space.

coordinates are rotated in the opposite direction (hence α is replaced by $-\alpha$), one obtains

$$x' = x \cos\alpha + y \sin\alpha$$
$$y' = -x \sin\alpha + y \cos\alpha$$

(1.22)

Invert these equations to express x and y as a function of x' and y':

$$x = x' \cos\alpha - y' \sin\alpha$$
$$y = x' \sin\alpha + y' \cos\alpha$$

(1.23)

The partial derivatives needed in the chain rule can now be obtained by direct derivation:

$$\frac{\partial x}{\partial x'} = \cos\alpha$$

$$\frac{\partial y}{\partial x'} = \sin\alpha$$

$$\frac{\partial x}{\partial y'} = -\sin\alpha$$

$$\frac{\partial y}{\partial y'} = \cos\alpha$$

(1.24)

Hence, the transformation of the derivatives is entirely similar to the transformation of the x, y functions themselves:

$$\hat{R}\left(\frac{\partial}{\partial x} \quad \frac{\partial}{\partial y}\right) = \left(\frac{\partial}{\partial x} \quad \frac{\partial}{\partial y}\right)\begin{pmatrix} \cos\alpha & -\sin\alpha \\ \sin\alpha & \cos\alpha \end{pmatrix}$$

(1.25)

In an operator formalism, we should denote this as

$$\left[\hat{R}, \frac{\partial}{\partial x}\right] = \cos\alpha \frac{\partial}{\partial x} + \sin\alpha \frac{\partial}{\partial y}$$

$$\left[\hat{R}, \frac{\partial}{\partial y}\right] = -\sin\alpha \frac{\partial}{\partial x} + \cos\alpha \frac{\partial}{\partial y}$$

(1.26)

As a further example, consider a symmetry transformation of a symmetry operator itself. Take, for instance, a rotation, $\hat{C}_2^x$, corresponding to a rotation about the x-axis of $180°$ and rotate this $90°$ counterclockwise about the z-direction by $\hat{C}_4^z$. Applying the general expression for an operator transformation yields

$$\left(\hat{C}_2^x\right)' = \hat{C}_4^z \hat{C}_2^x \left(\hat{C}_4^z\right)^{-1}$$

(1.27)

The result of this transformation corresponds to an equivalent twofold rotation around the y-direction, $\hat{C}_2^y$. The rotation around x is thus mapped onto a rotation

around y by a fourfold rotation axis along the z direction. In Chap. 3, we shall see that this relation installs an equivalence between both twofold rotations whenever such a $\hat{C}_4^z$ is present.

1.4 An Aide Mémoire

- Use a right-handed coordinate system.
- Always leave the Cartesian directions unchanged.
- Symmetry operations are defined in an active sense.
- Rotations through positive angles appear counterclockwise, when viewed from the rotational pole; "counterclockwise is positive."
- The transformation of the coordinates of a point is written in a column vector notation.
- The transformation of a function space is written in a row vector notation.
- There is a dual relationship between the transformations of functions and of coordinates: $\hat{R}f(\mathbf{r}) = f(\hat{R}^{-1}\mathbf{r})$.
- The transformation of an operator $\mathcal{O}$ is given by $\hat{R}\mathcal{O}\hat{R}^{-1}$.

1.5 Problems

1.1 Use the stereographic representation of Fig. 1.1 to show that $[\hat{\imath}, \hat{C}_2^z] = 0$.
1.2 The square of the radial distance of the point P_1 in the xy plane may be obtained by multiplying the coordinate column by its transposed row:

$$r^2 = x_1^2 + y_1^2 = \begin{pmatrix} x_1 & y_1 \end{pmatrix} \begin{pmatrix} x_1 \\ y_1 \end{pmatrix} \tag{1.28}$$

Show that this scalar product is invariant under a rotation about the z-axis.
1.3 Derive the general form of a 2×2 matrix that leaves this radial distance invariant.
1.4 The translation operator $\mathcal{T}_a$ displaces a point with x-coordinate x_1 to a new position $x_1 + a$. Apply this operator to the wavefunction e^{ikx}.
1.5 Construct a differential operator such that its action on the coordinate functions x and y matches the matrix transformation in Eq. (1.16). What is the angular derivative of this operator as the rotation angle tends to zero? Can you relate this limit to the angular momentum operator $\mathcal{L}_z$?

References

1. Berry, M.V.: In: Shapere, A., Wilczek, F. (eds.) Geometric Phases in Physics. Advanced Series in Mathematical Physics, vol. 5, pp. 3–28. World Scientific, Singapore (1989)

Chapter 2
Function Spaces and Matrices

Abstract This chapter refreshes such necessary algebraic knowledge as will be needed in this book. It introduces function spaces, the meaning of a linear operator, and the properties of unitary matrices. The homomorphism between operations and matrix multiplications is established, and the Dirac notation for function spaces is defined. For those who might wonder why the linearity of operators need be considered, the final section introduces time reversal, which is anti-linear.

Contents

2.1 Function Spaces

In the first chapter, we saw that if we wanted to rotate the $2p_x$ function, we automatically also needed its companion $2p_y$ function. If this is extended to out-of-plane rotations, the $2p_z$ function will also be needed. The set of the three p-orbitals forms a prime example of what is called a *linear vector space*. In general, this is a space that consists of components that can be combined linearly using real or complex numbers as coefficients. An n-dimensional linear vector space consists of a set of n vectors that are linearly independent. The components or basis vectors will be denoted as f_l, with l ranging from 1 to n. At this point we shall introduce the Dirac notation [1] and rewrite these functions as $|f_l\rangle$, which characterizes them as so-called *ket*-functions. Whenever we have such a set of vectors, we can set up a complementary set of so-called *bra*-functions, denoted as $\langle f_k|$. The scalar product of a bra and a ket yields a number. It is denoted as the bracket: $\langle f_k|f_l\rangle$. In other words, when a bra collides with a ket on its right, it yields a scalar number. A bra-vector is completely defined when its scalar product with every ket-vector of the vector space is given.

For linearly independent functions, we have

$$\forall\, k \neq l : \langle f_k | f_l \rangle = 0 \tag{2.1}$$

The basis is orthonormal if all vectors are in addition normalized to $+1$:

$$\forall\, k : \langle f_k | f_k \rangle = 1 \tag{2.2}$$

This result can be summarized with the help of the Kronecker delta, δ_{ij}, which is zero unless the subscript indices are identical, in which case it is unity. Hence, for an orthonormal basis set,

$$\langle f_k | f_l \rangle = \delta_{kl} \tag{2.3}$$

In quantum mechanics, the bra-function of f_k is simply the complex-conjugate function, $\bar{f}_k$, and the bracket or scalar product is defined as the integral of the product of the functions over space:

$$\langle f_k | f_l \rangle = \int \int \int \bar{f}_k f_l \, dV \tag{2.4}$$

One thus also has

$$\overline{\langle f_k | f_l \rangle} = \langle f_l | f_k \rangle \tag{2.5}$$

2.2 Linear Operators and Transformation Matrices

A linear operator is an operator that commutes with multiplicative scalars and is distributive with respect to summation: this means that when it acts on a sum of functions, it will operate on each term of the sum:

$$\hat{R} c | f_k \rangle = c \hat{R} | f_k \rangle$$
$$\hat{R} \big(| f_k \rangle + | f_l \rangle \big) = \hat{R} | f_k \rangle + \hat{R} | f_l \rangle \tag{2.6}$$

If the transformations of functions under an operator can be expressed as a mapping of these functions onto a linear combination of the basis vectors in the function space, then the operator is said to leave the function space *invariant*. The corresponding coefficients can then be collected in a transformation matrix. For this purpose, we arrange the components in a row vector, $(|f_1\rangle, |f_2\rangle, \ldots, |f_n\rangle)$, as agreed upon in Chap. 1. This row precedes the transformation matrix. The usual symbols are $\hat{R}$ for the operator and $\mathbb{D}(R)$ for the corresponding matrix:

$$\hat{R}\big(|f_1\rangle | f_2\rangle \cdots | f_n\rangle\big) = \big(|f_1\rangle | f_2\rangle \cdots | f_n\rangle\big) \begin{pmatrix} & & \\ & \mathbb{D}(R) & \\ & & \end{pmatrix}$$

i.e.,

$$\hat{R}|f_i\rangle = \sum_{j=1}^{n} D_{ji}(R)|f_j\rangle \tag{2.7}$$

When multiplying this equation left and right with a given bra-function in an orthonormal basis, one obtains

$$\langle f_k|\hat{R}|f_i\rangle = \sum_{j=1}^{n} D_{ji}(R)\langle f_k|f_j\rangle = \sum_{j=1}^{n} D_{ji}(R)\delta_{kj} = D_{ki}(R) \tag{2.8}$$

where the summation index j has been restricted to k by the Kronecker delta. Hence, the elements of the transformation matrix are recognized as matrix elements of the symmetry operators. The transformation of bra-functions runs entirely parallel with the transformation of ket-functions, except that the complex conjugate of the transformation matrix has to be taken, and hence,

$$\hat{R}\langle f_i| = \sum_{j=1}^{n} \bar{D}_{ji}(R)\langle f_j| \tag{2.9}$$

For convenience, we sometimes abbreviate the row vector of the function space as $|\mathbf{f}\rangle$, so that the transformation is written as

$$R|\mathbf{f}\rangle = |\mathbf{f}\rangle \mathbb{D}(R) \tag{2.10}$$

When the bra-functions are also ordered in a row vector, we likewise have:

$$\hat{R}\langle\mathbf{f}| = \langle\mathbf{f}|\bar{\mathbb{D}}(R) \tag{2.11}$$

A product of two operators is executed consecutively, and hence the one closest to the ket acts first. In detail,

$$\hat{R}\hat{S}|f_i\rangle = \hat{R}\sum_j D_{ji}(S)|f_j\rangle$$

$$= \sum_{k,j} D_{kj}(R)D_{ji}(S)|f_k\rangle$$

$$= \sum_k \big[\mathbb{D}(R) \times \mathbb{D}(S)\big]_{ki}|f_k\rangle \tag{2.12}$$

Here, the symbol $\times$ refers to the product of two matrices.

$$\hat{R}\hat{S}|\mathbf{f}\rangle = |\mathbf{f}\rangle \mathbb{D}(R) \times \mathbb{D}(S) \tag{2.13}$$

This is an important result. It shows that the consecutive action of two operators can be expressed by the product of the corresponding matrices. The matrices are said to

Fig. 2.1 Matrix
representation of a group: the
operators (*left*) are mapped
onto the transformations
(*right*) of a function space.
The consecutive action of two
operators on *the left*
(symbolized by ●) is replaced
by the multiplication of two
matrices on *the right*
(symbolized by ×)
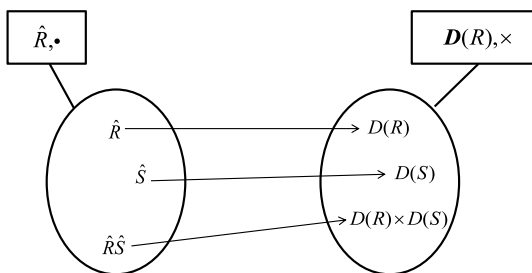
represent the action of the corresponding operators. The relationship between both
is a mapping. In this mapping the operators are replaced by their respective matrices,
and the product of the operators is mapped onto the product of the corresponding
matrices. In this mapping the order of the elements is kept.

$$\mathbb{D}(RS) = \mathbb{D}(R) \times \mathbb{D}(S) \tag{2.14}$$

In mathematical terms, such a mapping is called a *homomorphism* (see Fig. 2.1). In
Eq. (2.14) both the operators and matrices that represent them are *right-justified*; that
is, the operator (matrix) on the *right* is applied first, and then the operator (matrix)
immediately to the left of it is applied to the result of the action of the right-hand op-
erator (matrix). The conservation of the order is an important characteristic, which
in the active picture entirely relies on the convention for collecting the functions in a
row vector. In the column vector notation the order would be reversed. Further con-
sequences of the homomorphism are that the unit element is represented by the unit
matrix, $\mathbb{I}$, and that an inverse element is represented by the corresponding inverse
matrix:

$$\mathbb{D}(E) = \mathbb{I}$$
$$\mathbb{D}\left(R^{-1}\right) = \left[\mathbb{D}(R)\right]^{-1} \tag{2.15}$$

2.3 Unitary Matrices

A matrix is unitary if its rows and columns are orthonormal. In this definition the
scalar product of two rows (or two columns) is obtained by adding pairwise prod-
ucts of the corresponding elements, $\bar{A}_{ij} A_{kj}$, one of which is taken to be complex
conjugate:

$$\sum_j \bar{A}_{ij} A_{kj} = \sum_j \bar{A}_{ji} A_{jk} = \delta_{ik} \leftrightarrow \mathbb{A} \text{ is unitary} \tag{2.16}$$

A unitary matrix has several interesting properties, which can easily be checked
from the general definition:

- The inverse of a unitary matrix is obtained by combining complex conjugation and transposition:

$$\mathbb{A}^{-1} = \bar{\mathbb{A}}^{\mathrm{T}} \tag{2.17}$$

Here, T denotes transposition of rows and columns. This result implies that $A_{ij}^{-1} = \bar{A}_{ji}$.
- The inverse and the transpose of a unitary matrix are unitary.
- The product of unitary matrices is a unitary matrix.
- The determinant of a unitary matrix has an absolute value of unity.

To prove the final property, we note that the determinant of a product of matrices is equal to the product of the determinants of the individual matrices, and we also note that the determinant does not change upon transposition of a matrix. By definition, $\mathbb{I} = \mathbb{A} \times \mathbb{A}^{-1}$, and it then follows:

$$
\begin{aligned}
\det\left(\mathbb{A} \times \mathbb{A}^{-1}\right) &= \det(\mathbb{A}) \det\left(\mathbb{A}^{-1}\right) \\
&= \det(\mathbb{A}) \det\left(\bar{\mathbb{A}}^{\mathrm{T}}\right) \\
&= \det(\mathbb{A}) \det(\bar{\mathbb{A}}) \\
&= \det(\mathbb{A}) \overline{\det(\mathbb{A})} \\
&= \left|\det(\mathbb{A})\right|^2 = \det(\mathbb{I}) = 1
\end{aligned}
\tag{2.18}
$$

Now consider a function space $|\mathbf{f}\rangle$ and a linear transformation matrix, $\mathbb{A}$, which recombines the basis functions to yield a transformed basis set, say $|\mathbf{f}'\rangle$. Such a linear transformation of an orthonormal vector space preserves orthonormality *if and only if the transformation matrix $\mathbb{A}$ is unitary*. Assuming that $\mathbb{A}$ is unitary, the forward implication is easily proven:

$$
\begin{aligned}
\langle f_k'|f_l'\rangle &= \sum_{ij} \bar{A}_{ik} A_{jl} \langle f_i|f_j\rangle \\
&= \sum_{ij} \bar{A}_{ik} A_{jl} \delta_{ij} \\
&= \sum_i \bar{A}_{ik} A_{il} \\
&= \delta_{kl}
\end{aligned}
\tag{2.19}
$$

The converse implication is that if a transformation preserves orthonormality, the corresponding representation matrix will be unitary. Here, the starting point is the assumption that the basis remains orthonormal after transformation:

$$\sum_i \bar{A}_{ik} A_{il} = \delta_{kl} \tag{2.20}$$

This result may be recast in a matrix multiplication as

$$\sum_i \bar{A}_{ki}^{\mathrm{T}} A_{il} = \left[\bar{\mathbb{A}}^{\mathrm{T}} \times \mathbb{A}\right]_{kl} = \delta_{kl} \tag{2.21}$$

or $\bar{\mathbb{A}}^{\mathrm{T}} \times \mathbb{A} = \mathbb{I}$. In order to prove the unitary property, we also have to prove that the matrix order in this multiplication may be switched. This is achieved[1] as follows:

$$\bar{\mathbb{A}}^{\mathrm{T}} \times \mathbb{A} = \mathbb{I}$$
$$\mathbb{A} \times \bar{\mathbb{A}}^{\mathrm{T}} \times \mathbb{A} = \mathbb{A}$$
$$\mathbb{A} \times \bar{\mathbb{A}}^{\mathrm{T}} = \mathbb{A} \times \mathbb{A}^{-1} \tag{2.22}$$
$$\mathbb{A} \times \bar{\mathbb{A}}^{\mathrm{T}} = \mathbb{I}$$

Left or right multiplication by $\bar{\mathbb{A}}^{\mathrm{T}}$ thus turns the matrix $\mathbb{A}$ into the unit matrix, and the inverse of a matrix is unique; it thus follows that the inverse of $\mathbb{A}$ is obtained by taking the complex-conjugate transposed form, which means that the matrix is unitary. Note that the result in Eq. (2.22) is valid only if the matrix $\mathbb{A}$ is nonsingular. However, this will certainly be the case since

$$\det\left(\bar{\mathbb{A}}^T\right)\det(\mathbb{A}) = \left|\det(\mathbb{A})\right|^2 = 1 \tag{2.23}$$

Spatial symmetry operations are linear transformations of a coordinate function space. When choosing the space in orthonormal form, symmetry operations will conserve orthonormality, and hence all transformations will be carried out by unitary matrices. This will be the case for all spatial representation matrices in this book. When all elements of a unitary matrix are real, it is called an *orthogonal* matrix. As unitary matrices, orthogonal matrices have the same properties except that complex conjugation leaves them unchanged. The determinant of an orthogonal matrix will thus be equal to ± 1. The rotation matrices in Chap. 1 are all orthogonal and have determinant $+1$.

2.4 Time Reversal as an Anti-linear Operator

The fact that an operator cannot change a scalar constant in front of the function on which it operates seems to be evident. However, in quantum mechanics there is one important operator that does affect a scalar constant and turns it into its complex conjugate. This is the operator of *time reversal*, i.e., the operator which inverts time, $t \to -t$, and sends the system back to its own past. If we are looking at a stationary

---

[1] Adapted from: [2, Problem 8, p. 59].

state, with no explicit time dependence, time inversion really means reversal of the direction of motion, where all angular momenta will be changing sign, including the "spinning" of the electrons. We shall denote this operator as $\hat{\vartheta}$. It has the following properties:

$$\hat{\vartheta}(|f_k\rangle + |f_l\rangle) = \hat{\vartheta}|f_k\rangle + \hat{\vartheta}|f_l\rangle$$
$$\hat{\vartheta}c|f_k\rangle = \bar{c}\hat{\vartheta}|f_k\rangle \tag{2.24}$$

These properties are characteristic of an *anti-linear* operator. As a rationale for the complex conjugation upon commutation with a multiplicative constant, we consider a simple case-study of a stationary quantum state. The time-dependent Schrödinger equation, describing the time evolution of a wavefunction, Ψ, defined by a Hamiltonian $\mathcal{H}$, is given by

$$-\frac{\hbar}{i}\frac{\partial \Psi}{\partial t} = \mathcal{H}\Psi \tag{2.25}$$

For a stationary state, the Hamiltonian is independent of time, and the wavefunction is characterized by an eigenenergy, E; hence the right-hand side of the equation is given by $\mathcal{H}\Psi = E\Psi$. The solution for the stationary state then becomes

$$\Psi(t) = \Psi(t_0)\exp\left(-\frac{iE(t-t_0)}{\hbar}\right) \tag{2.26}$$

Hence, the phase of a stationary state is "pulsating" at a frequency given by $E/\hbar$. Now we demonstrate the anti-linear character, using Wigner's argument that a perfect looping in time would bring a system back to its original state.[2] Such a process can be achieved by running backwards in time over a certain interval and then returning to the original starting time. Let $T_{\Delta t}$ represent a displacement in time toward the future over an interval Δt, and $T_{-\Delta t}$ a displacement over the same interval but toward the past. The consecutive action of $T_{\Delta t}$ and $T_{-\Delta t}$ certainly describes a perfect loop in time, and thus we can write:

$$\hat{T}_{\Delta t}\hat{T}_{-\Delta t} = \hat{E} \tag{2.27}$$

The reversal of the translation in time is the result of a reversal of the time variable. We thus can apply the operator transformation under $\hat{\vartheta}$, in line with the previous results in Sect. 1.3:

$$\hat{T}_{-\Delta t} = \hat{\vartheta}\hat{T}_{\Delta t}\hat{\vartheta}^{-1} \tag{2.28}$$

The complete loop can thus be written as follows:

$$T_{\Delta t}\hat{\vartheta}T_{\Delta t}\hat{\vartheta}^{-1} = \hat{E} \tag{2.29}$$

---

[2]Adapted from [3, Chap. 26].

This equation decomposes the closed path in time in four consecutive steps. Reading Eq. (2.29) from right to left, one sets off at time t_0 and reverses time $(\hat{\vartheta}^{-1})$. Now time runs for a certain interval Δt along the reversed time axis. A positive interval actually means that we are returning in time since the time axis has been oriented toward the past. This operation is presented by the displacement $\hat{T}_{\Delta t}$. Then one applies the time reversal again and now runs forward over the same interval to close the loop. The forward translation corresponds to the same $\hat{T}_{\Delta t}$ operator since again the interval is positive. Now multiply both sides of the equation, on the right, by $\hat{\vartheta}\,\hat{T}_{-\Delta t}$:

$$\hat{T}_{\Delta t}\hat{\vartheta} = \hat{\vartheta}\,\hat{T}_{-\Delta t} \tag{2.30}$$

The actions of the translations on the wavefunction are given by

$$
\begin{aligned}
T_{\Delta t}\Psi(t_0) &= \Psi(t_0)\exp\!\left(-\frac{iE\Delta t}{\hbar}\right) \\
T_{-\Delta t}\Psi(t_0) &= \Psi(t_0)\exp\!\left(\frac{iE\Delta t}{\hbar}\right)
\end{aligned}
\tag{2.31}
$$

Applying now both sides of Eq. (2.30) to the initial state yields

$$
\begin{aligned}
T_{\Delta t}\vartheta\Psi(t_0) &= \vartheta\,T_{-\Delta t}\Psi(t_0) \\
&= \vartheta\exp\!\left(\frac{iE\Delta t}{\hbar}\right)\Psi(t_0)
\end{aligned}
\tag{2.32}
$$

Since the Hamiltonian that we have used is invariant under time reversal, the function $\vartheta\Psi(t_0)$ on the left-hand side of Eq. (2.32) will be characterized by the same energy, E, and thus translate in time with the same phase factor as $\Psi(t_0)$ itself. Then the equation becomes

$$\exp\!\left(-\frac{iE\Delta t}{\hbar}\right)\vartheta\Psi(t_0) = \vartheta\exp\!\left(\frac{iE\Delta t}{\hbar}\right)\Psi(t_0) \tag{2.33}$$

which shows that time reversal will invert scalar constants to their complex conjugate, and hence it will be an anti-linear operator.

Note that in the present derivation we avoided providing an explicit form for the inverse of the time reversal operator. As a matter of fact, while space inversion is its own inverse, applying time reversal twice may give rise to an additional phase factor, which is $+1$ for systems with an even number of electrons, but -1 for systems with an odd number of electrons. We shall demonstrate this point later in Sect. 7.6. Hence, $\vartheta^{-1} = \pm\vartheta$, or

$$\hat{\vartheta}^2 = \pm 1 \tag{2.34}$$

2.5 Problems

2.1 A complex number can be characterized by an absolute value and a phase. A 2×2 complex matrix thus contains eight parameters, say

$$\mathbb{C} = \begin{pmatrix} |a|e^{i\alpha} & |b|e^{i\beta} \\ |c|e^{i\gamma} & |d|e^{i\delta} \end{pmatrix}$$

Impose now the requirement that this matrix is unitary. This will introduce relationships between the parameters. Try to solve these by adopting a reduced set of parameters.

2.2 The cyclic waves $e^{ik\phi}$ and $e^{-ik\phi}$ are defined in a circular interval $\phi \in [0, 2\pi[$. Normalize these waves over the interval. Are they mutually orthogonal?

2.3 A matrix $\mathbb{H}$ which is equal to its complex-conjugate transpose, $\mathbb{H} = \bar{\mathbb{H}}^{\mathrm{T}}$, is called *Hermitian*. It follows that the diagonal elements of such a matrix are real, while corresponding off-diagonal elements form complex-conjugate pairs:

$$\mathbb{H} \text{ Hermitian } \to H_{ii} \in \mathcal{R}; \quad H_{ij} = \bar{H}_{ji}$$

Prove that the eigenvalues of a Hermitian matrix are real. If the matrix is *skew-Hermitian*, $\mathbb{H} = -\bar{\mathbb{H}}^{\mathrm{T}}$, the eigenvalues are all imaginary.

References

1. Dirac, P.A.M.: The Principles of Quantum Mechanics. Clarendon Press, Oxford (1958)
2. Altmann, S.L.: Rotations, Quaternions, and Double Groups. Clarendon Press, Oxford (1986)
3. Wigner, E.P.: Group Theory. Academic Press, New York (1959)

Chapter 3
Groups

Abstract The concept of a group is introduced using the example of the symmetry group of the ammonia molecule. In spite of its tiny size, this molecule has a structural symmetry that is the same as the symmetry of a macroscopic trigonal pyramid. From the mathematical point of view, a group is an elementary structure that proves to be a powerful tool for describing molecular properties. Three ways of dividing (and conquering) groups are shown: subgroups, cosets, and classes. An overview of molecular symmetry groups is given. The relationship between rotational groups and chirality is explained, and symmetry lowerings due to applied magnetic and electric fields are determined.

Contents

3.1 The Symmetry of Ammonia

The umbrella shape of the ammonia molecule has trigonal symmetry with, in addition, three vertical reflection planes through the hydrogen atoms. Together these symmetry elements form a point group, which, in the Schoenflies notation, is denoted as C_{3v}. It is good practice to start the treatment by making a simple sketch of the molecule and putting it in a right-handed Cartesian frame, as shown in Fig. 3.1. By convention, the z-axis is defined as the principal threefold axis. One of the hydrogens is put in the xz plane as shown in the figure. We attach labels A, B, C to distin-

Fig. 3.1 Group theory of the ammonia molecule, with three sets of labels: x, y, z label the Cartesian axes, $\hat{\sigma}_1, \hat{\sigma}_2, \hat{\sigma}_3$ label the symmetry planes, and A, B, C label the hydrogen atoms
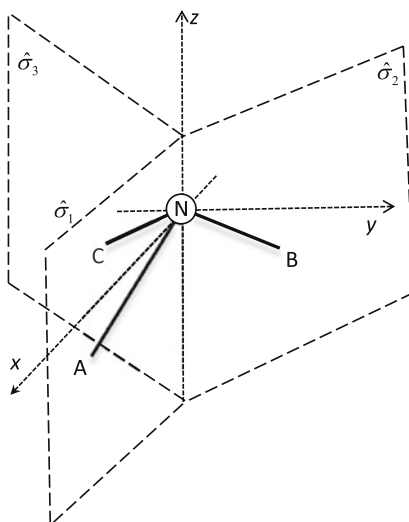
guish the equivalent hydrogen atoms. In the active view, which we keep throughout, the atoms will be displaced while the symmetry elements remain tied to the immobile Cartesian frame. We shall thus not label the reflection planes by A,B,C, but we shall instead denote them as $\hat{\sigma}_1, \hat{\sigma}_2, \hat{\sigma}_3$. The $\hat{\sigma}_1$ reflection plane coincides with the xz coordinate plane. The action of the symmetry elements will be to permute the atoms. The threefold axis, rotating counterclockwise about z, moves the atom A to the position of B, which itself is displaced to the position originally occupied by C. Finally, C travels to the place previously occupied by atom A. The $\hat{\sigma}_1$ plane will leave A unchanged and will interchange B and C. Now consider the combination $\hat{\sigma}_1 \hat{C}_3$ of these two elements. We place the structure to the right of the right-justified operators and then simply work out the action from right to left; hence, first the $\hat{C}_3$ axis, and then the plane. This is shown in a pictorial way in Fig. 3.2. First, the axis will permute the atoms so that C takes the place of A. Consequently, the $\hat{\sigma}_1$ plane will now conserve C and interchange A and B. The combined action is itself again one of the symmetry elements, viz., $\hat{\sigma}_2$. The reverse product order yields a different result. In summary,

$$\hat{\sigma}_1 \hat{C}_3 = \hat{\sigma}_2$$
$$\hat{C}_3 \hat{\sigma}_1 = \hat{\sigma}_3$$

(3.1)

In this way we can easily work out the full set of binary products, keeping in mind that applying the threefold rotation three times, or the symmetry planes twice, leaves every atom in place and thus corresponds to the unit element. The results are gathered in the 6×6 multiplication Table 3.1. This table should be read from left to right, i.e., the product $\hat{R}_i \hat{R}_j$ is found in the ith row and jth column. We may symbolically denote the matrix elements in the table as

$$M_{ij} = \hat{R}_i \hat{R}_j$$

(3.2)
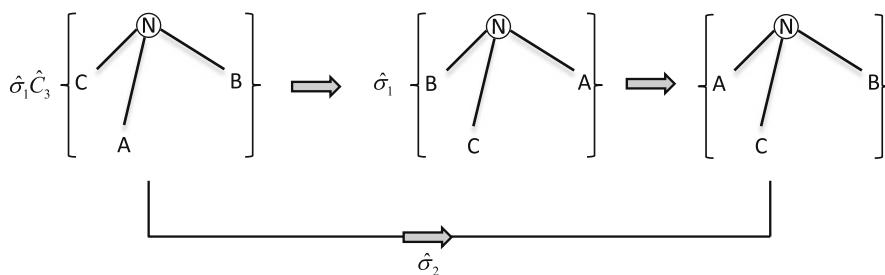
Fig. 3.2 Applying $\hat{\sigma}_1\hat{C}_3$ to the starting structure is equivalent to applying $\hat{\sigma}_2$

Table 3.1 Multiplication table for the point group C_{3v}

C_{3v}	$\hat{E}$	$\hat{C}_3$	$\hat{C}_3^2$	$\hat{\sigma}_1$	$\hat{\sigma}_2$	$\hat{\sigma}_3$
$\hat{E}$	$\hat{E}$	$\hat{C}_3$	$\hat{C}_3^2$	$\hat{\sigma}_1$	$\hat{\sigma}_2$	$\hat{\sigma}_3$
$\hat{C}_3$	$\hat{C}_3$	$\hat{C}_3^2$	$\hat{E}$	$\hat{\sigma}_3$	$\hat{\sigma}_1$	$\hat{\sigma}_2$
$\hat{C}_3^2$	$\hat{C}_3^2$	$\hat{E}$	$\hat{C}_3$	$\hat{\sigma}_2$	$\hat{\sigma}_3$	$\hat{\sigma}_1$
$\hat{\sigma}_1$	$\hat{\sigma}_1$	$\hat{\sigma}_2$	$\hat{\sigma}_3$	$\hat{E}$	$\hat{C}_3$	$\hat{C}_3^2$
$\hat{\sigma}_2$	$\hat{\sigma}_2$	$\hat{\sigma}_3$	$\hat{\sigma}_1$	$\hat{C}_3^2$	$\hat{E}$	$\hat{C}_3$
$\hat{\sigma}_3$	$\hat{\sigma}_3$	$\hat{\sigma}_1$	$\hat{\sigma}_2$	$\hat{C}_3$	$\hat{C}_3^2$	$\hat{E}$

As has already been shown, these operations can also be performed directly in function space. Choosing the xy-plane $2p$-orbitals on nitrogen, $\{p_x, p_y\}$, as a suitable basis set, we may represent all the symmetry elements by transformation matrices. The resulting matrices are summarized in Table 3.2. Note that all six matrices are different. The mapping between the symmetry elements and the matrices is therefore one-to-one, and the representation is said to be *faithful*. For the $\hat{C}_3$ axis, the matrix corresponds to the one in Eq. (1.13), with rotation angle $\alpha = 2\pi/3$, and for the $\hat{C}_3^2$ axis, one has $\alpha = 4\pi/3$, which is equivalent to the inverse angle $\alpha = -2\pi/3$. The $\hat{\sigma}_1$ element leaves p_x unchanged and inverts p_y. The other reflection planes are similar to $\hat{\sigma}_1$, which means that they can be obtained by a symmetry transformation of this operator, using the results in Sect. 1.3; hence,

$$\hat{\sigma}_2 = \hat{C}_3\hat{\sigma}_1\hat{C}_3^{-1}$$
$$\hat{\sigma}_3 = \hat{C}_3\hat{\sigma}_2\hat{C}_3^{-1}$$

(3.3)

The set of the six matrices in Table 3.2 offers an alternative algebraic way of constructing the multiplication table by direct matrix multiplication. The product $\hat{C}_3\hat{\sigma}_1$ is then replaced by the matrix multiplication $\mathbb{D}(C_3) \times \mathbb{D}(\sigma_1)$:

$$\begin{pmatrix} -\frac{1}{2} & -\frac{\sqrt{3}}{2} \\ +\frac{\sqrt{3}}{2} & -\frac{1}{2} \end{pmatrix} \times \begin{pmatrix} 1 & 0 \\ 0 & -1 \end{pmatrix} = \begin{pmatrix} -\frac{1}{2} & +\frac{\sqrt{3}}{2} \\ +\frac{\sqrt{3}}{2} & +\frac{1}{2} \end{pmatrix}$$

(3.4)

which yields the representation matrix for $\hat{\sigma}_3$, in line with Eq. (3.1).

Table 3.2 Representation matrices for the (p_x, p_y) basis in C_{3v}

$$\mathbb{D}(E) = \begin{pmatrix} 1 & 0 \\ 0 & 1 \end{pmatrix} \qquad \mathbb{D}(\sigma_1) = \begin{pmatrix} 1 & 0 \\ 0 & -1 \end{pmatrix}$$

$$\mathbb{D}(C_3) = \begin{pmatrix} -\frac{1}{2} & -\frac{\sqrt{3}}{2} \\ +\frac{\sqrt{3}}{2} & -\frac{1}{2} \end{pmatrix} \qquad \mathbb{D}(\sigma_2) = \begin{pmatrix} -\frac{1}{2} & -\frac{\sqrt{3}}{2} \\ -\frac{\sqrt{3}}{2} & +\frac{1}{2} \end{pmatrix}$$

$$\mathbb{D}(C_3^2) = \begin{pmatrix} -\frac{1}{2} & +\frac{\sqrt{3}}{2} \\ -\frac{\sqrt{3}}{2} & -\frac{1}{2} \end{pmatrix} \qquad \mathbb{D}(\sigma_3) = \begin{pmatrix} -\frac{1}{2} & +\frac{\sqrt{3}}{2} \\ +\frac{\sqrt{3}}{2} & +\frac{1}{2} \end{pmatrix}$$

3.2 The Group Structure

The set of symmetry operations of ammonia is said to form a *group*, G. This is a fundamental mathematical structure consisting of a set of elements and a multiplication rule with the following characteristics:

- Existence of a unit element, $\hat{E}$, which leaves all elements unchanged:

$$\hat{E}\hat{R} = \hat{R}\hat{E} = \hat{R} \tag{3.5}$$

In the list of elements the unit element is placed in front. As a result, the first row and first column of the multiplication table will simply repeat the ordered list of symmetry elements on which the table was based.

- Existence of an inverse element, $\hat{R}^{-1}$, for every element $\hat{R}$:

$$\hat{R}\hat{R}^{-1} = \hat{R}^{-1}\hat{R} = \hat{E} \tag{3.6}$$

Hence every action can also be undone. If this were not the case, we would have produced a monster that can only continue to grow. In the multiplication table, a unit element at position ij indicates that $\hat{R}_i$ and $\hat{R}_j$ are mutual inverses. Clearly, for the unit element, as well as for the reflection planes, $\hat{R}$ and $\hat{R}^{-1}$ coincide, while, for the $\hat{C}_3$ axis, the inverse is equal to $\hat{C}_3^2$, which completes a full turn.

- Closure:

$$\forall \hat{R} \in G \quad \& \quad \hat{S} \in G \Rightarrow \hat{R}\hat{S} \in G \& \hat{S}\hat{R} \in G \tag{3.7}$$

In the multiplication table, this is apparent by the fact that no entries are left open.

- Associativity:

$$\hat{R}(\hat{S}\hat{T}) = (\hat{R}\hat{S})\hat{T} \tag{3.8}$$

It is difficult to imagine that such a simple set of rules can give rise to such a powerful structure on which entire properties of molecules will depend. Note that, compared with a number system, a group is an even more primitive concept since it contains only one operation, multiplication, by means of which two elements of the group may be combined. In contrast, the set of numbers allows for addition and multiplication, which results in two kinds of unit elements, zero for addition and unity for multiplication. A closer look at the multiplication table of the group shows that it

has very remarkable properties. Each row and each column represent a permutation of the ordered set of elements, but in such a way that every element occurs only once in each row and column. This is a direct consequence of the group properties. As in many group-theoretical proofs, the simplest way to show this is by a *reductio ad absurdum*. Suppose that a given element, $\hat{T}$, occurred at entries ij and ik, with $\hat{R}_k \neq \hat{R}_j$. Then one would have, by applying the rules:

$$\hat{R}_i \hat{R}_j = \hat{R}_i \hat{R}_k$$

$$\hat{R}_i^{-1}(\hat{R}_i \hat{R}_j) = \hat{R}_i^{-1}(\hat{R}_i \hat{R}_k)$$

$$\left(\hat{R}_i^{-1}\hat{R}_i\right)\hat{R}_j = \left(\hat{R}_i^{-1}\hat{R}_i\right)\hat{R}_k \qquad (3.9)$$

$$\hat{E}\hat{R}_j = \hat{E}\hat{R}_k$$

$$\hat{R}_j = \hat{R}_k$$

which would contradict the original supposition. Along the same lines it is easy to prove that the inverse of a product is equal to the product of the inverses in the opposite order:

$$(\hat{R}_i \hat{R}_j)^{-1} = \hat{R}_j^{-1}\hat{R}_i^{-1} \qquad (3.10)$$

As a matter of principle, the group multiplication table contains everything there is to know about the group. It is, though, not necessary to store the whole multiplication table. A more compact way uses *generators*. The generators are defined as a minimal set of elements capable of generating the whole group. For the present example, two generators are needed, e.g., $\hat{C}_3$ and $\hat{\sigma}_1$. It is sufficient to make all binary combinations of these two operators in order to generate all remaining elements:

$$\hat{C}_3\hat{C}_3 = \hat{C}_3^2$$

$$\hat{\sigma}_1\hat{\sigma}_1 = \hat{E}$$

$$\hat{C}_3\hat{\sigma}_1 = \hat{\sigma}_3 \qquad (3.11)$$

$$\hat{\sigma}_1\hat{C}_3 = \hat{\sigma}_2$$

Alternatively, any pair of reflection planes would suffice as generators, say $\hat{\sigma}_1$ and $\hat{\sigma}_2$, but in this case the remaining symmetry plane can be obtained only by a further multiplication:

$$\hat{\sigma}_1\hat{\sigma}_1 = \hat{E}$$

$$\hat{\sigma}_2\hat{\sigma}_2 = \hat{E}$$

$$\hat{\sigma}_1\hat{\sigma}_2 = \hat{C}_3 \qquad (3.12)$$

$$\hat{\sigma}_2\hat{\sigma}_1 = \hat{C}_3^2$$

$$\hat{\sigma}_1\hat{\sigma}_2\hat{\sigma}_1 = \hat{\sigma}_3$$

Fig. 3.3 Cayley graph of the C_{3v} point group. The generators are $c = \hat{C}_3$ and $s = \hat{\sigma}_1$
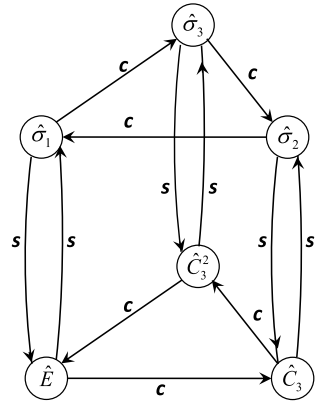
A *presentation* of a group is a set of generators, together with a minimal set of relations that are sufficient to work out any product of two elements. As an example, let us denote the $\hat{C}_3, \hat{\sigma}_1$ generators as c, s. Just three relations among these generators are sufficient to derive the whole multiplication table: $c^3 = s^2 = e, sc = c^2s$. The generation of the six elements of the group follows from Eq. (3.11):

$$\hat{E} = e$$
$$\hat{C}_3 = c$$
$$\hat{C}_3^2 = c^2$$
$$\hat{\sigma}_1 = s \qquad\qquad (3.13)$$
$$\hat{\sigma}_2 = sc$$
$$\hat{\sigma}_3 = cs$$

Any product of these elements can be shown to be closed using only the presentation. As an example, the rule $\hat{\sigma}_2 \hat{\sigma}_3 = \hat{C}_3$, is expressed in the presentation as follows:

$$sccs = s\left(c^2 s\right) = s(sc) = s^2 c = c \qquad\qquad (3.14)$$

In this way the whole multiplication table can be derived.

The structure of the group can also be encoded in a graph known as the Cayley graph. A graph is an abstract mathematical object consisting of a set of points, or nodes, and a set of lines connecting pairs of these points. In a *directed graph* these pairs are ordered, which means that directional arrows are added to the connecting lines. In the Cayley graph every element of the group corresponds to a node. The lines correspond to the action of the group generators. The generator $\hat{g}$ connects a given node $\langle \hat{R}_i \rangle$ by a directed line to the resulting node $\langle \hat{g} \hat{R}_i \rangle$. The action of the group on its own Cayley graph will not only map nodes onto nodes, but will also preserve the directed connections. As a result, the symmetry group will map the graph onto itself. Such a mapping is called an *automorphism*. The group G is

Table 3.3 Multiplication table for the point group D_2

D_2	$\hat{E}$	$\hat{C}_2^x$	$\hat{C}_2^y$	$\hat{C}_2^z$
$\hat{E}$	$\hat{E}$	$\hat{C}_2^x$	$\hat{C}_2^y$	$\hat{C}_2^z$
$\hat{C}_2^x$	$\hat{C}_2^x$	$\hat{E}$	$\hat{C}_2^z$	$\hat{C}_2^y$
$\hat{C}_2^y$	$\hat{C}_2^y$	$\hat{C}_2^z$	$\hat{E}$	$\hat{C}_2^x$
$\hat{C}_2^z$	$\hat{C}_2^z$	$\hat{C}_2^y$	$\hat{C}_2^x$	$\hat{E}$

thus isomorphic to the automorphism group of its Cayley graph. The Cayley graph corresponding to the group C_{3v}, generated by $\hat{C}_3$ and $\hat{\sigma}_1$, is shown in Fig. 3.3. It resembles a trigonal prism, but with opposite directions in the upper and the lower triangle. The $\hat{\sigma}_1$ generator corresponds to the upright edges of the prism. Since this generator is its own inverse, these edges can be traversed in both directions, so they are really undirected.

3.3 Some Special Groups

Abelian groups[1] are groups with a commutative multiplication rule, i.e.,

$$\forall \hat{R} \in G \quad \& \quad \hat{S} \in G \Rightarrow \hat{R}\hat{S} = \hat{S}\hat{R} \tag{3.15}$$

Hence, in an abelian group, the multiplication table is symmetric about the diagonal. Clearly, our group C_{3v} is not abelian.

Cyclic groups are groups with only one generator. They are usually denoted as C_n. The threefold axis gives rise to the cyclic group C_3. Its elements consist of products of the generator. By analogy with number theory, such multiple products are called powers; hence, $C_3 = \{\hat{C}_3, \hat{C}_3^2, \hat{C}_3^3\}$, where the third power is of course the unit element. Similarly, the reflection planes yield a cyclic group of order 2. The standard notation for this group is not C_2 but C_s. Cyclic groups are of course abelian because the products of elements give rise to a sum of powers and summation is commutative:

$$\hat{C}^i \hat{C}^j = \hat{C}^{i+j} = \hat{C}^{j+i} = \hat{C}^j \hat{C}^i \tag{3.16}$$

By contrast, not all abelian groups are cyclic. A simple example is the group[2] D_2 of order 4, which is presented in Table 3.3. It needs two perpendicular twofold axes as generators and thus cannot be cyclic. Nonetheless, it is abelian since its generators commute.

The *symmetric* group, S_n, is the group of all permutations of the elements of a set of cardinality n. The order of S_n is equal to $n!$. As it happens, our C_{3v} group is isomorphic to S_3. The permutations are defined on the ordered set of the three

---

[1]Named after the Norwegian mathematician Niels Henrik Abel (1802–1829).

[2]This group is isomorphic to Felix Klein's four-group (*Vierergruppe*).

hydrogen atomic labels ⟨ABC⟩. Interchange of A and B means that, in this row, the element A is replaced by B and vice versa. Another way to express this is that "A becomes B, and B becomes A," and hence (A → B → A). This interchange is a *transposition* or 2-cycle, which will be denoted as (AB). The operation for the entire set is then written as a sequence of two disjunct cycles (C)(AB), where the 1-cycle indicates that the element C remains unchanged. The 3-cycle (ABC) corresponds to a cyclic permutation of all three elements: (A → B → C → A). The successive application of both operations, acting on the letter string, can be worked out as follows:

$$⟨ABC⟩$$
$$(C)\,(AB) \quad ⇓$$
$$⟨BAC⟩ \tag{3.17}$$
$$(ABC) \quad ⇓$$
$$⟨CBA⟩$$

The result is to permute A and C, and leave B invariant. This result defines the product of the two operations as

$$(ABC) \cdot (C)(AB) = (B)(AC) \tag{3.18}$$

The multiplication table for the whole group is given in Table 3.4. The group multiplication tables of S_3 and C_{3v} clearly have the same structure, but the isomorphism can be realized in six different ways, as there are six ways to associate the three letters with the three trigonal sites. It is important to keep in mind that the two kinds of groups have a very different meaning. The C_{3v} operations refer to spatial symmetry operations of the ammonia molecule, while the permutational group is a set-theoretic concept and acts on elements in an ordered set. As an example, one might easily identify the $\hat{\sigma}_1$ reflection plane with the (A)(BC) permutation operation since it indeed leaves A invariant and swaps B and C. However, as shown in Fig. 3.2, when this reflection is preceded by a trigonal symmetry axis, the atom C has taken the place of A, and the $\hat{\sigma}_1$ plane now should be described as (C)(AB). For a proper definition of the relationship between nuclear permutations and spatial symmetry operations, we refer to Sect. 5.4, where the molecular symmetry group is introduced.

In S_3 the number of transpositions, i.e., pairwise interchanges of atoms, is zero for the unit element, one for the reflection planes, and two for the threefold axes. *Odd permutations* are defined by an odd number of transpositions. The product of two even permutations is an even permutation, and for this reason, the even permutations alone will also form a group, known as the *alternating group*, A_n. In the present example, the alternating group A_3 is isomorphic to the cyclic group C_3. By contrast, the product of two odd permutations is not odd, but even. So odd permutations cannot form a separate group.

Table 3.4 Multiplication table for the symmetric group S_3. The unit element can also be expressed as three 1-cycles: (A)(B)(C)

S_3	$\hat{E}$	(ABC)	(ACB)	(A)(BC)	(B)(AC)	(C)(AB)
$\hat{E}$	$\hat{E}$	(ABC)	(ACB)	(A)(BC)	(B)(AC)	(C)(AB)
(ABC)	(ABC)	(ACB)	$\hat{E}$	(C)(AB)	(A)(BC)	(B)(AC)
(ACB)	(ACB)	$\hat{E}$	(ABC)	(B)(AC)	(C)(AB)	(A)(BC)
(A)(BC)	(A)(BC)	(B)(AC)	(C)(AB)	$\hat{E}$	(ABC)	(ACB)
(B)(AC)	(B)(AC)	(C)(AB)	(A)(BC)	(ACB)	$\hat{E}$	(ABC)
(C)(AB)	(C)(BA)	(A)(BC)	(B)(AC)	(ABC)	(ACB)	$\hat{E}$

The group multiplication table contains all there is to know about a group. It hides a wealth of internal structure that is directly relevant to the physical phenomena to which the group applies. In order to elucidate this structure, three ways of delineating subsets of the group are useful: subgroups, cosets, and classes.

3.4 Subgroups

A subgroup H of G, denoted $H \subset G$, is a subset of elements of G, which itself has the group property. Trivial subgroups are the group containing the identity alone, denoted as $C_1 = \{\hat{E}\}$, and the group G itself. Besides these, in the case of the group of ammonia, C_{3v}, there are four nontrivial subgroups: $C_3 = \{\hat{E}, \hat{C}_3, \hat{C}_3^2\}$, and $C_s = \{\hat{E}, \hat{\sigma}_i\}$ with $i = 1, 2$, or 3. The three C_s groups are equivalent. We can construct a simplified genealogical tree, which shows the subgroup structure (Fig. 3.4). In chemistry and physics, subgroup structures are highly relevant since the distortions of a symmetric system can be described as a descent down the genealogical tree. We shall describe this in Sect. 4.6 as the subduction process. For the moment, we retain Cayley's theorem:

Theorem 1 *Every group of order n is isomorphic with a subgroup of the symmetric group S_n.*

This theorem is immediately clear from the multiplication table. A given row of the table shows how the corresponding element maps the entire set of elements onto itself. This mapping is a permutation of the n elements, and every element gives rise to a different permutation since no two rows are the same. Thus, G must be a subgroup of S_n. The importance of this theorem is especially evident from the mathematical point of view. It tells us that the symmetric groups exhaust all the possible structures of finite groups.

Fig. 3.4 Genealogical tree,
representing progressive
symmetry breaking of the
C_{3v} point group. The C_s box
stands for the three equivalent
reflections groups
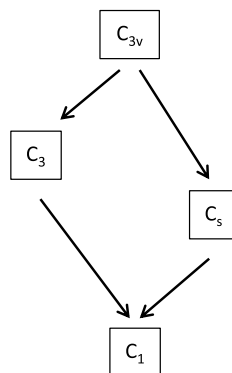
3.5 Cosets

A genuine *partitioning* of a group is achieved when the set of elements is divided
into separate subsets that do not exhibit any overlap and, together, constitute the
whole group. Subgroups clearly do not form a partitioning since, for instance, they
all share the same unit element. On the other hand, cosets do form a partitioning.
In molecules, the natural realizations of the cosets are the sets of equivalent sites.
These are atoms or groups of atoms that are permuted by the action of the molec-
ular symmetry group. In the example of the ammonia molecule, each of the three
hydrogen atoms occupies an equivalent site with C_s symmetry. The nitrogen atom,
however, occupies a unique site that has the full C_{3v} symmetry. Now consider the
site of one particular hydrogen atom, say A. The C_s subgroup that leaves this site
invariant consists of only two symmetry elements: $\hat{E}$ and $\hat{\sigma}_1$. This subgroup is called
the *stabilizer* of the site. When we multiply each element of this subgroup (on the
left) with an element outside it, say $\hat{C}_3$, we obtain two new elements, $\hat{C}_3$ and $\hat{\sigma}_3$,
which both share the property that they map A onto B. They form a (left) coset of
the original C_s subgroup, and the element that we used to form this coset is the
coset-representative. There is still another coset, which may be generated by one
of the remaining elements, say $\hat{C}_3^2$. In this way, one finds the coset, $\{\hat{C}_3^2, \hat{\sigma}_2\}$, of
elements which have the property that they both map A onto C. The sum of all the
cosets forms the total set, and hence,

$$C_{3v} = \{\hat{E}, \hat{\sigma}_1\} + \{\hat{C}_3, \hat{\sigma}_3\} + \{\hat{C}_3^2, \hat{\sigma}_2\} \tag{3.19}$$

We can rewrite this in general as

$$G = \sum_n \hat{R}_n H \tag{3.20}$$

where $\hat{R}_n$ denotes a coset representative, and the product $\hat{R}_n H$ denotes the nth coset,
obtained by multiplying every element of the subgroup on the left by the generator.
The choice of coset representatives is not unique since every element of a given
coset may act as representative. In the case of the present group, we can choose all

representatives as powers of the threefold axis, which allows introduction of a cyclic summation:

$$C_{3v} = \sum_{n=1}^{3} (\hat{C}_3)^n C_s \tag{3.21}$$

This expression forms a nice illustration of how representatives make different maps of the subgroup. These cosets form an *orbit* inside the group. Note that the way cosets are defined here is based on left multiplication by the generators, giving rise to what are also denoted as *left cosets*. An analogous partitioning of the group can also be based on right cosets. The partitioning of a group in cosets gives rise to the famous Lagrange theorem:

Theorem 2 *The order of a subgroup of a finite group is a divisor of the order of the group.*

Consider a group G and subgroup H with respective orders $|G|$ and $|H|$. The theorem states that $|G|/|H|$ is an integer. The proof is based on two elements. One first has to prove that all elements in a given coset are different and further that different cosets do not manifest any overlap.

Consider a coset $\hat{R}_i H$ with elements $\hat{R}_i \hat{h}_x$. For $\hat{h}_x \neq \hat{h}_y$, $\hat{R}_i \hat{h}_x$ must be different from $\hat{R}_i \hat{h}_y$, simply because two elements in the same row in the multiplication table can never be equal, as was proven in Eq. (3.9). Hence, the size of the coset will be equal to $|H|$. Then we consider an element $\hat{R}_j \notin \hat{R}_i H$. This new element will in turn be the representative of a new coset, $\hat{R}_j H$, and we must prove that this new coset does not overlap with the previous one. This can easily be demonstrated by *reductio ad absurdum*. Suppose that there is an element $\hat{R}_j \hat{h}_x$ in the second coset that also belongs to the first coset, as $\hat{R}_i \hat{h}_y$. We then have:

$$\begin{aligned} \hat{R}_j \hat{h}_x &= \hat{R}_i \hat{h}_y \\ \hat{R}_i^{-1} \hat{R}_j &= \hat{h}_y \hat{h}_x^{-1} \end{aligned} \tag{3.22}$$

Since the subgroup H has the group property, the inverse element $\hat{h}_x^{-1}$ is also an element of H, and so is its product with $\hat{h}_y$. Hence, the product $\hat{R}_i^{-1} \hat{R}_j$ will be an element of H, say $\hat{h}_z = \hat{h}_y \hat{h}_x^{-1}$. The first coset will of course contain the element $\hat{R}_i \hat{h}_z$, which reduces to

$$\hat{R}_i \hat{h}_z = \hat{R}_i \hat{h}_y \hat{h}_x^{-1} = \hat{R}_i \hat{R}_i^{-1} \hat{R}_j = \hat{R}_j \tag{3.23}$$

Hence, $\hat{R}_j \in \hat{R}_i H$, contrary to the assumption. The expansion of the group in cosets thus leads to a complete partitioning in subsets of equal sizes. It starts by the subset formed by the subgroup H. If H is smaller than G, take an element outside H and form with this element a coset, which will have the same dimension as H. If there are still elements outside, use one of these to form a new coset, again containing $|H|$

elements, etc. Each time a coset is formed, a block of size $|H|$ is occupied till the full territory of the group is occupied by subsets of the same size. Their order must thus be a divisor of the group order. In a sense, one could describe this collection of cosets as the quotient, resulting from the "division" of the group by a subgroup. We shall make use of this concept in the induction of representations in Sect. 4.6. In the present example, the point group of ammonia is of order 6, with divisors 1, 2, 3, and 6, and for each of these, there are indeed subgroups. This is rather exceptional, though. It is *not* the case that for every divisor there should be a subgroup. As a further corollary, groups with an order which is a prime number have no nontrivial subgroups.

3.6 Classes

Probably, the most natural way to partition a group is by putting all elements "of the same kind" into separate classes. Hence, in the group C_{3v} we could put the three planes in one class; the unit element is of course a separate class, but what about the $\hat{C}_3$ and $\hat{C}_3^2$ axes? Are they of the same kind or not? Clearly, we need a rigorous definition of what it means for two symmetry elements to be equivalent. We can use as a criterion the symmetry transformations of an operator, as explained in Sect. 1.3. Hence, two elements $\hat{A}$ and $\hat{B}$ will belong to the same class, $\hat{A} \sim \hat{B}$, if there exists (denoted as $\exists$) a symmetry operation $\hat{U}$ that belongs to the group and transforms $\hat{B}$ into $\hat{A}$:

$$\hat{A} \sim \hat{B} : \exists \hat{U} \in G \rightarrow \hat{A} = \hat{U}\hat{B}\hat{U}^{-1} \tag{3.24}$$

In C_{3v}, the symmetry planes will map $\hat{C}_3$ onto $\hat{C}_3^2$. Hence, we can safely say that the two threefold elements belong to the same class, because of the existence of symmetry planes, which can reverse the direction of rotation. Synonyms for "to belong to the same class" are: "to be (class-)conjugate" or "to be similarity transforms." If the element $\hat{U}$ transforms $\hat{B}$ to $\hat{A}$, then the inverse element, $\hat{U}^{-1}$, which because of the group properties also belongs to G, will do the reverse and will transform $\hat{A}$ into $\hat{B}$. Hence, conjugation is reflexive. It is, furthermore, transitive:

$$(\hat{A} \sim \hat{B}) \& (\hat{B} \sim \hat{C}) \rightarrow (\hat{A} \sim \hat{C}) \tag{3.25}$$

The set of all elements that are conjugate with a given element is a *conjugacy class* or simply a class. A class is fully denoted by specifying any one of its elements in the same way as a coset is defined by any one of its representatives. The total group is of course the sum of all its classes. In abelian groups, the similarity transformation will always return the element on which it was acting; hence, in this case, all classes will be singletons (sets of order 1). The unit element is unique, so it is always in its own class.

Theorem 3 *The number of elements in a class is a divisor of the group order.*

The proof makes use of the coset concept. We start by considering all elements that stabilize a given element, say $\hat{A}_0$, of the group. One can prove that these elements constitute a subgroup $H \subset G$. Hence, we write:

$$\hat{h}_x \in H \Leftrightarrow \hat{h}_x \hat{A}_0 \hat{h}_x^{-1} = \hat{A}_0 \tag{3.26}$$

The proof consists of a check of the four group criteria. The closure, for instance, is proven as follows: suppose that both $\hat{h}_x$ and $\hat{h}_y$ stabilize $\hat{A}_0$; then their product will also be a stabilizer:

$$\hat{h}_x \hat{h}_y \hat{A}_0 (\hat{h}_x \hat{h}_y)^{-1} = \hat{h}_x \hat{h}_y \hat{A}_0 \hat{h}_y^{-1} \hat{h}_x^{-1} = \hat{h}_x \hat{A}_0 \hat{h}_x^{-1} = \hat{A}_0 \tag{3.27}$$

where we use the result of Eq. (3.10) that the inverse of a product is equal to the product of the inverses in the reverse order. Next, we expand G in cosets of this newly found subgroup H. All elements of a coset $\hat{R}_i H$, with $\hat{R}_i \notin H$, will transform $\hat{A}_0$ into the same new element $\hat{A}_i$:

$$\hat{R}_i \hat{h}_x \hat{A}_0 (\hat{R}_i \hat{h}_x)^{-1} = \hat{R}_i \hat{h}_x \hat{A}_0 \hat{h}_x^{-1} \hat{R}_i^{-1} = \hat{R}_i \hat{A}_0 \hat{R}_i^{-1} = \hat{A}_i \tag{3.28}$$

The result must be different from $\hat{A}_0$ because, otherwise, $\hat{R}_i$ would be an element of H. In order to prove the theorem, the following remaining questions have to be decided. Do different cosets give rise to different similarity transforms? Does one obtain all elements of a class by finding all transforms of a given starting element? The answers to both questions are affirmative. For the first question, if $\hat{R}_i$ and $\hat{R}_j$ represent different cosets, one should conclude that $\hat{A}_i \neq \hat{A}_j$. Suppose that the opposite is true:

$$\hat{R}_i \hat{A}_0 \hat{R}_i^{-1} = \hat{R}_j \hat{A}_0 \hat{R}_j^{-1}$$
$$\hat{R}_i^{-1} \hat{R}_j \hat{A}_0 \hat{R}_j^{-1} \hat{R}_i = \hat{A}_0 \tag{3.29}$$
$$\hat{R}_i^{-1} \hat{R}_j \hat{A}_0 (\hat{R}_i^{-1} \hat{R}_j)^{-1} = \hat{A}_0$$

This implies that $\hat{R}_i^{-1} \hat{R}_j$ stabilizes $\hat{A}_0$ and thus must belong to H, where it corresponds to, say, $\hat{h}_z$. But one then again has

$$\hat{R}_i \hat{h}_z = \hat{R}_i \hat{R}_i^{-1} \hat{R}_j = \hat{R}_j \tag{3.30}$$

and thus $\hat{R}_j$ is a representative of the same coset as $\hat{R}_i$, which contradicts the starting assumption. Hence, there will be at least as many equivalent elements in the class as there are cosets of the stabilizing subgroup. Have we then generated the entire class? Yes, because by going through all the cosets, we run through the entire group. In this way, we have found all elements that are conjugate to a given one, but, because of transitivity, this also means that there cannot be other conjugate elements. The one-to-one mapping between conjugate elements and cosets implies that the number in a class is equal to the number of cosets of the stabilizing subgroup and hence—by Lagrange's theorem—must be a divisor of the group order.

The proof illustrates the connection between cosets and conjugacy classes. A special example of this arises in the case of *normal*, or *invariant*, subgroups. A subgroup H is normal if its left and right cosets coincide, i.e., if $\hat{R}_i H = H \hat{R}_i$. This implies that all the elements of the group will map the subgroup onto itself or, for a normal subgroup H,

$$\forall \hat{U} \in G \quad \& \quad \hat{h}_x \in H : \hat{U}\hat{h}_x\hat{U}^{-1} \in H \tag{3.31}$$

Normal subgroups are thus made up of entire conjugacy classes of G. As an example, the group C_3 is a normal subgroup of C_{3v} since it contains the whole conjugacy class of the trigonal elements. A molecular site that is stabilized by a normal subgroup must be unique since it can be mapped only onto itself. Such is the case for the nitrogen atom in ammonia. By contrast, the C_s subgroups stabilizing the hydrogen sites in ammonia are not normal since they are based on only one reflection plane, while there are three symmetry planes in the corresponding conjugacy class. Accordingly, the hydrogen sites are not unrelated.

3.7 Overview of the Point Groups

The highest point group symmetry is that of the spherical symmetry group. The gradual descent in symmetry from the sphere provides a practical tool to determine and classify molecular symmetry groups. Molecules with a symmetry that is closest to the sphere are *isotropic*, in the sense that there is no unique direction to orient them. The corresponding symmetry groups are the cubic and icosahedral groups.

Breaking spherical symmetry gives rise to symmetry groups based on the cylinder. Cylindrical symmetry splits 3D space into an axial 1D component and an equatorial 2D space, which remains isotropic. Molecules with cylindrical shapes have a unique anisotropy axis, along which they may be oriented in space. Conventionally this direction is denoted as the z-direction. Along this direction they have a principal n-fold rotation or rotation–reflection axis, which is responsible for the remaining in-plane isotropy. Finally, further removal of all $\hat{C}_n$ or $\hat{S}_n$ with $n > 2$ leads to molecules that are completely anisotropic and have at most orthorhombic symmetry, D_{2h}. In this section we will provide a concise overview of the point groups, following a path of descent in symmetry. We thereby refer to the list of point groups presented in the character tables in Appendix A.

Spherical Symmetry and the Platonic Solids

Any plane through the center of a sphere is a reflection plane, and any axis through the center is a rotation axis, as well as a rotation–reflection axis. In addition, the sphere also is centrosymmetric, which means that the center is a point of inversion. The resulting infinite-dimensional symmetry group of the sphere is usually denoted

Table 3.5 The Platonic solids and their point groups. The numbers count the triangles, squares, and pentagons, that intersect in a vertex of the solid

	Triangle	Square	Pentagon
3	Tetrahedron (T_d)	Cube (O_h)	Dodecahedron (I_h)
4	Octahedron (O_h)		
5	Icosahedron (I_h)		

as $O(3)$, which refers to the orthogonal group in three dimensions. This assignment is based on the one-to-one correspondence between the symmetry operations of the sphere and the set of 3×3 orthogonal matrices. This will be explained in more detail in Sect. 7.1. Only isolated atoms exhibit spherical symmetry. Molecular shapes that approximate perfect spherical symmetry are based on the *regular polyhedra*, the building blocks of which are *regular polygons*. These polygons are obtained by distributing n points around a circle in such a way that all points are equivalent, i.e., that the distances between any two neighboring points are the same, implying that the angles subtended by adjacent edges are also the same. In this way the circle may circumscribe an equilateral triangle, a square, a regular pentagon, etc.

In fact, for any integer n with $3 \leq n \leq \infty$, a regular n-gon can be obtained, though not all of them can be drawn by use of a ruler and compass. In 3D things are quite different. Defining regular polyhedra by distributing n points over a sphere in such a way that all vertices, edges, and faces of the resulting structures are the same cannot be realized in infinitely many ways: quite on the contrary, only five solutions are possible.[3] These are known as the Platonic solids, and they are listed in Table 3.5. They played an important role in Pythagorean tradition, as well as in Eastern philosophy and religion. The fact that in 3D only five solutions exist was considered to reveal a fundamental truth about nature, to the extent that Plato, in his *Timaeus*, based his natural philosophy on these solids. The ancient doctrine of the four elements was placed in correspondence with four of the solids. The tetrahedron (or 4-plane), with symmetry T_d, has the most acute angles and was associated with fire. The cube, or hexahedron (6-plane), with symmetry O_h, is clearly the most stable structure and refers to the earth. The icosahedron (20-plane), with symmetry I_h, contains twenty faces and is therefore closest to a globular surface, which symbolizes the most fluid element, water. Both cube and icosahedron have a dual partner, which is obtained by replacing vertices by faces and vice versa. The dual of the cube is the octahedron (8-plane), which figured for air. In Table 3.5, the octahedron is placed between the tetrahedron and the icosahedron, and this seemed appropriate for air because it is intermediate between fire and water in its mobility, sharpness, and ability to penetrate. The dual of the icosahedron is the regular dodecahedron (12-plane). There being only four elements, the discovery of the fifth solid caused some embarrassment, which found an elegant solution by its being assigned to the substance of the

---

[3]The sum of the angles subtended at a vertex of a Platonic solid must be smaller than a full angle of 2π. Hence, no more than five triangles, three squares, or three pentagons can meet in a vertex; regular hexagons are already excluded since the junction of three such hexagons already gives rise to an angle of 2π at the shared vertex.

Fig. 3.5 Genealogical tree
for the cubic and icosahedral
point groups
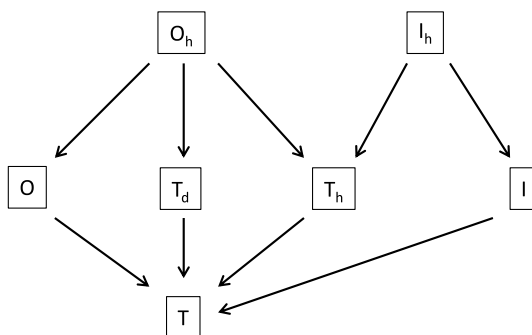
heavens. The dodecahedron and its intriguing symmetry were considered worthy of the stars, with their perfect cosmic order. Besides the three point groups, T_d, O_h, and I_h, represented by the Platonic solids, there are four more groups that belong to the isotropic family: T_h, T, O, and I. They are subgroups of the octahedral and icosahedral groups, as shown in Fig. 3.5.

The Tetrahedron

T_d symmetry (Fig. 3.6(a)) plays a crucial role in chemistry. It is the symmetry of the valence structure of aliphatic carbon. The attribution of this symmetry to carbon by Van't Hoff[4] as early as 1874, i.e., well before the modern concept of molecular structure and some two and a half millennia after Pythagoras, remains a tribute to the Greek vision that the fundamental structure of matter consists of ideal symmetric shapes. The tetrahedron is the most fundamental of the solids since it is the *simplex* of 3D space. A simplex is a figure consisting of vertices that are all equivalent and are equidistant from each other.[5] In an n-dimensional space the simplex contains $n + 1$ vertices, e.g., in 2D Euclidean space exactly three points can be distributed in such a way that they are equidistant, viz., by occupying the vertices of an equilateral triangle. In 3D space only four points can be distributed in such a way that they have this property, the solution being the tetrahedron. The perfect permutational symmetry of the vertices of the n-simplex implies that the corresponding symmetry group is isomorphic to the symmetric group S_n. We have already seen that the triangular symmetry of the hydrogens in ammonia could be described by S_3; in the same way the tetrahedral symmetry group is isomorphic to S_4. The rotational subgroup of T_d is the group T, which, in turn, is isomorphic to the alternating group A_4. An extraordinary member of the tetrahedral family is the group T_h, which has the same

---

[4]Van't Hoff published his findings in 1874 in Utrecht. In the same year, Le Bel came to the same conclusion, based on the investigation of optical rotatory power. An English translation of the original papers of both chemists can be found in: [1].

[5]In graph theory the graph of a simplex with n vertices is the complete n-graph, K_n. In such a graph, each of the n vertices is connected to all the other $(n - 1)$ vertices. There is only one simplex for each dimension.
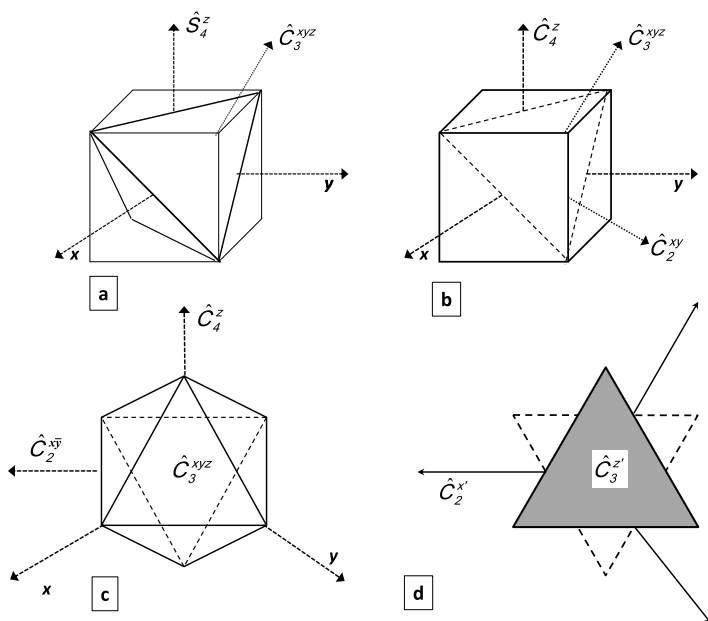
Fig. 3.6 The tetrahedral and octahedral symmetry groups: (**a**) tetrahedron, inscribed in a cube by connecting four alternating corners; (**b**) orientation of the cube based on fourfold axes along the Cartesian directions; $\hat{C}_2^{xy}$ lies along the acute bisector of the x and y directions; the dashed triangle is one face of the inscribed tetrahedron; (**c**) construction drawing of the octahedron in the same fourfold setting; the $\hat{C}_2$ axis shown is the bisector of the positive x and negative y direction; and (**d**) same drawing of the octahedron with a trigonal coordinate orientation: the z' direction is along the $\hat{C}_3$ axis, and the x'-direction is along the bisector of the positive x- and negative y-directions

order as T_d and also contains T as its rotational subgroup. Molecular examples of this group are quite rare and will mostly be encountered as symmetry lowering of cubic or icosahedral molecules (see later, Fig. 3.8).

The Cube and Octahedron

The group O_h contains 48 elements and is the symmetry group of the octahedron and the cube (see Fig. 3.6(b)). The system of Cartesian axes itself has octahedral symmetry, and, as such, this symmetry group is the natural representative of 3D space. It is ubiquitous in ionic crystals, where it corresponds to coordination numbers 6 (as in rock salt, NaCl) or 8 (as in caesium chloride, CsCl). It is also the dominant symmetry group of coordination compounds. The rotational subgroup is the group O with 24 elements. The octahedron provides us with an insight into the basic architecture of polyhedra. There are three structural elements: vertices, edges, and faces. Through each of these runs a rotational symmetry axis: a $\hat{C}_4$ axis through the vertices, a $\hat{C}_2$ axis through the edge, and a $\hat{C}_3$ axis through the face center. In
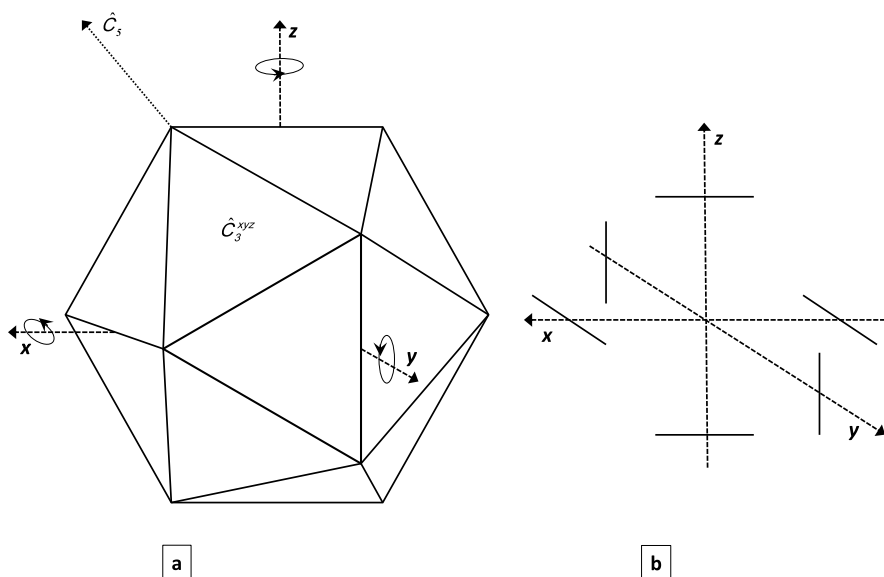
Fig. 3.7 (**a**) Icosahedron in a D_{2h} setting, (**b**) T_h structure based on the icosahedral edges through the Cartesian coordinate axes

a triangular face, the product of the three rotations equals the unit element. For the triangle that is turned toward the viewer in Fig. 3.6(c), this is

$$\hat{C}_2^{xz}\hat{C}_3^{xyz}\hat{C}_4^{z} = \hat{E} \tag{3.32}$$

The symmetry elements are labeled by the indices x, y, and z, which refer to their orientation in the Cartesian coordinate system, e.g., $\hat{C}_3^{xyz}$ indicates the $\hat{C}_3$ axis, which is the diagonal of the positive Cartesian directions. This notation emphasizes that symmetry elements are tied to the coordinate system and stay fixed in space.

The Icosahedron and Dodecahedron

Icosahedral symmetry is less obvious and thus more intriguing than cubic symmetry. Whilst tetrahedral and octahedral molecules were already known before the turn of the nineteenth/twentieth century, the first structural study of an icosahedral molecule was the closo-dodecaborane, $B_{12}H_{12}^{2-}$, in 1960. More examples would follow: in 1984, dodecahedrane, $C_{20}H_{20}$, and then the supermolecule Buckminster-fullerene, C_{60}, which has the shape of a truncated icosahedron [2–4]. Icosahedral structures can be drawn inside a regular hexagon, as shown in Fig. 3.7(a). The coordinate axes in this figure are chosen in such a way that each of the Cartesian directions coincides with a twofold axis. These axes together form a D_{2h} subgroup. This orientation thus corresponds to a D_{2h} setting. Figure 3.7(b) shows the orientation of the edges through the Cartesian directions. When going from one axis to a
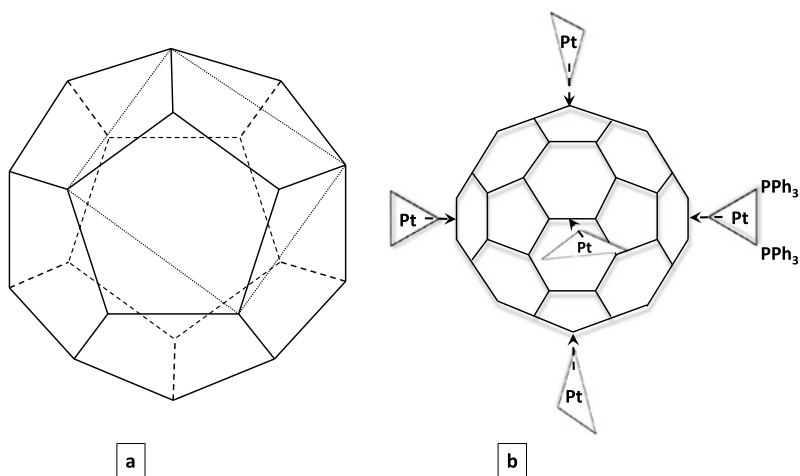
Fig. 3.8 (**a**) Dodecahedron, the square is the top face of an inscribed cube; (**b**) supramolecular complex of C_{60} Buckminsterfullerene with six η^2-platina-bis(triphenyl)phosphine adducts on double bonds adjacent to two hexagons; the adducts adopt a D_{2h} setting and reduce the icosahedral symmetry of the buckyball to T_h

neighboring axis, one always rotates the edges by 90°. In fact, there are two ways to realize this D_{2h} setting either with the top edge in the xz plane, as in Fig. 3.7(b), or in the yz plane [5]. The reason is that the O_h symmetry of the Cartesian frame is not a subgroup of I_h since $|O_h|$ is not a divisor of $|I_h|$. Their highest common subgroup is the 24-element group T_h, as indicated in Fig. 3.5. The structure of the six edges in Fig. 3.7(b) does indeed have T_h symmetry. Note that T_h is a normal subgroup of O_h, but not of I_h. The dual of the icosahedron is the dodecahedron, shown in Fig. 3.8(a). In a dodecahedron, one can select a set of eight vertices that form the corners of a cube. The dashed square in the figure is the top face of such an inscribed cube. Euclid already demonstrated that a cube could be drawn inside a dodecahedron in such a way that its twelve edges each lie in one of the twelve faces of the dodecahedron. In turn, in the center of each of the faces of this cube there lies a dodecahedral edge, which breaks the fourfold symmetry axes of the cube. The stabilizer of the cube inside I_h is the subgroup T_h. The icosahedral group can be partitioned into five cosets of T_h, which can be generated in a cyclic orbit by a pentagonal generator:

$$I_h = \sum_{n=1}^{5} (\hat{C}_5)^n T_h \tag{3.33}$$

Each of the cosets refers to an inscribed cube, exactly as the three C_s cosets in C_{3v} ammonia refer to the three equivalent hydrogen sites. Hence, in a dodecahedron there will be five inscribed cubes. Since the order of the I_h group is 120, which equals 5!, it is tempting to think of this group as isomorphic to S_5, permuting the five inscribed cubes. This, however, is not the case since I_h contains 10-fold

rotation-reflection axes, which are not present in S_5. On the other hand, the rotational subgroup I is indeed isomorphic to the alternating group A_5. The icosahedral rotations act transitively on the set of five cubes. The icosahedron also contains six-fold rotation–reflection axes, $\hat{S}_6$. These symmetry elements act transitively on the set of the six pentagonal directions. C_{60} (Buckminsterfullerene) has perfect I_h symmetry and corresponds to a truncated icosahedron. Bonds that are adjacent to two hexagons have pronounced double-bonding character. Metal fragments can coordinate [6] to these bonds, as shown in Fig. 3.8(b). A hexa-adduct is formed with near T_h symmetry.

Cylindrical Symmetries

Cylinders, Prisms, Antiprisms

The full symmetry group of an ideal cylinder is denoted by $D_{\infty h}$. The D stands for *dihedral*[6] and h for *horizontal*. Like the spherical group, the cylindrical symmetry group is a continuous symmetry group, which has an infinite number of elements. It contains any rotation or rotation–reflection about the z-axis, any $\hat{C}_2$ axis in the equator and any vertical symmetry plane, $\hat{\sigma}_v$. In addition there are four singleton classes, viz. the identity, the $\hat{C}_2^z$ rotation, the unique horizontal symmetry plane, and spatial inversion. Cylindrical symmetry is met only in linear molecules such as homonuclear diatomics. Obviously, in nonlinear molecules the rotational symmetry of the cylinder is replaced by a finite cyclic symmetry. Two shapes are realizations of maximal finite subgroups of the cylinder: prisms and antiprisms with respective symmetries D_{nh} and D_{nd}. In both structures the principal axis is a $\hat{C}_n$ axis, perpendicular to which there are n twofold axes. The horizontal symmetry plane is conserved only in prisms, and not in antiprisms. In Fig. 3.9(a), the staggered configuration in ferrocene exemplifies a pentagonal antiprism, while the eclipsed configuration in ruthenocene is a pentagonal prism. The presence of inversion symmetry depends on the parity of n. It is present only in D_{2nh} prisms and $D_{(2n+1)d}$ antiprisms. The cylindrical symmetries reach their lower limit when the principal rotation axis is twofold. In the D_{2h} case, the equatorial directions are no longer equivalent, and we have a rectangular parallelepiped that is an *orthorhombic* structure with three different and mutually perpendicular directions. By contrast, in the twofold antiprism, with symmetry D_{2d}, we have a scalenohedron that has two directions perpendicular to the z-axis, which are equivalent. In fact, the highest symmetry element in this case is an $\hat{S}_4$ rotation–reflection axis, which is responsible for the equivalence of the

---

[6]Dihedral means literally "having two planes." The dihedral angle is an important molecular descriptor. The dihedral angle of the central B−C bond in an A−B−C−D chain is the angle between the ABC and BCD faces. In the present context, the term dihedral originates from crystallography, such as when two plane faces meet in an apex of a crystal.
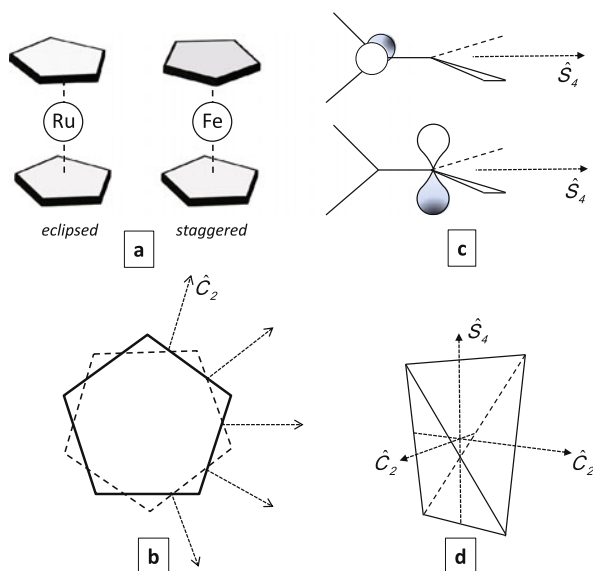
Fig. 3.9 Molecular realizations of cylindrical symmetry: (**a**) D_{5h} ruthenocene in an eclipsed pentagonal prismatic conformation and D_{5d} ferrocene in a staggered pentagonal antiprismatic conformation; (**b**) top view of the pentagonal antiprism with the position of the five twofold axes perpendicular to the pentagonal direction; (**c**) staggered conformation of triplet ethylene with D_{2d} symmetry and horizontal $\hat{S}_4$ axis (in the triplet the two carbon $2p$-orbitals shown are singly occupied); (**d**) alternative view of the D_{2d} symmetry of a bisphenoid, with vertical $\hat{S}_4$ axis

in-plane $\hat{C}_2$ axes. The triplet excited state of ethylene adopts a staggered conformation, which has D_{2d} symmetry (Fig. 3.9(c)). Benzene has prismatic D_{6h} symmetry. In this case, there are two classes of perpendicular twofold axes, which are distinguished in the tables by the labels $\hat{C}_2'$ and $\hat{C}_2''$, and, likewise, two classes of vertical symmetry planes, $\hat{\sigma}_v$ and $\hat{\sigma}_d$. The standard choice for orienting these elements in the hexagonal molecular frame is shown in Fig. 3.10. This choice is conventional and may be changed, but note that the two symmetries are coupled in that the $\hat{\sigma}_v$ planes contain the $\hat{C}_2'$ axes and, similarly, the $\hat{\sigma}_d$ planes contain the $\hat{C}_2''$ axes.

The Rotating Cylinder

Other than geometrical distortions, symmetry breaking of a cylinder may also be realized by a dynamic effect, as in a *rotating cylinder*. In this case, only symmetry elements that will not change the direction of rotation are allowed. As a result, the twofold rotation axes have to be removed, and the cylindrical symmetry is reduced to that of the point group, $C_{\infty h}$. This is the symmetry of an *axial* vector or pseudovector. It corresponds to the spatial symmetry of a magnetic field. Note that this group is abelian, and so are its molecular subgroups, with symmetry C_{nh}. Again, the parity of n is important here. $C_{(2n+1)h}$ groups are cyclic. They have one generator,

Fig. 3.10 Hexagonal D_{6h} symmetry of benzene: Orientation of twofold symmetry elements. $\hat{C}_2'$ and $\hat{\sigma}_v$ pass through opposite atoms; $\hat{C}_2''$ and $\hat{\sigma}_d$ bisect opposite bonds
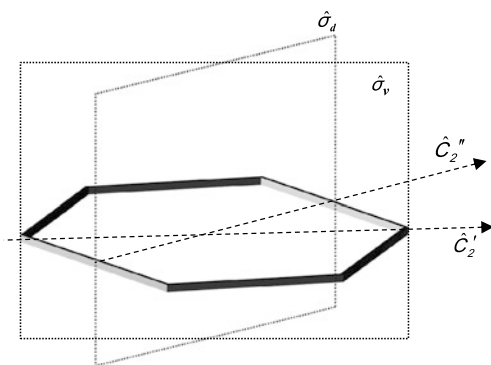
Fig. 3.11 The rotating cylinder has the symmetry of a magnetic field, B, along the cylinder axis. (**a**) shows a tetra-imine macrocycle, with the bridging CH_2 groups below and above the molecular plane; the resulting symmetry group is C_{2h}; (**b**) shows stereographic projections of C_{2h} and S_4
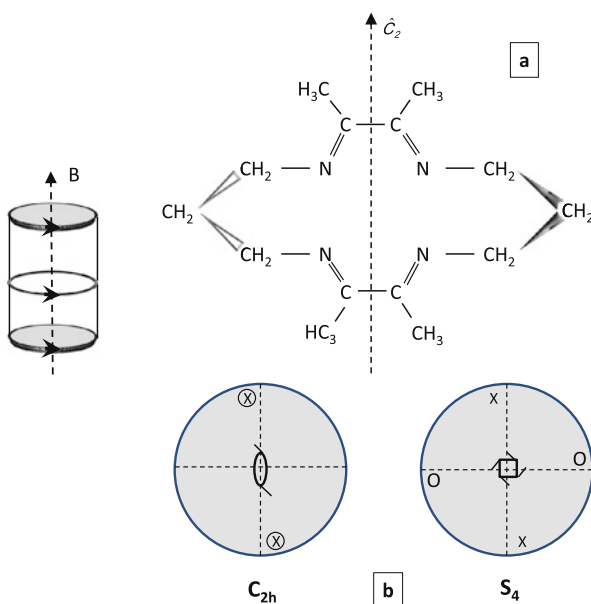
which is a reflection axis, $\hat{S}_{2n+1}$, of order $4n + 2$. For rotations of even order, two kinds of subgroups arise: the C_{2nh} groups and the S_{2n} groups. The latter are not to be confused with the symmetric groups but designate cyclic groups, generated by a $2n$-fold rotation–reflection axis. Figure 3.11 shows the stereographic projections for C_{2h} and S_4, and a molecular realization of C_{2h}. Note that the latter symmetry group is a combination of the three different kinds of binary symmetry elements of the point groups: a twofold rotation, the reflection plane, and the spatial inversion. It reminds us of the famous Euler identity $e^{i\pi} = -1$, which brings together three special numbers: the base of natural logarithms (e), the square-root of -1 (i), and the ratio of the circumference to the diameter of a circle (π).

Fig. 3.12 The twisted cylinder. On the right is a cartoon of the green fluorescent protein (GFP). It adopts a β-barrel structure. Eleven β-sheet strands are wound in a helix around the central fluorophore. The approximate symmetry is D_{11}. In the barrel a cleft is opened to provide interactions with the surrounding solvent
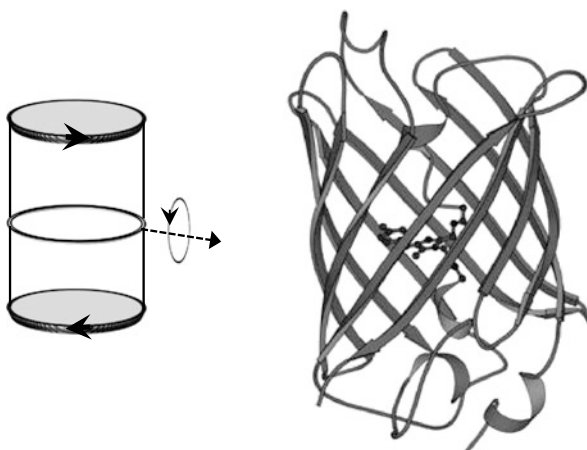
The Twisted Cylinder

An alternative symmetry lowering of the cylinder is attained in the twisted cylinder. Here, all improper symmetry elements are broken, the remaining group being the rotational subgroup, D_∞ (see Fig. 3.12). The twist itself can be in two opposite directions, which are mirror images of each other. Molecules of this type may be formed by applying a twist to prisms or antiprisms. A simple example is ethane. In the eclipsed high-energy conformation this is a prism with D_{3h} symmetry, while in the staggered conformation it is an antiprism, D_{3d}. By rotating the two methyl groups with respect to each other in opposite senses about the threefold axis, we may interconvert these two conformations. In between the two extremal conformations the frame adopts the largest common subgroup, which is D_3.

Cones

A cone can be considered as a deformation of a cylinder, in which the poles of the uniaxial direction are no longer equivalent. The symmetry group is reduced accordingly to $C_{\infty v}$, where only the vertical symmetry planes remain. Conical symmetry is exemplified by hetero-nuclear diatomic molecules, but it is also the symmetry of a *polar* vector, such as a translation in a given direction, or a polarized medium or an electric field, etc. Conical molecules have C_{nv} symmetries, as was the case for the ammonia model. Again, the smallest trivial member of this series is C_{2v}, which is fully anisotropic. This is the point group of the water molecule.

The Rotating Cone

Adding a rotation to the cone will destroy the vertical symmetry planes, since reflection in these planes would alter the sense of the rotation. As a result, only rotations
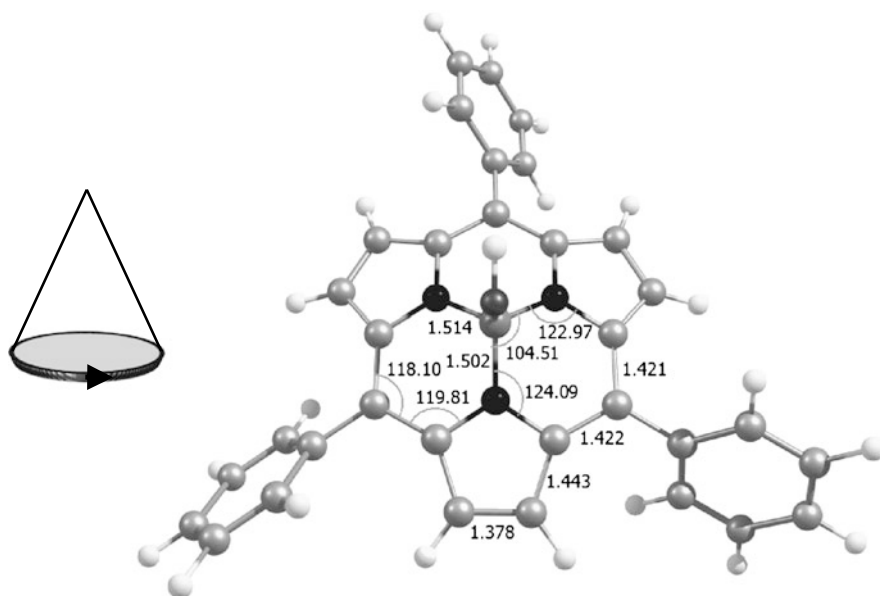
Fig. 3.13 The rotating cone. The molecule is a subporphyrin and consists of a central boron in a tri-pyrrole macrocycle. The subporphyrin itself has the shape of a trigonal dome and exhibits C_{3v} symmetry. Three phenyl substituents at the meso-positions are arranged like a propeller and reduce the symmetry to C_3. A further symmetry lowering to C_1 is caused by an apical hydroxyl substituent at the boron position, with its hydrogen pointing in the direction of the upper phenyl group

around the axis of the cone are retained, limiting the symmetry group to C_∞. Its molecular point groups are the cyclic groups, C_n. These symmetries are encountered in propeller-like molecules. An example of a subporphyrin [7] is shown in Fig. 3.13. The smallest nontrivial C_n group is found for $n = 2$. This is the symmetry of the Möbius strip, which may also be attained in Möbius-type annulenes.

3.8 Rotational Groups and Chiral Molecules

The symmetry operations that we have encountered are either *proper* or *improper*. Proper symmetry elements are rotations, also including the unit element. The improper rotations comprise planes of symmetry, rotation–reflection axes, and spatial inversion. All improper elements can be written as the product of spatial inversion and a proper rotation (see, e.g., Fig. 1.1). The difference between the two kinds of symmetry elements is that proper rotations can be carried out in real space, while improper elements require the inversion of space and thus a mapping of every point onto its antipode. This can only be done in a virtual way by looking at the structure via a mirror. From a mathematical point of view, this difference is manifested

in the sign of the determinant of the corresponding representation matrices in the (x, y, z) basis. For proper rotations, the determinant is equal to $+1$. For improper rotations, it is equal to -1. This minus sign comes from the representation matrix for the inversion centre, which corresponds to minus the unit matrix:

$$\hat{\imath} \begin{pmatrix} x & y & z \end{pmatrix} = \begin{pmatrix} x & y & z \end{pmatrix} \begin{pmatrix} -1 & 0 & 0 \\ 0 & -1 & 0 \\ 0 & 0 & -1 \end{pmatrix} \tag{3.34}$$

Since the determinant of a matrix product is the product of the determinants of the individual matrices, multiplication of proper rotations will yield again a proper rotation, and for this reason, the proper rotations form a rotational group. In contrast, the product of improper rotations will square out the action of the spatial inversion and thus yield a proper rotation. For this reason, improper rotations cannot form a subgroup, only a coset. Since the inversion matrix is proportional to the unit matrix, the result also implies that spatial inversion will commute with all symmetry elements.

In all the point groups with improper rotations, we shall thus always also have a rotational subgroup, like D_n in D_{nd} or D_{nh}, or T in T_d and T_h, etc. Moreover, this rotational subgroup is always a halving subgroup, i.e., its order is half the order of the full group. This can easily be demonstrated. Let H_{rot} be the rotational subgroup of G, and consider an improper symmetry element, $\hat{S}_i$, as coset generator. The coset $\hat{S}_i H_{\text{rot}}$ will contain only improper symmetry elements, and its order will be equal to $|H_{\text{rot}}|$. Now is it possible that the group contains additional improper elements, outside this coset? Suppose that we find such an element, say $\hat{S}_j$. Of course, the product $\hat{S}_i^{-1} \hat{S}_j$ is the combination of two improper elements and thus must be a proper rotation, included in the rotational subgroup. Let us denote this element as $\hat{R}_z$. Hence, it follows that

$$\hat{S}_i \hat{R}_z = \hat{S}_i \hat{S}_i^{-1} \hat{S}_j = \hat{S}_j \tag{3.35}$$

This result confirms that S_j is included in the coset of $\hat{S}_i$ and thus implies that there is only one coset of improper rotations, covering half of the set of symmetry elements.

A group is a *direct product* of two subgroups, H_1 and H_2, if the operations of H_1 commute with the operations of H_2 and every operation of the group can be written uniquely as a product of an operation of H_1 and an operation of H_2. This may be denoted in general as

$$G = H_1 \times H_2 \tag{3.36}$$

This is certainly the case when a group is *centrosymmetric*, i.e., when it contains an inversion centre. Since the inversion operation commutes with all operations, a centrosymmetric group can be written as the direct product $C_i \times H_{\text{rot}}$, where $C_i = \{\hat{E}, \hat{\imath}\}$. However, direct product groups are not limited to centrosymmetry. In the group D_{3h}, for example, the horizontal symmetry plane forms a separate conjugacy class, which means that it commutes with all the operations of the group. It thus

Fig. 3.14 Dimethyl
substituted allene occurs in
two chiral forms, which are
the mirror image of each
other, and cannot be
superimposed; the point
group of each form is C_2
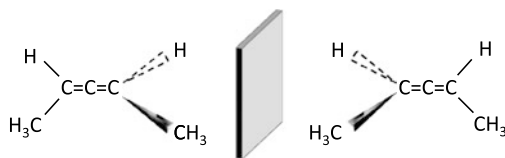
generates a normal C_s subgroup. The full group D_{3h} can then be written as a direct
product of this normal subgroup and the rotational subgroup:

$$D_{3h} = C_s \times D_3 \tag{3.37}$$

When the symmetry of a molecule is a purely rotational group, then the molecule
does not coincide with its mirror image, and there will be two copies of it, which re-
late to each other as do right and left hands. This is illustrated in Fig. 3.14. Molecules
with only rotational symmetry are *chiral*, meaning that the molecule and its reflec-
tion form optical antipodes. A synonym is *enantiomeric*, which literally means: on
both sides of the mirror. By contrast, when a molecular point group contains any
improper symmetry element, the molecule will be congruent to its mirror image
and is *achiral*. Why does the absence of an improper symmetry element prevent the
molecule's coinciding with its mirror image? Congruence operations are whole ro-
tations and/or translations that are performed in order to superimpose the image on
the object. As we have shown, when reflecting a molecule through a mirror, spatial
inversion is implied, and this cannot be undone by rotations or translations, but only
by another improper symmetry element that restores the inversion. Such symmetry
elements are absent in molecules with only rotational point group symmetries, and,
hence, they cannot be made to coincide with their mirror image. Molecular chiral-
ity thus derives from an obvious and basic symmetry characteristic; nonetheless, it
has far reaching physical and chemical consequences. Chiral molecules are opti-
cally active, which means that the plane of polarization of linearly polarized light
is rotated when passing through a medium with chiral molecules. The absorption
coefficients of chiral molecules for left- and right-circularly polarized light are also
different, giving rise to natural circular dichroism (CD) spectra. This will be illus-
trated in Sect. 6.8. The chemical consequences of chirality are of vital importance:
living organisms are based on biochemical molecules with strict chirality.

3.9 Applications: Magnetic and Electric Fields

In many spectroscopic applications external magnetic or electric fields are applied
to a molecular sample. For magnetic fields, the perturbing influence of the field
is known as the Zeeman effect. Electric fields give rise to the Stark effect. As we
have seen, uniform magnetic and electric fields have symmetries $C_{\infty h}$ and $C_{\infty v}$,
respectively. In this case, the symmetry group of the experiment will be constrained
to these operations, which leave the {molecule + field} combination invariant. It

Table 3.6 Symmetries of a tetrahedral molecule in a uniform magnetic (B) or electric (E) field

	$\hat{E}$	$8\hat{C}_3$	$3\hat{C}_2$	$6\hat{S}_4$	$6\hat{\sigma}_d$	$T_d \cap C_{\infty h}$
$B \parallel \hat{S}_4$	$\hat{E}$		$\hat{C}_2$	$2\hat{S}_4$		S_4
$B \parallel \hat{C}_3$	$\hat{E}$	$2\hat{C}_3$				C_3
$B \perp \hat{\sigma}_d$	$\hat{E}$				$\hat{\sigma}_d$	C_s
						$T_d \cap C_{\infty v}$
$E \parallel \hat{S}_4$	$\hat{E}$		$\hat{C}_2$		$2\hat{\sigma}_d$	C_{2v}
$E \parallel \hat{C}_3$	$\hat{E}$	$2\hat{C}_3$			$3\hat{\sigma}_d$	C_{3v}
$E \in \hat{\sigma}_d$	$\hat{E}$				$\hat{\sigma}_d$	C_s

will thus consist only of symmetry elements that are common to both parts. These elements form the *intersection* of both symmetry groups. The elements of an intersection themselves form a group, which is the largest common subgroup of both symmetry groups. This can be written as follows:

$$\text{magnetic field} : H = G \cap C_{\infty h}$$
$$\text{electric field} : H = G \cap C_{\infty v}$$

(3.38)

This intersection group will depend on the orientation of the field in the molecular frame. In Table 3.6 we work out an example of a tetrahedral molecule. The top row lists the symmetry elements of T_d. The fields can be oriented along several directions. The highest symmetry positions are along the fourfold or threefold axes. A lower symmetry position is within or perpendicular to a symmetry plane, or finally along an arbitrary direction with no symmetry at all. In Appendix B we list representative intersection groups for several point groups and orientations. Note that in the case of a magnetic field, the resulting intersection group is always abelian. This is of course a consequence of $C_{\infty h}$ being abelian.

3.10 Problems

3.1 The multiplication table of a set of elements is given below. Does this set form a group?

	A	B	C	D
A	C	D	A	B
B	D	C	B	A
C	A	B	C	D
D	B	A	D	C

3.2 Use molecular ball and stick models to construct examples of molecules that have a reflection plane as the only symmetry element. Similarly, for a center of inversion and for a twofold axis. In each case find the solution with the smallest

number of atoms! Explain your reasoning. What is the smallest molecule with no symmetry at all?

3.3 The 2D analogue of a polyhedron is a polygon. In a regular polygon all vertices, edges, and angles between adjacent edges are identical. A 2D plane can be tessellated in identical regular polygons, which then form a covering of the plane. In how many ways can this be performed?

3.4 Why is the order of a rotational axis of a polyhedral object always an integer?

3.5 Prove that a halving subgroup is always a normal subgroup.

3.6 Determine the point group of a soccer ball, a tennis ball, a basketball, and a trefoil knot.

3.7 The parameter equations defining a helix in Cartesian space are given by

$$x(t) = a \cos\left(\frac{nt}{a}\right)$$

$$y(t) = a \sin\left(\frac{nt}{a}\right)$$

$$z(t) = t$$

Here a is the radius. Is this helix left- or right-handed? Write down the parameterization of its enantiomer. The symmetry of a helix is based on a screw axis, which corresponds to a translation in t. It is composed of a translation along the z-direction with a concomitant rotation in the xy-plane. Now decorate the helix with atoms at points $t_k/a = 2\pi k/m$, where k and m are integers. Determine the screw symmetry of this molecular helix. If n/m is irrational, the helix is *noncommensurate*. Will it still have a symmetry in this case?

References

1. Benfey, O.T. (ed.): Classics in the Theory of Chemical Combination, pp. 151–171. Dover Publications, New York (1963)
2. Wunderlich, J.A., Lipscomb, W.N.: The structure of $B_{12}H_{12}^{2-}$ ion. J. Am. Chem. Soc. **82**, 4427 (1960)

3. Paquette, L.A.: Dodecahedrane—the chemical transliteration of Plato's universe. Proc. Natl. Acad. Sci. USA **79**, 4495 (1982)
4. Kroto, H.W., Heath, J.R., O'Brien, S.C., Curl, R.F., Smalley, R.E.: C_{60} Buckminsterfullerene. Nature **318**, 162 (1985)
5. Boyle, L.L., Schäffer, C.E.: Alternative equivalent icosahedral irreducible tensors. Int. J. Quant. Chem. **8**, 153 (1974)
6. Fagan, P.J., Calabrese, J.C., Malone, B.: The chemical nature of Buckminsterfullerene and the characterization of a platinum derivative. Science **252**, 1160 (1991)
7. Takeuchi, Y., Matsuda, A., Kobayashi, N.: Synthesis and characterization of meso-triarylsubporphyrins. J. Am. Chem. Soc. **129**, 8271 (2007)

Chapter 4
Representations

Abstract Having made acquaintance with the basic properties of groups, we now turn our attention to the structure of the matrices that represent the group action in a function space. It turns out that there exists only a limited set of standard patterns. These are called the irreducible representations. They form the principal mathematical concept on which this monograph is based, and much care is devoted to acquire a gradual understanding of what this concept really means. Then the character theorem, matrix theorems, and projection operators are introduced. The concepts of subduction and induction relate the representations of subgroups and those of their parent groups. The chapter also offers a detailed group-theoretical analysis of three chemical applications: the tetrahedral hybridization of carbon, the molecular vibrations of UF_6, and the electronic structure of conjugated hydrocarbons, according to the Hückel model and the method of the London model of gauge-invariant atomic orbitals.

Contents

4.1 Symmetry-Adapted Linear Combinations of Hydrogen Orbitals in Ammonia

From now on we shall no longer be working with the nuclei, but with electronic orbital functions that are anchored on the nuclei. As an example, we take the $1s$ orbitals on the hydrogen atoms in ammonia. The $|1s_A\rangle$ is defined in Eq. (4.1), where $\mathbf{R}_A$ denotes the position vector of atom A with respect to the Cartesian origin; a_0 is the Bohr radius (0.529 Å), which is the atomic unit of length.

$$|1s_A\rangle = \frac{1}{\sqrt{\pi}} \left(\frac{1}{a_0}\right)^{3/2} \exp\left(-\frac{|\mathbf{r} - \mathbf{R}_A|}{a_0}\right) \tag{4.1}$$

Following Sect. 1.2, the transformation of this function by the threefold axis is given by

$$\hat{C}_3 |1s_A\rangle = \frac{1}{\sqrt{\pi}} \left(\frac{1}{a_0}\right)^{3/2} \exp\left(-\frac{|[\hat{C}_3^{-1}\mathbf{r}] - \mathbf{R}_A|}{a_0}\right) \tag{4.2}$$

The distance between the electron at position $\hat{C}_3^{-1}\mathbf{r}$ and nucleus A is equal to the distance between the electron at position $\mathbf{r}$ and nucleus B. This can be established by working out the distances as functions of the Cartesian coordinates, but a straightforward demonstration is based on the fact that the distance does not change if we rotate *both* nuclei and electrons:

$$\left|[\hat{C}_3^{-1}\mathbf{r}] - \mathbf{R}_A\right| = \hat{\mathcal{Q}}_3 \left|[\hat{C}_3^{-1}\mathbf{r}] - \mathbf{R}_A\right| = \left|[\hat{\mathcal{Q}}_3 \hat{C}_3^{-1}\mathbf{r}] - \hat{\mathcal{Q}}_3 \mathbf{R}_A\right| = |\mathbf{r} - \mathbf{R}_B| \quad (4.3)$$

Here, we have denoted the bodily rotation of the entire molecule as $\hat{\mathcal{Q}}_3$ in order to indicate that its action also involves the nuclei, as opposed to $\hat{C}_3$, which is reserved for electrons. In the expression of Eq. (4.1), $\mathbf{R}_A$ is replaced by $\mathbf{R}_B$, or

$$\hat{C}_3 |1s_A\rangle = |1s_B\rangle \tag{4.4}$$

This confirms the active view, propagated from the beginning, as applied to the functions. We rotate the $|1s_A\rangle$ orbital itself counterclockwise over 120°. The result is equal to the $|1s_B\rangle$ orbital. We now put the three components of the function space together in a row vector:

$$|\mathbf{f}\rangle = \left(|1s_A\rangle \quad |1s_B\rangle \quad |1s_C\rangle\right) \tag{4.5}$$

The action of the operator in the function space now reads as follows:

$$\hat{C}_3 |\mathbf{f}\rangle = |\mathbf{f}\rangle \mathbb{D}(C_3) \tag{4.6}$$

where the representation matrix is given by

$$\mathbb{D}(C_3) = \begin{pmatrix} 0 & 0 & 1 \\ 1 & 0 & 0 \\ 0 & 1 & 0 \end{pmatrix} \tag{4.7}$$

While the function space is clearly invariant, i.e., it transforms into itself under the rotation, the individual components are not: they are mutually permuted. Our objective is to find *symmetry-adapted linear combinations* (SALCs) that are invariant under the operator, except, possibly, for a phase factor. The combinations we are looking for are thus nothing other than eigenfunctions of the symmetry operator, in the same way as solutions of the Schrödinger equation are eigenfunctions of the Hamiltonian. Unlike the Hamiltonian eigenfunctions, however, which will usually consist of linear combinations in an infinite Hilbert space, the present exercise is carried out in a space of three functions only since this space is already closed under the operator. We shall solve this symmetry eigenvalue problem in a purely algebraic way. Let $|\psi_m\rangle$ be a SALC:

$$|\psi_m\rangle = \sum_{X=A,B,C} c_X |1s_X\rangle \tag{4.8}$$

which we shall again write as the product of a row vector and a column vector:

$$|\psi_m\rangle = \left(|1s_A\rangle \quad |1s_B\rangle \quad |1s_C\rangle\right) \begin{pmatrix} c_A \\ c_B \\ c_C \end{pmatrix} \tag{4.9}$$

The transformation of this function is then given by

$$\hat{C}_3|\psi_m\rangle = |\mathbf{f}\rangle \begin{pmatrix} 0 & 0 & 1 \\ 1 & 0 & 0 \\ 0 & 1 & 0 \end{pmatrix} \begin{pmatrix} c_A \\ c_B \\ c_C \end{pmatrix} \tag{4.10}$$

We now require this function to be an eigenfunction of the threefold rotation operator with eigenvalue λ:

$$\hat{C}_3|\psi_m\rangle = \lambda|\psi_m\rangle \tag{4.11}$$

Combining Eqs. (4.10) and (4.11), we see that the function is an eigenfunction if the product of the $\mathbb{D}$ matrix with the column vector of the coefficients returns the coefficient column, multiplied by the eigenvalue λ, i.e.,

$$\begin{pmatrix} 0 & 0 & 1 \\ 1 & 0 & 0 \\ 0 & 1 & 0 \end{pmatrix} \begin{pmatrix} c_A \\ c_B \\ c_C \end{pmatrix} = \lambda \begin{pmatrix} c_A \\ c_B \\ c_C \end{pmatrix} \tag{4.12}$$

This equation can also be rewritten as

$$\begin{pmatrix} -\lambda & 0 & 1 \\ 1 & -\lambda & 0 \\ 0 & 1 & -\lambda \end{pmatrix} \begin{pmatrix} c_A \\ c_B \\ c_C \end{pmatrix} = \mathbf{0} \tag{4.13}$$

Equation (4.13) forms a homogeneous system of equations in the three unknowns. It will have solutions only if the matrix preceding the column vector of the unknowns

has determinant zero. This requirement is written as

$$\left|\mathbb{D}(C_3) - \lambda\mathbb{I}\right| = 0 \tag{4.14}$$

Here, the vertical bars denote the determinant. Equation (4.14) is called the *secular equation*. It has the form of a simple cubic equation in the eigenvalue λ:

$$-\lambda^3 + 1 = 0 \tag{4.15}$$

This equation is the Euler equation. It has three roots:

$$\lambda_m = \exp\left(\frac{2m\pi i}{3}\right) \tag{4.16}$$

where m can take the values $-1, 0, +1$. What we have just performed is a matrix diagonalization of the representation matrix. We obtain at once not one but three eigenvalues. The eigenfunction corresponding to a given root can now be found by introducing this λ value in the system of equations, Eq. (4.13). Since the system is homogeneous, the three unknown coefficients can be determined only up to a constant factor. We find the absolute values of these vector coefficients by invoking a normalization condition that requires the vectors to be of unit length. The simplified normalization condition, neglecting overlap integrals, reads:

$$|c_A|^2 + |c_B|^2 + |c_C|^2 = 1 \tag{4.17}$$

In this way we obtain three SALCs, each characterized by a different eigenvalue for the symmetry operator:

$$|\psi_0\rangle = \frac{1}{\sqrt{3}}\left(|1s_A\rangle + |1s_B\rangle + |1s_C\rangle\right)$$

$$|\psi_{+1}\rangle = \frac{1}{\sqrt{3}}\left(|1s_A\rangle + \bar{\epsilon}|1s_B\rangle + \epsilon|1s_C\rangle\right) \tag{4.18}$$

$$|\psi_{-1}\rangle = \frac{1}{\sqrt{3}}\left(|1s_A\rangle + \epsilon|1s_B\rangle + \bar{\epsilon}|1s_C\rangle\right)$$

where $\epsilon = \exp 2\pi i/3$. The set of corresponding eigenvalues is called the spectrum of the operator. It will be evident that this spectrum consists of the cube roots of 1, since operating with $\hat{C}_3$ three times in succession is equivalent to applying the identity operator:

$$\hat{C}_3^3|\psi_m\rangle = \lambda^3|\psi_m\rangle = \hat{E}|\psi_m\rangle \tag{4.19}$$

For any operator, one can find eigenfunctions by simply diagonalizing the corresponding representation matrix. However, our objective is more ambitious. We want to obtain functions that are not only adapted to a single symmetry element but to the group as a whole. This really amounts to finding SALCs for the set of group generators, since adaptation to the generators implies that the function is adapted to any

combination of generators and, hence, to the whole group. So, in the case of C_{3v}, we have to examine the behavior of the $|\psi_m\rangle$ functions under a vertical symmetry plane as well, say $\hat{\sigma}_1$. This plane will leave $|1s_A\rangle$ unchanged and will interchange $|1s_B\rangle$ and $|1s_C\rangle$. Its effect on the trigonal eigenfunctions is thus given by

$$\hat{\sigma}_1|\psi_0\rangle = |\psi_0\rangle$$
$$\hat{\sigma}_1|\psi_{+1}\rangle = |\psi_{-1}\rangle \qquad (4.20)$$
$$\hat{\sigma}_1|\psi_{-1}\rangle = |\psi_{+1}\rangle$$

What does this result tell us? The SALC $|\psi_0\rangle$ is simultaneously an eigenfunction of both $\hat{C}_3$ and $\hat{\sigma}_1$; hence, it forms in itself a one-dimensional function space that is completely adapted to the full group. This symmetry characteristic will be denoted by the totally symmetric representation A_1. However, the other two SALCs are transformed into each other. We can easily turn them into eigenfunctions of $\hat{\sigma}_1$ and in this way obtain alternative eigenfunctions, one of which is symmetric under reflection and one of which is antisymmetric. These will be labeled as x and y, respectively, since their symmetry under reflection mimics the symmetries of p_x and p_y:

$$|\psi_x\rangle = \frac{1}{\sqrt{2}}\left(|\psi_{+1}\rangle + |\psi_{-1}\rangle\right) = \frac{1}{\sqrt{6}}\left(2|1s_A\rangle - |1s_B\rangle - |1s_C\rangle\right)$$
$$|\psi_y\rangle = \frac{i}{\sqrt{2}}\left(|\psi_{+1}\rangle - |\psi_{-1}\rangle\right) = \frac{1}{\sqrt{2}}\left(|1s_B\rangle - |1s_C\rangle\right) \qquad (4.21)$$

A schematic drawing of these eigenfunctions is shown in Fig. 4.1. The downside of this symmetry adaptation is that it has destroyed the diagonalization along the trigonal axis. Indeed, one has:

$$\hat{C}_3\left(|\psi_x\rangle \quad |\psi_y\rangle\right) = \left(|\psi_x\rangle \quad |\psi_y\rangle\right)\begin{pmatrix} \cos(2\pi/3) & -\sin(2\pi/3) \\ \sin(2\pi/3) & \cos(2\pi/3) \end{pmatrix} \qquad (4.22)$$

Hence, it is impossible to resolve the function space formed by $|\psi_{\pm1}\rangle$ into simultaneous eigenfunctions of both generators. The action of the symmetry group ties these functions together into a two-dimensional space, which is thus *irreducible*. This symmetry characteristic is denoted by the degenerate irreducible representation E. We have learned form this simple example the following. The construction of SALCs of a symmetry group is based on simultaneous diagonalization of the representation matrices of the group generators. This will resolve the function space into separate blocks, which may consist of one function, or which may form a subspace that cannot be further reduced. The results are functions that transform as irreducible representations (irreps). Why is such a resolution important? The irreducible subspaces into which the function space has been separated are invariant under the actions of the actual symmetry group. This means that there are no operators that send SALCs from one irreducible subspace into SALCs from another irreducible subspace. This also implies that the eigenenergies associated with these

Fig. 4.1 Hydrogen SALCs in ammonia. The size of the circles is proportional to the eigenfunction coefficients. $|\psi_0\rangle$ transforms as the totally symmetric irrep A_1; $|\psi_x\rangle$ and $|\psi_y\rangle$ are components of the degenerate E representation
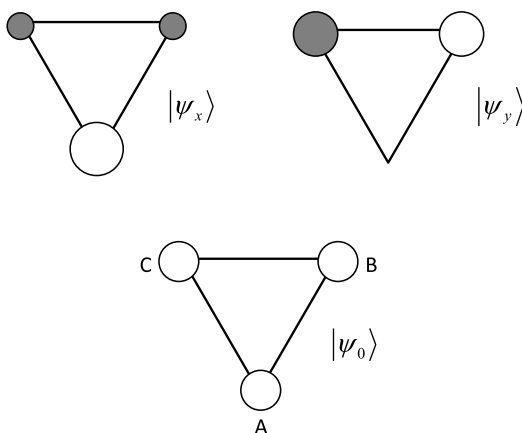
irreducible blocks are not be related. We will return to this in much more detail in Sect. 5.2. The algebraic treatment also provides an insight into the meaning of degeneracy. The two components of the E irrep are locked in the same function space because it is not possible to diagonalize the representation matrices for both generators simultaneously. If two operators commute, it is always possible to find solutions that are simultaneous eigenfunctions of both. However, the two generators of C_{3v} do not commute as this group is not abelian. The fact that the corresponding representation matrices also do not commute explains why it is impossible to block-diagonalize the E irrep.

4.2 Character Theorems

When examining a function space from a symmetry point of view, we note that there are two basic questions to be asked:

1. What are the symmetry ingredients of the function space; in other words, which irreps describe the symmetry of this space?
2. What do the corresponding SALCs look like?

The present section on characters deals with the first question and provides an elegant description of the symmetries of function spaces. In the subsequent sections, matrix theorems are used for the construction of projection operators that will carry out the job of obtaining the suitable SALCs. The intuitive algebraic approach that we have demonstrated in the previous section has been formalized by Schur, Frobenius,[1] and others into a fully fledged character theory, which reveals which irreps

---

[1]The papers by Schur and Frobenius have been edited as C. Frobenius, The Collected Works of Frobenius (1849–1917), J.-P. Serre (ed.), Springer, Berlin (1968), 3 vols.; I. Schur, Gesammelte Abhandlungen, A. Brauer and H. Rohrbach (eds.) Springer, Berlin (1973), 3 vols.

a given group can sustain and how to analyze the irreducible contents of a given function space. Characters are nothing other than the traces (that is, the sum of the diagonal elements) of representation matrices. They will be represented as $\chi(R)$:

$$\chi(R) = \sum_i D_{ii}(R) \tag{4.23}$$

If the functional basis of a representation is transformed by a unitary transformation, the trace does not change, as can easily be demonstrated. Define $|\mathbf{f}'\rangle = |\mathbf{f}\rangle \mathbb{U}$. Then the corresponding representation matrices, $\mathbb{D}'(R)$, also undergo a unitary transformation:

$$
\begin{aligned}
\hat{R}|\mathbf{f}'\rangle = \hat{R}|\mathbf{f}\rangle \mathbb{U} &= |\mathbf{f}\rangle \mathbb{D}(R)\mathbb{U} \\
&= |\mathbf{f}'\rangle \mathbb{U}^{-1}\mathbb{D}(R)\mathbb{U} \\
&= |\mathbf{f}'\rangle \mathbb{D}'(R)
\end{aligned} \tag{4.24}
$$

from which it follows that

$$\mathbb{D}'(R) = \mathbb{U}^{-1}\mathbb{D}(R)\mathbb{U} \tag{4.25}$$

or, for unitary $\mathbb{U}$, that

$$
\begin{aligned}
D'_{ij}(R) &= \sum_{kl} \bar{U}^T_{ik} D_{kl}(R) U_{lj} \\
&= \sum_{kl} \bar{U}_{ki} D_{kl}(R) U_{lj}
\end{aligned} \tag{4.26}
$$

The invariance of the character then follows from the orthogonality of the rows of the unitary matrix:

$$
\begin{aligned}
\chi'(R) &= \sum_i D'_{ii}(R) \\
&= \sum_{kl} D_{kl}\left(\sum_i \bar{U}_{ki} U_{li}\right) \\
&= \sum_{kl} D_{kl}(R)\delta_{kl} \\
&= \sum_k D_{kk}(R) \\
&= \chi(R)
\end{aligned} \tag{4.27}
$$

Hence, sets of characters literally characterize representations since they are immune to the effects of unitary transformations, such as occur in Eq. (4.21) between the complex functions $|\psi_{+1}\rangle$, $|\psi_{-1}\rangle$ and the real functions $|\psi_x\rangle$, $|\psi_y\rangle$. The characters for the irreps are brought together in a character table. Here, the conjugacy class

Table 4.1 Character table for
the group C_{3v} and reducible
characters of the hydrogen $1s$
functions $\chi(1s)$ and
hydrogen bends $\chi(\Delta\phi)$. The
$\chi(1s)$ row is equal to the sum
of the A_1 and E rows, and the
$\chi(\Delta\phi)$ row is equal to the
sum of the A_2 and E rows

C_{3v}	$\hat{E}$	$2\hat{C}_3$	$3\hat{\sigma}_v$	$\langle\chi\mid\chi\rangle$
A_1	1	1	1	6
A_2	1	1	-1	6
E	2	-1	0	6
$\chi(1s)$	3	0	1	12
$\chi(\Delta\phi)$	3	0	-1	12

concept comes in very useful. Indeed, since all elements belonging to the same class
are similarity transforms, their representation matrices are unitary transforms and,
hence, all have the same character. We can thus group elements together in classes.
In Table 4.1 we show the character table for C_{3v} as can be obtained by algebraic
techniques such as the one we used in the previous section. We recognize at once
the characters for the totally symmetric A_1 and the twofold-degenerate E irrep. In
addition, there is another one-dimensional irrep, A_2, which is symmetric under the
threefold axis and antisymmetric under the reflection planes.

Let us denote an irrep as Γ_i and the string of characters, arranged in a row over
the full group, in a Dirac form as $|\chi^{\Gamma_i}\rangle$. The norm of this string[2] will then be denoted
as a bracket, i.e.,

$$\langle\chi^{\Gamma_i}\mid\chi^{\Gamma_i}\rangle = \sum_{R\in G}\bar{\chi}^{\Gamma_i}(R)\chi^{\Gamma_i}(R) \tag{4.28}$$

Since the matrices are unitary, we could also replace the complex-conjugate char-
acter by the character of the inverse element:

$$\bar{\chi}^{\Gamma_i}(R) = \chi^{\Gamma_i}(R^{-1}) \tag{4.29}$$

The character strings obey the following character theorem:

Theorem 4 *The norm of the character string is equal to the order of the group if
and only if the characters refer to an irreducible representation. The scalar product
of two character strings of different irreps is equal to zero.*

This theorem can be expressed as follows:

$$\langle\chi^{\Gamma_i}\mid\chi^{\Gamma_j}\rangle = \sum_{R\in G}\bar{\chi}^{\Gamma_i}(R)\chi^{\Gamma_j}(R) = \delta_{ij}|G| \tag{4.30}$$

where Γ_i and Γ_j refer to irreducible representations, and $|G|$ is the order of the
group. This theorem provides an elegant and simple solution for determining the ir-

---

[2]Since elements in the same class have the same character, we can also simplify the expression to
a summation over all classes, provided that we then multiply each term by the number of elements
in the class under consideration.

Fig. 4.2 Symmetry coordinates for the in-plane bending of the hydrogen atoms in ammonia. The length of *the arrows* is proportional to the SALC coefficients
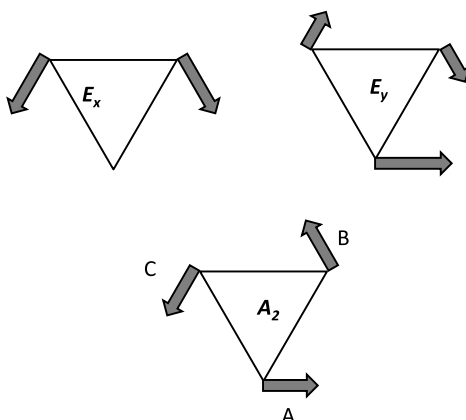
rep content of a function space. One first determines the characters of the representation matrices, $\chi(R)$. They will be equal to the sums of the traces of the individual irreducible symmetry blocks. This can be expressed as follows:

$$\chi(R) = \sum_i c_i \chi^{\Gamma_i}(R) \tag{4.31}$$

Here, the important quantities are the c_i coefficients. These are integers that tell how many times a given irrep Γ_i is contained in the function space. They can easily be calculated by using the character theorems. All one has to do is to evaluate the scalar product of a given irreducible character, say Γ_k, and the reducible character, and then divide by the group order.

$$\frac{1}{|G|}\langle \chi^{\Gamma_k}|\chi\rangle = \frac{1}{|G|}\sum_i c_i \langle \chi^{\Gamma_k}|\chi^{\Gamma_i}\rangle = \sum_i c_i \delta_{ki} = c_k \tag{4.32}$$

It is also clear that the norm of the reducible character is a multiple of the group order, since

$$\langle \chi|\chi\rangle = \sum_{ij} c_i c_j \langle \chi^{\Gamma_i}|\chi^{\Gamma_j}\rangle = \sum_i c_i^2 |G| \tag{4.33}$$

This procedure may seem quite complicated, but it is in fact very simple. Let us demonstrate this for the previous example, the set of the three $1s$-orbitals on the hydrogens in NH_3. We first determine the reducible character of this set (see $\chi(1s)$ in Table 4.1). We do not have to do this for all six elements of C_{3v} but only for one representative of each class since conjugate elements have the same characters. For the unit element, the representation matrix is of course the 3×3 unit matrix, and its trace is equal to three, the dimension of the set. For the other elements, we do not need to know the full matrix representation; indeed, *we need only the elements on the diagonal*. Now a diagonal entry in a representation matrix can differ from zero only if a component function is turned into itself, or at least into a fraction of itself.

The threefold axis moves all three $1s$-orbitals around and hence has zeros only on the diagonal; thus, $\chi(C_3) = 0$ (see Eq. (4.7)). For the reflection planes, one element is stabilized, while the other two are interchanged; hence, there is only one nonzero diagonal element, which will be equal to $+1$ since the orbital is not affected; hence, $\chi(\sigma_1) = +1$. The norm of the character string is given by

$$\langle \chi | \chi \rangle = 3^2 + 2 \times 0 + 3 \times 1^2 = 12 = 2|C_{3v}| \tag{4.34}$$

Since the norm is twice the order of the group, we know for certain that the symmetry of the function space is reducible. In fact, we also predict that it will reduce to two irreps, each of which occurs once, since the sum of the squares of the multiplicities in Eq. (4.33) is equal to 2. These coefficients can now be obtained by calculating the character brackets, which yields the previous result: $c_{A_1} = 1, c_{A_2} = 0, c_E = 1$. From Table 4.1 one can also verify that the sum of χ^{A_1} and χ^E equals $\chi(1s)$. This is sometimes also expressed in a formal way as

$$\Gamma = A_1 + E \tag{4.35}$$

As a further example, we can take the set of the two in-plane $2p$-orbitals on nitrogen, p_x and p_y. Here, the character for the threefold axis is

$$\chi^{p_x, p_y}(C_3) = 2\cos(2\pi i/3) = -1 \tag{4.36}$$

Under the $\hat{\sigma}_1$ plane of symmetry, one of the orbitals is antisymmetric, while the other is symmetric, and so the trace of the matrix vanishes. The characters of this p-set are thus precisely the ones for the E irrep, and we can therefore state that the set $\{p_x, p_y\}$ transforms irreducibly as the E representation. As a final example, let us take the alternative set consisting of three counterclockwise displacement vectors of the hydrogen atoms, along a tangent to the (imagined) circumscribed circle through the hydrogens, as indicated in Fig. 4.2. In this example the function space is the set of three bendings: $\Delta\phi_A, \Delta\phi_B, \Delta\phi_C$. We must realize that in this case the function on which we are operating is actually the distortion itself, and to rotate this distortion in an active sense means to take the distortion vector and displace it to the next nucleus. Hence, nuclei are left immobile: only the distortions are moved. One could easily reconcile this view with the previous orbital rotations by thinking of the distortions as little tangent p-orbitals with positive and negative lobes corresponding to the head and tail of the vectors, respectively. Hence, as an example, one has

$$\hat{C}_3 \Delta\phi_A = \Delta\phi_B \tag{4.37}$$

Since all distortions are cyclically permuted, the character under this generator is zero. On the other hand, for the reflection plane, one has:

$$\begin{aligned}
\hat{\sigma}_1 \Delta\phi_A &= -\Delta\phi_A \\
\hat{\sigma}_1 \Delta\phi_B &= -\Delta\phi_C \\
\hat{\sigma}_1 \Delta\phi_C &= -\Delta\phi_B
\end{aligned} \tag{4.38}$$

In this case, the only contribution to the trace comes from the distortion of A, which is mapped onto minus itself; hence, $\chi(\sigma_1) = -1$. The resulting character string also has norm 12, but in this case it decomposes into $A_2 + E$. As shown in Fig. 4.2, the A_2 component is the sum of the three distortions, which corresponds to a bodily rotation of the molecule around its vertical axis. The E components are given by

$$Q_{E_x} = \frac{1}{\sqrt{2}}(\Delta\phi_C - \Delta\phi_B)$$

$$Q_{E_y} = \frac{1}{\sqrt{6}}(2\Delta\phi_A - \Delta\phi_B - \Delta\phi_C)$$

(4.39)

Perhaps the most surprising result is that the symmetry eigenfunctions of the C_{3v} group can be only of three different types: A_1, A_2, and E. In fact, this is another result derived by Schur.

Theorem 5 *The number of irreps in a group is equal to the number of conjugacy classes.*

The fact that there are only a few canonical ways of representing a symmetry group can be rationalized in a general way as follows. Consider a molecule with symmetry group G and a function that is localized on an arbitrary point in the molecule, i.e., a point which is lying neither on an axis of symmetry, nor in a reflection plane, nor in the inversion center or the center of a rotation–reflection axis. We shall denote this function as $|f_E\rangle$ since it is stabilized by, and only by, the unit element. Any other element would move this function to some other point that is a copy of the original one. We write this as

$$\hat{R}|f_E\rangle = |f_R\rangle \qquad (4.40)$$

In this way the entire group generates a set of $|G|$ functions, which all are different. Indeed, suppose that, for $\hat{R} \neq \hat{S}$, the two corresponding functions are the same; then the product operation $\hat{S}^{-1}\hat{R}$ maps $|f_E\rangle$ onto itself. This contradicts the assumption that $|f_E\rangle$ is stabilized only by the unit element. Furthermore, the closure of the group also guarantees that this set of functions forms an invariant function space. This function space transforms according to a reducible representation, which is called the *regular* representation, Γ_{reg}. This representation describes the most general function basis that one can consider since it is based on functions that have no symmetry whatsoever. Now let us determine the symmetry ingredients of this space using the standard character procedure. The character of the regular representation is equal to $|G|$ for the unit element and zero for all other elements since none of the functions is stabilized:

$$\chi^{\Gamma_{reg}}(R) = |G|\delta_{ER} \qquad (4.41)$$

Inserting this result into the expression for the multiplicity coefficients yields

$$c_k = \frac{1}{|G|}\langle\chi^{\Gamma_k}|\chi^{\Gamma_{reg}}\rangle = \bar{\chi}^{\Gamma_k}(E) = \dim(\Gamma_k) \qquad (4.42)$$

Hence, every irrep occurs as many times as its own dimension. The sum of all these irreducible blocks must yield the regular representation. Thus one has

$$\sum_k c_k \dim(\Gamma_k) = \sum_k \left[\dim(\Gamma_k)\right]^2 = |G| \tag{4.43}$$

This result tells us that, in a group of order $|G|$, there are exactly $|G|$ independent vectors. Rewriting these vectors in the form of SALCs exhausts all possible symmetries that can be realized in this group. If a group is abelian, every class is a singleton, and hence the number of classes is equal to the order of the group. In this case, Eq. (4.43) can be fulfilled only if all irreps are one-dimensional. Hence, in an abelian group all irreps are one-dimensional.

4.3 Character Tables

In Appendix A, we reproduce the character tables for the point groups and the symmetric groups, following the standard form introduced by Mulliken [1]. The top row of the table lists the conjugacy classes. In some cases the designations of the symmetry operations can be ambiguous, and additional labels are added, such as h, v, and d for *horizontal*, *vertical*, and *dihedral*, respectively (see also, e.g., Fig. 3.10). In the final columns of the tables we list some simple functions, which transform according to the corresponding irreps. Irreps are denoted by letters that are related to their degeneracy. A and B stand for one-dimensional irreps, which are symmetric or antisymmetric with respect to some principal symmetry element. E and T are used for two- and three-dimensional irreps, respectively. Sometimes, in physics textbooks, T is replaced by F. This alphabetical order is then continued for the fourfold- and fivefold-degenerate irreps in the icosahedral symmetry, which are denoted as G and H. Further subscripts are added to distinguish symmetry characteristics with respect to secondary symmetry elements. Best known are the g and u subscripts, which distinguish between even (*gerade*) and odd (*ungerade*) symmetries with respect to spatial inversion. Primes or double primes are used to distinguish symmetric versus antisymmetric behavior with respect to a horizontal symmetry plane in groups such as $D_{(2n+1)h}$ or $C_{(2n+1)h}$. In addition, numerical indices can appear as subscripts, such as in A_1, A_2 in the C_{3v} group. It should be clear that this labeling is somewhat ad hoc, and one should consult the actual tables in order to find out the precise meaning of the symbols used.

Some point groups, viz. the cyclic groups C_n, $C_{(2n+1)h}$, S_{2n}, and also T and T_h, have irreps with complex characters. In these cases, for an irrep Γ_k with complex characters, there will always be a complementary irrep with a complex-conjugate character string, which is denoted as $\bar{\Gamma}_k$. Hence, one has

$$\chi^{\bar{\Gamma}_k}(R) = \bar{\chi}^{\Gamma_k}(R) \tag{4.44}$$

Note that if Γ_k fulfills the character theorems, then $\bar{\Gamma}_k$ also does, and hence it, too, must be irreducible. The two irreps are said to be complex conjugates. They are orthogonal to each other, and hence there is no point group operation that can turn a function belonging to Γ_k into a function belonging to $\bar{\Gamma}_k$. For this reason, we also should denote them by two separate labels. However, in the absence of external magnetic fields, symmetry is not restricted to spatial symmetry, but also includes time-reversal symmetry. As we have seen in Sect. 2.4, this symmetry will precisely turn functions into their complex conjugates and thus also interchange the corresponding conjugate irreps. Complex-conjugate irreps thus remain degenerate under time reversal, and for this reason, they are usually indicated by means of a brace.

4.4 Matrix Theorem

Determining the symmetry contents of a function space is only a first step. We would also like to know what are the SALCs that correspond to the different irreps. To carry out this task, we have to work with the representation matrices themselves. In the group C_{3v} the matrices for the one-dimensional irreps A_1 and A_2 are trivial since these are simply equal to the corresponding characters. For the E irrep, we need to determine the generator matrices and perform the proper multiplications in order to generate all $\mathbb{D}^E(R)$ for the whole group. These matrices are already available from Table 3.2 for the standard basis of the p_x and p_y orbitals. An important theorem, known as the *Great Orthogonality Theorem* (GOT), is due to Schur.

Theorem 6 *Let Ω and Ω' be two irreducible representations of a group G, and consider vectors formed by taking elements $\{ij\}$ and $\{kl\}$ from the respective representation matrices for every element of the group. Then these vectors are orthogonal to each other, and their squared norm is equal to the order of the group, divided by the dimension of the irrep*:

$$\sum_{R \in G} \bar{D}_{ij}^{\Omega}(R) D_{kl}^{\Omega'}(R) = \frac{|G|}{\dim(\Omega)} \delta_{\Omega,\Omega'} \delta_{ik} \delta_{jl} \qquad (4.45)$$

The theorem thus proceeds as follows: take a given entry ij in the representation matrix of the irrep Ω for every R and order these elements to form a vector of length $|G|$. Do the same with another entry, kl, for a different representation, Ω', and also arrange these to form a vector. Then take the scalar product of these two vectors, bearing in mind that, in this process, the complex conjugate of one of them should be taken (it does not matter which one since the scalar product is always real). The theorem states that this scalar product is zero unless the same irrep is taken, and in this irrep the same row and column index are selected. In that case, the scalar product yields the norm of the vector equal to $|G|/\dim(\Omega)$.

Let us apply this to C_{3v}. For this group, the total number of $\{\Omega, i, j\}$ combinations that can be formed according to the GOT procedure is equal to 6. These

Table 4.2 Complete set of matrix element strings for the group C_{3v}

C_{3v}	$\hat{E}$	$\hat{C}_3$	$\hat{C}_3^2$	$\hat{\sigma}_1$	$\hat{\sigma}_2$	$\hat{\sigma}_3$	$\langle D_{ij}^{\Omega}|D_{ij}^{\Omega}\rangle$
A_1	1	1	1	1	1	1	6
A_2	1	1	1	-1	-1	-1	6
E_{11}	1	$-\frac{1}{2}$	$-\frac{1}{2}$	1	$-\frac{1}{2}$	$-\frac{1}{2}$	3
E_{21}	0	$+\frac{\sqrt{3}}{2}$	$-\frac{\sqrt{3}}{2}$	0	$-\frac{\sqrt{3}}{2}$	$+\frac{\sqrt{3}}{2}$	3
E_{12}	0	$-\frac{\sqrt{3}}{2}$	$+\frac{\sqrt{3}}{2}$	0	$-\frac{\sqrt{3}}{2}$	$+\frac{\sqrt{3}}{2}$	3
E_{22}	1	$-\frac{1}{2}$	$-\frac{1}{2}$	-1	$+\frac{1}{2}$	$+\frac{1}{2}$	3

are listed in Table 4.2, based on the matrices in Table 3.2. In general, this number is always equal to the order of the group since, for every irrep, the number of $\{i, j\}$ combinations is equal to the squared dimension of that irrep, and, according to Eq. (4.43), the sum of these squares is equal to $|G|$. The strings in Table 4.2 thus form a set of six linearly independent vectors. This is in accord with our earlier finding that the set of arbitrary functions that form the most general function space for a group has dimension $|G|$. The GOT thus offers the complete list of coefficients from which SALCs may be constructed. How this can be done is shown in the next section. Note that the trace theorem in the previous section is a direct consequence of the GOT that is obtained by taking diagonal matrix entries ii and kk and summing over i and k:

$$
\begin{aligned}
\langle \chi^{\Omega}|\chi^{\Omega'}\rangle &= \sum_{i,k}\sum_{R\in G} \bar{D}_{ii}^{\Omega}(R)D_{kk}^{\Omega'}(R) \\
&= \frac{|G|}{\dim(\Omega)}\delta_{\Omega,\Omega'}\sum_{ik}\delta_{ik} \\
&= \frac{|G|}{\dim(\Omega)}\delta_{\Omega,\Omega'}\dim(\Omega) \\
&= \delta_{\Omega,\Omega'}|G|
\end{aligned}
\tag{4.46}
$$

4.5 Projection Operators

We recapitulate what we have so far: a group G has been identified, and a function space $|\mathbf{f}\rangle$ was constructed, which is invariant under the action of the group. Next, the characters were determined for each conjugacy class and arranged in a character string, $|\chi\rangle$, which was mapped onto the irreducible characters in the table. Nonzero brackets determined which irreps are present in the function space. Now, the final step is to carry out the actual symmetry adaptation and to obtain the resulting SALCs, say $|\Phi_i^{\Omega}\rangle$. The SALCs are characterized by two indices: the

upper index, Ω, which stands for the irrep, and the lower index, i. The latter index is sometimes called the subrepresentation and also contains a specific piece of information. It determines the component of the irrep, i.e., it refers to a particular column in the irreducible representation matrix that describes the transformation of this component:

$$\hat{R}|\Phi_i^{\Omega}\rangle = \sum_j |\Phi_j^{\Omega}\rangle D_{ji}^{\Omega}(R) \tag{4.47}$$

This symbol of course makes sense only if we do not limit ourselves to the characters, but also determine the representation matrices for all nondegenerate irreps of the group. These will depend on the choice of a particular canonical basis set. Tabular material containing suitable sets of irrep matrices is rather sparse. Some standard choices are provided in Appendix C. Now we construct the projector $\hat{P}$ based on the available matrices:

$$\hat{P}_{kl}^{\Omega'} = \frac{\dim(\Omega')}{|G|} \sum_{R \in G} \bar{D}_{kl}^{\Omega'}(R)\hat{R} \tag{4.48}$$

Let us apply this projector to the SALC $|\Phi_i^{\Omega}\rangle$. This requires the combination of Eqs. (4.47) and (4.48) and exploits the full GOT potential:

$$\begin{aligned}
\hat{P}_{kl}^{\Omega'}|\Phi_i^{\Omega}\rangle &= \frac{\dim(\Omega')}{|G|} \sum_{R \in G} \sum_j \bar{D}_{kl}^{\Omega'}(R) D_{ji}^{\Omega}(R)|\Phi_j^{\Omega}\rangle \\
&= \sum_j \delta_{\Omega',\Omega}\delta_{kj}\delta_{li}|\Phi_j^{\Omega}\rangle \\
&= |\Phi_k^{\Omega'}\rangle\delta_{\Omega',\Omega}\delta_{li} \tag{4.49}
\end{aligned}$$

The action of the projector entails a twofold selection, both at the level of the representation and of the subrepresentation, indicated by the two Kronecker deltas. First, it compares the irreps of the operator and of the SALC. If they do not match, then the SALC is simply destroyed. Second, the δ_{li} selection rule comes into play—under the "protection," as it were, of the first Kronecker delta, which assures that the second selection rule will matter only when we are already inside the same irrep. This second rule compares index l of the projection operator with index i of the target, and annihilates the target unless they are the same; it therefore selectively picks out the SALC that transforms exactly as the lth component of the Ω' irrep. Third, instead of delivering as result this particular component, the projector also has a built-in ability to act as a ladder operator and turn the lth component so obtained into a kth component. If we do not want this ladder aspect, we simply use the diagonal projection operator with $k = l$. Let us illustrate this for the Q_{Ex} hydrogen bending mode in Fig. 4.2. If we want to obtain from this the Q_{Ey} component, we should use a projection operator that recognizes the x and replaces it by y; hence, it must belong to the E irrep, its row index should be 2, and its column index 1. This

indeed generates the y component of Eq. (4.39):

$$
\begin{aligned}
\hat{P}_{21}^E Q_{E_x} &= \frac{1}{3}\frac{\sqrt{3}}{2}\big[\hat{C}_3 - \hat{C}_3^2 - \hat{\sigma}_2 + \hat{\sigma}_3\big]\frac{1}{\sqrt{2}}(\Delta\phi_C - \Delta\phi_B) \\
&= \frac{1}{2\sqrt{6}}\big[(\Delta\phi_A - \Delta\phi_C) - (\Delta\phi_B - \Delta\phi_A) \\
&\quad - (-\Delta\phi_A + \Delta\phi_B) + (-\Delta\phi_C + \Delta\phi_A)\big] \\
&= \frac{1}{\sqrt{6}}(2\Delta\phi_A - \Delta\phi_B - \Delta\phi_C) \\
&= Q_{E_y} \tag{4.50}
\end{aligned}
$$

For a given irrep, the number of projectors that can be constructed is equal to the number of all possible $\{k,l\}$ combinations, which equals $\dim(\Omega')^2$. By varying the row index, k, one can obtain all the components of the invariance space of a given irrep. This is demonstrated by acting on the operators with an element $\hat{S}$:

$$
\begin{aligned}
\hat{S}\hat{P}_{kl}^{\Omega'} &= \frac{\dim(\Omega')}{|G|}\sum_{R\in G}\sum_{j}\bar{D}_{kl}^{\Omega'}(R)\hat{S}\hat{R} \\
&= \frac{\dim(\Omega')}{|G|}\sum_{T\in G}\bar{D}_{kl}^{\Omega'}(S^{-1}T)\hat{T} \\
&= \frac{\dim(\Omega')}{|G|}\sum_{T\in G}\Big(\sum_m \bar{D}_{km}^{\Omega'}(S^{-1})\bar{D}_{ml}^{\Omega'}(T)\Big)\hat{T} \\
&= \frac{\dim(\Omega')}{|G|}\sum_m D_{mk}^{\Omega'}(S)\Big(\sum_{T\in G}\bar{D}_{ml}^{\Omega'}(T)\hat{T}\Big) \\
&= \sum_m D_{mk}^{\Omega'}(S)\hat{P}_{ml}^{\Omega'} \tag{4.51}
\end{aligned}
$$

In this derivation we have used the substitution $\hat{S}\hat{R} = \hat{T}$. The result shows that the set of projectors with fixed index l forms a complete basis set for the Ω' irrep. On the other hand, by changing the column index l we have access to different sets of SALCs with the same symmetry. This applies only when the function space has multiplicities, c_Γ, greater than one. This can be illustrated for the $\{|f_R\rangle\}$ function space transforming as the regular representation that has the maximal degree of freedom. Two projectors with the same k index, but different l indices, will project out two functions that are linearly independent, as the following overlap calculation shows:

$$
\begin{aligned}
\big\langle \hat{P}_{kl}^{\Omega} f_E \big| \hat{P}_{kl'}^{\Omega} f_E \big\rangle &= \frac{\dim(\Omega)^2}{|G|^2}\Big\langle \sum_R \bar{D}_{kl}^{\Omega}(R)\hat{R}f_E \Big| \sum_S \bar{D}_{kl}^{\Omega}(S)\hat{S}f_E \Big\rangle \\
&= \frac{\dim(\Omega)^2}{|G|^2}\sum_{R,S} D_{kl}^{\Omega}(R)\bar{D}_{kl}^{\Omega}(S)\langle f_R|f_S\rangle
\end{aligned}
$$

$$= \frac{\dim(\Omega)^2}{|G|^2} \sum_{R,S} D_{kl}^{\Omega}(R) \bar{D}_{kl}^{\Omega}(S) \delta_{R,S}$$

$$= \frac{\dim(\Omega)^2}{|G|^2} \sum_{R} D_{kl}^{\Omega}(R) \bar{D}_{kl'}^{\Omega}(R)$$

$$= \frac{\dim(\Omega)}{|G|} \delta_{l,l'} \tag{4.52}$$

Hence, if the multiplicity is greater than one, an additional label preceding the irrep label has to be introduced in order to distinguish SALCs with the same symmetry, and, by varying the l index of the projector, all these can be projected out. Note that the maximal invariance space of a symmetry group is bound to be the regular representation; hence, multiplicities of an invariant function space cannot exceed the dimensions of the irreps and thus will always be covered by the variation of index l. If the multiplicity is smaller than $\dim(\Omega)$, variation of l will give rise to redundancies.

The action of the projector on an arbitrary function can be written as

$$\hat{P}_{kl}^{\Gamma} | f_x \rangle = S_x^{\Gamma l} | \Phi_k^{\Gamma} \rangle \tag{4.53}$$

Hence, the projector takes out of the function an irreducible part that transforms as the $| \Phi_k^{\Gamma} \rangle$ SALC multiplied by an overlap factor, $S_x^{\Gamma l}$, which indicates the extent to which the $| \Phi_l^{\Gamma} \rangle$ SALC is present in this function. A very concise formulation of this result can be achieved by the use of the Dirac notation. In this notation, the projector is written as

$$\hat{P}_{kl}^{\Gamma} = | \Phi_k^{\Gamma} \rangle \langle \Phi_l^{\Gamma} | \tag{4.54}$$

In the ket–bra combination, all the aspects of the projector come together. Let us apply this to our function:

$$\hat{P}_{kl}^{\Gamma} | f_x \rangle = | \Phi_k^{\Gamma} \rangle \langle \Phi_l^{\Gamma} | | f_x \rangle$$

$$= | \Phi_k^{\Gamma} \rangle \langle \Phi_l^{\Gamma} | f_x \rangle \tag{4.55}$$

where the convention is followed that the juxtaposition of two vertical lines is contracted to one. Comparing Eqs. (4.54) and (4.55), one can identify the bracket:

$$S_x^{\Gamma l} = \langle \Phi_l^{\Gamma} | f_x \rangle \tag{4.56}$$

When the projection operator acts (on the left) on a function $| f_x \rangle$, it forms a bracket, which is the overlap factor measuring how much of the $| \Phi_l^{\Gamma} \rangle$ SALC is present in the target. This is the "recognition" part of the projection. It then returns, as a result, the desired SALC $| \Phi_k^{\Gamma} \rangle$ multiplied by the overlap factor. This is the ladder aspect. As an example, consider the action of the $\hat{P}^E$ projection operators on the $| 1s_A \rangle$ orbital

in ammonia. One has:

$$\hat{P}_{11}|1s_A\rangle = \frac{1}{3}\left[2|1s_A\rangle - |1s_B\rangle - |1s_C\rangle\right] = \frac{\sqrt{2}}{\sqrt{3}}|\psi_x\rangle$$

$$\hat{P}_{21}|1s_A\rangle = \frac{\sqrt{2}}{\sqrt{3}}|\psi_y\rangle \tag{4.57}$$

$$\hat{P}_{12}|1s_A\rangle = 0$$

$$\hat{P}_{22}|1s_A\rangle = 0$$

Note that the bracket $\langle\psi_y|1s_A\rangle$ vanishes because $|1s_A\rangle$ does not occur in the $|\psi_y\rangle$ target, and this gives rise to the zeros in Eq. (4.57). If one wants to avoid the cumbersome construction of the irreducible representation matrices, one can construct trace projectors by putting $k = l$ and summing over all k:

$$\sum_k \hat{P}_{kk}^{\Gamma} = \frac{\dim(\Gamma)}{|G|} \sum_k \sum_R \bar{D}_{kk}^{\Gamma}(R)\hat{R}$$

$$= \frac{\dim(\Gamma)}{|G|} \sum_R \bar{\chi}^{\Gamma}(R)\hat{R} \tag{4.58}$$

In this case, only the character tables are needed in order to construct such projectors. They will certainly destroy all parts of the function space that do not belong to the irrep Γ, but, on the other hand, one loses the additional information in the subrepresentation. As we will see in the subsequent chapters, these little auxiliary indices are nonetheless valuable. A further remarkable property of a projector is that if it is applied twice with inverted kl indices, one again obtains a projector:

$$\hat{P}_{lk}^{\Gamma}\hat{P}_{kl}^{\Gamma} = \frac{\dim(\Gamma)^2}{|G|^2} \sum_{RS} \bar{D}_{lk}^{\Gamma}(R)\bar{D}_{kl}^{\Gamma}(S)\hat{R}\hat{S}$$

$$= \frac{\dim(\Gamma)^2}{|G|^2} \sum_{RT} \bar{D}_{lk}^{\Gamma}(R)\bar{D}_{kl}^{\Gamma}(R^{-1}T)\hat{T}$$

$$= \frac{\dim(\Gamma)^2}{|G|^2} \sum_T \sum_m \sum_R \bar{D}_{lk}^{\Gamma}(R)\bar{D}_{km}^{\Gamma}(R^{-1})\bar{D}_{ml}^{\Gamma}(T)\hat{T}$$

$$= \frac{\dim(\Gamma)^2}{|G|^2} \sum_T \sum_m \left(\sum_R \bar{D}_{lk}^{\Gamma}(R)D_{mk}^{\Gamma}(R)\right)\bar{D}_{ml}^{\Gamma}(T)\hat{T}$$

$$= \frac{\dim(\Gamma)}{|G|} \sum_T \left(\sum_m \delta_{m,l}\bar{D}_{ml}^{\Gamma}(T)\right)\hat{T}$$

$$= \hat{P}_{ll}^{\Gamma} \tag{4.59}$$

This also implies that the diagonal operator $\hat{P}_{kk}$ is *idempotent*, i.e., applying it twice gives exactly the same result as applying it once:

$$\hat{P}_{kk}^{\Gamma} \hat{P}_{kk}^{\Gamma} = \hat{P}_{kk}^{\Gamma} \tag{4.60}$$

Finally, summing over all diagonal projectors gives rise to the unit element:

$$\sum_{\Gamma} \sum_{i} \hat{P}_{ii}^{\Gamma} = \hat{E} \tag{4.61}$$

The proof is as follows:

$$\begin{aligned}
\sum_{\Gamma} \sum_{i} \hat{P}_{ii}^{\Gamma} &= \frac{1}{|G|} \sum_{\Gamma} \dim(\Gamma) \sum_{i} \sum_{R} \bar{D}_{ii}^{\Gamma}(R) \hat{R} \\
&= \frac{1}{|G|} \sum_{\Gamma} \dim(\Gamma) \sum_{R} \bar{\chi}^{\Gamma}(R) \hat{R} \\
&= \frac{1}{|G|} \sum_{R} \left(\sum_{\Gamma} \dim(\Gamma) \chi^{\Gamma}(R) \right) \hat{R} \\
&= \sum_{R} \delta_{R,E} \hat{R} \\
&= \hat{E} \tag{4.62}
\end{aligned}$$

Here, we have made use of the fact that the sum over all characters multiplied by the dimension of the irrep is the character of the regular representation, and this vanishes for all R except for the unit element, where it is equal to $|G|$ (see Eq. (4.41)). In Dirac terminology this reads

$$\sum_{\Gamma} \sum_{i} |\Phi_i^{\Gamma}\rangle\langle\Phi_i^{\Gamma}| = 1 \tag{4.63}$$

This relation is also known as the *closure* relation. It is frequently applied in the context of the crystal field theory of the lanthanides.

4.6 Subduction and Induction

Many applications are concerned with the reduction of symmetry by external or internal perturbations. Subduction corresponds to the lowering a symmetry group G to one of its subgroups, H, and is denoted by $G \downarrow H$. It can consist of a chain of consecutive symmetry lowerings, following a path of descent in symmetry down the genealogical tree of the group. In physics a typical form of *external* symmetry breaking is through application of a uniform magnetic or electric field. It leads to a subgroup that is the intersection of the molecular point group and the axial or

Table 4.3 Subduction of T_{1u} in $O_h \downarrow D_{3d}$

O_h	$\hat{E}$	$8\hat{C}_3$	$6\hat{C}_2$	$6\hat{C}_4$	$3\hat{C}_2$	$\hat{\imath}$	$6\hat{S}_4$	$8\hat{S}_6$	$3\hat{\sigma}_h$	$6\hat{\sigma}_d$
T_{1u}	3	0	-1	1	-1	-3	-1	0	1	1
D_{3d}	$\hat{E}$	$2\hat{C}_3$	$3\hat{C}_2$			$\hat{\imath}$		$2\hat{S}_6$		$3\hat{\sigma}_d$
T_{1u}	3	0	-1			-3		0		1
A_{2u}	1	1	-1			-1		-1		1
E_u	2	-1	0			-2		1		0

polar symmetry of the applied field, as discussed in Sect. 3.9. In chemistry a common approach to external symmetry breaking is to substitute one or more atoms or atomic groups by homologues, or to interchange sites, which may give rise to different stereo-isomers. *Internal* symmetry breaking is more subtle and may arise as a consequence of the Jahn–Teller effect. In this case the presence of a degenerate electronic state in the high-symmetry conformation of the molecule may provoke a spontaneous geometric distortion of the nuclear frame, leading to a lower symmetry in which the degeneracy is removed. This effect involves the coupling of representations and will be discussed in Sect. 6.6. Our concern here is what will happen to the irreps of G when the symmetry is reduced to H. This can easily be decided on the basis of the character theorem. We simply have to determine the character of the representation in the subgroup. The procedure consists of three steps. One first identifies the correspondence between the elements of G and the elements of H. Then the characters of the irrep in G are transferred to the characters for the corresponding operations in the subgroup. Third, the character string in the subgroup is reduced according to the standard procedure of the character theorem. Hence, let Γ denote an irrep of the parent group, and γ an irrep of the subgroup. The number of times that this subgroup representation occurs in the subduction $G \downarrow H$ is given by

$$c_\gamma(\Gamma G \downarrow H) = \frac{1}{|H|} \sum_{h \in H} \bar{\chi}^\gamma(h) \chi^\Gamma(h) \tag{4.64}$$

In Table 4.3 we follow as an example the fate of the octahedral T_{1u} irrep for the subduction $O_h \downarrow D_{3d}$. When the subduction is performed, the anchoring of the correspondences in the first step of the procedure is very important. For instance, the octahedron has two conjugacy classes of $\hat{C}_2$ axes. The $6\hat{C}_2$ class collects the twofold axes which bisect the Cartesian directions, while the $3\hat{C}_2$ class is made up of the $\hat{C}_4^2$ axes along the Cartesian directions. In the case of subduction to D_{3d}, the three axes perpendicular to the trigonal direction belong to the $6\hat{C}_2$ class. As the table indicates, in D_{3d} the threefold-degenerate representation becomes reducible by splitting into two trigonal irreps:

$$O_h \downarrow D_{3d} : T_{1u} \rightarrow A_{2u} + E_u \tag{4.65}$$

In some cases a subgroup can be reached via two different symmetry breakings. An example is the subduction $O_h \downarrow D_{2h}$. Here, two pathways for symmetry breaking
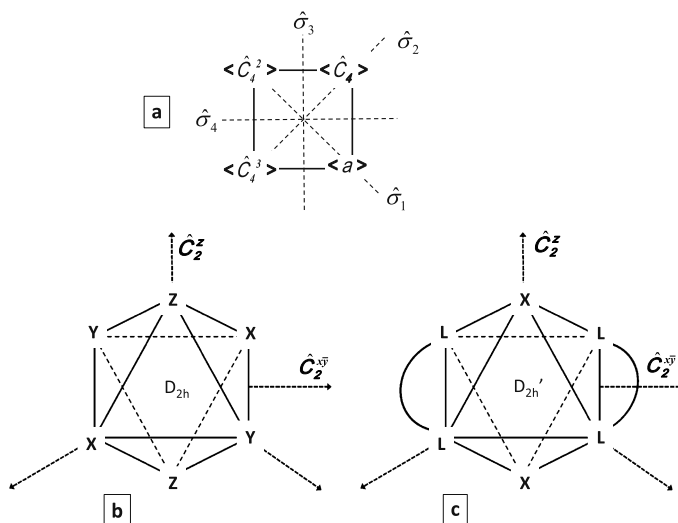
Fig. 4.3 (a) generation of equivalent sites in a square starting from $\langle a \rangle$, (b) substitutional symmetry lowering of $O_h \downarrow D_{2h}$ in the $MX_2Y_2Z_2$ complex isomer, and (c) $O_h \downarrow D'_{2h}$ symmetry lowering by bidentate ligands in *trans*-$M(L-L)_2X_2$

Table 4.4 Subduction of T_{2g} under $O_h \downarrow D_{2h}$

O_h	$\hat{E}$		$3\hat{C}_2$		$\hat{i}$		$3\hat{\sigma}_h$	
	$\downarrow$	$\swarrow$	$\downarrow$	$\searrow$	$\downarrow$	$\swarrow$	$\downarrow$	$\searrow$
D_{2h}	$\hat{E}$	$\hat{C}_2^x$	$\hat{C}_2^y$	$\hat{C}_2^z$	$\hat{i}$	$\hat{\sigma}_{xy}$	$\hat{\sigma}_{xz}$	$\hat{\sigma}_{yz}$
T_{2g}	3	−1	−1	−1	3	−1	−1	−1
B_{1g}	1	−1	−1	1	1	1	−1	−1
B_{2g}	1	−1	1	−1	1	−1	1	−1
B_{3g}	1	1	−1	−1	1	−1	−1	1

are present. The three $\hat{C}_2$ axes of the orthorhombic symmetry are either based on the $3\hat{C}_2$ class, $\{\hat{C}_2^x, \hat{C}_2^y, \hat{C}_2^z\}$, or on a mixture of the two classes, as in $\{\hat{C}_2^z, \hat{C}_2^{xy}, \hat{C}_2^{\bar{x}y}\}$. We shall denote the latter group as D'_{2h}. Simple molecular examples of both are shown in Fig. 4.3. Tables 4.4 and 4.5 present the splitting of the T_{2g} irrep over these two subduction paths. The corresponding splitting schemes are as follows:

$$O_h \downarrow D_{2h} : T_{2g} \rightarrow B_{1g} + B_{2g} + B_{3g}$$
$$O_h \downarrow D'_{2h} : T_{2g} \rightarrow A_g + B_{2g} + B_{3g}$$

(4.66)

Subduction tables are available in Appendix D.

The opposite process to subduction is induction. Here, we start from an irrep in a subgroup H. By coset expansion, this subgroup is put on an orbit inside a higher symmetry group. This leads to an extension of the function space and generates

Table 4.5 Subduction of T_{2g} under $O_h \downarrow D'_{2h}$

O_h	$\hat{E}$	$6\hat{C}_2$			$3\hat{C}_2$	$\hat{\imath}$	$3\hat{\sigma}_h$	$6\hat{\sigma}_d$	
	$\downarrow$	$\downarrow$	$\searrow$		$\downarrow$	$\downarrow$	$\downarrow$	$\downarrow$	$\searrow$
D'_{2h}	$\hat{E}$	$\hat{C}_2^x$	$\hat{C}_2^y$		$\hat{C}_2^z$	$\hat{\imath}$	$\hat{\sigma}_{xy}$	$\hat{\sigma}_{xz}$	$\hat{\sigma}_{yz}$
T_{2g}	3	1	1		-1	3	-1	1	1
A_g	1	1	1		1	1	1	1	1
B_{2g}	1	-1	1		-1	1	-1	1	-1
B_{3g}	1	1	-1		-1	1	-1	-1	1

irreps of the parent group. The outcome of the induction is determined by the reciprocity theorem due to Frobenius.

Theorem 7 *The number of times that a given irrep Γ of a parent group G occurs in the induction $H \uparrow G$ of a subgroup irrep γ is equal to the number of times that γ is present in the subduction $G \downarrow H$ of that irrep Γ.*

We shall present the proof here since it introduces the important concept of the *ground* representation [2, 3]. This concept is especially useful when considering a polyhedral molecular cluster or complex consisting of several equivalent sites. Typically, these sites could be the atoms in a network covering a hollow cage, or ligands in a metal complex. In the case of ammonia, the sites are simply the three hydrogen atoms. Usually, the site group is of type C_{nv}. We choose site $\langle a \rangle$ as the starting site, which is stabilized by the subgroup H_A. The group G is expanded in cosets of this subgroup, with coset representatives $\hat{g}_\kappa$:

$$G = \sum_\kappa \hat{g}_\kappa H_A \tag{4.67}$$

As we have seen in the previous chapter, the coset representatives each address a copy of site $\langle a \rangle$, which we shall label as $\langle \kappa \rangle$. The site group that stabilizes this site is isomorphic to H_A and is denoted by H_κ. We thus have the following mappings:

$$\begin{aligned}
\langle \kappa \rangle &= \hat{g}_\kappa \langle a \rangle \\
H_\kappa &= \hat{g}_\kappa H_A \hat{g}_\kappa^{-1}
\end{aligned} \tag{4.68}$$

The mapping of the stabilizer, $H_A \rightarrow H_\kappa$, is recognized as a similarity transformation of the whole subgroup. Two different sites can share the same site group. As an example, in a square pyramidal complex, with parent group C_{4v} and site groups C_s, two ligands, *trans* to each other, have the same site group. With reference to the square in Fig. 4.3a, the cosets may be generated as follows:

$$C_{4v} = \sum_{k=0}^{3} \hat{C}_4^k \{\hat{E}, \hat{\sigma}_1\} = \{\hat{E}, \hat{\sigma}_1\} + \{\hat{C}_4, \hat{\sigma}_4\} + \{\hat{C}_4^2, \hat{\sigma}_2\} + \{\hat{C}_4^3, \hat{\sigma}_3\} \tag{4.69}$$

Hence, the four sites of the square are denoted by the coset generators as $\langle a \rangle$, $\langle \hat{C}_4 \rangle$, $\langle \hat{C}_4^2 \rangle$, and $\langle \hat{C}_4^3 \rangle$. Now we also introduce a functional basis on site $\langle a \rangle$, which is represented by the irrep γ, with component labeling m_γ:

$$\hat{h}_A |\gamma m_\gamma; a\rangle = \sum_{m'_\gamma} |\gamma m'_\gamma; a\rangle D^\gamma_{m'_\gamma m_\gamma}(h_A) \tag{4.70}$$

The coset generators will once again take this functional space around in an orbit which visits all the equivalent sites. Local basis sets are thus defined as

$$|\gamma m_\gamma; \kappa\rangle = \hat{g}_\kappa |\gamma m_\gamma; a\rangle \tag{4.71}$$

The total induction space is the sum of all these basis sets on the different sites.

As we have seen, the operators of the group act transitively on the cosets. This means that the cosets are permuted among themselves. The permutation matrix is denoted as $\mathbb{P}(g)$. One has

$$\hat{g}(\hat{g}_\kappa H_A) = \sum_\lambda P_{\lambda\kappa}(g)\hat{g}_\lambda H_A \tag{4.72}$$

with

$$\begin{aligned} P_{\lambda\kappa}(g) &= 1 \quad \text{if } \hat{g}(\hat{g}_\kappa H_A) = \hat{g}_\lambda H_A \\ P_{\lambda\kappa}(g) &= 0 \quad \text{if } \hat{g}(\hat{g}_\kappa H_A) \neq \hat{g}_\lambda H_A \end{aligned} \tag{4.73}$$

This permutational representation is also called the *ground* representation. It describes the transformation of the coset space. The dimension of this coset space is $|G|/|H|$. In the case of a cluster, where each coset corresponds to a site, it represents the permutation of the positions of the sites. For this reason, it is also called the *positional* representation. Indeed, Eq. (4.72) may equally well be written as

$$\hat{g}\langle \kappa\rangle = \sum_\lambda P_{\lambda\kappa}(g)\langle\lambda\rangle \tag{4.74}$$

For the λ-value, which marks the position of the nonzero element in the κth column of the matrix $\mathbb{P}$, the product $\hat{g}_\lambda^{-1}\hat{g}\hat{g}_\kappa$ is an element of H_A. We call this the *subelement* of $\hat{g}$ in H_A. As an example, for the case of the pyramidal complex, the matrices of the positional representation are listed in Table 4.6. If $\hat{g} = \hat{g}_\kappa \hat{h}\hat{g}_\kappa^{-1}$, the diagonal element will be nonzero: $P_{\kappa\kappa}(g) = 1$. The following sum rules will thus hold, as can be verified from Table 4.6:

$$\begin{aligned} \sum_\kappa P_{\kappa\kappa}\left(g_\kappa h g_\kappa^{-1}\right) &= \frac{|G|}{|H|} \\ \sum_{h\in H} P_{\kappa\kappa}\left(g_\kappa h g_\kappa^{-1}\right) &= |H| \end{aligned} \tag{4.75}$$

Table 4.6 Ground or positional representation of the four equatorial ligand sites in a square pyramidal complex; the sites are ordered as in Fig. 4.3(a)

$$\mathbb{P}(E) = \begin{pmatrix} 1 & 0 & 0 & 0 \\ 0 & 1 & 0 & 0 \\ 0 & 0 & 1 & 0 \\ 0 & 0 & 0 & 1 \end{pmatrix} \qquad \mathbb{P}(\sigma_1) = \begin{pmatrix} 1 & 0 & 0 & 0 \\ 0 & 0 & 0 & 1 \\ 0 & 0 & 1 & 0 \\ 0 & 1 & 0 & 0 \end{pmatrix}$$

$$\mathbb{P}(C_4) = \begin{pmatrix} 0 & 0 & 0 & 1 \\ 1 & 0 & 0 & 0 \\ 0 & 1 & 0 & 0 \\ 0 & 0 & 1 & 0 \end{pmatrix} \qquad \mathbb{P}(\sigma_2) = \begin{pmatrix} 0 & 0 & 1 & 0 \\ 0 & 1 & 0 & 0 \\ 1 & 0 & 0 & 0 \\ 0 & 0 & 0 & 1 \end{pmatrix}$$

$$\mathbb{P}(C_4^2) = \begin{pmatrix} 0 & 0 & 1 & 0 \\ 0 & 0 & 0 & 1 \\ 1 & 0 & 0 & 0 \\ 0 & 1 & 0 & 0 \end{pmatrix} \qquad \mathbb{P}(\sigma_3) = \begin{pmatrix} 0 & 0 & 0 & 1 \\ 0 & 0 & 1 & 0 \\ 0 & 1 & 0 & 0 \\ 1 & 0 & 0 & 0 \end{pmatrix}$$

$$\mathbb{P}(C_4^3) = \begin{pmatrix} 0 & 1 & 0 & 0 \\ 0 & 0 & 1 & 0 \\ 0 & 0 & 0 & 1 \\ 1 & 0 & 0 & 0 \end{pmatrix} \qquad \mathbb{P}(\sigma_4) = \begin{pmatrix} 0 & 1 & 0 & 0 \\ 1 & 0 & 0 & 0 \\ 0 & 0 & 0 & 1 \\ 0 & 0 & 1 & 0 \end{pmatrix}$$

We are now ready to start the proof. The total induction space is invariant under the operations of the group G. As an example, we can act with an operator of the group on one of the functions on one of the sites:

$$\hat{g}|\gamma m_\gamma; \kappa\rangle = \hat{g}\hat{g}_\kappa |\gamma m_\gamma; a\rangle = \sum_\lambda P_{\lambda\kappa}(g)\hat{g}_\lambda \left[\hat{g}_\lambda^{-1}\hat{g}\hat{g}_\kappa\right]|\gamma m_\gamma; a\rangle \qquad (4.76)$$

where we have placed the subelement of $\hat{g}$ in square brackets. This subelement belongs to H_A, under the protection of the $P_{\lambda\kappa}(g)$ prefactor, which will be nonzero only for values of $\hat{g}$ for which this is indeed the case. We can thus introduce the representation matrix for the local on-site transformations:

$$\hat{g}|\gamma m_\gamma; \kappa\rangle = \sum_\lambda \sum_{m'_\gamma} P_{\lambda\kappa}(g)\hat{g}_\lambda |\gamma m'_\gamma; a\rangle D^\gamma_{m'_\gamma m_\gamma}\left(g_\lambda^{-1} g g_\kappa\right)$$

$$= \sum_\lambda \sum_{m'_\gamma} P_{\lambda\kappa}(g)|\gamma m'_\gamma; \lambda\rangle D^\gamma_{m'_\gamma m_\gamma}\left(g_\lambda^{-1} g g_\kappa\right) \qquad (4.77)$$

This result provides the matrix transformation that shows how the basis functions of the total induction space are transformed under the operations of G. We shall denote this matrix as $\mathbb{D}^{H\uparrow G}$. The structure of this matrix is based on the permutational structure of the ground representation, but the zeros are replaced by small zero blocks of dimension $\dim(\gamma) \times \dim(\gamma)$, and, instead of the ones, the $\mathbb{D}^\gamma(g_\lambda^{-1} g g_\kappa)$ matrices are inserted. A diagonal element of this matrix will be given by $P_{\kappa\kappa}(g)D^\gamma_{m_\gamma m_\gamma}(\hat{g}_\kappa^{-1}\hat{g}\hat{g}_\kappa)$.

Knowing the diagonal elements of the induction matrix, we can now calculate the frequency of a given Γ irrep of the main group, using the character theorem:

$$c_\Gamma(\gamma H \uparrow G) = \frac{1}{|G|} \sum_{g \in G} \bar{\chi}^\Gamma(g) \text{Tr}\left[\mathbb{D}^{H\uparrow G}(g)\right]$$

$$= \frac{1}{|G|} \sum_{g \in G} \bar{\chi}^\Gamma(g) \sum_\kappa P_{\kappa\kappa}(g) \chi^\gamma\left(g_\kappa^{-1} g g_\kappa\right) \qquad (4.78)$$

The only elements $\hat{g}$ that are allowed in the summation over κ are the ones such that $(\hat{g}_\kappa^{-1} \hat{g} \hat{g}_\kappa) \in H_A$. For other elements, $P_{\kappa\kappa}(g)$ are zero. Let us denote by $\hat{h}$ the subelement that allows us to express $\hat{g}$ as

$$\hat{g} = \hat{g}_\kappa \hat{h} \hat{g}_\kappa^{-1} \qquad (4.79)$$

Introducing this substitution in Eq. (4.78) yields

$$c_\Gamma(\gamma H \uparrow G) = \frac{1}{|G|} \sum_{h \in H} \sum_\kappa \bar{\chi}^\Gamma\left(g_\kappa h g_\kappa^{-1}\right) \chi^\gamma(h) P_{\kappa\kappa}\left(g_\kappa h g_\kappa^{-1}\right) \qquad (4.80)$$

The first character in this equation belongs to the full group and is the same for all elements of a conjugacy class, and hence,

$$\chi^\Gamma\left(g_\kappa h g_\kappa^{-1}\right) = \chi^\Gamma(h) \qquad (4.81)$$

Substituting the result of Eq. (4.81) and the sum rule in Eq. (4.75) into the character expression finally gives

$$c_\Gamma(\gamma H \uparrow G) = \frac{1}{|G|} \sum_{h \in H} \sum_\kappa \bar{\chi}^\Gamma(h) \chi^\gamma(h) P_{\kappa\kappa}\left(g_\kappa h g_\kappa^{-1}\right)$$

$$= \frac{1}{|G|} \sum_{h \in H} \bar{\chi}^\Gamma(h) \chi^\gamma(h) \left(\sum_\kappa P_{\kappa\kappa}\left(g_\kappa h g_\kappa^{-1}\right)\right)$$

$$= \frac{1}{|H|} \sum_{h \in H} \bar{\chi}^\Gamma(h) \chi^\gamma(h)$$

$$= c_\gamma(\Gamma G \downarrow H) \qquad (4.82)$$

which concludes the proof. Armed with the subduction tables, we can now read these at once in the opposite sense and obtain the corresponding induction frequencies. As a simple example, consider a hydrogen atom in ammonia. The site symmetry is C_s, and the subduction from C_{3v} reads:

$$A_1 \rightarrow a$$
$$A_2 \rightarrow b \qquad (4.83)$$
$$E \rightarrow a + b$$

Fig. 4.4 Tetrahedral SALCs
in methane. *The open circles
are positive and the filled
circles are negative.* The T_2
orbitals match the sign
pattern of central p-orbitals

$$T_{2x} \qquad\qquad T_{2y} \qquad\qquad T_{2z}$$
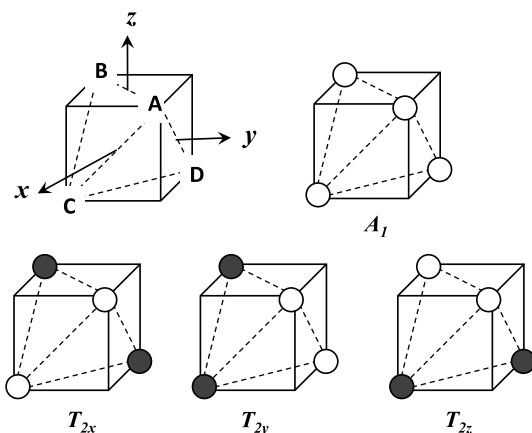
Using reciprocity, we can thus immediately infer the SALC symmetries of the hydrogen basis functions by selecting the C_{3v} irreps that subduce a in the case of the $1s$ orbitals and b in the case of the bending coordinates:

$$\text{Hydrogen } 1s : aC_s \uparrow C_{3v} = A_1 + E$$
$$\text{Hydrogen } \Delta\phi : bC_s \uparrow C_{3v} = A_2 + E \tag{4.84}$$

Some induction schemes for σ, π, and δ orbital basis sets on C_{nv} sites of polyhedral complexes are to be found in Appendix D. In addition to the Frobenius theorem, there is also a stronger result for induction theory based on the concept of a fiber bundle. This requires the coupling of representations and will be considered in Sect. 6.9.

4.7 Application: The sp^3 Hybridization of Carbon

Methane is the prototype of the saturated aliphatic hydrocarbons. The four hydrogen atoms occupy the corners of a regular tetrahedron, as in Fig. 4.4. Their site symmetry is C_{3v}. The $1s$ atomic orbital on hydrogen is totally symmetric in the site group. The symmetries of the corresponding SALCs can of course be obtained by the standard character procedure, as for the case of ammonia, but we might as well directly obtain them by induction:

$$\Gamma(a_1 C_{3v} \uparrow T_d) = A_1 + T_2 \tag{4.85}$$

The corresponding SALCs can easily be projected:

$$\begin{pmatrix} |A_1\rangle & |T_{2x}\rangle & |T_{2y}\rangle & |T_{2z}\rangle \end{pmatrix}$$
$$= \begin{pmatrix} |1s_A\rangle & |1s_B\rangle & |1s_C\rangle & |1s_D\rangle \end{pmatrix} \times \mathbb{T} \tag{4.86}$$

with

$$\mathbb{T} = \frac{1}{2} \begin{pmatrix} 1 & 1 & 1 & 1 \\ 1 & -1 & -1 & 1 \\ 1 & 1 & -1 & -1 \\ 1 & -1 & 1 & -1 \end{pmatrix} \tag{4.87}$$

SALCs are normalized to unity, neglecting overlap between the sites. The matrix $\mathbb{T}$ transforms the localized orbitals on the sites to delocalized molecular orbitals with irreducible symmetry characteristics. The inverse matrix $\mathbb{T}^{-1}$ fulfills the opposite role and localizes the molecular orbital set back on the atomic sites.

The valence shell of the central carbon atom contains four orbitals, which incidentally also transform as $A_1 + T_2$. The precise correspondence is as follows:

$$\begin{aligned} |2s\rangle &\leftrightarrow A_1 \\ |2p_x\rangle &\leftrightarrow T_{2x} \\ |2p_y\rangle &\leftrightarrow T_{2y} \\ |2p_z\rangle &\leftrightarrow T_{2z} \end{aligned} \tag{4.88}$$

Hence, we can match the central valence shell with the hydrogen SALCs. In fact, this correspondence provides a simple pictorial method for obtaining the SALCs immediately. The weighting coefficients for a given SALC are simply taken as proportional to the local amplitude of the central $2s$ or $2p$ function, with the same symmetry, as is illustrated in Fig. 4.4. In this way one obtains a SALC that has the same nodal characteristics and thus the same symmetry as the central orbital. Note that this procedure also aligns the phases of the peripheral and central orbitals.

Starting from on-site localized atomic orbitals, we have thus transformed these into SALCs using the $\mathbb{T}$ matrix and then found a perfect matching with the central valence orbitals on carbon. What would now be the effect of applying the inverse transformation, $\mathbb{T}^{-1}$, not to the hydrogen SALCs but to the central carbon orbitals? This yields an interesting result. The inverse matrix, which transforms delocalized SALCs back into localized orbitals, reshapes the carbon valence orbitals by projecting out linear combinations, of mixed or *hybrid* character, which are maximally directed to a single site of the tetrahedron. These are the ubiquitous sp^3 hybrids of Pauling, which we can label with the site labels A, B, C, and D:

$$\begin{pmatrix} |sp_A^3\rangle & |sp_B^3\rangle & |sp_C^3\rangle & |sp_D^3\rangle \end{pmatrix}$$

$$= \begin{pmatrix} |2s\rangle & |2p_x\rangle & |2p_y\rangle & |2p_z\rangle \end{pmatrix} \frac{1}{2} \begin{pmatrix} 1 & 1 & 1 & 1 \\ 1 & -1 & 1 & -1 \\ 1 & -1 & -1 & 1 \\ 1 & 1 & -1 & -1 \end{pmatrix} \tag{4.89}$$

The components of the valence shell of carbon being a scalar ($2s$) and a vector ($2p$), the tetrahedron is the optimal geometry that provides four valence sites, which together transform precisely as scalar and vector. The alternative high-symmetry

four-site structure is the square, but, from the tables in Appendix D, the induction from the C_{2v} sites in a square-planar structure yields

$$\Gamma(a_1 C_{2v} \uparrow D_{4h}) = A_{1g} + B_{2g} + E_u \tag{4.90}$$

This matches the symmetry of $sp^2 d$ hybrids. It is thus not suitable for carbon, but indeed describes the valence structure of square-planar transition-metal complexes where d-orbitals are involved in the bonding.

4.8 Application: The Vibrations of UF$_6$

As we have already mentioned, representations not only apply to orbitals, but equally well to vibrational coordinates. The function space in such a case consists of a set of distortions. When applying symmetry operations we do not move the atoms, but the distortions. Let us consider the vibrations of an octahedral complex, such as UF$_6$, which can be brought into the gas phase and which has been studied in great detail since it is the carrier of uranium in the gas diffusion process for enrichment of nuclear fuel. The atoms are labeled as in Fig. 4.5, and on each atom we define a local coordinate system that parallels the central system. In the notation adopted, ΔY_2 is a variable for a displacement of atom 2 over a distance Δ in the positive y-direction. A symmetry operation such as $\hat{C}_4^z$ transforms this ΔY_2 into $-\Delta X_3$. The seven atoms give rise to 21 distortions, which include six spurious modes, corresponding to three translations and three rotations. The seven atoms form two different orbits: the orbit containing the six fluoride ligands and the one-atom orbit of the central uranium atom. The displacements of one ligand can further be separated into a radial or σ-mode and two tangential or π-modes, which, in the C_{4v} site group, transform as a_1 and e, respectively. Altogether, the distortion space thus contains three different basis sets: the central atom, the ligand σ-modes, and the ligand π-modes. For each of these, the symmetry content may be determined by directly applying the character theorem, or—for the case of the ligands—by using induction. The three displacements of the uranium atom transform as the T_{1u} irrep of the central translation mode. The ligand inductions are as follows:

$$
\begin{aligned}
\text{F}\sigma &: \Gamma(a_1 C_{4v} \uparrow O_h) = A_{1g} + E_g + T_{1u} \\
\text{F}\pi &: \Gamma(e C_{4v} \uparrow O_h) = T_{1g} + T_{2g} + T_{1u} + T_{2u}
\end{aligned} \tag{4.91}
$$

We can now determine the symmetry-adapted coordinates by applying the projection operators, but the results can be written down almost immediately by again using the criterion of overlap with central symmetry functions. The A_{1g}, T_{1u}, and $E_g + T_{2g}$ SALCs reflect the nodal patterns of central s, p, and d functions, respectively. The T_{1g} mode corresponds to the rotation and evidently consists of tangential displacements of ligands in the equator perpendicular to the rotation axis. Finally, the T_{2u} is a buckling mode, which has the symmetry of central f orbitals, viz.

Fig. 4.5 Ligand numbering
and displacement coordinates
for UF$_6$
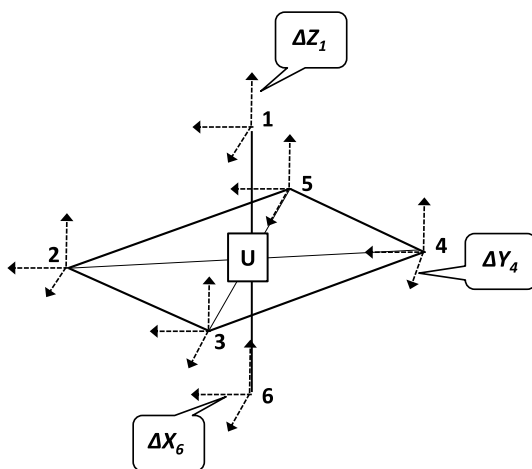
Table 4.7   Symmetry coordinates for UF$_6$

U$T_{1u}p_x$	ΔX_0
U$T_{1u}p_y$	ΔY_0
U$T_{1u}p_z$	ΔZ_0
F$\sigma A_{1g}s$	$1/\sqrt{6}(\Delta Z_1 + \Delta X_2 + \Delta Y_3 - \Delta X_4 - \Delta Y_5 - \Delta Z_6)$
F$\sigma E_g d_{z^2}$	$1/\sqrt{12}(2\Delta Z_1 - \Delta X_2 - \Delta Y_3 + \Delta X_4 + \Delta Y_5 - 2\Delta Z_6)$
F$\sigma E_g d_{x^2-y^2}$	$1/2(\Delta X_2 - \Delta Y_3 - \Delta X_4 + \Delta Y_5)$
F$\sigma T_{1u}p_x$	$1/\sqrt{2}(\Delta X_2 + \Delta X_4)$
F$\sigma T_{1u}p_y$	$1/\sqrt{2}(\Delta Y_3 + \Delta Y_5)$
F$\sigma T_{1u}p_z$	$1/\sqrt{2}(\Delta Z_1 + \Delta Z_6)$
F$\pi T_{1g}x$	$1/2(-\Delta Y_1 + \Delta Z_3 - \Delta Z_5 + \Delta Y_6)$
F$\pi T_{1g}y$	$1/2(\Delta X_1 - \Delta Z_2 - \Delta X_6 + \Delta Z_4)$
F$\pi T_{1g}z$	$1/2(\Delta Y_2 - \Delta X_3 - \Delta Y_4 + \Delta X_5)$
F$\pi T_{2g}d_{yz}$	$1/2(\Delta Y_1 + \Delta Z_3 - \Delta Z_5 - \Delta Y_6)$
F$\pi T_{2g}d_{xz}$	$1/2(\Delta X_1 + \Delta Z_2 - \Delta X_6 - \Delta Z_4)$
F$\pi T_{2g}d_{xy}$	$1/2(\Delta Y_2 + \Delta X_3 - \Delta Y_4 - \Delta X_5)$
F$\pi T_{1u}p_x$	$1/2(\Delta X_1 + \Delta X_3 + \Delta X_5 + \Delta X_6)$
F$\pi T_{1u}p_y$	$1/2(\Delta Y_1 + \Delta Y_2 + \Delta Y_4 + \Delta Y_6)$
F$\pi T_{1u}p_z$	$1/2(\Delta Z_2 + \Delta Z_3 + \Delta Z_4 + \Delta Z_5)$
F$\pi T_{2u}f_{x(y^2-z^2)}$	$1/2(-\Delta X_1 + \Delta X_3 + \Delta X_5 - \Delta X_6)$
F$\pi T_{2u}f_{y(z^2-x^2)}$	$1/2(\Delta Y_1 - \Delta Y_2 - \Delta Y_4 + \Delta Y_6)$
F$\pi T_{2u}f_{z(x^2-y^2)}$	$1/2(\Delta Z_2 - \Delta Z_3 + \Delta Z_4 - \Delta Z_5)$

$f_{z(x^2-y^2)}$, and its cyclic permutations $f_{x(y^2-z^2)}$ and $f_{y(z^2-x^2)}$. In Table 4.7 we list
all 21 symmetry coordinates by category, using labels that refer to the central har-
monic functions. We may denote the 21 symmetry coordinates by a row vector **S**.

The kinetic energy is then given by

$$T = \frac{1}{2} \sum_{i=1}^{21} m_i \left(\frac{\mathrm{d}S_i}{\mathrm{d}t} \right)^2$$

$$= \frac{M}{2} \sum_{i=1}^{3} \left(\frac{\mathrm{d}S_i}{\mathrm{d}t} \right)^2 + \frac{m}{2} \sum_{i=4}^{21} \left(\frac{\mathrm{d}S_i}{\mathrm{d}t} \right)^2 \tag{4.92}$$

Here, M is the atomic mass of uranium, and m is the atomic mass of fluorine. The kinetic energy can be reduced to a uniform scalar product by mass weighting the coordinates, i.e., by multiplying the S coordinates with the square root of the atomic mass of the displaced atom. We shall denote these as the vector $\mathbf{Q}$. Hence, $Q_i = \sqrt{m_i} S_i$:

$$T = \frac{1}{2} \sum_i \left(\frac{\mathrm{d}Q_i}{\mathrm{d}t} \right)^2 = \frac{1}{2} \sum_i \dot{Q}_i^2 \tag{4.93}$$

where the dot over Q denotes the time derivative. The potential energy will be approximated by second-order derivatives of the potential energy surface $V(\mathbf{Q})$ in the mass-weighted coordinates:

$$V_{ij} = \frac{\partial^2 V}{\partial Q_i \partial Q_j} \tag{4.94}$$

These derivatives are the elements of the Hessian matrix, $\mathbb{V}$, which is symmetric about the diagonal. The potential minimum coincides with the octahedral geometry. The resulting potential energy is

$$V = \frac{1}{2} \sum_{i,j} V_{ij} Q_i Q_j \tag{4.95}$$

The kinetic and potential energies are combined to form the Lagrangian, $L = T - V$. The equation of motion is given by

$$\frac{\partial L}{\partial Q_k} = \frac{\mathrm{d}}{\mathrm{d}t} \frac{\partial L}{\partial \dot{Q}_k} \tag{4.96}$$

The partial derivatives in this equation are given by

$$\frac{\partial L}{\partial Q_k} = -\frac{\partial V}{\partial Q_k} = -V_{kk} Q_k - \frac{1}{2} \sum_{i \neq k} (V_{ik} + V_{ki}) Q_i$$

$$= -V_{kk} Q_k - \sum_{i \neq k} V_{ki} Q_i = -\sum_i V_{ki} Q_i \tag{4.97}$$

$$\frac{\mathrm{d}}{\mathrm{d}t} \frac{\partial L}{\partial \dot{Q}_k} = \frac{\mathrm{d}}{\mathrm{d}t} \frac{\partial T}{\partial \dot{Q}_k} = \frac{\mathrm{d}}{\mathrm{d}t} \dot{Q}_k = \ddot{Q}_k \tag{4.98}$$

Table 4.8 Vibrational spectrum of UF$_6$

Symmetry	Type	$\bar{\nu}(\text{cm}^{-1})$	Calc.	Technique
$\nu_1(A_{1g})$	Breathing	667	669	Raman (very strong)
$\nu_2(E_g)$	Stretching	533	534	Raman (weak)
$\nu_3(T_{1u})$	Stretching	626	624	IR
$\nu_4(T_{1u})$	Bending	186	181	IR
$\nu_5(T_{2g})$	Bending	202	191	Raman (weak)
$\nu_6(T_{2u})$	Buckling	142	140	Overtone

It will be assumed that the coordinates vary in a harmonic manner with an angular frequency ω; hence, $Q_k = Q_k^{\max} \cos \omega t$. The second derivative is then given by

$$\ddot{Q}_k = -\omega^2 Q_k = -(2\pi \nu)^2 Q_k \tag{4.99}$$

where ν is the vibrational frequency in Hertz. The equation of motion then is turned into a set of homogeneous linear equations:

$$\forall k: \quad \sum_i \left(V_{ki} - \delta_{ki}\omega^2\right)Q_i = 0 \tag{4.100}$$

This set of equations is solved in the standard way by diagonalizing the Hessian matrix, as

$$\left|\mathbb{V} - \omega^2 \mathbb{I}\right| = 0 \tag{4.101}$$

The eigenvalues of the secular equation yield the frequencies of the normal modes, which are usually expressed as wavenumbers, $\bar{\nu}$, preferentially in reciprocal centimetres, cm^{-1} by dividing the frequency by the speed of light, c.

$$\bar{\nu} = \frac{\nu}{c} = \frac{\omega}{2\pi c} \tag{4.102}$$

In Table 4.8 we present the experimental results [4] for U^{238}F$_6$, as compared with the Hessian eigenvalues, based on extensive relativistic calculations [5]. The eigenfunctions of the Hessian matrix are the corresponding normal modes. The Hessian matrix will be block-diagonal over the irreps of the group and, within each irrep, over the individual components of the irrep. Moreover, the blocks are independent of the components. All this illustrates the power of symmetry, and the reasons for it will be explained in detail in the next chapter. As an immediate consequence, symmetry coordinates, which belong to irreps that occur only once, are exact normal modes of the Hessian. Five irreps fulfil this criterion: the T_{1g} mode, which corresponds to the overall rotations, and the vibrational modes, $A_{1g} + E_g + T_{2g} + T_{2u}$. Only the T_{1u} irrep gives rise to a triple multiplicity. In this case, the actual normal modes will depend on the matrix elements in the Hessian. Let us study this in detail
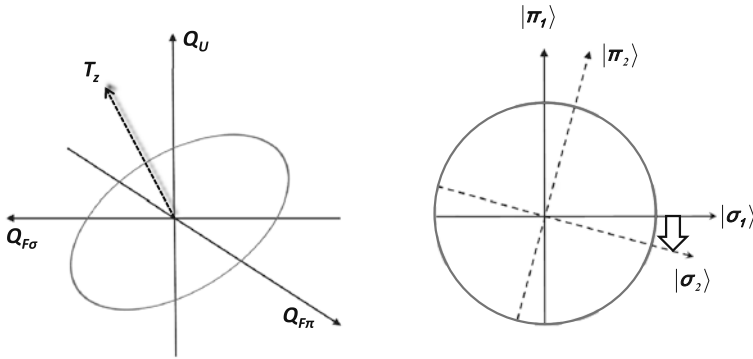
Fig. 4.6 T_{1u} distortion space for UF$_6$ with coordinates as defined in Eq. (4.103); T_z is the translation of mass. The circle, perpendicular to this direction, is the space of vibrational stretching and bending, with coordinates defined in Eqs. (4.104) and (4.105). The angle $\langle \sigma_2 | \sigma_1 \rangle$ is $-10.5°$

for the three $T_{1u}z$-components, which we shall abbreviate as follows:

$$Q_U = \sqrt{M}\Delta Z_0$$

$$Q_\sigma = \frac{\sqrt{m}}{\sqrt{2}}(\Delta Z_1 + \Delta Z_6) \tag{4.103}$$

$$Q_\pi = \frac{\sqrt{m}}{2}(\Delta Z_2 + \Delta Z_3 + \Delta Z_4 + \Delta Z_5)$$

This space is still reducible since it includes the translation in the z-direction. The translation coordinate corresponds to the displacement of the center of mass in the z-direction. It is given by $\sum_i m_i \Delta Z_i$, which can be expressed as follows:

$$T_z = M\Delta Z_0 + m(\Delta Z_1 + \Delta Z_2 + \Delta Z_3 + \Delta Z_4 + \Delta Z_5 + \Delta Z_6)$$
$$= \sqrt{M}Q_U + \sqrt{2m}Q_\sigma + \sqrt{4m}Q_\pi \tag{4.104}$$

We can remove this degree of freedom from the function space by a standard orthogonalization procedure. One option is to construct first a pure stretching mode, which does not involve the Q_π coordinate. This mode is denoted by $|\sigma_1\rangle$. The remainder of the function space, which is orthogonal both to the translation and to this pure stretching mode, is then denoted by $|\pi_1\rangle$. Normalizing these modes with respect to mass-weighted coordinates yields:

$$|\sigma_1\rangle = \frac{-\sqrt{2m}Q_U + \sqrt{M}Q_\sigma}{\sqrt{M + 2m}}$$

$$|\pi_1\rangle = \frac{-\sqrt{4mM}Q_U - m\sqrt{8}Q_\sigma + (M + 2m)Q_\pi}{\sqrt{(M + 2m)(M + 6m)}} \tag{4.105}$$

An alternative option would be to construct a pure bending mode, based on the tangent motions. Let us denote this by $|\pi_2\rangle$. The remainder is then denoted by $|\sigma_2\rangle$.

$$
\begin{aligned}
|\sigma_2\rangle &= \frac{-\sqrt{2mM}\,Q_U + (M+4m)\,Q_\sigma - m\sqrt{8}\,Q_\pi}{\sqrt{(M+4m)(M+6m)}} \\
|\pi_2\rangle &= \frac{-\sqrt{4m}\,Q_U + \sqrt{M}\,Q_\pi}{\sqrt{M+4m}}
\end{aligned}
\tag{4.106}
$$

In Fig. 4.6 we present both choices of bases. The angle, α, between both basis sets is defined by

$$
\cos\alpha = \sqrt{\frac{M(M+6m)}{(M+2m)(M+4m)}}
\tag{4.107}
$$

In the case of UF$_6$ ($m = 18.998$, $M = 238.050$) this angle is $-10.5°$. The actual eigenmodes are found by setting up the Hessian in one of these coordinate sets and diagonalizing it. This Hessian matrix is symmetric and thus contains three independent parameters: the two diagonal elements and the single off-diagonal element. The sum of the resulting eigenvalues is equal to the trace of the matrix, and the product is equal to its determinant; this leaves still one degree of freedom, which can be associated with the *composition* of the normal mode, viz. the angle of rotation in the diagram. It is important to realize that this composition also gives rise to observables, albeit not the eigenfrequencies, but a variety of other properties, such as the intensities of the vibrational transition, isotope shifts and isotope splittings, or electron diffraction amplitudes. For most octahedral complexes, as in the case of UF$_6$, the rotation angle for the actual T_{1u} eigenmodes lies in the interval $[0, \alpha]$. This means that the modes may approximately be assigned as a stretching and a bending mode. In the spectrum their frequencies are denoted as ν_3 and ν_4, respectively. The isotope effect of the radioactive nucleus U^{235}, as distinct from U^{238}, is absent for all modes, except for the T_{1u} modes, since these involve the displacement of uranium. Of the latter two, the strongest effect is expected for the stretching vibration, since this involves the largest displacement of the central atom. The pure stretching mode, $|\sigma_1\rangle$, can be expressed in terms of the displacements along the z-direction as

$$
|\sigma_1\rangle = \sqrt{\frac{2mM}{M+2m}}\left(-\Delta Z_0 + \frac{\Delta Z_1 + \Delta Z_6}{2}\right)
\tag{4.108}
$$

This is precisely the antisymmetric mode for a triatomic F–U–F oscillator. The square root preceding the modes corresponds to a mass weighting by the reduced mass, μ, for such an oscillator:

$$
\mu = \left(\frac{1}{M} + \frac{1}{2m}\right)^{-1} = \frac{2mM}{M+2m}
\tag{4.109}
$$

Substitution of U^{238} by the U^{235} isotope will reduce this effective mass by a factor 0.9982. The frequency is accordingly increased by the square root of this factor.

This gives an increase of frequency of 0.56 cm^{-1}, which is close to the experimental value [6] of 0.60 cm^{-1}. This confirms the dominant stretching character of the ν_3 mode.

What have we learned from this example? The Hessian matrix is block diagonal over the irreps of the point group, and, as a result, the normal modes are characterized by symmetry labels. These labels are exact spectral assignments. In the long run their relevance for the study of symmetry may be more important than the temporary gain in computational time for evaluation and diagonalization of the Hessian matrix.

4.9 Application: Hückel Theory

The Hückel model for the chemist (or the analogous tight-binding model for the condensed-matter physicist) is an extremely simplified molecular orbital model [7], which nevertheless continues to play an important role in our understanding of electronic structures and properties. It emphasizes the molecule–graph analogy and uses what is now regarded as spectral graph theory [8, 9] in order to obtain molecular orbitals. Its strength comes from the fact that, in spite of the approximations involved, it incorporates the essential topological and symmetry aspects of electronic structures, and, as we keep repeating, these are simple but exact properties of complex molecular quantum-systems. Hückel theory is preferentially applied to molecular systems where each atom or node carries one atomic orbital, say $|\phi_i\rangle$. Molecular orbitals will be denoted as $|\Phi_k\rangle$. To find the molecular orbitals, one sets up the Hückel Hamiltonian matrix, which in its most simplified form is proportional to the adjacency matrix, $\mathbb{A}$, of the molecular graph. Elements of the adjacency matrix are zero, unless row and column index refer to neighboring nodes, in which case the matrix element is equal to one. The Hamiltonian matrix then is given by

$$\langle \phi_i | \mathcal{H} | \phi_j \rangle = \alpha \delta_{ij} + \beta A_{ij} \qquad (4.110)$$

or, in operator form,

$$\mathcal{H} = \sum_i \alpha |\phi_i\rangle\langle\phi_i| + \sum_{i \neq j} \beta A_{ij} |\phi_i\rangle\langle\phi_j| \qquad (4.111)$$

Here, α is the so-called Coulomb integral, which corresponds to the on-site interaction element. It defines the zero-point of energy and thus has only a symbolic significance in homogeneous systems. However, in hetero-atomic systems, it is important to differentiate the atoms. As an example, the Coulomb integral for nitrogen will be more negative than the one for carbon because the heavier nitrogen nucleus exerts a greater attraction on the electrons. The β parameter is the resonance or inter-site hopping integral. It represents a bonding interaction and thus is negative. The Hückel eigenvalues are thus of opposite sign as compared with the corresponding eigenvalues of the adjacency matrix. The molecular symmetry group is called in

to transform the atomic basis into SALCs according to the irreps of the point group. Molecular orbitals have a definite irrep and component symmetry and thus contain only SALCs with these same symmetry characteristics. Transforming the atomic basis into SALCs will reduce the Hamiltonian matrix to a set of smaller symmetry blocks. From the eigenfunctions one can determine π-contributions to properties such as the on-site atomic population, q_r, and the inter-site π-bond order, p_{rs}. The population of atom r and the bond order of the bond between atoms r and s are given by

$$
\begin{aligned}
q_r &= \sum_k n_k |c_r^k|^2 \\
p_{rs} &= \sum_k n_k \overline{c_r^k} c_s^k
\end{aligned}
\tag{4.112}
$$

Here, the index k runs over the eigenfunctions: n_k is the occupation number (0,1, or 2) of the kth eigenlevel, and c_r^k is the coefficient of the $|\phi_r\rangle$ atomic orbital for the normalized eigenfunction. The atomic populations are simply the densities or weights at the atomic sites and may vary between 0 and 2. The neutral atom has a population of one p_z-electron, and sites with $q_r < 1$ are cationic and with $q_r > 1$ anionic. The bond order adopts the form of a correlation coefficient between two sites. The π-bond order for a full π-bond in ethylene is equal to 1, and for benzene, it is 2/3. Below we shall examine in detail some special cases where symmetry plays an important role.

Cyclic Polyenes

Cyclic polyenes, also known as *annulenes*, are hydrocarbon rings, C_nH_n. Each carbon atom contributes one p_z-orbital, perpendicular to the plane of the ring, which gives rise to conjugated π-bonding. The prototype is the aromatic molecule benzene. The adjacency matrix has the form of a *circulant* matrix. This is a matrix where each row is rotated one element to the right relative to the preceding row. Because each atom is linked to only two neighbors, each row contains only two elements. These are arranged left and right of the diagonal, which is characteristic for a chain, but with additional nonzero elements in the upper right and lower left corners, where both ends of the chain meet. For benzene, it is given by

$$
\mathbb{A} =
\begin{pmatrix}
0 & 1 & 0 & 0 & 0 & 1 \\
1 & 0 & 1 & 0 & 0 & 0 \\
0 & 1 & 0 & 1 & 0 & 0 \\
0 & 0 & 1 & 0 & 1 & 0 \\
0 & 0 & 0 & 1 & 0 & 1 \\
1 & 0 & 0 & 0 & 1 & 0
\end{pmatrix}
\tag{4.113}
$$

The symmetry of an N-atom ring is D_{Nh}, but in practice the cyclic group C_N is sufficient to solve the eigenvalue problem. Atoms are numbered from 0 to $N-1$. The cyclic projection operator, $\hat{P}_k$, is given by

$$\hat{P}_k = \frac{1}{N} \sum_{j=0}^{N-1} \exp\left(2\pi i \frac{jk}{N}\right) \hat{C}_N^j \tag{4.114}$$

Projectors are characterized by an integer k in a periodic interval. We may choose the range $]-N/2, +N/2]$ as the standard interval. The total number of integers in this interval is N. Keeping in mind the active view, where the rotation axis will rotate all the orbitals one step further in a counterclockwise way, we now act with the projection operator on the starting orbital, $|\phi_0\rangle$:

$$\hat{P}_k|\phi_0\rangle = \frac{1}{N} \sum_{j=0}^{N-1} \exp\left(2\pi i \frac{jk}{N}\right) |\phi_j\rangle \tag{4.115}$$

The result is an unnormalized SALC, which we denote as $|\Phi_k\rangle$. Neglecting overlap between adjacent atoms, we obtain the normalized SALC as

$$|\Phi_k\rangle = \sqrt{N}\,\hat{P}_k|\phi_0\rangle \tag{4.116}$$

The transformation properties of this SALC under the rotation axis are characterized as

$$\hat{C}_N|\Phi_k\rangle = \frac{1}{\sqrt{N}} \sum_{j=0}^{N-1} \exp\left(2\pi i \frac{jk}{N}\right) |\phi_{j+1}\rangle$$

$$= \frac{1}{\sqrt{N}} \sum_{j=0}^{N-1} \exp\left(2\pi i \frac{(j-1)k}{N}\right) |\phi_j\rangle$$

$$= \exp\left(-2\pi i \frac{k}{N}\right) |\Phi_k\rangle \tag{4.117}$$

Applying this symmetry element N times is identical to the unit operation and raises the exponential factor in this expression to the Nth power:

$$\left(\exp\left(-2\pi i \frac{k}{N}\right)\right)^N = \exp(-2\pi i k) = 1 \tag{4.118}$$

Each integer value of k in the periodic interval $]-N/2, +N/2]$ thus characterizes a different SALC. The corresponding energy eigenvalues are also easily extracted:

$$E_k = \langle \Phi_k | \mathcal{H} | \Phi_k \rangle$$

$$= \frac{1}{N} \sum_{j,j'=0}^{N-1} \exp\left(2\pi i \frac{k(-j+j')}{N}\right) \langle \phi_j | \mathcal{H} | \phi_{j'} \rangle$$

Fig. 4.7 Hückel orbital
energy spectrum of benzene
as a function of index k, with
allowed values $0, \pm1, \pm2, 3$
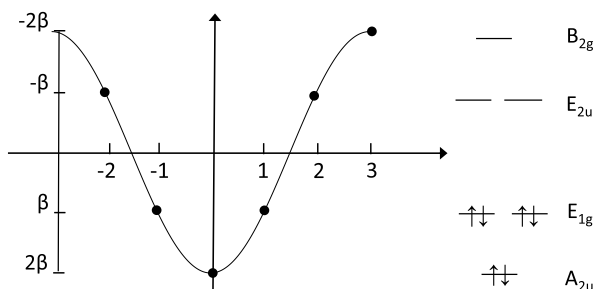
$$= \frac{1}{N} \sum_{j=0}^{N-1} \left(\alpha + \beta \left[\exp(-2\pi i k/N) + \exp(+2\pi i k/N) \right] \right)$$

$$= \alpha + 2\beta \cos(2\pi k/N) \tag{4.119}$$

The energies are thus seen to form N discrete levels, which are points on a cosine curve, as shown in Fig. 4.7. Except for $k = 0$, and in the case of N even, $k = N/2$, all levels E_k and E_{-k} are twofold-degenerate. Closed-shell structures thus will be realized for $N = 4n + 2$, which is the famous Hückel condition for aromaticity. These cyclic labels can easily be expanded to the full irrep designations of the D_{6h} symmetry group for benzene. The atomic p_z-orbitals transform as b_1 in the C_{2v} site group. In accord with the conventions for the D_{6h} point group symmetry, as pictured in Fig. 3.10, this site group is based on operators of type $\hat{C}'_2$ and $\hat{\sigma}_v$. The induced irrep of the six atomic orbitals then becomes

$$\Gamma(b_1 C_{2v} \uparrow D_{6h}) = A_{2u} + E_{1g} + E_{2u} + B_{2g} \tag{4.120}$$

Since each irrep occurs only once, there is a one-to-one correlation between these irreps and the cycle index k, which can be retrieved from the $D_{6h} \downarrow C_6$ subduction rules :

$$
\begin{aligned}
A_{2u} &\longrightarrow A \quad (k = 0) \\
E_{1g} &\longrightarrow E_1 \quad (k = \pm1) \\
E_{2u} &\longrightarrow E_2 \quad (k = \pm2) \\
B_{2g} &\longrightarrow B \quad (k = 3)
\end{aligned}
\tag{4.121}
$$

We will now engage in a more elaborate application of Hückel theory, which demonstrates the power of this simple model. The purpose is to determine the energy shifts of the eigenvalues when an annulene is brought into a uniform magnetic field, **B**. This field is independent of position and time. It can be defined as the "curl" (or rotation) of a vector potential **A**, and, in terms of a position vector **r** from a given

origin, the relevant relations are as follows:

$$\mathbf{B} = \nabla \wedge \mathbf{A}$$
$$\mathbf{A} = \frac{1}{2}\mathbf{B} \wedge \mathbf{r} \tag{4.122}$$

This implies that the divergence of the vector potential is zero, and hence $\mathbf{A}$ and ∇ commute: $[\nabla, \mathbf{A}] = \mathbf{0}$. The introduction of the magnetic field will add an extra term in the kinetic energy operator, which becomes

$$\begin{aligned}
T &= \frac{1}{2m}\left(\frac{\hbar}{i}\nabla + e\mathbf{A}\right)^2 \\
&= -\frac{h^2}{8\pi^2 m}\left(\nabla + i\frac{e}{\hbar}\mathbf{A}\right)^2 \\
&= -\frac{h^2}{8\pi^2 m}\left(\Delta + i\frac{e}{\hbar}\mathbf{A}\cdot\nabla + i\frac{e}{\hbar}\nabla\cdot\mathbf{A} - \frac{e^2}{\hbar^2}A^2\right) \\
&= -\frac{h^2}{8\pi^2 m}\left(\Delta + 2i\frac{e}{\hbar}\mathbf{A}\cdot\nabla - \frac{e^2}{\hbar^2}A^2\right)
\end{aligned} \tag{4.123}$$

where we have taken into account that the "del" (or nabla) operator and the vector potential commute. The electron charge is $-e$. London proposed that the atomic basis functions should be multiplied by a phase factor, which explicitly depends on the vector potential [10]. In this London gauge the atomic orbitals are rewritten as

$$|\chi_j\rangle = \exp\left(-i\frac{e}{\hbar}\mathbf{A}_j\cdot\mathbf{r}\right)|\phi_j\rangle \tag{4.124}$$

where $\mathbf{A}_j$ is the vector potential at the position of the jth atom. The effect of this phase factor is to move the origin of the vector potential from an arbitrary origin to the local position of atom j. The action of the del operator and Laplacian on this gauge is given by

$$\nabla\exp\left(-i\frac{e}{\hbar}\mathbf{A}_j\cdot\mathbf{r}\right) = \exp\left(-i\frac{e}{\hbar}\mathbf{A}_j\cdot\mathbf{r}\right)\left(-i\frac{e}{\hbar}\mathbf{A}_j + \nabla\right)$$
$$\Delta\exp\left(-i\frac{e}{\hbar}\mathbf{A}_j\cdot\mathbf{r}\right) = \exp\left(-i\frac{e}{\hbar}\mathbf{A}_j\cdot\mathbf{r}\right)\left(-\frac{e^2}{\hbar^2}A_j^2 - 2i\frac{e}{\hbar}\mathbf{A}_j\cdot\nabla + \Delta\right) \tag{4.125}$$

Combining this result with Eqs. (4.123) and (4.124) yields

$$T|\chi_j\rangle = -\frac{h^2}{8\pi^2 m}\exp\left(-i\frac{e}{\hbar}\mathbf{A}_j\cdot\mathbf{r}\right)$$
$$\times\left[\Delta + 2i\frac{e}{\hbar}(\mathbf{A}-\mathbf{A}_j)\cdot\nabla - \frac{e^2}{\hbar^2}(\mathbf{A}-\mathbf{A}_j)\cdot(\mathbf{A}-\mathbf{A}_j)\right]|\phi_j\rangle \tag{4.126}$$

The first term in the brackets is the usual kinetic energy term, while the second term produces the orbital Zeeman effect. The third term describes the second-order interactions corresponding to the atomic contribution to the susceptibility. The second term can easily be converted into the more familiar form of the Zeeman operator as follows:

$$\frac{e}{m}(\mathbf{A} - \mathbf{A}_j) \cdot \left(\frac{\hbar}{i}\nabla\right) = \frac{e}{2m}\mathbf{B} \cdot \left[(\mathbf{r} - \mathbf{R}_j) \wedge \mathbf{p}\right]$$
$$= \frac{e}{2m}\boldsymbol{l} \cdot \mathbf{B}$$
$$= -\boldsymbol{m} \cdot \mathbf{B} \tag{4.127}$$

Here, $\mathbf{p}$ is the momentum operator of the electron in atom j, $\boldsymbol{l}$ is the corresponding angular momentum operator, and $\boldsymbol{m}$ is the magnetic dipole operator. These operators are related by

$$\boldsymbol{m} = -\frac{e}{2m}\boldsymbol{l} = -\frac{\mu_B}{\hbar}\boldsymbol{l} \tag{4.128}$$

Here μ_B is the Bohr magneton. Angular momentum is thus expressed in units of $\hbar$, and the magnetic moment in units of the Bohr magneton. The basis atomic orbitals will be eigenfunctions of the first two operators. So to first order the London basis orbitals are eigenfunctions of the total Hamiltonian. Moreover, for a p_z-orbital, the Zeeman effect for a magnetic field along the z-axis vanishes. As a result, the on-site parameter α is independent of the London gauge:

$$\langle\chi_j|\mathcal{H}|\chi_j\rangle = \alpha\langle\chi_j|\chi_j\rangle = \alpha \tag{4.129}$$

However, the inter-site integrals, which depend on the potential energy, V, are influenced by the gauge factors:

$$\langle\chi_i|V|\chi_j\rangle = \left\langle\phi_i\left|V\exp\left(i\frac{e}{\hbar}(\mathbf{A}_i - \mathbf{A}_j)\cdot\mathbf{r}\right)\right|\phi_j\right\rangle \tag{4.130}$$

At this point London introduced an important approximation by replacing the variable position vector in this equation by the position vector (relative to the arbitrary origin) of the center of the bond between the two atoms:

$$\mathbf{r} = (\mathbf{R}_i + \mathbf{R}_j)/2 \tag{4.131}$$

In this approximation the phase factor is turned into a constant, which can be removed from the brackets. One has:

$$\frac{1}{2}(\mathbf{A}_i - \mathbf{A}_j)\cdot(\mathbf{R}_i + \mathbf{R}_j) = \frac{1}{4}\left[(\mathbf{B}\wedge\mathbf{R}_i)\cdot\mathbf{R}_j - (\mathbf{B}\wedge\mathbf{R}_j)\cdot\mathbf{R}_i\right]$$
$$= \frac{1}{2}\mathbf{B}\cdot(\mathbf{R}_i \wedge \mathbf{R}_j)$$
$$= \mathbf{B}\cdot\mathbf{S}_{ij} \tag{4.132}$$

Fig. 4.8 Triangular surface
vector: $\mathbf{S}_{j,j+1} = \frac{1}{2}\mathbf{R}_j \wedge \mathbf{R}_{j+1}$
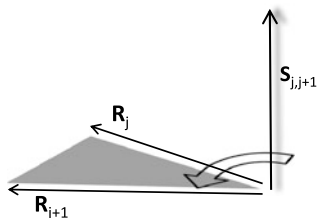
Here $\mathbf{S}_{ij}$ is the directed area of the triangle formed by the position vectors of the atoms i and j from the origin, as shown in Fig. 4.8. The orientation of the vector $\mathbf{S}_{ij}$ follows the right thumb rule. So if the atom numbers increase counterclockwise, this vector will be oriented in the positive z-direction. One also has:

$$\mathbf{S}_{ij} = -\mathbf{S}_{ji} \tag{4.133}$$

The interaction elements in the Hückel matrix are thus replaced by

$$\langle\chi_i|V|\chi_j\rangle = \exp\left(i\frac{e}{\hbar}\mathbf{B}\cdot\mathbf{S}_{ij}\right)\beta$$
$$\langle\chi_j|V|\chi_i\rangle = \exp\left(-i\frac{e}{\hbar}\mathbf{B}\cdot\mathbf{S}_{ij}\right)\beta \tag{4.134}$$

We further define a vector $\mathbf{S}$ as

$$\sum_{j=0}^{N-1}\mathbf{S}_{j,j+1} = \mathbf{S} \tag{4.135}$$

The magnitude of this vector is equal to the area of the polygon. Because of cyclic symmetry, we can also write

$$\mathbf{S}_{j,j+1} = \frac{1}{N}\mathbf{S} \tag{4.136}$$

The action of the symmetry operators on the London gauge is as follows:

$$\hat{C}_N \exp\left(-i\frac{e}{\hbar}\mathbf{A}_j\cdot\mathbf{r}\right) = \exp\left[-i\frac{e}{\hbar}\mathbf{A}_j\cdot(\hat{C}_N^{-1}\mathbf{r})\right]$$
$$= \exp\left(-i\frac{e}{\hbar}\mathbf{A}_{j+1}\cdot\mathbf{r}\right) \tag{4.137}$$

which may easily be proven by writing out $\mathbf{A}_j$ and $\hat{C}_N^{-1}\mathbf{r}$ in full. Hence, the rotation axis will perform a cyclic permutation of the $|\chi_j\rangle$ kets, exactly in the same way as for the $|\phi_j\rangle$ kets. The magnetic field reduces the D_{nh} symmetry of the regular polygon to C_{nh} (see Appendix B), so the cyclic symmetry is conserved, and thus the projection operators of Eq. (4.114) remain valid, and so do the eigenfunctions.

We shall denote these as $|\Psi_k\rangle$. One has:

$$|\Psi_k\rangle = \frac{1}{\sqrt{N}} \sum_{j=0}^{N-1} \exp\left(2\pi i \frac{jk}{N}\right)|\chi_j\rangle \tag{4.138}$$

The corresponding eigenvalues can be worked out in the same way as in the absence of the field (see Eq. (4.119)):

$$E_k = \langle \Psi_k|\mathcal{H}|\Psi_k\rangle$$

$$= \frac{1}{N} \sum_{j,j'=0}^{N-1} \exp\left(2\pi i \frac{k(-j+j')}{N}\right)\langle\chi_j|\mathcal{H}|\chi_{j'}\rangle$$

$$= \alpha + \frac{1}{N} \sum_{j=0}^{N-1} \beta\left[\exp\left(-\frac{2\pi i k}{N} + i\frac{e}{\hbar}\mathbf{B}\cdot\mathbf{S}_{j,j-1}\right) + \exp\left(\frac{2\pi i k}{N} + i\frac{e}{\hbar}\mathbf{B}\cdot\mathbf{S}_{j,j+1}\right)\right]$$

$$= \alpha + 2\beta\cos\left[\frac{2\pi}{N}\left(k + \frac{e}{\hbar}\mathbf{B}\cdot\mathbf{S}\right)\right] \tag{4.139}$$

The result is of the same form as in the absence of the field, except for a shift of the quantum number k under the influence of the magnetic field. The magnitude of this shift, $e/\hbar\mathbf{B}\cdot\mathbf{S}$, is equal to the magnetic flux through the area of the ring, multiplied by the constant $e/\hbar$. As a result of this shift, the energy levels that were originally degenerate now display a Zeeman splitting. For $\mathbf{B}\cdot\mathbf{S} > 0$, the Zeeman contribution adds to k in the energy expression. This implies that the points on the k axis in Fig. 4.7 are displaced to the right. The roots with $k = 1, 2$ thus increase in energy, while their counterparts, $k = -1, -2$, become lower in energy. Likewise, the root at the bottom ($k = 0$) increases in energy, while the root at the top, $k = 3$, decreases, but the changes in these extremal points are only of second order.

This simple model is at the basis of a whole corpus of electromagnetic studies of conjugated polyenes, involving, inter alia, the calculation of magnetic susceptibilities, current densities, ring currents, and chemical shifts in nuclear magnetic resonance (NMR). From the point of view of symmetry, it is to be noted that the magnetic field has removed all degeneracies. The time-reversal symmetry is indeed no longer valid. However, if one reverses the momenta, $k \to -k$, and at the same time switches the magnetic field, $\mathbf{B} \to -\mathbf{B}$, the energies are still invariant. This operation is no longer an invariance operation of one measurement though, but rather a comparison between two separate experiments with opposite fields.

Polyhedral Hückel Systems of Equivalent Atoms

The polygonal system of the annulenes can be extended to polyhedral systems of equivalent atoms. Atoms are equivalent if the symmetry group of the molecule—or

more generally the automorphism group of the molecular graph—acts transitively on the set of atomic nodes. So, for any pair of atoms $\langle k \rangle \langle l \rangle$, there is a symmetry element that will map $\langle k \rangle$ onto $\langle l \rangle$, and then of course there is always an inverse element that maps $\langle l \rangle$ onto $\langle k \rangle$. The solution of the Hamiltonian matrix for such a system can almost entirely be performed by symmetry arguments. The first step consists in the construction of SALCs, using the projection operators on the atomic orbital on site $\langle a \rangle$:

$$|\Phi_{ik}^{\Omega}\rangle = \hat{P}_{ik}^{\Omega}|\phi_{\mathrm{A}}\rangle = \frac{\dim(\Omega)}{|G|} \sum_{R \in G} \bar{D}_{ik}^{\Omega}(R)\hat{R}|\phi_{\mathrm{A}}\rangle \qquad (4.140)$$

These functions are not yet normalized. This can be done later. Let us first consider a general matrix element:

$$\langle \Phi_{ik}^{\Omega}|\mathcal{H}|\Phi_{jl}^{\Omega'}\rangle = \frac{\dim(\Omega)^2}{|G|^2} \sum_{R,S} D_{ik}^{\Omega}(R)\bar{D}_{jl}^{\Omega'}(S)\langle \hat{R}\phi_{\mathrm{A}}|\mathcal{H}|\hat{S}\phi_{\mathrm{A}}\rangle$$

$$= \frac{\dim(\Omega)^2}{|G|^2} \sum_{R,Q} D_{ik}^{\Omega}(R)\bar{D}_{jl}^{\Omega'}(RQ)\langle \hat{R}\phi_{\mathrm{A}}|\mathcal{H}|\hat{R}\hat{Q}\phi_{\mathrm{A}}\rangle$$

$$= \frac{\dim(\Omega)^2}{|G|^2} \sum_{R,Q} \sum_{m} D_{ik}^{\Omega}(R)\bar{D}_{jm}^{\Omega'}(R)\bar{D}_{ml}^{\Omega'}(Q)\langle \phi_{\mathrm{A}}|\hat{R}^{-1}\mathcal{H}\hat{R}|\hat{Q}\phi_{\mathrm{A}}\rangle$$

$$= \frac{\dim(\Omega)}{|G|}\delta_{\Omega\Omega'}\delta_{ij} \sum_{Q} \bar{D}_{kl}^{\Omega}(Q)\langle \phi_{\mathrm{A}}|\mathcal{H}|\hat{Q}\phi_{\mathrm{A}}\rangle \qquad (4.141)$$

The by-now experienced reader has recognized in the second line of this derivation the use of a substitution, $\hat{S} \to \hat{R}\hat{Q}$, as well as the invariance of the Hamiltonian under the symmetry transformation in the third line. Let us now use this equation to normalize the SALCs. This can be done by simply setting the Hamiltonian equal to unity. Adopting the Hückel approximation, which neglects all overlaps between the sites, we obtain:

$$\langle \Phi_{ik}^{\Omega}|\Phi_{ik}^{\Omega}\rangle = \frac{\dim(\Omega)}{|G|} \sum_{Q} \bar{D}_{kk}^{\Omega}(Q)\delta_{Q,E} = \frac{\dim(\Omega)}{|G|} \qquad (4.142)$$

Hence, the normalized SALCs should be redefined as

$$|\Phi_{ik}^{\Omega}\rangle = \sqrt{\frac{\dim(\Omega)}{|G|}} \sum_{R \in G} \bar{D}_{ik}^{\Omega}(R)\hat{R}|\phi_{\mathrm{A}}\rangle \qquad (4.143)$$

The matrix elements are accordingly simplified to

$$\langle \Phi_{ik}^{\Omega}|\mathcal{H}|\Phi_{il}^{\Omega}\rangle = \sum_{Q} \bar{D}_{kl}^{\Omega}(Q)\langle \phi_{\mathrm{A}}|\mathcal{H}|\hat{Q}\phi_{\mathrm{A}}\rangle \qquad (4.144)$$
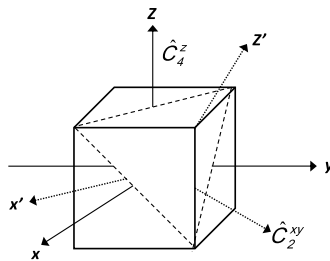
The Hückel approximation considers only hopping between nearest neighbors, and hence the sum in this expression is limited to only those operators that link the starting site to its neighbours. We thus do not need all the irrep matrices, but only a few of them. As an example, the cube is a trivalent polyhedron, i.e., each atom has three bonds to its neighbors. The neighbors of site $\langle a \rangle$ can be reached by $\hat{C}_4$, $\hat{C}_4^{-1}$, $\hat{C}_2^{xy}$, where the twofold axis belongs to the $6\hat{C}_2'$ class. We thus need to know the irrep matrices for these three elements only. In principle, according to the above derivation, for each component of each irrep, we can, by varying the index k, construct a number of projection operations which is equal to $\dim(\Omega)$. As we have already discussed, we effectively need all these only when the induced representation of the atoms is equal to the regular representation. This is the case if the number of atoms is equal to the order of the group, i.e., when there are no symmetry elements "going through" the atoms, so that their site group is the trivial C_1. For octahedral symmetry, this is a polyhedron with 48 vertices. It belongs to the family of the Archimedean solids and is known as the *great rhombicuboctahedron*. The highest Archimedean solid is a polyhedron with 120 equivalent vertices, which is known as the *great rhombicosidodecahedron*.[3] The representation of its vertices is the regular representation of the group I_h. In the case where the number of atoms is less, and thus the site symmetry is higher, the projection operators will give rise to redundancies. To avoid these, we can make use of the Frobenius reciprocity theorem. The number of times a given irrep occurs in the induction is exactly equal to the number of times it subduces the totally symmetric irrep at the site group. The number of projection operations should thus also be restricted to this number. This can be achieved when the $\mathbb{D}^\Omega$ matrices are constructed in such a way that they are block diagonal in the stabilizing sitegroup of site $\langle a \rangle$. In that case the k indices of the projection operators should then be chosen in such a way that they correspond to components that are totally symmetric in that sitegroup.[4] As an example, consider the cube. The site group is C_{3v}, and induction tells us that the function space, spanned by the 8 atoms, is given by

$$\Gamma(a_1 C_{3v} \uparrow Oh) = A_{1g} + T_{2g} + T_{1u} + A_{2u} \tag{4.145}$$

---

[3]Calculations predict that a C_{120} molecular realization of this solid should exist. See [11, 12].

[4]For more elaborate treatments, including the use of the Cayley graph, see [13, 14].

All these irreps occur only once; hence, when we choose a trigonal symmetry adaptation for constructing representation matrices, for all these matrices, there will be exactly one index k that labels the component that is totally symmetric in C_{3v}. For this value, the matrix elements read

$$\langle \Phi_{ik}^{\Omega}|\mathcal{H}|\Phi_{ik}^{\Omega}\rangle = \beta\big[\bar{D}_{kk}^{\Omega}(C_4) + \bar{D}_{kk}^{\Omega}\big(C_4^{-1}\big) + \bar{D}_{kk}^{\Omega}(C_2)\big] \tag{4.146}$$

To obtain these eigenvalues, we thus have to mould the representation matrices for O_h in a trigonal setting. For the one-dimensional irreps, A_{1g} and A_{2u}, this is trivial since the matrix elements in Eq. (4.146) are simply the characters. We thus obtain:

$$E(A_{1g}) = \beta\big[\chi^{A_{1g}}(C_4) + \chi^{A_{1g}}\big(C_4^{-1}\big) + \chi^{A_{1g}}(C_2)\big] = 3\beta$$
$$E(A_{2u}) = \beta\big[\chi^{A_{2u}}(C_4) + \chi^{A_{2u}}\big(C_4^{-1}\big) + \chi^{A_{2u}}(C_2)\big] = -3\beta \tag{4.147}$$

For the T_{1u} irrep, we can use the set of the p-orbitals. In the standard Cartesian orientation, this set is adapted to the tetragonal site symmetry. In Fig. 4.9 we illustrate an alternative trigonal basis (see also Fig. 3.6(d)). The transformation between the two sets is given by

$$|p_z'\rangle = \frac{1}{\sqrt{3}}\big(|p_x\rangle + |p_y\rangle + |p_z\rangle\big)$$

$$|p_x'\rangle = \frac{1}{\sqrt{2}}\big(|p_x\rangle - |p_y\rangle\big) \tag{4.148}$$

$$|p_y'\rangle = \frac{1}{\sqrt{6}}\big(|p_x\rangle + |p_y\rangle - 2|p_z\rangle\big)$$

Here, the first component points in the threefold direction and thus is adapted to the C_{3v} site symmetry. We require only the diagonal matrix elements for this component. They can easily be obtained by expressing these elements in the standard canonical set:

$$D_{z'z'}(C_4) = \langle p_z'|\hat{C}_4|p_z'\rangle$$

$$= \frac{1}{3}\big(\langle p_x| + \langle p_y| + \langle p_z|\big)\hat{C}_4\big(|p_x\rangle + |p_y\rangle + |p_z\rangle\big)$$

$$= \frac{1}{3}\big(\langle p_x| + \langle p_y| + \langle p_z|\big)\big(|p_y\rangle - |p_x\rangle + |p_z\rangle\big) = \frac{1}{3}$$

$$D_{z'z'}\big(C_4^{-1}\big) = \langle p_z'|\hat{C}_4^{-1}|p_z'\rangle$$

$$= \frac{1}{3}\big(\langle p_x| + \langle p_y| + |p_z\rangle\big)\hat{C}_4^{-1}\big(|p_x\rangle + |p_y\rangle + |p_z\rangle\big)$$

$$= \frac{1}{3}\big(\langle p_x| + \langle p_y| + \langle p_z|\big)\big(-|p_y\rangle + |p_x\rangle + |p_z\rangle\big) = \frac{1}{3}$$

$$D_{z'z'}(C_2') = \langle p_z' | \hat{C}_2' | p_z' \rangle$$

$$= \frac{1}{3} (\langle p_x | + \langle p_y | + \langle p_z |) \hat{C}_2' (|p_x\rangle + |p_y\rangle + |p_z\rangle)$$

$$= \frac{1}{3} (\langle p_x | + \langle p_y | + \langle p_z |) (|p_y\rangle + |p_x\rangle - |p_z\rangle) = \frac{1}{3} \quad (4.149)$$

An entirely similar derivation can be made for the T_{2g} irrep, using the d-orbital set. The results are:

$$\begin{aligned} E(T_{1u}) &= \beta \\ E(T_{2g}) &= -\beta \end{aligned} \quad (4.150)$$

Triphenylmethyl Radical and Hidden Symmetry

As a final application, we discuss an example of a molecular radical, where more symmetry is present than the eye meets. The triphenylmethyl radical, $C_{19}H_{15}$, is a planar, conjugated, hydrocarbon-radical, with 19 π-electrons. The molecular point group for the planar configuration is D_{3h}, but, since all valence $2p_z$-orbitals are antisymmetric with respect to the horizontal symmetry plane, the relevant symmetry of the valence shell is only C_{3v} as seen from Fig. 4.10. The molecular symmetry group distributes the 19 atoms over five trigonal orbits of atoms that, under C_{3v}, can solely be permuted with partners in the same orbit.

1. The central atom $\{o\}$.
2. The three atoms that are adjacent to o: $\{a, b, c\}$.
3. The six atoms in the *ortho* positions: $\{d, e, f, g, h, i\}$.
4. The six atoms in the *meta* positions: $\{p, q, r, s, t, u\}$.
5. The three atoms in the *para* positions: $\{x, y, z\}$.

The separate rotation of a single phenyl group by 180° around its twofold direction will not change the connectivity of the graph. Yet this cannot be achieved by elements of the point group. It is, however, a legitimate symmetry operation as far as the graph is concerned since it preserves the connectivity. The resulting automorphism group is thus larger than the point group and in fact is isomorphic to O_h [15]. The three phenyl groups can be associated with the three Cartesian directions of this octahedral group. The six atoms in the ortho orbit can be formally associated with the six corners of this octahedron, each connected to a meta position (Fig. 4.10). This implies that the ortho and meta atoms occupy C_{4v} sites. The three-atom orbits correspond to the three tetragonal directions in the octahedron. The site group that leaves such a tetragonal direction invariant is not of the conical C_{nv} type, but D_{4h}. These correspondences allow identification of all the permutations. As examples, the $\hat{C}_4$ symmetry element through the upper phenyl group and the $\hat{S}_6$ rotation–reflection
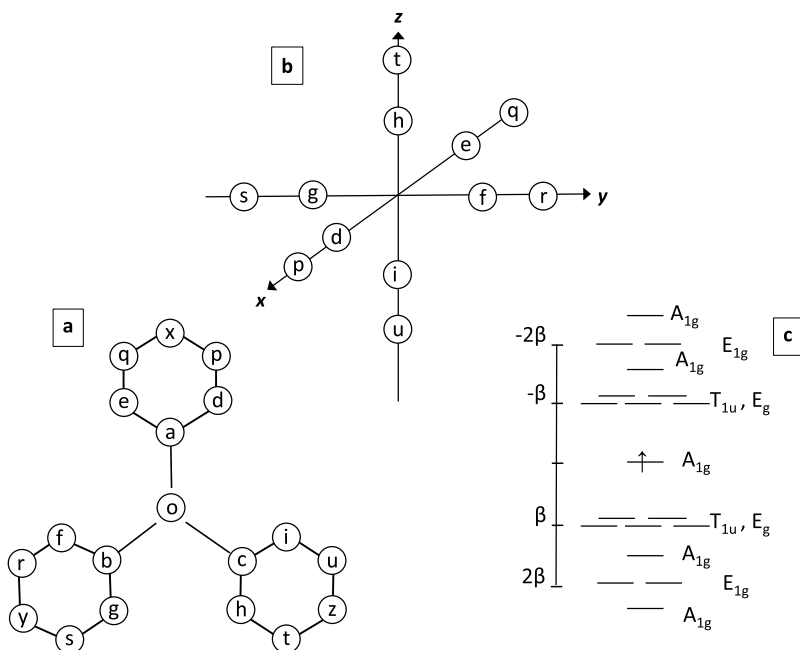
Fig. 4.10 (**a**) molecular graph of triphenylmethyl, (**b**) correspondence between ortho and meta sites and octahedral C_{4v} positions, and (**c**) Hückel spectrum

extension along the threefold direction of the trigonal axis of the molecular frame permute the atoms as follows:

$$\hat{C}_4 \rightarrow (o)(a)(d)(p)(x)(q)(e)(b,c)(y,z)(f,h,g,i)(r,t,s,u)$$

$$\hat{S}_6 \rightarrow (o)(a,c,b)(x,z,y)(d,i,f,e,h,g)(p,u,r,q,t,s)$$

$$(4.151)$$

A horizontal coordinate plane, $\hat{\sigma}_h$, of the octahedron has the effect of flipping one single phenyl group around. We can at once determine the irreps of the different orbits by induction:

$$\{a,b,c\} : \Gamma(a_{1g}D_{4h} \uparrow O_h) = A_{1g} + E_g$$

$$\{x,y,z\} : \Gamma(a_{1g}D_{4h} \uparrow O_h) = A_{1g} + E_g$$

$$\{d,e,f,g,h,i\} : \Gamma(a_1C_{4v} \uparrow O_h) = A_{1g} + E_g + T_{1u}$$

$$\{p,q,r,s,t,u\} : \Gamma(a_1C_{4v} \uparrow O_h) = A_{1g} + E_g + T_{1u}$$

$$(4.152)$$

The central atom is invariant in O_h and thus transforms as A_{1g}. The total induced representation of the function space thus is given by

$$\Gamma = 5A_{1g} + 4E_g + 2T_{1u} \tag{4.153}$$

The 19-dimensional Hückel matrix thus will be resolved into five blocks, one of dimension 5, two identical blocks of dimension 4, and three identical blocks of dimension 2. In Table 4.9 we display the blocks for each irrep and the corresponding SALCs for one component. The corresponding secular equations are:

$$A_{1g} : \lambda\left(\lambda^4 - 8\lambda^2 + 13\right)^2 = 0$$

$$E_g : \lambda^4 - 5\lambda^2 + 4 = 0$$

$$T_{1u} : \lambda^2 - 1 = 0 \tag{4.154}$$

Symmetry has taken us to a point where still quintic, quartic, and quadratic secular equations must be solved. However, a closer look at this equations shows that they can easily be solved. Apparently, a further symmetry principle is present, which leads to simple analytical solutions of the secular equations. Triphenylmethyl is an *alternant* hydrocarbon. In an alternant, atoms can be given two different colors in such a way that all bonds are between atoms of different colors; hence, no atoms of the same color are adjacent. A graph with this property is *bipartite*,[5] and its eigenvalue spectrum obeys the celebrated Coulson–Rushbrooke theorem [16].

Theorem 8 *The eigenvalues of an alternant are symmetrically distributed about the zero energy level. The corresponding eigenfunctions also show a mirror relationship, except for a difference of sign (only) in every other atomic orbital coefficient. The total charge density at any carbon atom in the neutral alternant hydrocarbon equals unity.*

Since triphenylmethyl is an odd alternant, there should be at least one eigenvalue at energy zero. This root will be necessarily of A_{1g} symmetry since this is the only irrep that occurs an odd number of times. All other roots occur in pairs of opposite energies. This is confirmed by the secular equations in Eq. (4.154), where the A_{1g} equation indeed has a root at $\lambda = 0$, and all remaining equations contain only even powers of λ. The roots are then easily determined (see also Fig. 4.10):

$$A_{1g} : \lambda = 0, \pm\sqrt{4 \pm \sqrt{3}}$$

$$E_g : \lambda = \pm 1, \pm 2 \tag{4.155}$$

$$T_{1u} : \lambda = \pm 1$$

---

[5]Note that in fact a molecular graph will always be bipartite unless it contains one or more odd-membered rings.

Table 4.9 SALCs and Hückel matrices, in units of β, for triphenylmethyl. For the degenerate irreps, only one component is given

A$_{1g}$

$\lvert o \rangle$	$-\lambda$	$\sqrt{3}$	0	0	0
$1/\sqrt{3}(\lvert a \rangle + \lvert b \rangle + \lvert c \rangle)$	$\sqrt{3}$	$-\lambda$	0	$\sqrt{2}$	0
$1/\sqrt{3}(\lvert x \rangle + \lvert y \rangle + \lvert z \rangle)$	0	0	$-\lambda$	0	$\sqrt{2}$
$1/\sqrt{6}(\lvert d \rangle + \lvert e \rangle + \lvert f \rangle + \lvert g \rangle + \lvert h \rangle + \lvert i \rangle)$	0	$\sqrt{2}$	0	$-\lambda$	1
$1/\sqrt{6}(\lvert p \rangle + \lvert q \rangle + \lvert r \rangle + \lvert s \rangle + \lvert t \rangle + \lvert u \rangle)$	0	0	$\sqrt{2}$	1	$-\lambda$

E$_g$

$1/\sqrt{2}(\lvert b \rangle - \lvert c \rangle)$	$-\lambda$	0	$\sqrt{2}$	0
$1/\sqrt{2}(\lvert y \rangle - \lvert z \rangle)$	0	$-\lambda$	0	$\sqrt{2}$
$1/2(\lvert f \rangle + \lvert g \rangle - \lvert h \rangle - \lvert i \rangle)$	$\sqrt{2}$	0	$-\lambda$	1
$1/2(\lvert r \rangle + \lvert s \rangle - \lvert t \rangle - \lvert u \rangle)$	0	$\sqrt{2}$	1	$-\lambda$

T$_{1u}$

$1/\sqrt{2}(\lvert d \rangle - \lvert e \rangle)$	$-\lambda$	1
$1/\sqrt{2}(\lvert p \rangle - \lvert q \rangle)$	1	$-\lambda$

The spectrum contains unexpected fivefold degeneracies at $E = \pm\beta$, where the T_{1u} and E_g levels coincide. This degeneracy is considered *accidental*, to the extent that it does not correspond to a single irrep of the automorphism group of the graph. However, the fivefold degeneracy can easily be rationalized as follows: $E = \beta$ is the eigenenergy of the degenerate highest occupied molecular orbital (HOMO) in an isolated phenyl-ring. The three rings thus give rise to six orbitals with this energy. The symmetry of this orbital space in O_h is equal to $A_{1g} + E_g + T_{1u}$. Of these only the A_{1g} combination is of the right symmetry to interact with the central atom. For the five others, there can be no communication between the phenyl rings since the channel via the central atom is open only to A_{1g} symmetries. As a result, for these solutions, there is no overlap between the rings, and five isolated phenyl solutions persist at $E = \beta$. A similar argument applies to the level $E = -\beta$, which stems from the phenyl lowest unoccupied orbital (LUMO).

Many features thus come together in triphenylmethyl. Besides the C_{3v} molecular point group, the Hückel matrix obeys an additional or hidden O_h symmetry. This is a typical feature of the nearest-neighbor approximation, which requires only that symmetry operations should preserve the connections with the nearest neighbors. This precisely complies with the definition of the automorphism group of the graph. Furthermore, the special bipartite properties of the graph further impose constraints on the spectrum, which in this case lead to a complete reduction of the secular equations. Finally, an unexpected additional degeneracy manifests itself, which is related

to the composite nature of the molecule being considered, with several fragments
bound to one central atom.

4.10 Problems

4.1 A Schlegel diagram of a polyhedron is a projection into a plane figure. The fig-
ure below shows the Schlegel diagram for a dodecahedron. As was explained
in the preceding chapter (see Fig. 3.8(a)), a dodecahedron contains five cubes,
e.g., the cube based on the nodes $\langle 1, 3, 9, 10, a, c, i, j \rangle$. Symmetry elements of
I_h permute these cubes. Construct the set of the five cubes and determine the
irreps of this set. Can you obtain this result by induction?
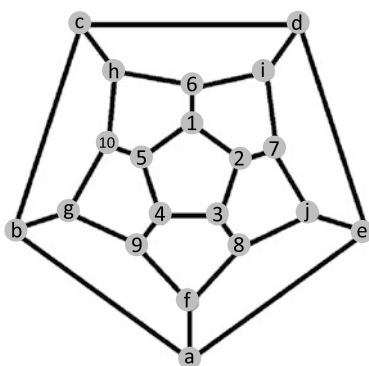
4.2 Consider the set of eight tangential π-orbitals on a tetrahedron. Derive the
irreducible representations in the T_d point group. How would you label the
canonical symmetry of the combinations that are shown in the figure below?
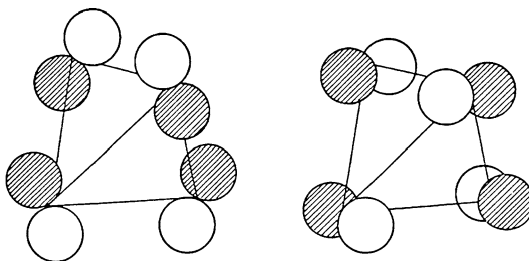
4.3 Consider the set of perpendicular p_z-orbitals in the polyaromatic planar
molecule coronene shown below. This set gives rise to a symmetry of molec-
ular orbitals of a_{1u} and b_{1g} . Can you draw both these orbitals? (Use the stan-
dard orientation of the central benzene frame, as shown in Fig. 3.10)
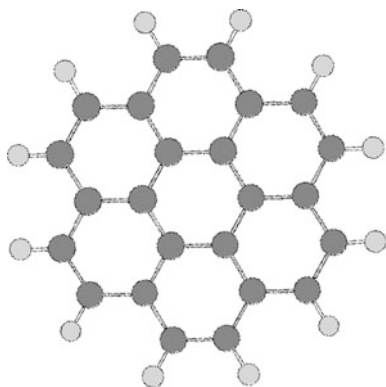
4.4 In dodecaborane, $B_{12}H_{12}^{2-}$, the twelve boron atoms occupy the vertices of an icosahedral cage. Determine the irreducible representations of the set of their tangential π-orbitals.

4.5 Consider a degenerate manifold, transforming as the irrep Γ_i. The appropriate projector was applied to the basis to yield one component of the degeneracy space. Which other projectors do you need to use to generate all the remaining components?

4.6 Consider the expression for a totally symmetric projection operator and demonstrate that it is indeed totally symmetric under any group element.

4.7 Construct the three sp^2 hybrids in the xy plane.

4.8 The picture below shows the distortion of an equilateral triangle. Determine the representation of this distortion.
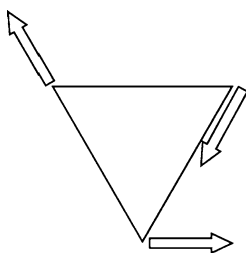
4.9 Construct the character table for a cyclic group of order 5.

4.10 In a molecule with D_{6h} symmetry, the choice of $\hat{C}_2'$ and $\hat{C}_2''$ directions is arbitrary, but, once the twofold directions are chosen, the $\hat{\sigma}_v$ and $\hat{\sigma}_d$ reflection planes are also fixed, as was indicated in Fig. 3.10. Show that these spatial relationships between the axes and the planes is in line with the character table for D_{6h}.

4.11 Consider a molecule with D_{3h} symmetry and apply a distortion mode that transforms according to the a_2'' irrep. A distortion along this coordinate breaks

the original symmetry to a subgroup of D_{3h}. Which subgroup? Try to generalize this example to a general rule.

4.12 Below is shown the Schlegel diagram for the C_{24} fullerene. It is a cage structure with hexagonal faces at top and bottom, capping a crown of twelve pentagons around its waist. The valence shell of this structure is formed by a set of 24 radial p_σ-orbitals, one on each carbon. Determine the point group of this molecule and the irreps describing the valence shell. (Hint: divide the set of 24 orbitals into two separate orbits.)
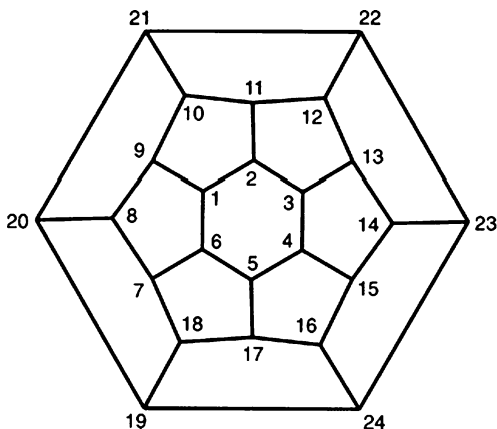
References

1. Mulliken, R.S.: Report on notation for the spectra of polyatomic molecules. J. Chem. Phys. **23**, 1997 (1955)
2. Altmann, S.L.: Induced Representations in Crystals and Molecules. Academic Press, London (1977)
3. Ceulemans, A.: The construction of symmetric orbitals for molecular clusters. Mol. Phys. **54**, 161 (1985)
4. Shimanouchi, T.: Tables of Molecular Vibrational Frequencies Consolidated, Vol. I. National Bureau of Standards, Gaithersburg, Maryland (1972)
5. Yun-Guang, Z., Yu-De, L.: Relativistic density functional investigation of UX$_6$ (X=F, Cl, Br and I). Chin. Phys. **19**, 033302 (2010)
6. Aldridge, J.P., et al.: Measurement and analysis of the infrared-active stretching fundamental (ν_3) of UF$_6$. J. Chem. Phys. **83**, 34 (1985)
7. Salem, L.: The Molecular Orbital Theory of Conjugated Systems. W. A. Benjamin, New York and Amsterdam (1966)
8. Coulson, C.A., O'Leary, B., Mallion, R.B.: Hückel Theory for the Organic Chemists. Academic Press, London (1978)
9. Cvetković, D.M., Doob, M., Sachs, H.: Spectra of Graphs, 3rd edn. Johann Ambrosius Barth Verlag, Heidelberg (1995)

10. London, F.: Théorie quantique des courants interatomiques dans les combinaisons aromatiques. J. Phys. Radium **8**, 397 (1937)
11. Schulman, J.M., Dish, R.L.: Archimedene. Chem. Phys. Lett. **262**, 813 (1996)
12. Bruns, D., Miura, H., Vollhardt, K.P., Stanger, A.: En route to archimedene: total synthesis of C_{3h}-symmetric [7]phenylene. Org. Lett. **5**, 549 (2003)
13. Fowler, P.W., Ceulemans, A., Chibotaru, L.F.: Eigenvalues of Hückel systems of equivalent points. Discrete Math. **212**, 75 (2000)
14. Samuel, S.: On the electronic structure of C_{60}. Int. J. Mod. Phys. B **7**, 3877 (1993)
15. Ojha, P.C.: Analysis of degeneracy in the spectrum of a class of molecular graphs. Int. J. Quant. Chem. **35**, 687 (1989)
16. Mallion, R.B., Rouvray, D.H.: The golden jubilee of the Coulson–Rushbrooke pairing theorem. J. Math. Chem. **5**(1), 399 (1990). See also J. Math. Chem. 8, 1991

Chapter 5
What has Quantum Chemistry Got to Do with It?

Abstract The time has come to see how the concept of irreducible representations ties in with quantum chemistry. After a brief introduction to the prequantum principles of symmetry, we will show that eigenfunctions of the Hamiltonian are also eigenfunctions of the symmetry operators that commute with the Hamiltonian. We further analyze the concept of a degeneracy and show how the degenerate components can be characterized by canonical symmetry relationships. The final section will then provide a detailed account of the symmetry operations that leave the Hamiltonian invariant.

Contents

5.1 The Prequantum Era

Nature around us is full of disorder and chaos, yet it also offers intriguing examples of perfect order and symmetry. Ever since prehistoric times, man has been admiring the circular geometry of a full moon or the perfectly flat surface of a calm sea. Crystals offer another example of almost ideal symmetrical shapes, and it is no surprise that early recognition of the important role of symmetry in physics was based on the study of properties of crystals. Two pioneers of the prequantum era, Franz Neumann and Pierre Curie [1], stand out for their important conjectures.

Theorem 9 *Neumann's principle states that the symmetry elements of any physical property of a crystal must include all the symmetry elements of the point group of the crystal.*

We can apply this directly to a molecule such as ammonia. Ammonia carries a permanent dipole moment, μ_z, which is oriented along the threefold axis. In-plane

components of the dipole moment are strictly forbidden. This is in agreement with the Neumann principle. A dipole moment corresponds to a displacement of charge, and the only displacement that does not destroy the molecular point group is along the z-direction. Hence, this is the only direction that is compatible with the Neumann principle.

Pierre Curie realized that this principle is not limited to crystals, but applies to physical phenomena in general, and not only to isolated systems, but also to systems subject to external perturbations. His proposition is known as the principle of *dissymmetry*.

Theorem 10 *The symmetry of a phenomenon is the maximal symmetry compatible with the existence of the phenomenon. In order for a phenomenon to exist, it is necessary that certain elements of symmetry are absent: dissymmetry creates the phenomenon.*

Curie understood that under stress, or in the presence of external electric or magnetic fields, the symmetry of a system is changed. The Neumann principle still applies but should no longer be based on the symmetry of the isolated crystal, but on that of the combined system of crystal and external field, as we have considered in Sect. 3.9. In the case of ammonia, application of an electric field has the $C_{\infty v}$ symmetry of a polar vector. The symmetry that results from the superposition of the field with the molecular point group C_{3v} depends on the orientation (see Appendix B). In the coordinate frame of Fig. 3.1 one has:

$$
\begin{aligned}
z &: C_{\infty v} \cap C_{3v} = C_{3v} \\
x &: C_{\infty v} \cap C_{3v} = C_s \\
y &: C_{\infty v} \cap C_{3v} = C_1
\end{aligned}
\tag{5.1}
$$

If the field is oriented along the z-direction, it will keep the C_{3v} symmetry of the molecule. This is also in line with the existence of a permanent dipole in the z-direction according to the Neumann principle since a charge dipole has the same symmetry as an electric field. If an external field is applied in the x-direction, the symmetry is reduced to the reflection group, $C_s = \{\hat{E}, \hat{\sigma}_1\}$. In the presence of such a field, displacement of charge in the x-direction is compatible with the extended symmetry principle, which means that ammonia can acquire an *induced* dipole moment in the x-direction. However, a field along x cannot induce a dipole moment in the y-direction since the σ_1 reflection plane is incompatible with the displacement of charge across the plane of symmetry.

The symmetry principles of Neumann and Curie can be recast in the language of irreducible representations. The requirement that physical properties be invariant under the symmetry elements of the point group simply means that they should transform as the totally symmetric irrep. For the dipole moment, the components

transform as follows:

$$\Gamma(\mu_z) = a_1$$
$$\Gamma(\mu_x, \mu_y) = e \tag{5.2}$$

Hence, only the z-component is compatible with the existence of a dipole moment.

The principles of Neumann and Curie are of course based on classical physics. They remain valid for quantum systems but do not include typical quantum phenomena, such as the existence of electronic degeneracy or transitions between quantum states. A proper quantum description of molecular symmetry is thus required.

5.2 The Schrödinger Equation

According to quantum mechanics, the stationary states of a molecule are described by the eigenfunctions of the Hamiltonian, $\mathcal{H}$, corresponding to a quantized set of eigenvalues,

$$\mathcal{H}|\Psi_j^k\rangle = E_k|\Psi_j^k\rangle \tag{5.3}$$

Here, E_k is a fixed eigenvalue, and $|\Psi_j^k\rangle$ is an associated eigenfunction. The index j takes into account the possibility that several eigenfunctions may be associated with the same eigenvalue. In this case the set of these functions forms an eigenspace $\{|\Psi_j^k\rangle\}_{j=1,...,n}$, where n denotes the dimension of this space, and the E_k eigenvalue is said to be n-fold *degenerate*. As usual, the eigenspace will be taken to be orthonormal. The Hamiltonian expresses the kinematics of the electrons in the frame of the nuclei subject to Coulomb forces. We shall study this in detail in Sect. 5.4. For the moment, all we need to know is that the operators of the molecular point group leave $\mathcal{H}$ invariant:

$$\forall \hat{R} \in G \rightarrow [\hat{R}, \mathcal{H}] = 0 \tag{5.4}$$

Now applying $\hat{R}$ to the Schrödinger equation yields

$$\hat{R}\mathcal{H}|\Psi_j^k\rangle = \mathcal{H}\hat{R}|\Psi_j^k\rangle = E_k\hat{R}|\Psi_j^k\rangle \tag{5.5}$$

Here, we have made use of the commutation relation in Eq. (5.4) and the property that $\hat{R}$ as a linear operator does not affect the constant eigenvalue. The equation signifies that if $|\Psi_j^k\rangle$ is an eigenfunction, the transformed function, $\hat{R}|\Psi_j^k\rangle$, also is an eigenfunction *with the same eigenvalue.* This is an important result, which ties quantum mechanics and group theory together, and is essentially the reason why group theory can be applied to chemistry! Now, there are two possibilities, depending on the degeneracy.

1. The electronic state is nondegenerate ($n = 1$). In this case the transformed eigenfunction must necessarily be proportional to the original one. Since the transformation does not change normalization, the proportionality constant must be a

unimodular number:

$$\hat{R}\big|\Psi^k\big\rangle = \exp(i\kappa_R)\big|\Psi^k\big\rangle \tag{5.6}$$

Here, we have dropped the index j since there is only one eigenfunction in this case. This equation indicates that this eigenfunction must transform as a nondegenerate irrep of the point group, say Γ_k, with

$$\exp(i\kappa_R) = \chi^{\Gamma_k}(R) \tag{5.7}$$

2. The electronic state is degenerate $(n > 1)$. In this case the transformed function may not be proportional to the original one, but in any case it is also an eigenfunction of H with the same eigenvalue. This means that it must be mapped onto a linear combination of the components of the eigenspace; hence, the eigenspace itself must form a function space that is invariant under G:

$$R\big|\Psi_j^k\big\rangle = \sum_{i=1}^{n} D_{ij}(R)\big|\Psi_i^k\big\rangle \tag{5.8}$$

Here, the eigenfunctions have again been arranged as a row vector, and the coefficients are gathered in a transformation matrix, $\mathbb{D}(R)$. There are now two possibilities:

- The matrix representation is an irrep of the point group.
  In this case the electronic degeneracy is equal to the dimension of an irrep of the point group.
- The matrix representation is reducible.
  In this case the eigenspace can always be separated in irreducible blocks by using projection operators.

This list of possibilities shows that eigenfunctions of the Hamiltonian will also be (or can be made to be) eigenfunctions of the symmetry group of the Hamiltonian. When there is a perfect match between the eigenfunctions and an irrep, the presence of degeneracy or nondegeneracy can directly be attributed to the symmetry of the eigenstates. The remaining possibility that the eigenspace may consist of several irreducible blocks could be described as a case of "accidental degeneracy", in the sense that symmetry cannot explain the fact that stationary states are degenerate. When this happens, it could mean that the symmetry of the system exceeds the apparent spatial symmetry group. This case is referred to as "hidden symmetry". A special case of this is Kramers' degeneracy, which is treated in Sect. 7.6. Or it could be that a simplified model Hamiltonian was used, such as, e.g., the nearest-neighbor Hamiltonian in Hückel theory, which may give rise to additional degeneracies, as we have explained for the example of triphenylmethyl in the previous chapter. In addition to these possibilities—in the words of Griffith [2]—experience tells that "accidents don't happen, at least in that part of physics which is understood".

The significance of these observations can hardly be overestimated. The derivation refers to the properties of the exact Hamiltonian and its eigenfunctions. In actual

calculations one must usually introduce approximate Hamiltonians and eigenspaces. However, there is at least one simple way to endow these approximate eigenfunctions with an exact property, i.e., by making sure that they are eigenfunctions of the symmetry group of the exact Hamiltonian. The great success of semiempirical theories, such as ligand-field theory for transition-metal and lanthanide complexes, is in fact due to this consistent use of atomic and molecular symmetry. But also in computational chemistry the effort of symmetrizing the orbital basis pays off in a considerable gain of computation time, and it facilitates the assignment of spectroscopic data.

5.3   How to Structure a Degenerate Space

The eigenfunctions of an n-fold degenerate state are defined up to unitary equivalence, which means that any complex linear combination of eigenfunctions is again an eigenfunction. It is convenient to define a standard basis, which brings some structure in this degenerate space. The tool that can be used for this is furnished by the following lemma due to Schur.

Theorem 11 *If a matrix commutes with all the matrices of an irreducible representation, the matrix must be a multiple of the unit matrix*:

$$\forall \, \hat{R} \in G : \mathbb{U}\mathbb{D}(R) = \mathbb{D}(R)\mathbb{U} \to \mathbb{U} \sim \mathbb{I} \tag{5.9}$$

This theorem implies that, if we combine the basis functions of a space in such a way that their representation matrices of the group generators coincide with a canonical choice, then the entire basis set will be completely fixed, up to a global phase factor. This remaining phase freedom is external to the symmetry group. A basis set that complies with a specified set of representation matrices is called a *canonical* basis. A convenient strategy for defining a canonical basis is founded on a *splitting field*. In this case the basis is chosen in such a way that it is diagonal with respect to a particular generator, usually a principal axis of rotation. The components then appear as eigenfunctions of the splitting field. In order for the splitting to be unequivocal, all eigenvalues should be different. The splitting field then "recognizes" each component by its individual eigenvalue. As an example, consider the twofold degenerate E-state in an octahedron. As a splitting field, we take the $\hat{C}_4$ axis along the z-direction. The standard components, which are recognized individually by this field, are denoted as $|E\theta\rangle$ and $|E\epsilon\rangle$. They are respectively symmetric and anti-symmetric with respect to the rotation axis:

$$\hat{C}_4^z|E\theta\rangle = |E\theta\rangle$$
$$\hat{C}_4^z|E\epsilon\rangle = -|E\epsilon\rangle \tag{5.10}$$

In octahedral transition-metal complexes, the d-orbitals, which transform as the E irrep, are d_{z^2} and $d_{x^2-y^2}$. They are seen to match $|E\theta\rangle$ and $|E\epsilon\rangle$, respectively. The

conventional choice of the real d-orbitals is thus based on a tetragonal splitting field. Once the splitting field has been applied, the eigenspace is already nearly fixed; the only freedom that remains is the *relative* phases of the components. To freeze these phases, one can sometimes use an extra ladder operator, which moves from one component to the other, thereby imposing a phase convention. For the E-state, one uses a threefold axis to connect the two components, and the corresponding representation matrix is defined by

$$\hat{C}_3 \left(|E\theta\rangle \quad |E\epsilon\rangle \right) = \left(|E\theta\rangle \quad |E\epsilon\rangle \right) \begin{pmatrix} -1/2 & -\sqrt{3}/2 \\ \sqrt{3}/2 & -1/2 \end{pmatrix} \tag{5.11}$$

This operator connects the two components, and, therefore, if we require that the matrix be of the specified form, then the relative phase freedom is lifted. With such a connecting element, one can indeed easily construct a proper ladder operator:

$$\frac{2}{\sqrt{3}} \left[\hat{C}_3 + \frac{1}{2}\hat{E} \right] |\hat{E}\theta\rangle = |\hat{E}\epsilon\rangle$$

$$-\frac{2}{\sqrt{3}} \left[\hat{C}_3 + \frac{1}{2}\hat{E} \right] |\hat{E}\epsilon\rangle = |\hat{E}\theta\rangle \tag{5.12}$$

In Appendix D we list standard conventions that are frequently used to define canonical basis sets for degenerate irreps.

For the octahedral T_1 state, the standard basis complies with the transformation properties of the real p-orbitals and is marked as $|T_{1x}\rangle, |T_{1y}\rangle, |T_{1z}\rangle$. If we diagonalize this set under a fourfold splitting field, we obtain the complex p-orbitals. In applications where real functions are preferred, the $\hat{C}_4$ axis is represented as

$$\hat{C}_4 \left(|T_{1x}\rangle \quad |T_{1y}\rangle \quad |T_{1z}\rangle \right) = \left(|T_{1x}\rangle \quad |T_{1y}\rangle \quad |T_{1z}\rangle \right) \begin{pmatrix} 0 & -1 & 0 \\ 1 & 0 & 0 \\ 0 & 0 & 1 \end{pmatrix} \tag{5.13}$$

Here, $|T_{1z}\rangle$ is recognized as a totally symmetric eigenfunction, and it is uniquely defined by this eigenvalue since the other eigenvalues are $\pm i$. The splitting field is thus operating only partially; nonetheless, it uniquely picks the z-component. Then the $\hat{C}_3$ axis is a perfect ladder operator, effecting a cyclic permutation of z to x, and further to y.

5.4 The Molecular Symmetry Group

So far, the symmetry of the Hamiltonian was defined as the set of all operations that leave the Hamiltonian invariant. This invariance group was assumed to coincide with the point group of the nuclear frame of the molecule, but it is now time to provide a clear explanation of this connection. This section relies on the definition of the

symmetry groups of nonrigid molecules proposed by Longuet-Higgins [3]. We start by writing down in explicit form the Schrödinger Hamiltonian for a molecule:

$$\mathcal{H} = T_e + T_N + V_{NN} + V_{eN} + V_{ee} \tag{5.14}$$

The T operators are the kinetic energy operators for electrons and nuclei:

$$
\begin{aligned}
T_e &= -\frac{\hbar^2}{2m_e} \sum_i \left(\frac{\partial^2}{\partial x_i^2} + \frac{\partial^2}{\partial y_i^2} + \frac{\partial^2}{\partial z_i^2} \right) \\
T_N &= -\frac{\hbar^2}{2} \sum_n \frac{1}{m_n} \left(\frac{\partial^2}{\partial X_n^2} + \frac{\partial^2}{\partial Y_n^2} + \frac{\partial^2}{\partial Z_n^2} \right)
\end{aligned}
\tag{5.15}
$$

The V operators are the Coulomb interactions between the particles:

$$
\begin{aligned}
V_{NN} &= \sum_{n<m} \frac{Z_n Z_m e^2}{4\pi \epsilon_0 |\mathbf{R}_n - \mathbf{R}_m|} \\
V_{eN} &= -\sum_{i,n} \frac{Z_n e^2}{4\pi \epsilon_0 |\mathbf{R}_n - \mathbf{r}_i|} \\
V_{ee} &= \sum_{i<j} \frac{e^2}{4\pi \epsilon_0 |\mathbf{r}_i - \mathbf{r}_j|}
\end{aligned}
\tag{5.16}
$$

The Hamiltonian may contain additional terms describing coupling between orbital and spin momenta. Longuet-Higgins stated that this full Hamiltonian must be invariant under the following types of transformations:

1. Any permutation of the positions and spins of the electrons.
2. Any rotation of the positions and spins of all particles (electrons and nuclei) about any axis through the center of mass.
3. Any over-all translation in space.
4. The reversal of all particle momenta and spins.
5. The simultaneous inversion of the positions of all particles in the center of mass.
6. Any permutation of the positions and spins of any set of identical nuclei.

The complete group of the Hamiltonian is the combination of all these possible symmetries. This derivation is directly evident from the mathematical form of the Hamiltonian and expresses fundamental properties of molecular space and time. Yet it took 40 years, from Schrödinger to Longuet-Higgins, to obtain a clear definition of the molecular-symmetry group. Three kinds of symmetries may be identified:

- Space symmetries. Space is uniform, isotropic, and has inversion symmetry. This is clear from the fact that the kinetic energy Laplacian operators are trace operators of second derivatives; hence, they are invariant under a sign change of all coordinates and isotropic under rotations. All potential-energy operators depend only on relative distances between particles and thus do not change under translations, rotations, or inversion.

- Time symmetry. The reversal of all momenta and spins is nothing other than the time-reversal operator we introduced earlier. As long as no external magnetic fields are present, time is reversible.
- Elementary particles of the same kind are indistinguishable. The remaining symmetries do not refer to space or time but to the permutational symmetry of a set of particles. All electrons are the same, and thus the Hamiltonian does not change when we permute electron labels. This symmetry becomes apparent only when multielectronic wavefunctions are considered, and these will be treated in the next chapter. Likewise, identical nuclei can be permuted without changing the Hamiltonian. This is reflected in the potential energy terms, which consist of sums over all pairwise interactions. Permutations of particle labels change only the order of the terms in these summations.

As an example, in Fig. 5.1 we return to our favored ammonia molecule and list all nuclear permutations, with and without the all-particle inversion operator, that leave the full Hamiltonian invariant. Nuclear permutations are defined here in the same way as in Sect. 3.3. A permutation such as (ABC) means that the letters A, B, and C are replaced by B, C, and A, respectively.[1] The inversion operator, $\hat{E}^*$, inverts the positions of all particles through a common inversion center, which can be conveniently chosen in the mass origin. In total, 12 combinations of such operations are found, which together form a group that is isomorphic to D_{3h}. How is this related to our previous C_{3v} point group? At this point it is very important to recall that the state of a molecule is not only determined by its Hamiltonian but also, and to an equal extent, by the boundary conditions. The eigenvalue equation is a differential equation that has a very extensive set of mathematical solutions, but not all these solutions are also acceptable states of the physical system. The role of the boundary conditions is to define constraints that filter out physically unacceptable states of the system. In most cases these constraints also lead to the quantization of the energies.

From our present perspective the invariance group should not only leave the Hamiltonian invariant, but also *it should not alter the boundary conditions*. Now, in most quantum-chemical applications a very stringent boundary condition is offered by the Born−Oppenheimer approximation. This simply states that the nuclei are considered immobile. It seriously restricts the Longuet-Higgins list. Indeed, we should retain only those operations that leave all nuclei in their rest positions. Applying this to ammonia, of the twelve operations we retain only those that do not affect the starting structure, i.e., only those combinations of permutations, permutation inversion, and overall rotations that, as a net result, keep the nuclei fixed in space. This immediately constrains the symmetry group to the familiar C_{3v} molecular point group. As an example, the permutation of nuclei B and C followed by the inversion of all particles gives rise to the structure, marked (A)(BC)* in Fig. 5.1, in which the ammonia molecule has been turned upside down. The nuclei can be moved back to their original positions by rotating the whole molecule by 180° about

---

[1] See also [4, Chap. 1].
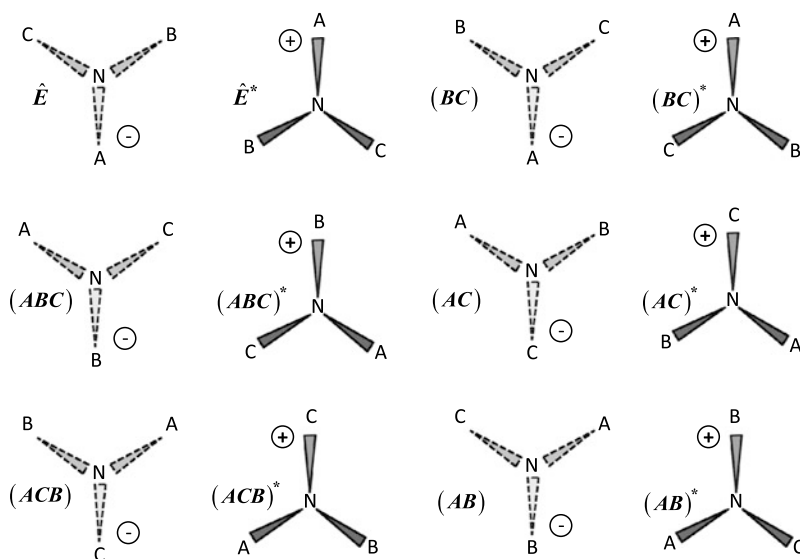
Fig. 5.1 Dynamic symmetry group of ammonia, with permutations of nuclei, and inversion of all particles (indicated by *an asterisk*). *The plus* (*minus*) *sign* indicates the position of an electron above (below) the plane of the hydrogen atoms

Table 5.1 Embedding of the C_{3v} point group in the Longuet-Higgins group. The symmetry elements of the point group act on the electrons. They are identified as the product of nuclear permutations, inversion of all particles (star operation), and bodily rotations of all particles ($\hat{\mathcal{Q}}$ operators) along particular directions

C_{3v}	Rotation	$\times$	Inversion	$\times$	Permutation
$\hat{E}$	$\hat{E}$		$\hat{E}$		$\hat{E}$
$\hat{C}_3$	$\hat{\mathcal{Q}}_3^z$		$\hat{E}$		(ABC)
$\hat{C}_3^2$	$(\hat{\mathcal{Q}}_3^z)^{-1}$		$\hat{E}$		(ACB)
$\hat{\sigma}_1$	$\hat{\mathcal{Q}}_2^{\perp\sigma_1}$		$\hat{E}^*$		(A)(BC)
$\hat{\sigma}_2$	$\hat{\mathcal{Q}}_2^{\perp\sigma_2}$		$\hat{E}^*$		(B)(AC)
$\hat{\sigma}_3$	$\hat{\mathcal{Q}}_2^{\perp\sigma_3}$		$\hat{E}^*$		(C)(AB)

an axis that is perpendicular to the $\hat{\sigma}_1$ reflection plane. The net result is that the electron, marked by the little circle in the figure, has been reflected in this plane. This operation thus leaves the nuclei in place, and only the positions of the electrons are changed. This is precisely the definition of symmetry operators that we have been using all along. The operators are displacing the electrons and in this way lead to transformations of the electronic wavefunctions. The complete embedding of C_{3v} in the Longuet-Higgins group is given in Table 5.1.

By contrast, an operation such as (A)(BC), not followed by spatial inversion of all particles, gives rise to an alternative arrangement of the nuclei, which cannot be brought into coincidence with the original positions by mere spatial rotations. As a result, this operation is not compatible with the Born−Oppenheimer boundary con-

ditions. On the other hand, going beyond the Born–Oppenheimer approximation, one may consider the dynamic states of ammonia that correspond to the tunnelling of the nitrogen through the triangle of the hydrogens. For the tunnelling states, the all-particle inversion operator, $\hat{E}^*$, is also a symmetry element, and the symmetry group of the nonrigid ammonia thus attains the full D_{3h} Longuet-Higgins group.

5.5 Problems

5.1 Prove that the electron-repulsion operator, V_{ee}, is invariant under the rotation around the z-axis.

5.2 Construct a splitting field and ladder operators for the canonical components of the icosahedral irreps in Appendix D.

5.3 Derive the permutation–inversion group for CH_3BF_2 (methyl-boron-difluoride) under the assumption that the methylgroup is almost freely rotating. This means that the result of a permutation inversion can be rotated back by a bodily rotation to a rotamer of the original structure. Determine the point group that is isomorphic to the resulting dynamic symmetry group.

5.4 The barrier to rotation of the cylopentadienyl rings in $Fe(C_5H_5)_2$ (ferrocene, see Fig. 3.9(a)), measured in the gas phase, is only a kcal/mol. Construct a dynamic symmetry group for this molecule.

References

1. Katzir, S.: The emergence of the principle of symmetry in physics. Historical Studies in the Physical Sciences **35**, 35 (2004)
2. Griffith, J.S.: The Theory of Transition-Metal Ions. Cambridge University Press, Cambridge (1961)
3. Longuet-Higgins, H.C.: The symmetry group of non-rigid molecules. Mol. Phys. **6**, 445 (1963)
4. Bunker, P.R.: Molecular Symmetry and Spectroscopy. Academic Press, New York (1979)

Chapter 6
Interactions

Abstract In quantum mechanics the observable phenomena are interactions, expressed as matrix elements of operators in a function space. These spaces and operators are like communicating vessels, reality is neither the operation nor the representation, but the interaction. The evaluation of the corresponding matrix elements requires the coupling of representations, and can be factorized into an intrinsic scalar quantity that contains the physics of the interaction, and a tensorial coupling coefficient that contains its symmetry. This factorization is first illustrated for the case of overlap integrals, where the operator is just the unit operator, and then extended to the case of non-trivial operators, such as the Hamiltonian, and electric and magnetic dipole operators. The Wigner–Eckart theorem is introduced, together with the symmetry selection rules, both at the level of representations and subrepresentations. The results are applied to chemical reaction theory, and to the theory of the Jahn–Teller effect. Selection rules are illustrated for linear and circular dichroism. Finally, the polyhedral Euler theorem is introduced and applied to valence-bond theory for clusters.

Contents

6.1 Overlap Integrals

Operations and representations are merely theoretical constructs. What is actually observed are the *interactions*. In quantum mechanics, interactions are expressed as matrix elements of operators in a function space. When the operator is the unit operator, the matrix elements are just overlap integrals. These are the simplest form of interactions.

We start our analysis by examining symmetry selection rules for overlap integrals. Consider the overlap integral between the ith component of a function space which transforms according to the irrep Γ, and the kth component of another function space transforming as Γ'. The overlap integral, S_{ki}, is a scalar quantity and thus must be invariant under the action of linear symmetry operators acting on the functions.

$$S_{ki} = \langle \phi_k^{\Gamma'} | \psi_i^{\Gamma} \rangle = \hat{R} \langle \phi_k^{\Gamma'} | \psi_i^{\Gamma} \rangle \tag{6.1}$$

An integral being an infinite sum, the operator can be brought inside the bracket and then transform the bra and ket parts directly.

$$\hat{R} \langle \phi_k^{\Gamma'} | \psi_i^{\Gamma} \rangle = \langle \hat{R}\phi_k^{\Gamma'} | \hat{R}\psi_i^{\Gamma} \rangle = \sum_{jl} \bar{D}_{lk}^{\Gamma'}(R) D_{ji}^{\Gamma}(R) \langle \phi_l^{\Gamma'} | \psi_j^{\Gamma} \rangle \tag{6.2}$$

By summing over all $\hat{R} \in G$ and dividing by the group order one obtains a form to which the GOT can be applied.

$$
\begin{aligned}
\langle \phi_k^{\Gamma'} | \psi_i^{\Gamma} \rangle &= \frac{1}{|G|} \sum_{R \in G} \hat{R} \langle \phi_k^{\Gamma'} | \psi_i^{\Gamma} \rangle \\
&= \frac{1}{|G|} \sum_{jl} \left(\sum_{R} \bar{D}_{lk}^{\Gamma'}(R) D_{ji}^{\Gamma}(R) \right) \langle \phi_l^{\Gamma'} | \psi_j^{\Gamma} \rangle \\
&= \delta_{\Gamma'\Gamma} \delta_{ik} \frac{1}{\dim(\Gamma)} \sum_{j} \langle \phi_j^{\Gamma'} | \psi_j^{\Gamma} \rangle
\end{aligned}
\tag{6.3}
$$

We now rewrite this result in terms of elements of the overlap matrix $\mathbb{S}$:

$$S_{ki} = \delta_{\Gamma'\Gamma} \delta_{ik} \frac{1}{\dim(\Gamma)} \sum_{j} S_{jj} = \delta_{\Gamma'\Gamma} \delta_{ik} \frac{1}{\dim(\Gamma)} \mathrm{Tr}(\mathbb{S}) \tag{6.4}$$

This simple derivation yields three important results:

1. Overlap integrals between functions which transform according to different irreps are zero.
2. Overlap integrals between functions which belong to different components of the same irrep are zero.
3. Overlap integrals between functions with the same symmetry properties, i.e. transforming as the *same component* of the *same irrep*, are independent of the component choice provided that both components are normalized.

These results clearly illustrate the importance of the GOT. It not only provides a selection rule at the level of the irreps, but also at the level of the components. Of course, the latter selection rule will work only if we ensured that the symmetry adaptation of the basis set has been carried out at the component level, as was explained in Sect. 5.3.

A further consequence is that SALCs on peripheral atom sites can quite often easily be derived from central symmetry-adapted orbitals. One simply has to make sure that the SALCs have the same nodal characteristics as the central functions, so as to guarantee maximal overlap. This is well illustrated in Fig. 4.4.

6.2 The Coupling of Representations

Overlap integrals are scalar products of a bra and a ket function. A general matrix element is an integral of the outer product of a bra, an operator, and a ket, giving rise to a triad of irreps. The evaluation of such elements is based on the *coupling* of irreps. This concept refers to the formation of a product space. The simplest example is the formation of a two-electron wavefunction, obtained by multiplying two one-electron functions. This section will be devoted entirely to the formation of such product spaces.

Consider two sets of orbitals, transforming as the irreps Γ_a and Γ_b respectively, each occupied by one electron. A two-electron wavefunction with electron 1 in the γ_a component of the first set, and electron 2 in the γ_b component of the second set is written as a simple product function: $|\Gamma_a\gamma_a(1)\rangle|\Gamma_b\gamma_b(2)\rangle$. Clearly, since the one-electron function spaces are invariants of the group, their product space is invariant, too. Now the question is to determine the symmetry of this new space. The recipe to find this symmetry can safely be based on the character theorem: first determine the character string for the product basis, and then carry out the reduction according to the character theorem. Symmetry operators are all-electron operators affecting all particles together; hence, the effect of a symmetry operation on a ket product is to transform both kets simultaneously.

$$\hat{R}\big(|\Gamma_a\gamma_a(1)\rangle|\Gamma_b\gamma_b(2)\rangle\big) = \sum_{\gamma_a'}\sum_{\gamma_b'} D^{\Gamma_a}_{\gamma_a'\gamma_a}(R) D^{\Gamma_b}_{\gamma_b'\gamma_b}(R) |\Gamma_a\gamma_a'(1)\rangle|\Gamma_b\gamma_b'(2)\rangle \quad (6.5)$$

The transformation of the product functions is thus expressed by a super matrix, each element of which is a product of two matrix elements for the individual orbital transformations. The trace of this super matrix is given by:

$$\chi^{\Gamma_a\times\Gamma_b}(R) = \sum_{\gamma_a\gamma_b} D^{\Gamma_a}_{\gamma_a\gamma_a}(R) D^{\Gamma_b}_{\gamma_b\gamma_b}(R)$$

$$= \chi^{\Gamma_a}(R)\chi^{\Gamma_b}(R) \quad (6.6)$$

This is a gratifying result. The character of a product space is simply the product of the characters of the factor spaces. Accordingly, the symmetry of the product space

Table 6.1 Direct product of $E_g \times T_{2g}$ in O_h symmetry

O_h	$\hat{E}$	$8\hat{C}_3$	$6\hat{C}_2$	$6\hat{C}_4$	$3\hat{C}_2$	$\hat{i}$	$6\hat{S}_4$	$8\hat{S}_6$	$3\hat{\sigma}_h$	$6\hat{\sigma}_d$
E_g	2	−1	0	0	2	2	0	−1	2	0
T_{2g}	3	0	1	−1	−1	3	−1	0	−1	1
$E_g \times T_{2g}$	6	0	0	0	−2	6	0	0	−2	0
T_{1g}	3	0	−1	1	−1	3	1	0	−1	−1
T_{2g}	3	0	1	−1	−1	3	−1	0	−1	1

is identified as the *direct product* of the orbital irreps, and is denoted as $\Gamma_a \times \Gamma_b$. If both irreps are degenerate, the direct product will be reducible. Let c_Γ be the number of times that the irrep Γ occurs in the direct product:

$$\Gamma_a \times \Gamma_b = \sum_\Gamma c_\Gamma \Gamma \tag{6.7}$$

By straightforward application of the character theorem one obtains:

$$c_\Gamma = \frac{1}{|G|} \sum_R \bar{\chi}^\Gamma(R) \chi^{\Gamma_a \times \Gamma_b}(R)$$

$$= \frac{1}{|G|} \sum_R \bar{\chi}^\Gamma(R) \chi^{\Gamma_a}(R) \chi^{\Gamma_b}(R) \tag{6.8}$$

Here we have, for the first time, a formula with a triad of irreps. This will form the basis for the symmetry evaluation of general matrix elements. The c_Γ coefficients are obtained by performing product manipulations on the character tables. As an example, Table 6.1 illustrates the reduction of the $E_g \times T_{2g}$ product in O_h, as given in Eq. (6.9). Product tables are given in Appendix E.

$$E_g \times T_{2g} = T_{1g} + T_{2g} \tag{6.9}$$

Let us now proceed with the two-electron problem and address the next question, which is that, after having determined which symmetry species are present, we should like to know what the corresponding two-electron wavefunctions look like, i.e. we should like to construct the SALCs. This construction does not pose any new problems; the projection operators that were introduced in Sect. 4.5 will do the job perfectly well. Some notation is important here. The product function will be written as:

$$\left| \Gamma \gamma(1,2) \right\rangle = \sum_{\gamma_a} \sum_{\gamma_b} c^{\Gamma\gamma}_{\gamma_a \gamma_b} \left| \Gamma_a \gamma_a(1) \right\rangle \left| \Gamma_b \gamma_b(2) \right\rangle \tag{6.10}$$

The combination coefficient is itself identified as a matrix element, by multiplying left and right with the one-electron bra functions and using orthonormality of the

basis orbitals.

$$c_{\gamma_a \gamma_b}^{\Gamma} = \langle \Gamma_a \gamma_a(1) \Gamma_b \gamma_b(2) | \Gamma \gamma(1, 2) \rangle$$
$$\equiv \langle \Gamma_a \gamma_a \Gamma_b \gamma_b | \Gamma \gamma \rangle \tag{6.11}$$

This coefficient is known as a Clebsch–Gordan (CG) coupling coefficient and de-noted by the 3Γ bracket $\langle \Gamma_a \gamma_a \Gamma_b \gamma_b | \Gamma \gamma \rangle$. It indicates how the orbital irreps Γ_a and Γ_b have to be combined to yield a product ket that transforms as $|\Gamma \gamma\rangle$. The CG-coefficients can be determined by using projection operators. The results are listed in Appendix F. It is often possible to obtain these results by a simpler procedure. We illustrate this for the components of the T_{1g} two-electron state, obtained in Eq. (6.9). The z-component of this state is the only component that is totally symmetric under the $\hat{C}_4$ splitting field. It is clear that this symmetry can be obtained only by multiplying the $|e_g \epsilon\rangle$ and $|t_{2g} \zeta\rangle$ components, since these are both antisymmetric and thus will form a symmetric product. From here on we will adopt for the product functions the usual notation of small letters for the orbitals and capital letters for the coupled states. Hence:

$$|T_{1g}z\rangle = |e_g \epsilon\rangle |t_{2g} \zeta\rangle \tag{6.12}$$

The coupling coefficient $\langle E_g \epsilon T_{2g} \zeta | T_{1g} z \rangle$ is thus equal to 1. The x and y compo-nents may then immediately be obtained by applying the cyclic $\hat{C}_3$ generator. As an example for the x-component:

$$|T_{1g}x\rangle = \hat{C}_3 |T_{1g}z\rangle$$
$$= \left(\hat{C}_3 |e_g \epsilon\rangle \right) \left(\hat{C}_3 |t_{2g} \zeta\rangle \right)$$
$$= \left(-\frac{\sqrt{3}}{2} |e_g \theta\rangle - \frac{1}{2} |e_g \epsilon\rangle \right) |t_{2g} \xi\rangle$$
$$= -\frac{\sqrt{3}}{2} |e_g \theta\rangle |t_{2g} \xi\rangle - \frac{1}{2} |e_g \epsilon\rangle |t_{2g} \xi\rangle \tag{6.13}$$

Thus: $\langle \theta \xi | x \rangle = -\sqrt{3}/2$; $\langle \epsilon \xi | x \rangle = -1/2$. The resulting coupling coefficients are shown in Table 6.2.

6.3 Symmetry Properties of the Coupling Coefficients

The CG-coefficients in the finite point groups stem from Wigner's celebrated cou-pling coefficients for the spherical symmetry group [1]. Wigner proposed reformu-lating these coefficients in terms of more primitive $3j$ symbols, which contain, in a uniform way, the permutational properties of the spherical coupling coefficients. Several attempts have been made to define similar 3Γ symbols for the point group, but this requires the introduction of quite detailed phase conventions, which lim-its the efficiency of this formalism [2, 3]. We shall therefore not engage in a further

Table 6.2 The coupling coefficients for the direct product $E_g \times T_{2g}$ in O_h symmetry

$E_g \times T_{2g}$	T_{1g}			T_{2g}		
	x	y	z	ξ	η	ζ
$\lvert\theta\rangle\lvert\xi\rangle$	$-\frac{\sqrt{3}}{2}$	0	0	$-\frac{1}{2}$	0	0
$\lvert\theta\rangle\lvert\eta\rangle$	0	$\frac{\sqrt{3}}{2}$	0	0	$-\frac{1}{2}$	0
$\lvert\theta\rangle\lvert\zeta\rangle$	0	0	0	0	0	1
$\lvert\epsilon\rangle\lvert\xi\rangle$	$-\frac{1}{2}$	0	0	$\frac{\sqrt{3}}{2}$	0	0
$\lvert\epsilon\rangle\lvert\eta\rangle$	0	$-\frac{1}{2}$	0	0	$-\frac{\sqrt{3}}{2}$	0
$\lvert\epsilon\rangle\lvert\zeta\rangle$	0	0	1	0	0	0

factorization of the coupling coefficients, but, express the important symmetry properties of the couplings at the level of the brackets. Two guidelines will thereby be used: when dealing with coupling coefficients it is important to bear in mind that the coupling is based on the formation of a product, as we have illustrated in the preceding section, and, secondly, that we should treat the coupling coefficients as far as possible as ordinary brackets.

A direct consequence of the latter viewpoint is that the rules for complex conjugation of brackets apply:

$$\overline{\langle \Gamma_a \gamma_a \Gamma_b \gamma_b | \Gamma \gamma \rangle} = \langle \Gamma \gamma | \Gamma_a \gamma_a \Gamma_b \gamma_b \rangle \tag{6.14}$$

Being expansion coefficients of SALCs, the coupling coefficients also obey two orthogonality rules. Column-wise orthonormality results from the orthonormal properties of the coupled states.

$$\sum_{\gamma_a \gamma_b} \langle \Gamma' \gamma' | \Gamma_a \gamma_a \Gamma_b \gamma_b \rangle \langle \Gamma_a \gamma_a \Gamma_b \gamma_b | \Gamma \gamma \rangle = \delta_{\Gamma \Gamma'} \delta_{\gamma \gamma'} \tag{6.15}$$

In addition, the scalar products along rows are orthonormal, because of the orthonormal properties of the basic kets. Note that the summation runs over the irreps of the entire product space: $\Gamma \in \Gamma_a \times \Gamma_b$.

$$\sum_{\Gamma \gamma} \langle \Gamma_a \gamma_a' \Gamma_b \gamma_b' | \Gamma \gamma \rangle \langle \Gamma \gamma | \Gamma_a \gamma_a \Gamma_b \gamma_b \rangle = \delta_{\gamma_a' \gamma_a} \delta_{\gamma_b' \gamma_b} \tag{6.16}$$

The permutational properties of the CG-coefficients refer to interchange of the bra and ket irreps. If Γ_a and Γ_b are not equivalent, their ordering will not affect the symmetry of the coupled state, since the factors in the direct product commute:

$$\Gamma_a \times \Gamma_b = \Gamma_b \times \Gamma_a \tag{6.17}$$

We can therefore define the coupling coefficients in such a way that interchange of the coupled irreps leaves the coefficient invariant:

$$\Gamma_a \neq \Gamma_b : \langle \Gamma_a \gamma_a \Gamma_b \gamma_b | \Gamma \gamma \rangle \equiv \langle \Gamma_b \gamma_b \Gamma_a \gamma_a | \Gamma \gamma \rangle \tag{6.18}$$

If the coupled electrons are equivalent, i.e. belong *to the same shell*, the situation is different. In this case, $\Gamma_a = \Gamma_b$, and the direct product becomes a *direct square*. For non-equivalent irreps, exchange of the components γ_a and γ_b was not possible, because they refer to different irreps. However, when they are components of the same irrep, this exchange is an important symmetry of the product space. Indeed, the squared space can be split into two separate blocks, one block which contains product functions that are symmetric under exchange of the component labels and one block which is antisymmetric. This implies that we can define two separate sets of direct square coupling coefficients, which are either symmetric or antisymmetric under exchange of the labels, i.e.: $\langle \Gamma_a\gamma_a\Gamma_a\gamma_b | \Gamma\gamma \rangle = \pm\langle \Gamma_a\gamma_b\Gamma_a\gamma_a | \Gamma\gamma \rangle$. The symmetrized part of the direct square is denoted as $[\Gamma_a]^2$. For $n = \dim(\Gamma_a)$, the dimension of this subspace is equal to the number of symmetric combinations:

$$\dim\big([\Gamma_a]^2\big) = \sum_{\gamma_a} 1 + \sum_{\gamma_a < \gamma_b} 1 = n + n(n-1)/2 = n(n+1)/2 \tag{6.19}$$

On the other hand, if the coupling coefficients are antisymmetric under exchange of the labels, the coupled state belongs to the antisymmetrized direct square, denoted as $\{\Gamma_a\}^2$. This product space is restricted to combinations with $\gamma_a \neq \gamma_b$; its dimension is equal to $n(n-1)/2$. The characters for either part of the square can be determined separately. For the character of the $\{\Gamma_a\}^2$ part the derivation runs as follows: one first applies a symmetry operator to an arbitrary antisymmetric function. The ket product $|\Gamma_a\gamma_a(1)\rangle|\Gamma_a\gamma_b(2)\rangle$ will be abbreviated here as: $\gamma_a(1)\gamma_b(2)$.

$$
\begin{aligned}
\hat{R}&\big(\gamma_a(1)\gamma_b(2) - \gamma_b(1)\gamma_a(2)\big) \\
&= \sum_{\gamma_a'\gamma_b'} \big(\gamma_a'(1)\gamma_b'(2) - \gamma_b'(1)\gamma_a'(2)\big) D^{\Gamma_a}_{\gamma_a'\gamma_a}(R) D^{\Gamma_a}_{\gamma_b'\gamma_b}(R) \\
&= \sum_{\gamma_a'\gamma_b'} \gamma_a'(1)\gamma_b'(2)\big(D^{\Gamma_a}_{\gamma_a'\gamma_a}(R) D^{\Gamma_a}_{\gamma_b'\gamma_b}(R) - D^{\Gamma_a}_{\gamma_a'\gamma_b}(R) D^{\Gamma_a}_{\gamma_b'\gamma_a}(R)\big) \\
&= \frac{1}{2} \sum_{\gamma_a'\gamma_b'} \big(\gamma_a'(1)\gamma_b'(2) - \gamma_b'(1)\gamma_a'(2)\big)\big(D^{\Gamma_a}_{\gamma_a'\gamma_a}(R) D^{\Gamma_a}_{\gamma_b'\gamma_b}(R) - D^{\Gamma_a}_{\gamma_a'\gamma_b}(R) D^{\Gamma_a}_{\gamma_b'\gamma_a}(R)\big)
\end{aligned}
$$

$$\tag{6.20}$$

Taking the trace then yields:

$$
\begin{aligned}
\chi^{\{\Gamma_a\}^2}(R) &= \frac{1}{2} \sum_{\gamma_a\gamma_b} \big(D^{\Gamma_a}_{\gamma_a\gamma_a}(R) D^{\Gamma_a}_{\gamma_b\gamma_b}(R) - D^{\Gamma_a}_{\gamma_a\gamma_b}(R) D^{\Gamma_a}_{\gamma_b\gamma_a}(R)\big) \\
&= \frac{1}{2}\Big(\big(\chi^{\Gamma_a}(R)\big)^2 - \sum_{\gamma_a} D^{\Gamma_a}_{\gamma_a\gamma_a}(R^2)\Big) \\
&= \frac{1}{2}\big(\big(\chi^{\Gamma_a}(R)\big)^2 - \chi^{\Gamma_a}(R^2)\big) \tag{6.21}
\end{aligned}
$$

Table 6.3 Direct square $H_g \times H_g$ in I_h symmetry

I_h	$\hat{E}$	$12\hat{C}_5$	$12\hat{C}_5^2$	$20\hat{C}_3$	$15\hat{C}_2$	$\hat{i}$	$12\hat{S}_{10}$	$12\hat{S}_{10}^3$	$20\hat{S}_6$	$15\hat{\sigma}$
χ^{H_g}	5	0	0	-1	1	5	0	0	-1	1
$\chi^{H_g{}^2}$	25	0	0	1	1	25	0	0	1	1
$\chi^{H_g}(R^2)$	5	0	0	-1	5	5	0	0	-1	5
$\chi^{[H_g]^2}$	15	0	0	0	3	15	0	0	0	3
$\chi^{\{H_g\}^2}$	10	0	0	1	-2	10	0	0	1	-2

The trace for the symmetrized product is then found by subtracting the trace in Eq. (6.21) from the total trace for the direct product.

$$
\begin{aligned}
\chi^{[\Gamma_a]^2}(R) &= \chi^{\Gamma_a{}^2}(R) - \chi^{\{\Gamma_a\}^2}(R) \\
&= \frac{1}{2}\left(\left(\chi^{\Gamma_a}(R)\right)^2 + \chi^{\Gamma_a}\left(R^2\right)\right)
\end{aligned}
\tag{6.22}
$$

In Table 6.3 these quantities are given for the direct product $H_g \times H_g$ in icosahedral symmetry. The product resolution is as follows:

$$
H_g \times H_g = [A_g + G_g + 2H_g] + \{T_{1g} + T_{2g} + G_g\}
\tag{6.23}
$$

Note that this product contains one totally-symmetric irrep, notably in the symmetrized part. In general, for irreps with real characters the totally-symmetric irrep, Γ_0, appears in a direct square only once. This can easily be derived from Eq. (6.8). When Γ_a is an irrep with *real characters*, one has:

$$
\begin{aligned}
\langle \chi^{\Gamma_0} | \chi^{\Gamma_a \times \Gamma_b} \rangle &= \sum_R \bar{\chi}^{\Gamma_0}(R)\chi^{\Gamma_a}(R)\chi^{\Gamma_b}(R) \\
&= \sum_R \chi^{\Gamma_a}(R)\chi^{\Gamma_b}(R) \\
&= |G|\delta_{\Gamma_a \Gamma_b}
\end{aligned}
\tag{6.24}
$$

In the case of irreps that can be represented by *real transformation matrices*, it is possible to show that this totally-symmetric irrep will belong to the symmetrized part. In order to apply the character theorem to Eq. (6.22), the following intermediate result is needed:

$$
\begin{aligned}
\sum_R \chi^{\Gamma_a}\left(R^2\right) &= \sum_R \sum_i \left[\mathbb{D}^{\Gamma_a}(R) \times \mathbb{D}^{\Gamma_a}(R)\right]_{ii} \\
&= \sum_R \sum_i \sum_j D_{ij}^{\Gamma_a}(R)D_{ji}^{\Gamma_a}(R) \\
&= \frac{|G|}{\dim(\Gamma_a)} \sum_i \sum_j \delta_{ij} = |G|
\end{aligned}
\tag{6.25}
$$

In order to arrive at this result we have made use of the GOT, on the assumption that the $\mathbb{D}$ matrices are real. Combining the results of Eqs. (6.24) and (6.25) with

Eq. (6.22) then leads to the conclusion that the unique totally-symmetric irrep belongs to the symmetrized part of the direct square:

$$\frac{1}{|G|}\langle \chi^{\Gamma_0}|\chi^{[\Gamma_a]^2}\rangle = \frac{1}{2|G|}\sum_R \chi^{\Gamma_0}(R)\big[\chi^{\Gamma_a^2}(R) + \chi^{\Gamma_a}(R^2)\big] = 1 \qquad (6.26)$$

For irreps with real characters, but transformation matrices that cannot be all real, the unique totally-symmetric product appears in the antisymmetrized part. This is the case for spin representations, which will be dealt with in Chap. 7. In summary, as far as complex-conjugation properties are concerned, we have three kinds of irreps:

1. Irreps with real characters, and for which all $\mathbb{D}(R)$ transformation matrices can be put in real form. In this case: $\Gamma_0 \in [\Gamma_a]^2$.
2. Irreps with real characters, but which cannot be represented by transformation matrices that are all real. In this case $\Gamma_0 \in \{\Gamma_a\}^2$.
3. Irreps with complex characters. In this case there is always a complex-conjugate irrep, and $\Gamma_0 \in \Gamma \times \bar{\Gamma}$.

Equation (6.23) further exemplifies a case of *product multiplicity*. This is when an irrep occurs more than once in the decomposition of a direct product. Both the H_g and G_g irreps appear twice in the direct product $H_g \times H_g$. In the point groups product multiplicity is quite rare. It occurs only in the icosahedral group for the products $G \times H$ and $H \times H$, as well for spin representations in cubic and icosahedral symmetries. Product multiplicity means that there are different coupling schemes for arriving at the product states. Each of these "channels" corresponds to a separate set of CG coupling coefficients. There are several ways of obtaining linearly-independent sets of coupling coefficients. For the separation of the two G_g irreps in Eq. (6.23) symmetrization of the product space is sufficient, since the symmetrized and antisymmetrized parts each contain one G_g. This strategy does not work for the two H_g irreps, which are both the result of symmetrized coupling. In this case, more elaborate splitting schemes have been constructed, based *inter alia* on higher symmetries [4, 5].

Last but not least, we should consider the relationship between coupling coefficients where irreps from bra and ket parts are interchanged. We shall limit the discussion here to the simplified case in which all ingredients of the coupling are taken to be real. A case with complex irreps will be treated in Chap. 7. Consider two related couplings: $\Gamma_a \times \Gamma_b = \Gamma$ and $\Gamma \times \Gamma_b = \Gamma_a$. The corresponding expansion coefficients are scalar matrix elements and are thus invariant under the group action. By importing the group action inside the brackets, as we have frequently done before, we obtain a set of equations in the CG-coefficients:

$$\langle \Gamma_a\gamma_a \Gamma_b\gamma_b|\Gamma\gamma\rangle = \sum_{\gamma_a'\gamma_b'\gamma'}\left[\frac{1}{|G|}\sum_R \bar{D}^{\Gamma_a}_{\gamma_a'\gamma_a}(R)\bar{D}^{\Gamma_b}_{\gamma_b'\gamma_b}(R)D^{\Gamma}_{\gamma'\gamma}(R)\right]\langle \Gamma_a\gamma_a' \Gamma_b\gamma_b'|\Gamma\gamma'\rangle$$

$$(6.27)$$

$$\langle \Gamma \gamma \Gamma_b \gamma_b | \Gamma_a \gamma_a \rangle = \sum_{\gamma_a' \gamma_b' \gamma} \left[\frac{1}{|G|} \sum_R D^{\Gamma_a}_{\gamma_a' \gamma_a}(R) \bar{D}^{\Gamma_b}_{\gamma_b' \gamma_b}(R) \bar{D}^{\Gamma}_{\gamma' \gamma}(R) \right] \langle \Gamma \gamma' \Gamma_b \gamma_b' | \Gamma_a \gamma_a' \rangle$$

$$(6.28)$$

These equations form a system of homogeneous linear equations from which the coupling coefficients can be obtained. At present, we shall use this result only in the simplified case where all components have been chosen to be real, so that Eqs. (6.27) and (6.28) form the same system of equations.[1] From this it follows that the corresponding coupling coefficients will be proportional to each other, independent of the components; hence:

$$\langle \Gamma_a \gamma_a \Gamma_b \gamma_b | \Gamma \gamma \rangle = x \langle \Gamma \gamma \Gamma_b \gamma_b | \Gamma_a \gamma_a \rangle \tag{6.29}$$

The proportionality constant can be determined by summing the square of the coefficients over all components and using the normalization result from Eq. (6.15).

$$\sum_{\gamma_a \gamma_b \gamma} \left| \langle \Gamma_a \gamma_a \Gamma_b \gamma_b | \Gamma \gamma \rangle \right|^2 = x^2 \sum_{\gamma_a \gamma_b \gamma} \left| \langle \Gamma \gamma \Gamma_b \gamma_b | \Gamma_a \gamma_a \rangle \right|^2$$

$$\dim(\Gamma) = x^2 \dim(\Gamma_a) \tag{6.30}$$

The permutation of irreps between bra and ket in the CG-coefficients thus requires a uniform dimensional renormalization:

$$\left[\dim(\Gamma) \right]^{-1/2} \langle \Gamma_a \gamma_a \Gamma_b \gamma_b | \Gamma \gamma \rangle = \pm \left[\dim(\Gamma_a) \right]^{-1/2} \langle \Gamma \gamma \Gamma_b \gamma_b | \Gamma_a \gamma_a \rangle \tag{6.31}$$

The renormalization leaves a phase factor undetermined. This phase factor is the same for the entire coupling table, and thus can be chosen in arbitrarity. As an example, in the group O (see Appendix F), the coefficients $\langle T_2 \xi T_1 x | E \theta \rangle$ and $\langle E \theta T_1 x | T_2 \xi \rangle$ are related as follows:

$$\frac{1}{\sqrt{2}} \langle T_2 \xi T_1 x | E \theta \rangle = \frac{1}{\sqrt{3}} \langle E \theta T_1 x | T_2 \xi \rangle = -\frac{1}{2} \tag{6.32}$$

Here the phase was chosen to be $+1$.

6.4 Product Symmetrization and the Pauli Exchange-Symmetry

In principle, the T_{1g} and T_{2g} coupled two-electron states, which we obtained in Table 6.2 of the previous section, could apply to the case of the $(t_{2g})^1 (e_g)^1$ excited states of a d^2 transition-metal ion in an octahedral ligand field, which splits the d

---

[1]The general case with complex irreps is exemplified for the coupling of spin representations in Sect. 7.4.

orbitals into a t_{2g} and an e_g shell. However, these coupled descriptions are not yet sufficient, since they make a distinction between electron 1, which resides in the t_{2g} orbital, and electron 2, which was promoted to the e_g level. The fundamental symmetry requirement that electrons must be indistinguishable is thus not fulfilled. The operator that permutes the two electrons is represented as $\hat{P}_{12}$:

$$\hat{P}_{12}|\Gamma\gamma(1,2)\rangle = |\Gamma\gamma(2,1)\rangle = \sum_{\gamma_a}\sum_{\gamma_b}\langle\Gamma_a\gamma_a\Gamma_b\gamma_b|\Gamma\gamma\rangle|\Gamma_a\gamma_a(2)\rangle|\Gamma_b\gamma_b(1)\rangle \quad (6.33)$$

The $|\Gamma\gamma(1,2)\rangle$ and $|\Gamma\gamma(2,1)\rangle$ states will have exactly the same symmetries, since the factors in the direct product commute:

$$\Gamma_a \times \Gamma_b = \Gamma_b \times \Gamma_a \quad (6.34)$$

As a result, $\hat{P}_{12}$ commutes with the spatial symmetry operators, and we can symmetrize the coupled states with respect to the electron permutation. The permutation operator is the generator of the symmetric group, S_2, which has only two irreps, one symmetric and one antisymmetric, corresponding, respectively, to the plus and minus combination in Eq. (6.35).

$$\begin{aligned}|\Gamma\gamma;\pm\rangle &= \frac{1}{\sqrt{2}}\big[|\Gamma\gamma(1,2)\rangle \pm |\Gamma\gamma(2,1)\rangle\big] \\ &= \frac{1}{\sqrt{2}}\sum_{\gamma_a}\sum_{\gamma_b}\langle\Gamma_a\gamma_a\Gamma_b\gamma_b|\Gamma\gamma\rangle \\ &\quad \times \big[|\Gamma_a\gamma_a(1)\rangle|\Gamma_b\gamma_b(2)\rangle \pm |\Gamma_b\gamma_b(1)\rangle|\Gamma_a\gamma_a(2)\rangle\big]\end{aligned} \quad (6.35)$$

These states have distinct permutation symmetries, and spatial symmetry operators cannot mix $+$ and $-$ states. This is a very general property of multi-particle states, to which no exceptions are known.

On the other hand the permutation symmetry of multi-electron wavefunctions is restricted by the Pauli principle.

Theorem 11 *The total wavefunction should be antisymmetric with respect to exchange of any pair of electrons. Hence, in the symmetric group S_2, or, for an n-electron system, the symmetric group, S_n, the total wavefunction should change sign under odd permutations, i.e. under permutations that consist of an odd number of transpositions of two elements, and should remain invariant under even permutations.*

Until now we have limited ourselves to the spatial part of the wavefunction. So far, only the antisymmetrized part obeys the Pauli principle. However, the principle places a requirement only on the *total* wavefunction. This also involves a spin part, which should be multiplied by the orbital part. Anticipating the results of Chap. 7, we here provide the spin functions for a two-electron system. Spin functions are characterized by a spin quantum number, S, and a component, M_S, in the range

$\{-S, -S+1, -S+2, \ldots, S-1, S\}$. The total number of components, hence the dimension of the spin-space for a given S, is equal to $2S+1$. This number is called the spin multiplicity. For a two-electron system, S can be 0 or 1; hence, there is one singlet state, and there are three components belonging to a triplet state. In a $|SM_S\rangle$ notation they are given by:

$$
\begin{aligned}
|0, 0\rangle &= \frac{1}{\sqrt{2}}\big[\alpha(1)\beta(2) - \beta(1)\alpha(2)\big] \\
|1, 1\rangle &= \alpha(1)\alpha(2) \\
|1, 0\rangle &= \frac{1}{\sqrt{2}}\big[\alpha(1)\beta(2) + \beta(1)\alpha(2)\big] \\
|1, -1\rangle &= \beta(1)\beta(2)
\end{aligned}
\tag{6.36}
$$

These functions also exhibit permutation symmetry: the triplet functions are symmetric under exchange of the two particles, while the singlet function is antisymmetric under such an exchange. The total wavefunction can thus always be put in line with the Pauli principle by combining the coupled orbital states with spin states of opposite permutation symmetry. Altogether we can thus construct four states: $^1T_{1g}, ^1T_{2g}, ^3T_{1g}, ^3T_{2g}$. This set of four states, totalling 24 wavefunctions, forms a *manifold*, representing all the coupled states resulting from the $(t_{2g})^1(e_g)^1$ configuration. The dimension of the manifold is equal to the product of the six possible t_{2g} substates (including spin), and the four possible e_g substates. In this case, where the coupling involves electrons belonging to different shells, the Pauli principle does not restrict the total dimension of the manifold, since all combinations remain possible. All states can be written as linear combinations of Slater determinants. As an example, for the $|^1T_{1g}z\rangle$ state, one writes:

$$
\begin{aligned}
|^1T_{1g}z\rangle &= \frac{1}{\sqrt{2}}\big(|\epsilon(1)\rangle|\zeta(2)\rangle + |\epsilon(2)\rangle|\zeta(1)\rangle\big)\frac{1}{\sqrt{2}}\big[\alpha(1)\beta(2) - \beta(1)\alpha(2)\big] \\
&= \frac{1}{\sqrt{2}}\big|(\epsilon\alpha)(\zeta\beta)\big| - \frac{1}{\sqrt{2}}\big|(\epsilon\beta)(\zeta\alpha)\big|
\end{aligned}
\tag{6.37}
$$

The situation is different when coupling two equivalent electrons; these are electrons that belong to *the same shell*. In this case, the coupled states are already eigenfunctions of the exchange operator as a result of the special symmetrization properties of the coupling coefficients for direct squares. Equation (6.10) will take the following form:

$$
\begin{aligned}
|\Gamma\gamma(1, 2)\rangle &= \sum_{\gamma_a\gamma_b}\langle\gamma_a\gamma_b|\Gamma\gamma\rangle|\gamma_a(1)\rangle|\gamma_b(2)\rangle = \sum_{\gamma_a}\langle\gamma_a\gamma_a|\Gamma\gamma\rangle|\gamma_a(1)\rangle|\gamma_a(2)\rangle \\
&\quad + \sum_{\gamma_a<\gamma_b}\big[\langle\gamma_a\gamma_b|\Gamma\gamma\rangle|\gamma_a(1)\rangle|\gamma_b(2)\rangle + \langle\gamma_b\gamma_a|\Gamma\gamma\rangle|\gamma_b(1)\rangle|\gamma_a(2)\rangle\big]
\end{aligned}
\tag{6.38}
$$

Now, if the product representation belongs to the symmetrized square, $\Gamma \in [\Gamma_a]^2$, this result simplifies to:

$$|\Gamma \gamma\rangle = \sum_{\gamma_a} \langle \gamma_a \gamma_a | \Gamma \gamma\rangle |\gamma_a(1)\rangle |\gamma_a(2)\rangle$$

$$+ \sum_{\gamma_a < \gamma_b} \langle \gamma_a \gamma_b | \Gamma \gamma\rangle \big(|\gamma_a(1)\rangle |\gamma_b(2)\rangle + |\gamma_b(1)\rangle |\gamma_a(2)\rangle \big) \qquad (6.39)$$

Hence, this function is symmetric under the $\hat{P}_{12}$ operator. It also obeys the normalization condition of Eq. (6.15). It should always be multiplied by an antisymmetric singlet spin-function in order to obey the Pauli exclusion principle. On the other hand, if the product representation belongs to the antisymmetrized square, $\Gamma \in \{\Gamma_a\}^2$, the coupled state is given by:

$$|\Gamma \gamma\rangle = \sum_{\gamma_a < \gamma_b} \langle \gamma_a \gamma_b | \Gamma \gamma\rangle \big(|\gamma_a(1)\rangle |\gamma_b(2)\rangle - |\gamma_b(1)\rangle |\gamma_a(2)\rangle \big) \qquad (6.40)$$

This function is antisymmetric under the $\hat{P}_{12}$ operator, and should be multiplied by a symmetric triplet spin-function in order to obey the Pauli principle. As an example, for the $(e_g)^2$ configuration the allowed states are:

$$e_g \times e_g = [A_{1g} + E_g] + \{A_{2g}\} \Rightarrow {}^1A_{1g} + {}^1E_g + {}^3A_{2g} \qquad (6.41)$$

For equivalent electrons the Pauli principle thus really does function as an exclusion principle, since the coupled states are either triplets or singlets, depending on their symmetrization. The dimension of the manifold is given by the binomial coefficient, where q is the number of equivalent substates (including spin), and n is the number of electrons:

$$\binom{q}{n} = \frac{q!}{n!(q-n)!} \qquad (6.42)$$

For the $(e_g)^2$ problem, one has $n = 2$ and $q = 4$; there are thus six two-electron states in this configuration (see Eq. (6.41)).

As a special result, we examine the symmetry of the maximal spin-multiplicity ground state of a system with a half-filled shell. The shell consists of the components $|f_1\rangle \cdots |f_n\rangle$, transforming according to the irrep Γ_a, and each will be occupied by one electron with α spin. The ground state corresponds to a single determinant:

$$|\Psi\rangle = |f_1\alpha \cdots f_2\alpha| = \frac{1}{\sqrt{n!}} \sum_{\sigma \in S_n} \text{sgn}(\sigma)\big[f_1\alpha(\sigma_1) \cdots f_n\alpha(\sigma_n)\big]$$

$$= \frac{1}{\sqrt{n!}} \sum_{\sigma \in S_n} \text{sgn}(\sigma)\big[f_{\sigma_1}\alpha(1) \cdots f_{\sigma_n}\alpha(n)\big] \qquad (6.43)$$

Here, $\sigma \in S_n$ is an element of the permutation group of the n electron labels, and $\text{sgn}(\sigma)$ is its parity.[2] Equation (6.43) indicates that this permutation can equally well be applied to the component labels, since the determinant is invariant under matrix transposition. We can now calculate the matrix element in the symmetry operator:

$$
\begin{aligned}
\langle \Psi | \hat{R} | \Psi \rangle &= \frac{1}{n!} \sum_{\sigma, \pi \in S_n} \text{sgn}(\sigma) \text{sgn}(\pi) \big[\langle f_{\sigma_1} \alpha(1) | \hat{R} | f_{\pi_1} \alpha(1) \rangle \cdots \langle f_{\sigma_n} \alpha(n) | \hat{R} | f_{\pi_n} \alpha(n) \rangle \big] \\
&= \frac{1}{n!} \sum_{\sigma, \pi \in S_n} \text{sgn}(\sigma) \text{sgn}(\pi) \big[D_{\sigma_1 \pi_1}^{\Gamma_a}(R) \cdots D_{\sigma_n \pi_n}^{\Gamma_a}(R) \big] \\
&= \sum_{\lambda \in S_n} \text{sgn}(\lambda) \big[D_{1 \lambda_1}^{\Gamma_a}(R) \cdots D_{n \lambda_n}^{\Gamma_a}(R) \big] \\
&= \det\big(\mathbb{D}^{\Gamma_a} \big)
\end{aligned}
\tag{6.44}
$$

In this equation we have used the result from Eq. (2.8), which identified matrix elements over symmetry operators as elements of the representation matrix. The double summation over permutations covers the permutation group twice and could be reduced to a single sum. The result indicates that the spatial symmetry of the half-filled shell ground state transforms as the determinant of the irrep of the shell. This is also called the *determinantal* representation. For the e_g shell the determinantal irrep is A_{2g}. The shell ground state is thus a $^3 A_{2g}$.

6.5 Matrix Elements and the Wigner–Eckart Theorem

A general interaction element is a bracket around an operator. Each of the three ingredients, bra, ket, and operator, can be put in symmetry-adapted form, so that it transforms according to a given irrep. Moreover, provided that the symmetry adaptation is done properly, not only the irrep itself but also the subrepresentation is well defined. Altogether, the matrix element will thus be characterized by six symmetry labels, as: $\langle \psi_\omega^\Omega | O_\lambda^\Lambda | \phi_\gamma^\Gamma \rangle$. The labels imply that the symmetry behaviour of each of these ingredients is fully known:

$$
\begin{aligned}
\hat{R} \langle \psi_\omega^\Omega | &= \sum_{\omega'} \bar{D}_{\omega' \omega}^\Omega(R) \langle \psi_{\omega'}^\Omega | \\
\hat{R} | \phi_\gamma^\Gamma \rangle &= \sum_{\gamma'} D_{\gamma' \gamma}^\Gamma(R) | \phi_{\gamma'}^\Gamma \rangle \\
\hat{R} | O_\lambda^\Lambda | R^{-1} &= \sum_{\lambda'} D_{\lambda' \lambda}^\Lambda(R) | O_{\lambda'}^\Lambda |
\end{aligned}
\tag{6.45}
$$

---

[2] Any permutation can be expressed as a sequence of transpositions of two elements. If the total number of transpositions is even, $\text{sgn}(\sigma) = +1$; if it is odd, $\text{sgn}(\sigma) = -1$. See also Sect. 3.3.

Note that the general form of the operator $|O_\lambda^\Lambda|$ refers to a component of an irreducible set. Such a set of operators is usually referred to as a *tensor operator*. Obvious examples are the components of the electric or magnetic dipole-moment operators. The Wigner–Eckart theorem introduces a symmetry factorization, which simplifies the evaluation of matrix elements.

Theorem 12 *A matrix element, involving a tensor operator, may be factorized into a product of an intrinsic scalar part and an appropriate 3Γ coupling coefficient.*

The scalar constant is denoted by $\langle \psi^\Omega \parallel O^\Lambda \parallel \phi^\Gamma \rangle$, and is called the *reduced matrix element*.

$$\langle \psi_\omega^\Omega | O_\lambda^\Lambda | \phi_\gamma^\Gamma \rangle = \langle \psi^\Omega \parallel O^\Lambda \parallel \phi^\Gamma \rangle \langle \Omega\omega | \Lambda\lambda\Gamma\gamma \rangle \tag{6.46}$$

To prove this theorem, one first considers the coupling of two ingredients of the matrix element, and then compares the result with the third one. We thus first consider the coupling of the operator and the ket. The transformation of their product does indeed correspond to the super matrix which is due to the direct product $\Lambda \times \Gamma$.

$$\hat{R} | O_\lambda^\Lambda | \phi_\gamma^\Gamma \rangle = \hat{R} | O_\lambda^\Lambda | \hat{R}^{-1} \hat{R} | \phi_\gamma^\Gamma \rangle = \sum_{\lambda'} \sum_{\gamma'} D_{\lambda'\lambda}^\Lambda(R) D_{\gamma'\gamma}^\Gamma(R) | O_{\lambda'}^\Lambda | \phi_{\gamma'}^\Gamma \rangle \tag{6.47}$$

This means that we couple the tensor operator and the ket to form product entities:

$$|(O\phi)_\pi^\Pi\rangle = \sum_{\lambda'} \sum_{\gamma'} | O_{\lambda'}^\Lambda | \phi_{\gamma'}^\Gamma \rangle \langle \Lambda\lambda'\Gamma\gamma' | \Pi\pi \rangle \tag{6.48}$$

We now invert this equation, using the unitary properties of the coupling coefficients, to yield:

$$| O_\lambda^\Lambda | \phi_\gamma^\Gamma \rangle = \sum_{\Pi'} \sum_{\pi'} |(O\phi)_{\pi'}^{\Pi'}\rangle \langle \Pi'\pi' | \Lambda\lambda\Gamma\gamma \rangle \tag{6.49}$$

Then we combine this expression with the bra.

$$\langle \psi_\omega^\Omega | O_\lambda^\Lambda | \phi_\gamma^\Gamma \rangle = \sum_{\Pi'} \sum_{\pi'} \langle \psi_\omega^\Omega |(O\phi)_{\pi'}^{\Pi'}\rangle \langle \Pi'\pi' | \Lambda\lambda\Gamma\gamma \rangle \tag{6.50}$$

The matrix elements on the right-hand side are now in fact reduced to an overlap integral where the direct product irreps are compared with the irrep of the bra. Hence, the selection rules for the overlap integrals apply:

$$\langle \Omega\omega |(O\phi)_{\pi'}^{\Pi'}\rangle = \delta_{\Omega,\Pi'} \delta_{\omega\pi'} \frac{1}{\dim(\Omega)} \sum_{\omega'} \langle \Omega\omega' |(O\phi)_{\omega'}^{\Omega'}\rangle \equiv \langle \psi^\Omega \parallel O^\Lambda \parallel \phi^\Gamma \rangle \tag{6.51}$$

The trace summation in this equation is identified as a scalar interaction constant, which is represented by the reduced matrix element.

Combination of Eqs. (6.50) and (6.51) then yields the Wigner–Eckart theorem of Eq. (6.46), where the total interaction is the product of a scalar interaction constant and a CG coupling coefficient. The former refers to the interaction itself, the latter extracts the transformation properties. In case of product multiplicity, there will be one reduced matrix element for every coupling channel, and the matrix element is decomposed into a sum over the channels. The Wigner–Eckart theorem or matrix-element theorem is at the heart of most chemical applications of group theory. It provides an elegant method for separating interactions into an intrinsic part and a part that depends only on the symmetry of the problem under consideration.

An important consequence of the matrix element theorem concerns the definition of selection rules. An interaction will be forbidden if the corresponding coupling coefficient in the Wigner–Eckart theorem is zero. The conditions that control the zero values of the coupling coefficients are called *triangular conditions*, since they involve the combination of three irreps. Two kinds of triangular conditions must be taken into account:

1. Selectivity on the representations: an interaction element is forbidden if the coupling of the three irreps involved is zero, i.e. if the direct product of the operator and ket parts does not include the irrep of the bra.

$$\Omega \notin \Lambda \times \Gamma \tag{6.52}$$

The triad of the three irreps may also be seen as a triple direct product, $\bar{\Omega} \times \Lambda \times \Gamma$, where the bra irrep appears in its complex-conjugate form. Equation (6.8) can now also be read as the character overlap between the totally-symmetric irrep and the triple product. Accordingly, the selection rule of Eq. (6.52) can also be reformulated as: an interaction will be forbidden if the triple product of the irreps does not contain the totally-symmetric irrep.

$$\Gamma_0 \notin \bar{\Omega} \times \Lambda \times \Gamma \tag{6.53}$$

2. Selectivity on the subrepresentations: subrepresentations that are defined in a splitting field must obey the triangular conditions for the subduced irreps in the corresponding subgroup.

6.6 Application: The Jahn–Teller Effect

In 1937 Jahn and Teller made the claim that degenerate states of molecules are intrinsically unstable [6, 7].

Theorem 13 *Non-linear molecules in a spatially-degenerate electronic state are subject to spontaneous symmetry-breaking forces that distort the molecule to a geometry of lower symmetry, where the degeneracy is removed.*

The theorem is based on a perturbation of the Hamiltonian by small displacements of the nuclei. A high-symmetry geometry is chosen as the origin, and the nuclear displacements are described by normal modes which transform as irreps of the point group. The nuclear positions are parameters in the electronic Hamiltonian. One has, to second-order:

$$\mathcal{H} = \mathcal{H}_0 + \mathcal{H}'$$

$$\mathcal{H}' = \sum_{Q_{\Gamma\gamma}} \left(\frac{\partial \mathcal{H}}{\partial Q_{\Gamma\gamma}} \right)_0 Q_{\Gamma\gamma} + \frac{1}{2} \sum_{Q_{\Gamma\gamma}} \sum_{Q_{\Gamma'\gamma'}} \left(\frac{\partial^2 \mathcal{H}}{\partial Q_{\Gamma\gamma} \partial Q_{\Gamma'\gamma'}} \right)_0 Q_{\Gamma\gamma} Q_{\Gamma'\gamma'} \tag{6.54}$$

The partial derivatives with respect to the normal modes will affect only the electrostatic V_{Ne} term in the Hamiltonian. These operators are thus electrostatic one-electron operators. At the coordinate origin, the electronic state is degenerate, and is described by a set of wavefunctions, $|\Gamma_a \gamma_a\rangle$, where Γ_a is a degenerate irrep. The energies as functions of the coordinates are obtained by diagonalizing the Hamiltonian matrix, $\mathbb{H}$, with elements:

$$H_{\gamma_a\gamma_b} = \langle \Gamma_a \gamma_a | \mathcal{H} | \Gamma_a \gamma_b \rangle = E_0 \delta_{\gamma_a\gamma_b} + \langle \Gamma_a \gamma_a | \mathcal{H}' | \Gamma_a \gamma_b \rangle \tag{6.55}$$

The matrix in $\mathcal{H}'$ is also called the Jahn–Teller (JT) matrix. The linear terms in this matrix are of type:

$$\left\langle \Gamma_a \gamma_a \left| \left(\frac{\partial \mathcal{H}}{\partial Q_{\Gamma\gamma}} \right)_0 Q_{\Gamma\gamma} \right| \Gamma_a \gamma_b \right\rangle = \left\langle \Gamma_a \gamma_a \left| \frac{\partial \mathcal{H}}{\partial Q_{\Gamma\gamma}} \right| \Gamma_a \gamma_b \right\rangle_0 Q_{\Gamma\gamma} \tag{6.56}$$

We have used the fact that the integration in this matrix element runs over electronic coordinates, and does not affect the nuclear coordinates. The Wigner–Eckart theorem can be applied to derive the selection rules. Since the Hamiltonian is invariant under the elements of the symmetry group, the transformation properties of the operator part in this matrix element will be determined by the partial derivatives, $\partial/\partial Q_{\Gamma\gamma}$. As we have seen in Sect. 1.3, a partial derivative in a variable has the same transformation properties as the variable itself.[3] The operator part is thus given by:

$$\left\langle \Gamma_a \gamma_a \left| \frac{\partial \mathcal{H}}{\partial Q_{\Gamma\gamma}} \right| \Gamma_a \gamma_b \right\rangle_0 = \langle \Gamma_a \parallel \Gamma \parallel \Gamma_a \rangle \langle \Gamma_a \gamma_a | \Gamma\gamma \Gamma_a \gamma_b \rangle \tag{6.57}$$

The coupling coefficient on the right-hand side of Eq. (6.57) restricts the symmetry of the nuclear displacements to the direct square of the irrep of the electronic wavefunction. This selection rule is made even more stringent by time-reversal symmetry. The Hamiltonian is based on displacement of nuclear charges, and not on momenta, so as an operator it is time-even or real.[4] For spatially-degenerate irreps, which are

---

[3] For complex variables, variable and derivative have complex-conjugate transformation properties.

[4] The general time-reversal selection rules are discussed in Sect. 7.6.

of the first kind, i.e. can be represented by real functions, JT matrix elements can thus be chosen to be entirely real, which implies:

$$\langle \Gamma_a \gamma_a | \mathcal{H}' | \Gamma_a \gamma_b \rangle = \langle \Gamma_a \gamma_b | \mathcal{H}' | \Gamma_a \gamma_a \rangle \tag{6.58}$$

Combining this result with Eq. (6.57) implies that the coupling coefficients, to first-order, should obey:

$$\langle \Gamma_a \gamma_a | \Gamma \gamma \Gamma_a \gamma_b \rangle = \langle \Gamma_a \gamma_b | \Gamma \gamma \Gamma_a \gamma_a \rangle \tag{6.59}$$

In view of Eq. (6.31) this condition can be rewritten as:

$$\langle \Gamma_a \gamma_a \Gamma_a \gamma_b | \Gamma \gamma \rangle = \langle \Gamma_a \gamma_b \Gamma_a \gamma_a | \Gamma \gamma \rangle \tag{6.60}$$

The JT distortion modes are thus restricted to the symmetrized square of the degenerate irrep of the electronic state, minus the totally-symmetric modes, since these cannot lower the symmetry:

$$\Gamma \in \left([\Gamma_a \times \Gamma_a] - \Gamma_0 \right) \tag{6.61}$$

Modes that obey this selection rule, are said to be *JT active*. The evaluation of the second-order matrix elements requires two steps. One first couples the two distortion modes to a composite tensor operator: $|\Omega \omega|$.

$$\left| \frac{\partial^2 \mathcal{H}}{\partial Q_{\Gamma \gamma} \partial Q_{\Gamma' \gamma'}} \right| = \sum_{\Omega \omega} |\Omega \omega \rangle \langle \Omega \omega | \Gamma \gamma \Gamma' \gamma' \rangle \tag{6.62}$$

The second-order matrix element then becomes:

$$\begin{aligned} &\left\langle \Gamma_a \gamma_a \left| \frac{\partial^2 \mathcal{H}}{\partial Q_{\Gamma \gamma} \partial Q_{\Gamma' \gamma'}} \right| \Gamma_a \gamma_b \right\rangle_0 \\ &= \sum_{\Omega \omega} \langle \Gamma_a \parallel \Omega \parallel \Gamma_a \rangle \langle \Omega \omega | \Gamma \gamma \Gamma' \gamma' \rangle \langle \Gamma_a \gamma_a | \Omega \omega \Gamma_a \gamma_b \rangle \end{aligned} \tag{6.63}$$

The second-order elements thus are related to a product of two 3Γ symbols.[5] A special element arises when Ω is totally symmetric. In this case, the coupling coefficients are given by:

$$\begin{aligned} \langle \Gamma_0 | \Gamma \gamma \Gamma' \gamma' \rangle &= \frac{1}{\sqrt{\dim(\Gamma)}} \delta_{\Gamma \Gamma'} \delta_{\gamma \gamma'} \\ \langle \Gamma_a \gamma_a | \Gamma_0 \Gamma_a \gamma_b \rangle &= \delta_{\gamma_a \gamma_b} \end{aligned} \tag{6.64}$$

---

[5]Such combinations can be cast in a higher-order symbol, known as 6Γ symbol, by analogy with the $6j$ coupling coefficients in atomic spectroscopy.

The second-order expressions then are reduced to a diagonal matrix element:

$$\langle \Gamma_a \parallel \Gamma_0 \parallel \Gamma_a \rangle \langle \Gamma_0 | \Gamma \gamma \Gamma' \gamma' \rangle \langle \Gamma_a \gamma_b | \Gamma_0 \Gamma_a \gamma_b \rangle$$

$$= \frac{1}{\sqrt{\dim(\Gamma)}} \langle \Gamma_a \parallel \Gamma_0 \parallel \Gamma_a \rangle \delta_{\Gamma \Gamma'} \delta_{\gamma \gamma'} \delta_{\gamma_a \gamma_b} = K_\Gamma \delta_{\Gamma \Gamma'} \delta_{\gamma \gamma'} \delta_{\gamma_a \gamma_b} \quad (6.65)$$

K_Γ in this equation is the harmonic force-constant. It gives rise to a constant diagonal term which provides an attractive potential around the minimum and keeps the surface bound at larger distances from the origin. The general expression for the potential-energy surface then becomes:

$$E_k(Q) = E_0 + \sum_\Gamma \frac{1}{2} K_\Gamma \left(\sum_\gamma Q_{\Gamma \gamma}^2 \right) + \varepsilon_k(Q) \quad (6.66)$$

Here, $\varepsilon_k(Q)$ represents the kth root of the Hamiltonian matrix. This equation describes a surface with multiple sheets, one for each root, which cross in the high-symmetry origin. In its simplest form the Hamiltonian can be restricted to the linear terms only. In the second-order approximation non-totally-symmetric second-order terms will also be included.

The prototype of the JT surface is the celebrated *Mexican hat* potential, which describes the effect of the twofold-degenerate cubic or trigonal E state. A typical example is the ^2E_g ground state of octahedral Cu^{2+} complexes, with $(t_{2g})^6(e_g)^3$ configuration. The JT-active mode in this case is restricted to an e_g mode, corresponding to the symmetrized square.

$$[E_g \times E_g] - A_{1g} = E_g \quad (6.67)$$

This distortion mode consists of the tetragonal and orthorhombic stretchings, which we already encountered as vibrational modes of UF_6, and are depicted in Fig. 6.1. By use of the appropriate $\langle Ei | Ej Ek \rangle$ coupling coefficients the JT matrix can easily be derived. The force element is defined as:

$$F_E = \left\langle E\theta \left| \frac{\partial \mathcal{H}}{\partial Q_\theta} \right| E\theta \right\rangle \quad (6.68)$$

The matrix then becomes:

$$\mathbb{H} = \left(E_0 + \frac{1}{2} K_E (Q_\theta^2 + Q_\epsilon^2) \right) \begin{bmatrix} 1 & 0 \\ 0 & 1 \end{bmatrix} + F_E \begin{bmatrix} Q_\theta & Q_\epsilon \\ Q_\epsilon & -Q_\theta \end{bmatrix} \quad (6.69)$$

To diagonalize this Hamiltonian, it is convenient to transform to cylindrical coordinates $\{\rho, \varphi\}$:

$$Q_\theta = \rho \cos \varphi$$
$$Q_\epsilon = \rho \sin \varphi \quad (6.70)$$
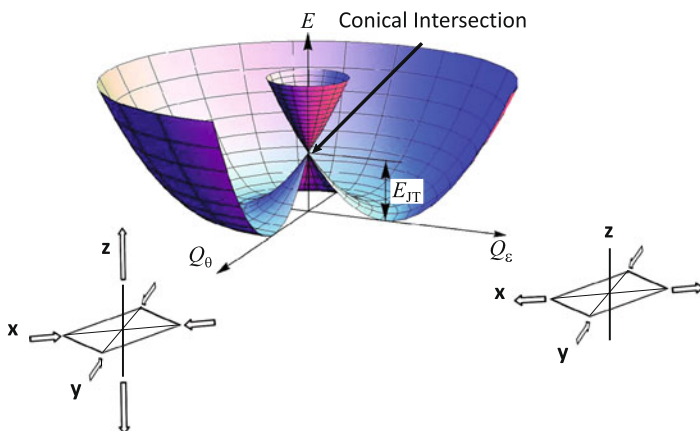
Fig. 6.1 The Mexican hat potential-energy surface of the $E \times e$ linear JT problem. The nuclear displacement coordinates are the tetragonal elongation, Q_θ, and the orthorhombic in-plane distortion, Q_ϵ

Then the secular equation of the force element matrix in Eq. (6.69) becomes:

$$\varepsilon_k^2 - F_E^2 \rho^2 \cos^2 \varphi - F_E^2 \rho^2 \sin^2 \varphi = 0 \tag{6.71}$$

Two roots are found, which are independent of the angular coordinate. The corresponding eigenfunctions are:

$$\epsilon_1 = F_E \rho \longrightarrow |\psi_1\rangle = \cos \frac{\varphi}{2} |E\theta\rangle + \sin \frac{\varphi}{2} |E\epsilon\rangle$$

$$\epsilon_2 = -F_E \rho \longrightarrow |\psi_2\rangle = -\sin \frac{\varphi}{2} |E\theta\rangle + \cos \frac{\varphi}{2} |E\epsilon\rangle \tag{6.72}$$

The surface consists of two sheets and exhibits rotational symmetry.

$$E_\pm = E_0 + \frac{1}{2} K_E \rho^2 \pm F_E \rho$$

$$= E_0 + \frac{1}{2} K_E (Q_\theta^2 + Q_\epsilon^2) \pm F_E \sqrt{Q_\theta^2 + Q_\epsilon^2} \tag{6.73}$$

A cross section of this surface looks like a two-well potential, with two displaced parabolæ. The depth of the well is called the JT stabilization energy:

$$E_{JT} = -\frac{F_E^2}{2K_E} \tag{6.74}$$

In the 2D space of the active modes these parabolæ revolve around the centre, giving rise to the Mexican hat appearance. At the origin this surface has the shape of a conical intersection, indicating that the high-symmetry point is unstable, and will spontaneously relax to the circular trough surrounding the degeneracy [8]. The

distorted system in the trough orbits around the origin. This motion is a *pseudo-rotation*, i.e. it is not a rotation of the molecular frame, but a gradual redistribution of the distortions between the Cartesian directions. We illustrate this in Fig. 6.2. The starting point is at $\varphi = 0$, in the direction of the Q_θ mode. In this mode the z-axis is elongated, and the xy-plane is contracted. A counterclockwise rotation activates the orthorhombic Q_ϵ mode, while the tetragonal Q_θ mode is receding. This introduces a difference between the x- and y-axes: the distortion in the x-direction becomes more pronounced, while the y-axis contracts further. At the same time the elongation of the z-axis diminishes. At an angle of $60°$ the x- and z-axes are both elongated to an equal extent, giving rise to a weak xz-plane and a strong y-axis. At the $90°$ point the Q_θ contribution vanishes, and the distortion is orthorhombic, with a short y-axis, an elongated x-axis, and an undistorted z-axis. At an angle of $120°$ we reach the point where the x-axis is weak, and the perpendicular yz-plane is strong. We thus have regained an elongated tetragonal configuration, but the elongation has been rotated from the z-axis to the x-axis. Continuing now at $240°$ we shall have travelled another third of the trough and reoriented the tetragonal axis along the y-direction. We can also follow the wavevector along the trough. If it is assumed that $F_E < 0$, the lower eigenfunction will be the $|\psi_1\rangle$ eigenfunction of Eq. (6.72). In the starting elongated tetragonal configuration the ground state coincides with the $|E\theta\rangle$ basis function. By the time we have reached the orthorhombic configuration at $\varphi = 90°$, the ground state has rotated by only half that angle and equals $1/\sqrt{2}(|E\theta\rangle + |E\epsilon\rangle)$. At $180°$, we reach a structure which is tetragonally compressed along the z-direction. Accordingly, the Q_θ mode has changed sign, in contrast to the eigenfunction, where $|E\theta\rangle$ is replaced by $|E\epsilon\rangle$. The observation of rotational symmetry is an unexpected feature, which is not related to the point group, but which stems from the limitation of the JT Hamiltonian to linear terms. To describe this symmetry we first reformulate the force element Hamiltonian in Eq. (6.69) in Dirac notation:

$$\mathcal{H}' = F_E\big(Q_\theta\big[|E\theta\rangle\langle E\theta| - |E\epsilon\rangle\langle E\epsilon|\big] + Q_\epsilon\big[|E\theta\rangle\langle E\epsilon| + |E\epsilon\rangle\langle E\theta|\big]\big) \qquad (6.75)$$

The angular momentum operator, corresponding to a rotation in coordinate space, is given by:

$$\mathcal{L} = \frac{\partial}{\partial\varphi} = \frac{\partial Q_\epsilon}{\partial\varphi}\frac{\partial}{\partial Q_\epsilon} + \frac{\partial Q_\theta}{\partial\varphi}\frac{\partial}{\partial Q_\theta} = Q_\theta\frac{\partial}{\partial Q_\epsilon} - Q_\epsilon\frac{\partial}{\partial Q_\theta} \qquad (6.76)$$

The partial derivatives were obtained from Eq. (6.70). The commutator of this operator with the Hamiltonian is:

$$\big[\mathcal{L}, \mathcal{H}'\big] = F_E\big(-Q_\epsilon\big[|E\theta\rangle\langle E\theta| - |E\epsilon\rangle\langle E\epsilon|\big] + Q_\theta\big[|E\theta\rangle\langle E\epsilon| + |E\epsilon\rangle\langle E\theta|\big]\big) \quad (6.77)$$

Surprisingly, this commutator does not vanish. This is an important observation, which directly points to the vibrational-electronic or *vibronic* coupling between the distortion modes and the electronic wavevector. When the system rotates around the origin in coordinate space, not only are the coordinates changing, but the wavevector is also rotating simultaneously, so we must also provide an angular momentum

Fig. 6.2 Rotation of the distortion in the trough of the Mexican hat. Along the Q_θ coordinate the complex is elongated along its z-axis. Rotation around the centre in the direction of Q_ϵ will shorten the z-axis and increase the x-axis. At an angle of revolution of 120° a tetragonally elongated structure is again found, but this time with the elongation along the x-direction, and similarly at 240°, with the elongation along the y-axis
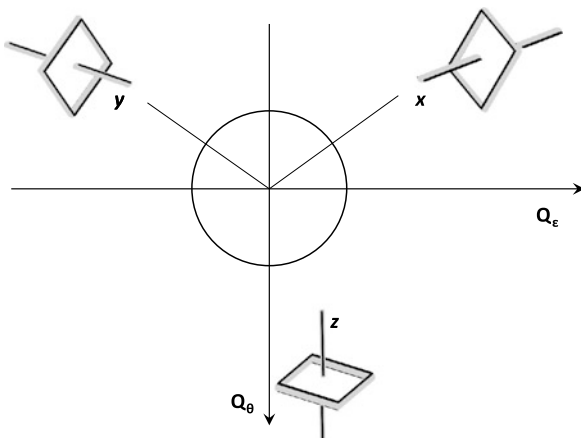
operator for a rotation in the function space (see [9]). We can construct this by analogy with Eq. (6.76), but with an important amendment: as we have argued while discussing Fig. 6.2, the coordinates rotate twice as quickly as the wavevector, and hence a prefactor of $1/2$ is required!

$$\mathcal{S} = \frac{1}{2}\big(|E\theta\rangle\langle E\epsilon| - |E\epsilon\rangle\langle E\theta|\big) \tag{6.78}$$

Only in this case does the total momentum operator $\mathcal{J} = \mathcal{L} + \mathcal{S}$ commute with the Hamiltonian:

$$\big[\mathcal{J}, \mathcal{H}'\big] = \big[\mathcal{L}, \mathcal{H}'\big] + \big[\mathcal{S}, \mathcal{H}'\big] = 0 \tag{6.79}$$

As the reader will have noticed, we have made use of the standard spectroscopic symbols for orbital angular momentum, spin momentum, and total momentum. Vibronic coupling is indeed analogous to coupling of spin and orbit momenta in cylindrical molecules. To form the vibronic wavefunction, describing the dynamics of the Mexican hat system, the electronic state has to be combined with nuclear wavefunctions. If the JT effect is pronounced, the vibronic levels take the form of a radial oscillator, describing transverse oscillations in the bottom of the through, and pseudo-rotational levels, describing the longitudinal motion along the bottom of the trough. The total vibronic wavefunction should of course be single-valued after a full turn around the trough, which takes the system back to the starting point. Hence, since the electronic part changes sign after a full turn, the vibrational part should also show a compensating sign change. This is indeed the case: the pseudo-rotational levels are characterized by half-integral angular momentum [10].

6.7 Application: Pseudo-Jahn–Teller interactions

Pseudo-JT interactions (PJT) refer to the second-order vibronic coupling between electronic states which are separated by a gap [11]. In this section we describe the

case of a non-degenerate ground state, $|\psi_{\Sigma\sigma}\rangle$, which is coupled to an excited manifold. The Hamiltonian is identical to the expression in Eq. (6.54). Application of the selection rules shows that the diagonal contribution, $\langle\psi_{\Sigma\sigma}|\mathcal{H}|\psi_{\Sigma\sigma}\rangle$, is limited to the totally-symmetric operator associated with the harmonic restoring-force, as in Eq. (6.66). Perturbation theory further provides interactions between the ground and excited states. These interactions are usually limited to first-order contributions, which give rise to a quadratic coordinate dependence. Hence one has, to second-order in the displacements:

$$
E(Q) = E_0 + \sum_{\Gamma} \frac{1}{2} K_{\Gamma} \left(\sum_{\gamma} Q_{\Gamma\gamma}^2 \right)
$$
$$
+ \sum_{\Lambda\lambda} \sum_{\Gamma\gamma} \frac{|\langle\psi_{\Lambda\lambda}| \frac{\partial\mathcal{H}}{\partial Q_{\Gamma\gamma}} |\psi_{\Sigma\sigma}\rangle_0|^2}{E_0 - E_{\Lambda}} Q_{\Gamma\gamma}^2 \tag{6.80}
$$

where we have used the property that the Hamiltonian matrix is hermitian. The selection rule in this process resides with the matrix elements in the enumerator of the bilinear term. The vibronic operator must couple ground and excited states; hence, it is required that their triple direct product contains the totally-symmetric irrep:

$$
\Gamma_0 \in \bar{\Gamma}_{\Lambda} \times \Gamma \times \Sigma \tag{6.81}
$$

Applying the Wigner–Eckart theorem to the matrix element yields:

$$
\left\langle \psi_{\Lambda\lambda} \left| \frac{\partial\mathcal{H}}{\partial Q_{\Gamma\gamma}} \right| \psi_{\Sigma\sigma} \right\rangle_0 = \langle\Lambda\lambda|\Gamma\gamma\Sigma\sigma\rangle\langle\Lambda \parallel \Gamma \parallel \Sigma\rangle \tag{6.82}
$$

The sum over the λ components of the excited state, transforming as the Λ irrep, can be simplified by using the orthonormality property of the coupling coefficients from Eq. (6.16).

$$
\sum_{\lambda\in\Lambda} \frac{|\langle\psi_{\Lambda\lambda}| \frac{\partial\mathcal{H}}{\partial Q_{\Gamma\gamma}} |\psi_{\Sigma\sigma}\rangle_0|^2}{E_0 - E_{\Lambda}} = \sum_{\lambda\in\Lambda} \frac{|\langle\Lambda\lambda|\Gamma\gamma\Sigma\sigma\rangle\langle\Lambda \parallel \Gamma \parallel \Sigma\rangle|^2}{E_0 - E_{\Lambda}}
$$
$$
= \frac{|\langle\Lambda \parallel \Gamma \parallel \Sigma\rangle|^2}{E_0 - E_{\Lambda}} \tag{6.83}
$$

Note that in case of a non-degenerate ground state the product $\Gamma \times \Sigma$ yields only one irrep, since the norm of the product character string equals the order of the group.

$$
\langle\chi^{\Gamma\times\Sigma}|\chi^{\Gamma\times\Sigma}\rangle = \langle\chi^{\Gamma}\chi^{\Sigma}|\chi^{\Gamma}\chi^{\Sigma}\rangle = \langle\chi^{\Gamma}|\chi^{\Gamma}\rangle = |G| \tag{6.84}
$$
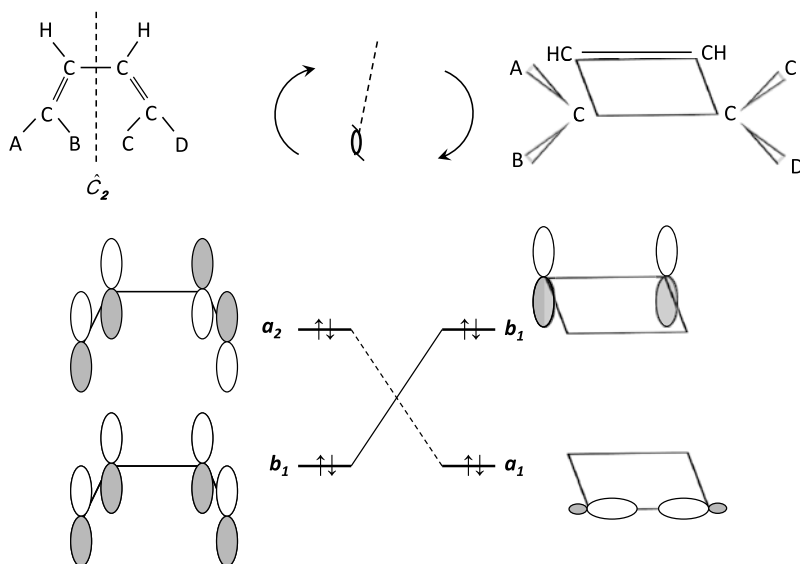
Fig. 6.3 Ring closure of *cis*-butadiene to *cyclo*-butene. In C_{2v} symmetry there is a symmetry mismatch between the a_2 and a_1 occupied orbitals. Vibronic orbital coupling requires a concerted mechanism, based on a conrotatory ring closure, which conserves only the $\hat{C}_2$ axis

The summation over $\lambda \in \Lambda$ thus covers the entire product space of $\Gamma \times \Sigma$. Combining the sum rule of Eq. (6.83) with the total expression for the PJT, one finds:

$$E(Q) = E_0 + \sum_\Gamma \left\{ \frac{1}{2} K_\Gamma + \sum_\Lambda \frac{|\langle \Lambda \, \| \, \Gamma \, \| \, \Sigma \rangle|^2}{E_0 - E_\Lambda} \right\} \left(\sum_\gamma Q_{\Gamma\gamma}^2 \right) \qquad (6.85)$$

Hence, when the ground state is non-degenerate, the first-order dependence of the energy on symmetry-lowering displacement vanishes, and the second-order term contains two contributions: the diagonal harmonic force constant, which is always positive, and the bilinear relaxation term, which is always negative. If the excited states are close in energy to the ground state, and if the vibronic coupling is strong, the relaxation term may be dominant, and a second-order symmetry-breaking effect will result. This is known as the pseudo-JT effect. There are two main applications of this effect: in geometry optimization, and in reaction dynamics.

In reaction dynamics the PJT may be responsible for stereoselectivity, because of the selection rules for vibronic coupling matrix elements. Via these relaxation matrix elements the Wigner–Eckart theorem is at the basis of the Woodward–Hoffmann rules [12]. We shall not discuss these rules in general, but consider some simple illustrations, related to electrocyclic reactions.[6] Take as a simple example the ring closure of *cis*-butadiene, as illustrated in Fig. 6.3. The relevant occupied orbitals are

[6]Based on [13].
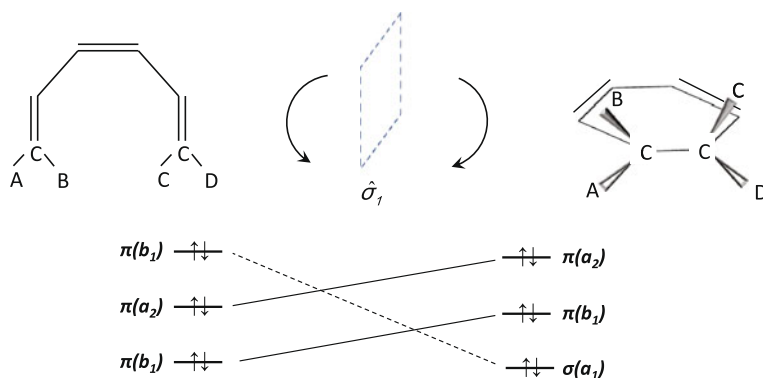
Fig. 6.4 Ring closure of *cis*-1, 3, 5-hexatriene to *cyclo*-hexadiene. In C_{2v} symmetry there is a symmetry mismatch between the b_1 and a_1 occupied orbitals. Vibronic orbital coupling requires a concerted mechanism, based on a disrotatory ring closure, which conserves only the $\hat{\sigma}_1$ plane

the π-bonds in the reagent, and the remaining π- and newly formed σ-bonds in the product. As the diagram shows, in the common C_{2v} point group there is a mismatch between the symmetries. In order for the reaction to occur, the reaction coordinate has to reduce the symmetry so that the a_2-orbital can interchange with an a_1-orbital. This interchange is taking place via a PJT mechanism which couples the a_2 occupied orbital to an a_1 virtual orbital in the reagent. As the reaction coordinate proceeds, this coupling is intensified and leads to an interchange of both. The relevant matrix element is thus an orbital vibronic coupling element:

$$\left\langle a_2 \left| \frac{\partial \mathcal{H}}{\partial Q_{\Gamma\gamma}} \right| a_1 \right\rangle \neq 0 \qquad (6.86)$$

Hence, a distortion coordinate is required which transforms as $a_2 \times a_1 = a_2$. The coordinate with this symmetry is the one that destroys the symmetry planes but keeps the twofold axis. This is typically a *conrotatory* reaction, where the extremal carbon atoms rotate simultaneously in the same sense, to form the σ-bond. Ring closure of substituted butadienes thus follows a conrotatory reaction stereochemistry, at least if the reaction is concerted.

This ring-closure selection rule is further confirmed by the closure reaction for the cis-1, 3, 5 hexatriene to 1, 3-cyclohexadiene, as illustrated in Fig. 6.4. Here, a b_1-orbital has to interchange with a virtual orbital of a_1 symmetry. The selection takes thus place at the level of the orbital matrix element:

$$\left\langle b_1 \left| \frac{\partial \mathcal{H}}{\partial Q_{\Gamma\gamma}} \right| a_1 \right\rangle \neq 0 \qquad (6.87)$$

Clearly, the distortion coordinate should now be of $b_1 \times a_1 = b_1$ symmetry, and this corresponds to the *disrotatory* mode, which destroys the $\hat{C}_2$ axis but keeps the vertical reflection plane.

6.8 Application: Linear and Circular Dichroism

Selection rules are of primary importance in spectroscopy, where they provide direct evidence concerning the nature of excited states. As an application, we study the linear and circular dichroism of tris-chelate transition-metal complexes [14]. The prototype is a divalent ruthenium complex with three $2, 2'$-bipyridyl ligands, which is an important chromophore for energy conversion. In this section we shall describe the charge transfer and intra-ligand transitions of this type of complex. The linear dichroism (LD) spectrum measures the absorption of the chromophore under plane-polarized incident light for different orientations of the polarization with respect to the molecular frame. This requires that the molecules should be embedded in an oriented phase, such as a crystalline host. Circular dichroism (CD) measures the difference in absorption between left and right circularly polarized light. Since this is based on the intrinsic helicity of the molecule, it can be performed in non-oriented medium, such as a solution.

As always, we start the treatment by making a simple sketch of the structure. Two sets of Cartesian axes are relevant. In the usual octahedral coordinate system the x, y, z-axes coincide with the metal-ligand bond directions, assuming that the ligator atoms form a perfect octahedron. In addition, in Fig. 3.6 of Chap. 3 a primed x', y', z'-coordinate system was introduced, which is adapted to the tris-chelate geometry. The z'-axis is along the threefold direction, and the x' axis is oriented along a twofold axis, coinciding with the bisector of the positive x and the negative y axes. Next, we determine the point group, which in the present case is D_3. This is a rotational group, which implies that the molecule is chiral. The figure shows the Δ-enantiomer.[7] Thirdly, we define the functional basis. The relevant orbitals are the metal t_{2g} orbitals, which are fully occupied in the Ru^{2+} ground state, and the frontier orbitals on the ligand. For conjugated bidentate ligands, such as $2, 2'$-bipyridyl (bipy) or 2, 4-pentanedionate (also named "acetylacetonate", acac$^-$), the frontier orbitals are of π-type. The essential parts of these orbitals are the contributions on the ligator atoms. These are either symmetric or antisymmetric with respect to the twofold axis through the bidentate ligand, as shown in Fig. 6.5. Following Orgel, we denote them as χ- or ψ-type, respectively [15]. The standard techniques of characters and projection operators yield SALCs for all these basis sets. The results are shown in Table 6.4. For the e-irrep the components are labelled as e_θ and e_ϵ, following the standard canonical format. As a splitting field we use the twofold axis along x'. Finally, we also include in the table the symmetries of the transition dipoles, which are the operators for the optical transitions. This completes the groundwork for the symmetry analysis.

---

[7]In tris-chelate complexes Δ refers to a right-handed (*dextro*) helix. A left-handed helix (*lævo*) is denoted as Λ.
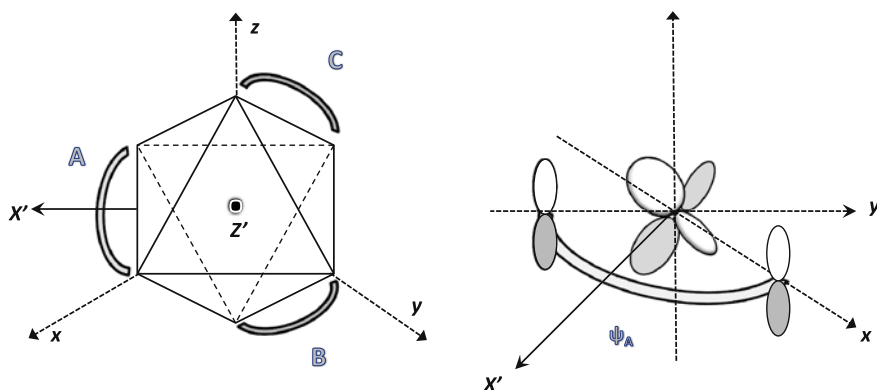
Fig. 6.5 Δ-enantiomer of tris-chelate octahedral complex of D_3 symmetry. The xyz-coordinate system passes through the ligator atoms; the primed coordinate system has the z'-direction along the threefold axis, and x' on a twofold axis through ligand A. The ligand orbital shown on the right is of ψ-type: it is antisymmetric under a rotation about the twofold axis through the ligator bridge. The ψ orbital on ligand A interacts with the $\frac{1}{\sqrt{2}}(d_{xz} - d_{yz})$-combination on the metal

Table 6.4 Symmetry-adapted zeroth-order metal and ligand orbital functions

t_{2g}-orbitals	dipole moments
$\lvert a_1\rangle = \frac{1}{\sqrt{3}}(d_{xy} + d_{xz} + d_{yz})$	$a_2 : \mu_{z'}$
$\lvert e_\theta\rangle = \frac{1}{\sqrt{6}}(-2d_{xy} + d_{xz} + d_{yz})$	$e_\theta : \mu_{x'}$
$\lvert e_\epsilon\rangle = \frac{1}{\sqrt{2}}(d_{xz} - d_{yz})$	$e_\epsilon : \mu_{y'}$

ψ-orbitals	χ-orbitals
$\lvert a_2\rangle = \frac{1}{\sqrt{3}}(\lvert\psi_A\rangle + \lvert\psi_B\rangle + \lvert\psi_C\rangle)$	$\lvert a_1\rangle = \frac{1}{\sqrt{3}}(\lvert\chi_A\rangle + \lvert\chi_B\rangle + \lvert\chi_C\rangle)$
$\lvert e_\theta\rangle = \frac{1}{\sqrt{2}}(\lvert\psi_C\rangle - \lvert\psi_B\rangle)$	$\lvert e_\theta\rangle = \frac{1}{\sqrt{6}}(2\lvert\chi_A\rangle - \lvert\chi_B\rangle - \lvert\chi_C\rangle)$
$\lvert e_\epsilon\rangle = \frac{1}{\sqrt{6}}(2\lvert\psi_A\rangle - \lvert\psi_B\rangle - \lvert\psi_C\rangle)$	$\lvert e_\epsilon\rangle = \frac{1}{\sqrt{2}}(\lvert\chi_B\rangle - \lvert\chi_C\rangle)$

Linear Dichroism

The linear dichroism is associated with the metal-to-ligand charge-transfer (CT) transitions [16]. Dipole-allowed transitions between the orbitals are governed by the appropriate D_3 coupling coefficients. However, since both donor and acceptor orbitals, as well as the transition operators, each involve two irreps, several symmetry-independent coupling channels are possible. As is often the case in transition-metal spectroscopy, it is not sufficient to identify the reduced matrix elements; for a deeper understanding a further development of the model is often required to compare the reduced matrix elements. In the case of the CT bands the model of Day and Sanders offers just that little extra [17]. According to this simple model, a charge-transfer

(CT) transition between metal and ligand gains intensity when the relevant metal and ligand orbitals interact.

We first calculate the interaction terms between the metal and isolated ligand orbitals. The bipy ligand has low-lying unoccupied levels of ψ-character, which form π-acceptor interactions with the metal t_{2g} orbitals. Let H_π represent the elementary interaction between a ligand ψ orbital and a metal t_{2g} orbital, directed towards one ligator. The allowed interactions are then obtained by cyclic permutation:

$$
\begin{aligned}
H_\pi &= \langle d_{xz}|\mathcal{H}|\psi^A \rangle = -\langle d_{yz}|\mathcal{H}|\psi^A \rangle \\
&= \langle d_{xy}|\mathcal{H}|\psi^B \rangle = -\langle d_{xz}|\mathcal{H}|\psi^B \rangle \\
&= \langle d_{yz}|\mathcal{H}|\psi^C \rangle = -\langle d_{xy}|\mathcal{H}|\psi^C \rangle
\end{aligned}
\tag{6.88}
$$

In order to apply the model of Day and Sanders, we now consider the CT transition between the ligand orbital on A and the t_{2g} combination that interacts with it. As shown in Fig. 6.5, the ψ^A-acceptor orbital is antisymmetric with respect to the $\hat{C}_2^{x'}$ axis and antisymmetric in the xy-plane. The only matching t_{2g} combination on the metal is the $|e_\epsilon(t_{2g})\rangle$ component (see Table 6.4). In the local C_{2v} symmetry, $|\psi_A\rangle$ and $|e_\epsilon(t_{2g})\rangle$ both transform as b_2 (taking the horizontal plane as the local $\hat{\sigma}_1$). Their interaction element is expressed as:

$$
\langle e_\epsilon(t_{2g})|\mathcal{H}|\psi^A \rangle = \frac{1}{\sqrt{2}}\langle d_{xz} - d_{yz}|\mathcal{H}|\psi^A \rangle = \sqrt{2}H_\pi
\tag{6.89}
$$

We now consider the transition dipole moment between these orbitals along the x' direction, with $\mu_{x'} = -ex'$. In C_{2v} symmetry this component transforms as a_1, while $\mu_{y'}$ and $\mu_{z'}$ are antisymmetric with respect to the $\hat{C}_2^{x'}$ axis. According to the Wigner–Eckart theorem, a transition dipole between two b_2 orbitals must transform as the direct product $b_2 \times b_2 = a_1$; hence, only the x'- component will be dipole-allowed. In a perturbative approach, which takes into account the symmetry-allowed interaction between the metal and ligand orbitals, one has:

$$
\mu\big(e_\epsilon(t_{2g}) \to \psi^A\big) = \langle e_\epsilon(t_{2g})|\mu_{x'}|\psi^A \rangle - \frac{\langle e_\epsilon(t_{2g})|\mathcal{H}|\psi^A \rangle}{E_\psi - E_{t_{2g}}}\langle \psi^A|\mu_{x'}|\psi^A \rangle
\tag{6.90}
$$

In this expression the first term is the *contact* term between the zeroth-order orbitals. The second term is the *transfer* term, arising from the interaction between the donor and acceptor orbitals. In the simplified model of Day and Sanders this term is the dominant contribution. The transfer-dipole matrix element in Eq. (6.90) is approximated as the dipole length of the transferred charge, which we will represent as μ_A.

$$
\langle \psi^A|\mu_{x'}|\psi^A \rangle = -e\langle \psi^A|x'|\psi^A \rangle \approx -e|\mathbf{R}_A| = -e\rho \equiv \mu_A
\tag{6.91}
$$

where $\mathbf{R}_A$ is the radius vector from the origin to the centre of ligand A, with length ρ. Since the three ligands are equivalent, we further write:

$$
\mu_A = \mu_B = \mu_C \equiv \mu^\perp
\tag{6.92}
$$

The three vectors of the ligand positions can be expressed in a row notation for the primed x', y', z' coordinate system as:

$$\mathbf{R}_A = \rho(1, 0, 0)$$

$$\mathbf{R}_B = \rho\left(-\frac{1}{2}, \frac{\sqrt{3}}{2}, 0\right) \tag{6.93}$$

$$\mathbf{R}_C = \rho\left(-\frac{1}{2}, -\frac{\sqrt{3}}{2}, 0\right)$$

The transfer term then becomes:

$$\boldsymbol{\mu}\left(e_\epsilon(t_{2g}) \rightarrow \psi^A\right) = -e\kappa\,\mathbf{R}_A = \kappa\,\boldsymbol{\mu}_A \tag{6.94}$$

where the parameter κ is an overlap factor which indicates what fraction of the charge is actually transferred:

$$\kappa = -\frac{\langle e_\epsilon(t_{2g})|\mathcal{H}|\psi^A\rangle}{E_\psi - E_{t_{2g}}} = -\frac{\sqrt{2}H_\pi}{E_\psi - E_{t_{2g}}} \tag{6.95}$$

Note that the transfer term is always polarized in the direction of the transferred charge.

    This parametrization can now be used to calculate the transfer term for the relevant trigonal transitions. The Hamiltonian operator is of course totally symmetric, so allowed interactions can take place only between orbitals with the same symmetry, and are independent of the component; hence:

$$\langle e_\epsilon(t_{2g})|\mathcal{H}|e_\epsilon(\psi)\rangle = \sqrt{3}H_\pi$$

$$\langle e_\theta(t_{2g})|\mathcal{H}|e_\theta(\psi)\rangle = \sqrt{3}H_\pi \tag{6.96}$$

    Symmetry prevents interaction between the $a_1(t_{2g})$ and $a_2(\psi)$ orbitals. The metal-ligand π acceptor interaction will thus stabilize the e-component of the t_{2g} shell, while leaving the a_1-orbital in place, as shown in the simple orbital-energy diagram in the left panel of Fig. 6.6. We can now calculate the transfer term for the $e \rightarrow e$ and $e \rightarrow a_2$ orbital transitions. In each case only one component needs to be calculated. The interaction element in this case is obtained from Eq. (6.96) and the transfer fraction reads:

$$-\frac{\sqrt{3}H_\pi}{E_\psi - E_{t_{2g}}} = \sqrt{\frac{3}{2}}\kappa \tag{6.97}$$

The transfer-dipole element is given by:

$$\frac{1}{6}\langle 2\psi^A - \psi^B - \psi^C|\boldsymbol{\mu}|2\psi^A - \psi^B - \psi^C\rangle = \frac{1}{6}[4\boldsymbol{\mu}_A + \boldsymbol{\mu}_B + \boldsymbol{\mu}_C] = \frac{1}{2}\boldsymbol{\mu}_A \tag{6.98}$$
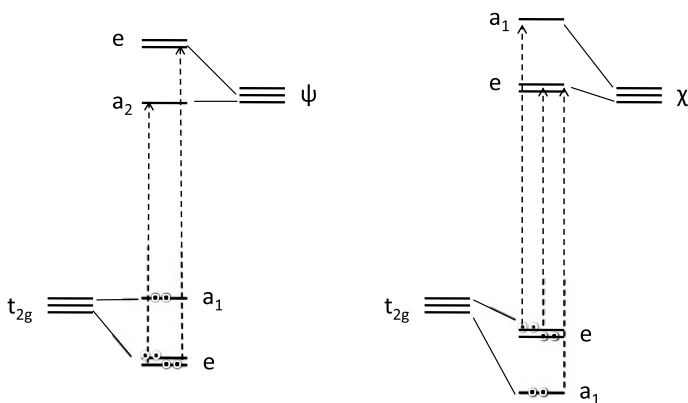
Fig. 6.6 Allowed CT transitions from the t_{2g} shell to ψ- or χ-type ligand acceptor orbitals for tris-chelate complexes with D_3 symmetry

Here, we have made use of the fact that the sum of the three dipole vectors vanishes. The effective transfer term thus becomes:

$$\boldsymbol{\mu}\big(e_\epsilon(t_{2g}) \rightarrow e_\epsilon(\psi)\big) = \sqrt{\frac{3}{8}}\kappa\boldsymbol{\mu}_A \tag{6.99}$$

In the Wigner–Eckart formalism, this matrix element is written as:

$$\big\langle e_\epsilon(t_{2g})|\mu_{x'}|e_\epsilon(\psi)\big\rangle = \langle E\epsilon|E\theta E\epsilon\rangle\big\langle e(t_{2g}) \parallel e(\mu) \parallel e(\psi)\big\rangle \tag{6.100}$$

The coupling coefficient in this equation is equal to $1/\sqrt{2}$. We can thus identify the reduced matrix element as:

$$\big\langle e(t_{2g}) \parallel e(\mu) \parallel e(\psi)\big\rangle = \frac{\sqrt{3}}{2}\kappa\mu_A \tag{6.101}$$

All other $e \rightarrow e$ transfer terms can then be obtained by simply varying the coupling coefficients. We give one more example of a transition that requires an operator which is $\mu_{y'}$ polarized:

$$\big\langle e_\theta(t_{2g})|\boldsymbol{\mu}|e_\epsilon(\psi)\big\rangle = \frac{1}{\sqrt{8}}\kappa\big\langle \psi^C - \psi^B|\boldsymbol{\mu}|2\psi^A - \psi^B - \psi^C\big\rangle$$

$$= \frac{1}{\sqrt{8}}\kappa(\boldsymbol{\mu}_B - \boldsymbol{\mu}_C) \tag{6.102}$$

The vector $\boldsymbol{\mu}_B - \boldsymbol{\mu}_C$ in this expression is directed in the $\mu_{y'}$ direction, as required by the selection rule. Moreover, the length of this vector is $\sqrt{3}\mu^\perp$:

$$(\boldsymbol{\mu}_B - \boldsymbol{\mu}_C) \cdot (\boldsymbol{\mu}_B - \boldsymbol{\mu}_C) = 2(\mu^\perp)^2 - 2\boldsymbol{\mu}_B \cdot \boldsymbol{\mu}_C = 3(\mu^\perp)^2 \tag{6.103}$$

Hence, the transfer-dipole length for this y'-polarized transition also measures $\sqrt{3/8}\kappa$, which is exactly the same as for the x'-polarized transition, given in Eq. (6.99). This is expected since the corresponding coupling coefficients, $\langle E\epsilon|E\theta\, E\epsilon\rangle$ and $\langle E\theta|E\epsilon\, E\epsilon\rangle$, are equal.

Using the transfer model, we can also express the reduced matrix elements for the $e \to a_2$ channel. Even though there is no overlap between these orbitals, they do give rise to a transfer-term intensity. Orbital interaction does indeed delocalize the $e(t_{2g})$ orbitals over the ligands. The dipole operators, centred on the complex origin, will then couple the $e(\psi)$ and $a_2(\psi)$ ligand-centred orbitals. Hence, we write:

$$\boldsymbol{\mu}\big(e_\epsilon(t_{2g}) \to a_2(\psi)\big) = -\frac{\langle e_\epsilon(t_{2g})|\mathcal{H}|e_\epsilon(\psi)\rangle}{E_\psi - E_{t_{2g}}}\langle e_\epsilon(\psi)|\boldsymbol{\mu}|a_2(\psi)\rangle$$

$$= \sqrt{\frac{3}{2}}\kappa\langle e_\epsilon(\psi)|\boldsymbol{\mu}|a_2(\psi)\rangle \tag{6.104}$$

The dipole matrix element in this expression can easily be evaluated:

$$\langle e_\epsilon(\psi)|\boldsymbol{\mu}|a_2(\psi)\rangle = \frac{1}{3\sqrt{2}}\langle 2\psi^A - \psi^B - \psi^C|\boldsymbol{\mu}|\psi^A + \psi^B + \psi^C\rangle$$

$$= \frac{1}{3\sqrt{2}}(2\boldsymbol{\mu}_A - \boldsymbol{\mu}_B - \boldsymbol{\mu}_C)$$

$$= \frac{1}{\sqrt{2}}\boldsymbol{\mu}_A \tag{6.105}$$

The total transfer term is obtained by combining Eqs. (6.104) and (6.105):

$$\boldsymbol{\mu}\big(e_\epsilon(t_{2g}) \to a_2(\psi)\big) = \frac{\sqrt{3}}{2}\kappa\boldsymbol{\mu}_A \tag{6.106}$$

A final task is to calculate the transition-moments between the corresponding multi-electronic states based on the orbital-transition moments obtained. In the tris-chelate complex under consideration, a $^1A_1 \to {}^1E$ state transition can be associated with each allowed orbital-transition. The $^1A_1$ corresponds to the closed-shell ground state, based on the $(t_{2g})^6$ configuration. Both the $e \to a_2$ and $e \to e$ transitions will give rise to a twofold-degenerate ^1E state. As an example, the θ states are written in determinantal notation as follows, where we write only the orbitals that are singly occupied:

$$\big|{}^1E_\theta(e \to a_2)\big\rangle = \frac{1}{\sqrt{2}}\big[\big|(e_\epsilon(t_{2g})\alpha)(a_2(\psi)\beta)\big| - \big|(e_\epsilon(t_{2g})\beta)(a_2(\psi)\alpha)\big|\big]$$

$$\big|{}^1E_\theta(e \to e)\big\rangle = \frac{1}{2}\big[\big|(e_\theta(t_{2g})\alpha)(e_\theta(\psi)\beta)\big| - \big|(e_\theta(t_{2g})\beta)(e_\theta(\psi)\alpha)\big| \tag{6.107}$$

$$- \big|(e_\epsilon(t_{2g})\alpha)(e_\epsilon(\psi)\beta)\big| + \big|(e_\epsilon(t_{2g})\beta)(e_\epsilon(\psi)\alpha)\big|\big]$$

Table 6.5 Transfer-term contributions to $^1A_1 \to {}^1E$ CT transitions, with ψ and χ acceptor orbitals

ψ ligand orbitals		χ ligand orbitals	
$^1E(a_1 \to e(\psi))$	0	$^1E(a_1 \to e(\chi))$	$\sqrt{2}\kappa'$
$^1E(e \to a_2(\psi))$	$\sqrt{\frac{3}{2}}\kappa$	$^1E(e \to a_1(\chi))$	$\frac{1}{\sqrt{2}}\kappa'$
$^1E(e \to e(\psi))$	$\sqrt{\frac{3}{2}}\kappa$	$^1E(e \to e(\chi))$	$\frac{1}{\sqrt{2}}\kappa'$

The resulting state transition-moments are then expressed in terms of orbital transition-moments as:

$$\left\langle {}^1A_1|\boldsymbol{\mu}|^1E_\theta(e \to a_2)\right\rangle = \sqrt{2}\left\langle e_\epsilon(t_{2g})|\boldsymbol{\mu}|a_2(\psi)\right\rangle = \sqrt{3/2}\kappa$$
$$\left\langle {}^1A_1|\boldsymbol{\mu}|^1E_\theta(e \to e)\right\rangle = 2\left\langle e_\theta(t_{2g})|\boldsymbol{\mu}|e_\theta(\psi)\right\rangle = \sqrt{3/2}\kappa \tag{6.108}$$

On the other hand, the $a_1(t_{2g})$ orbital does not delocalize over the ligands. As a result, there can be no transfer term associated with transitions from this orbital. One expects only a weak contact term. The lowest transition corresponds to $a_1(t_{2g}) \to a_2(\psi)$. The only non-zero coupling coefficient for this transition is $\langle A_1|A_2A_2\rangle$. This transition will thus be dipole allowed under $\mu_{z'}$. Polarized absorption spectra are in line with this analysis: the spectral onset of the CT region is characterized by a weak absorption band in parallel polarization, followed by two strong absorption bands in perpendicular polarization. This assignment is based on the assumption that the vertical Franck–Condon excitations reach delocalized charge-transfer states. At least in the case of $Ru(bipy)_3^{2+}$, this is supported by detailed spectral measurements [18]. An entirely similar analysis can be performed in the case when the ligand orbital is of χ-type. The transition-moments are collected in Table 6.5. In this case, the ligand and metal part both transform as $a_1 + e$ (see Table 6.4). As a result, three transitions are found to carry transfer-term intensity, as indicated in Fig. 6.6.

Circular Dichroism

The tris-chelate compounds are chiral compounds, with an apparent helical structure, which can easily be related to their circular-dichroic properties by use of symmetry selection rules. The CT transitions that we have just discussed cannot be responsible for the primary CD strength, since they are in-plane polarized, and thus do not carry intrinsic helicity. Instead, the prominent peaks in the CD spectrum are observed at higher energies, and are associated with the intra-ligand $\pi\pi^*$-transitions. These transitions take place between occupied and virtual ligand-centred orbitals which are of opposite signature, and hence are of type $\psi \to \chi$ or vice-versa. Such transitions are long-axis polarized, i.e. the transition dipole moment is oriented along the ligand bridge as shown in Fig. 6.7.
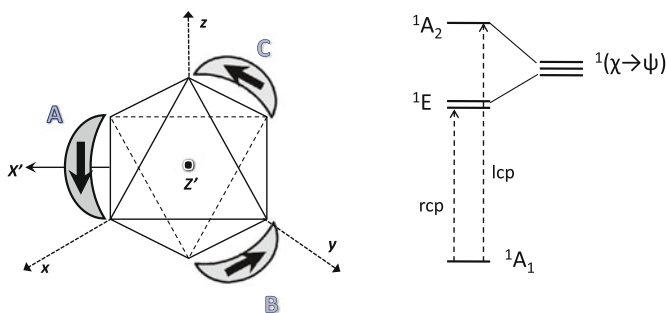
Fig. 6.7 Allowed intra-ligand transitions from χ- to ψ-type ligand orbitals for tris-chelate complexes with D_3 symmetry. The circular dichroism has a lower right-circularly polarized (rcp) band and an upper left-circularly polarized (lcp) band. This gives the CD spectrum the appearance of the first derivative of a Gaussian curve, with a negative part at longer wavelength and a positive part at shorter wavelength

We designate these dipole moments as $\boldsymbol{\mu}_A^{\|}, \boldsymbol{\mu}_B^{\|}, \boldsymbol{\mu}_C^{\|}$. These vectors can be expressed in a row notation for the primed x', y', z' coordinate system as follows:

$$\boldsymbol{\mu}_A^{\|} = \mu^{\|}\left(0, \frac{1}{\sqrt{3}}, \frac{\sqrt{2}}{\sqrt{3}}\right)$$

$$\boldsymbol{\mu}_B^{\|} = \mu^{\|}\left(-\frac{1}{2}, -\frac{1}{2\sqrt{3}}, \frac{\sqrt{2}}{\sqrt{3}}\right) \tag{6.109}$$

$$\boldsymbol{\mu}_C^{\|} = \mu^{\|}\left(\frac{1}{2}, -\frac{1}{2\sqrt{3}}, \frac{\sqrt{2}}{\sqrt{3}}\right)$$

The scalar products between these orientations are equal to $1/2$, which corresponds to angles of $60°$. Each of the three transitions gives rise to an excited state. In D_3 symmetry these states transform as $A_2 + E$. The composition of these *exciton* states[8] is as follows:

$$|^1A_2\rangle = \frac{1}{\sqrt{3}}\left[(\chi_A \rightarrow \psi_A)^1 + (\chi_B \rightarrow \psi_B)^1 + (\chi_C \rightarrow \psi_C)^1\right]$$

$$|^1E_\theta\rangle = \frac{1}{\sqrt{2}}\left[-(\chi_B \rightarrow \psi_B)^1 + (\chi_C \rightarrow \psi_C)^1\right] \tag{6.110}$$

$$|^1E_\epsilon\rangle = \frac{1}{\sqrt{6}}\left[2(\chi_A \rightarrow \psi_A)^1 - (\chi_B \rightarrow \psi_B)^1 - (\chi_C \rightarrow \psi_C)^1\right]$$

---

[8]The excitation creates an electron-hole pair, which can move from one ligand to another. This is called an exciton.

Here, the notation refers to a singlet orbital transition, which can be written in determinantal form as:

$$(\chi_A \to \psi_A)^1 = \frac{1}{\sqrt{2}}\big[\big|(\chi_A\alpha)(\psi_A\beta)\big| - \big|(\chi_A\beta)(\psi_A\alpha)\big|\big] \tag{6.111}$$

To first approximation, the metal centre is not taking part in the electronic properties, but merely serves as a structural template which keeps the ligands in place. Distant interactions between the three transitions can be described by a simple exciton-coupling model. In this model, the interaction between transitions is approximated by the electrostatic interaction potential between the corresponding transition dipoles. This potential is given by:

$$V_{ij} = \frac{1}{4\pi\epsilon_0}\left(\frac{\boldsymbol{\mu}^i \cdot \boldsymbol{\mu}^j}{R_{ij}^3} - \frac{3(\boldsymbol{\mu}^i \cdot \mathbf{R}_{ij})(\boldsymbol{\mu}^j \cdot \mathbf{R}_{ij})}{R_{ij}^5}\right) \tag{6.112}$$

where R_{ij} is the distance between the dipoles, and $\mathbf{R}_{ij} = \mathbf{R}_j - \mathbf{R}_i$. The length of the distance vector is thus $\sqrt{3}\rho$. The energies of the exciton states are then given by:

$$\langle {}^1A_2|V|{}^1A_2\rangle = \frac{(\mu^\|)^2}{4\pi\epsilon_0\rho^3}\frac{1}{6\sqrt{3}}$$

$$\langle {}^1E|V|{}^1E\rangle = -\frac{(\mu^\|)^2}{4\pi\epsilon_0\sqrt{3}\rho^3}\frac{1}{12\sqrt{3}} \tag{6.113}$$

The ${}^1A_2$ state thus goes up in energy twice as much as the ${}^1E$ state goes down, thus keeping the barycentre energy at the zeroth-order position. Now, in order to determine the CD strength, we need for the two states both the electric and the magnetic transition dipoles from the ground state. The electric dipoles are easily obtained by combining the state vectors:

$$\boldsymbol{\mu}\big({}^1A_1 \to {}^1A_2\big) = \frac{1}{\sqrt{3}}\big(\boldsymbol{\mu}_A^\| + \boldsymbol{\mu}_B^\| + \boldsymbol{\mu}_C^\|\big) = \sqrt{2}\mu^\|(0, 0, 1)$$

$$\boldsymbol{\mu}\big({}^1A_1 \to {}^1E_\epsilon\big) = \frac{1}{\sqrt{6}}\big(2\boldsymbol{\mu}_A^\| - \boldsymbol{\mu}_B^\| - \boldsymbol{\mu}_C^\|\big) = \frac{1}{\sqrt{2}}\mu^\|(0, 1, 0) \tag{6.114}$$

$$\boldsymbol{\mu}\big({}^1A_1 \to {}^1E_\theta\big) = \frac{1}{\sqrt{2}}\big(-\boldsymbol{\mu}_B^\| + \boldsymbol{\mu}_C^\|\big) = \frac{1}{\sqrt{2}}\mu^\|(1, 0, 0)$$

The calculation of the magnetic transition dipoles requires a preamble. The magnetic moment was already defined in Eq. (4.128) of Chap. 4. By explicitly writing the angular momentum operator in terms of the linear momentum operator as $\boldsymbol{r} \times \boldsymbol{p}$ one obtains:

$$\boldsymbol{m} = -\frac{e}{2m}\boldsymbol{l} = -\frac{e}{2m}\boldsymbol{r} \times \boldsymbol{p} \tag{6.115}$$

The commutator of the one-electron Hamiltonian with the position operator is given by:

$$[\mathcal{H}, \boldsymbol{r}] = \left[\left(\frac{\boldsymbol{p} \cdot \boldsymbol{p}}{2m} + V(\boldsymbol{r})\right), \boldsymbol{r}\right] = -\frac{i\hbar}{m}\boldsymbol{p} \qquad (6.116)$$

Here, we used the Heisenberg commutator relation between the conjugate position and momentum operators: $[x, p_x] = i\hbar$. The magnetic moment matrix element of the intra-ligand transition with respect to the common origin of the coordinate system is given by:

$$\boldsymbol{m}_A = \langle\psi_A|\boldsymbol{m}|\chi_A\rangle = -\frac{e}{2m}\langle\psi_A|(\boldsymbol{R}_A + \boldsymbol{r}) \times \boldsymbol{p}|\chi_A\rangle = -\frac{e}{2m}\boldsymbol{R}_A \times \langle\psi_A|\boldsymbol{p}|\chi_A\rangle \qquad (6.117)$$

where it was assumed that the chromophore has no intrinsic magnetic transition-moment. The momentum matrix element in this equation can now be evaluated with the help of Eq. (6.116):

$$\begin{aligned}
\langle\psi_A|\boldsymbol{p}|\chi_A\rangle &= \frac{im}{\hbar}\langle\psi_A|\mathcal{H}\boldsymbol{r} - \boldsymbol{r}\mathcal{H}|\chi_A\rangle \\
&= \frac{im}{\hbar}\left(\langle\mathcal{H}\psi_A|\boldsymbol{r}|\chi_A\rangle - \langle\psi_A|\boldsymbol{r}\mathcal{H}|\chi_A\rangle\right) \\
&= \frac{im}{\hbar}(E_\psi - E_\chi)\langle\psi_A|\boldsymbol{r}|\chi_A\rangle \\
&= 2\pi im\nu\langle\psi_A|\boldsymbol{r}|\chi_A\rangle \qquad (6.118)
\end{aligned}$$

Here, ν is the frequency of the intra-ligand transition. The combination of this result with Eq. (6.117) yields:

$$\begin{aligned}
\boldsymbol{m}_A &= i\pi\nu\left(\boldsymbol{R}_A \times \boldsymbol{\mu}_A^{\|}\right) = i\pi\nu\rho\mu^{\|}\left(0, -\frac{\sqrt{2}}{\sqrt{3}}, \frac{1}{\sqrt{3}}\right) \\
\boldsymbol{m}_B &= i\pi\nu\left(\boldsymbol{R}_B \times \boldsymbol{\mu}_B^{\|}\right) = i\pi\nu\rho\mu^{\|}\left(\frac{1}{\sqrt{2}}, \frac{1}{\sqrt{6}}, \frac{1}{\sqrt{3}}\right) \\
\boldsymbol{m}_C &= i\pi\nu\left(\boldsymbol{R}_C \times \boldsymbol{\mu}_C^{\|}\right) = i\pi\nu\rho\mu^{\|}\left(-\frac{1}{\sqrt{2}}, \frac{1}{\sqrt{6}}, \frac{1}{\sqrt{3}}\right)
\end{aligned} \qquad (6.119)$$

As we indicated the above formalism applies to chromophores that have no intrinsic magnetic moment.

$$\boldsymbol{m}({}^1A_1 \rightarrow {}^1A_2) = \frac{1}{\sqrt{3}}\left(\boldsymbol{m}_A^{\|} + \boldsymbol{m}_B^{\|} + \boldsymbol{m}_C^{\|}\right) = i\pi\nu\rho\mu^{\|}(0, 0, 1)$$

$$\boldsymbol{m}({}^1A_1 \rightarrow {}^1E_\epsilon) = \frac{1}{\sqrt{6}}\left(2\boldsymbol{m}_A^{\|} - \boldsymbol{m}_B^{\|} - \boldsymbol{m}_C^{\|}\right) = -i\pi\nu\rho\mu^{\|}(0, 1, 0) \qquad (6.120)$$

$$\boldsymbol{m}({}^1A_1 \rightarrow {}^1E_\theta) = \frac{1}{\sqrt{2}}\left(-\boldsymbol{m}_B^{\|} + \boldsymbol{m}_C^{\|}\right) = -i\pi\nu\rho\mu^{\|}(1, 0, 0)$$

A transition will be characterized by a helical displacement of the electron if the magnetic and electric transition dipoles are aligned. This is reflected in the Rosenfeld equation for the CD intensity or *rotatory strength*, $\mathcal{R}_{a \to j}$, for a transition from a ground state a to an excited state j in a collection of randomly-oriented molecules:

$$\mathcal{R}_{a \to j} = \mathrm{Im}\{\langle a|\boldsymbol{\mu}|j\rangle \cdot \langle j|\boldsymbol{m}|a\rangle\} \tag{6.121}$$

Straightforward application to the exciton bands yields:

$$\mathcal{R}({}^1 A_1 \to {}^1 A_2) = \sqrt{2}\pi \nu \rho (\mu^{\parallel})^2$$

$$\mathcal{R}({}^1 A_1 \to {}^1 E_\epsilon) = -\frac{1}{\sqrt{2}}\pi \nu \rho (\mu^{\parallel})^2 \tag{6.122}$$

$$\mathcal{R}({}^1 A_1 \to {}^1 E_\theta) = -\frac{1}{\sqrt{2}}\pi \nu \rho (\mu^{\parallel})^2$$

The out-of-plane polarized transition to the ${}^1 A_2$ state, which lies at higher energy, has a positive CD signal, while the in-plane polarized transition to the lower ${}^1 E$ state has a negative CD signal. The latter transition consists of two components along the two in-plane directions. Summing over the three components in Eq. (6.122), shows that the total rotatory strength, for randomly-oriented molecules, is exactly zero. This is a general sum rule for CD spectra. If one now takes the spectrum of the chiral antipode, the Λ tris-chelate complex, the spectra are exactly the same but the signs are reversed. Mirror image in actual geometry thus becomes reflection symmetry in the spectrum.

6.9 Induction Revisited: The Fibre Bundle

In Chap. 4 we left induction after the proof of the Frobenius reciprocity theorem. In that proof the important concept of the positional representation was introduced. This described the permutation of the sites under the action of the group elements. Further, we defined local functions on the sites which transformed as irreps of the site symmetry. As an example, if we want to describe the displacement of a cluster atom in a polyhedron, two local functions are required: a totally-symmetric one for the radial displacement and a twofold-degenerate one for the tangential displacements. In cylindrical symmetry, these are labelled σ and π, respectively. The *mechanical* representation, i.e. the representation of the cluster displacements, is then the sum of the two induced representations:

$$\Gamma_{\mathrm{mech}} = \Gamma(\sigma H \uparrow G) + \Gamma(\pi H \uparrow G) \tag{6.123}$$

As an example using the induction tables in Sect. C.2 for an octahedron, we have:

$$\Gamma_{\mathrm{mech}} = (A_{1g} + E_g + T_{1u}) + (T_{1g} + T_{2g} + T_{1u} + T_{2u}) \tag{6.124}$$

This is precisely the set of fluorine displacements that we constructed in Sect. 4.8 in order to describe the vibrational modes of UF_6. One remarkable result of induction theory is that the mechanical representation can also be obtained as the direct product of the positional representation and the translational representation, T_{1u}; this is the representation of the three displacements of the centre of the cluster.

$$\Gamma_{\text{mech}} = T_{1u} \times (A_{1g} + E_g + T_{1u})$$
$$= T_{1u} + (T_{1u} + T_{2u}) + (A_{1g} + E_g + T_{1g} + T_{2g}) \qquad (6.125)$$

It is as if the displacements of the central point of the octahedron were relocated to every ligand site. The elementary function space of the displacements of the central atom, which transforms as the translational irrep, T_{1u}, is called the *standard fibre*. This fibre is attached to every site of the cluster, and the set of these fibres is the *fibre bundle*. The action of the group permutes fibres of the bundle. The following induction theorem holds:

Theorem 14 *Consider a standard fibre, consisting of a function space that is invariant under the action of the group. In a cluster of equivalent sites, we can form a fibre bundle by associating this standard fibre with every site position. The induced representation of the fibre bundle is then the direct product of the irrep of the standard fibre with the positional representation.*

For $\mathcal{V}$ being the representation of the standard fibre, T_{1u} in our example, and $\mathcal{P}$ the positional representation of the set of equivalent sites in the molecule, one has for the induced representation:

$$\Gamma\big(\{\mathcal{V}\}H \uparrow G\big) = \mathcal{V} \times \mathcal{P}(H \uparrow G) \qquad (6.126)$$

For a proof of this theorem, we refer to the literature [19, 20]. The theorem is not only applicable to molecular vibrations but is also directly in line with the LCAO method in molecular quantum chemistry. In this method the molecular orbitals (MOs) are constructed from atomic basis sets that are defined on the constituent atoms. An atomic basis set, such as $3d$ or $4f$, corresponds to a fibre, emanating, as it were, from the atomic centre. Usually, such basis sets obey spherical symmetry, since they are defined for the isolated atoms. As such, they are also invariant under the molecular point group [21]. As an example, a set of $4f$ polarisation functions on a chlorine ligand in a $RhCl_6^{3-}$ complex is itself adapted to octahedral symmetry as $a_{2u} + t_{1u} + t_{2u}$. This representation thus corresponds to $\mathcal{V}$. In the C_{4v} site symmetry these irreps subduce: $a_1 + b_1 + b_2 + 2e$. According to the theorem, the LCAOs based on the $4f$ orbitals thus will transform as:

$$\Gamma\big(\{a_1 + b_1 + b_2 + 2e\}C_{4v} \uparrow O_h\big)$$
$$= (a_{2u} + t_{1u} + t_{2u}) \times (a_{1g} + e_g + t_{1u})$$
$$= a_{1g} + a_{2g} + 2e_g + 2t_{1g} + 3t_{2g} + a_{2u} + e_u + 3t_{1u} + 3t_{2u} \qquad (6.127)$$

In this LCAO space several irreps occur multiple times, but they can all be distinguished by the specific direct product from which they originated.

6.10 Application: Bonding Schemes for Polyhedra

Leonhard Euler dominated the mathematics of the 18th century. One of his famous discoveries was the polyhedral theorem, which marks the beginning of topology. A polyhedron has three structural elements: vertices, edges, and faces.[9] The numbers of these will be represented as v, e, and f, respectively. Then, for a polyhedron, the following theorem holds:

Theorem 15 *In a convex polyhedron the alternating sum of the numbers of vertices*, *edges*, *and faces is always equal to* 2.

$$v - e + f = 2 \qquad (6.128)$$

As an example, in a cube one has $v = 8$, $e = 12$, $f = 6$, and hence $8 - 12 + 6 = 2$. The 2 in the right-hand side of Eq. (6.128) is called the Euler invariant. It is a *topological* characteristic. Topology draws attention to properties of surfaces, which are not affected when surfaces are stretched or deformed, as one can do with objects made of rubber or clay. Topology is thus not concerned with regular shapes, and in this sense seems to be completely outside our subject of symmetry; yet, as we intend to show in this section, there is in fact a deep connection, which also carries over to molecular properties. The surface to which the 2 in the theorem refers is the surface of a sphere. A convex polyhedron is indeed a polyhedron which can be embedded or mapped on the surface of a sphere. Group theory, and in particular the induction of representations, provides the tools to understand this invariant. To this end, each of the terms in the Euler equation is replaced by an induced representation, which is based on the particular nature of the corresponding structural element. In Fig. 6.8 we illustrate the results for the case of the tetrahedron.

- The vertices, being zero-dimensional points, form a set of nodes, $\{\langle u \rangle\}$, which are permuted under the symmetry operations of the polyhedron. The representation of this set is the positional representation, $\Gamma_\sigma(v)$. The σ here refers to the fact that the sites themselves transform as totally-symmetric objects in the site group. If the cluster contains several orbits, the induced representation is of course the sum of the individual positional representations. In Fig. 6.8 the vertex representation is $A_1 + T_2$. In Sect. 4.7 we have already encountered these irreps, when discussing the sp^3 hybridization of carbon.

$$\Gamma_\sigma(v) = \Gamma(a_1 C_{3v} \uparrow T_d) = A_1 + T_2 \qquad (6.129)$$

---

[9]In geometry a *vertex* is a point were two or more lines meet.
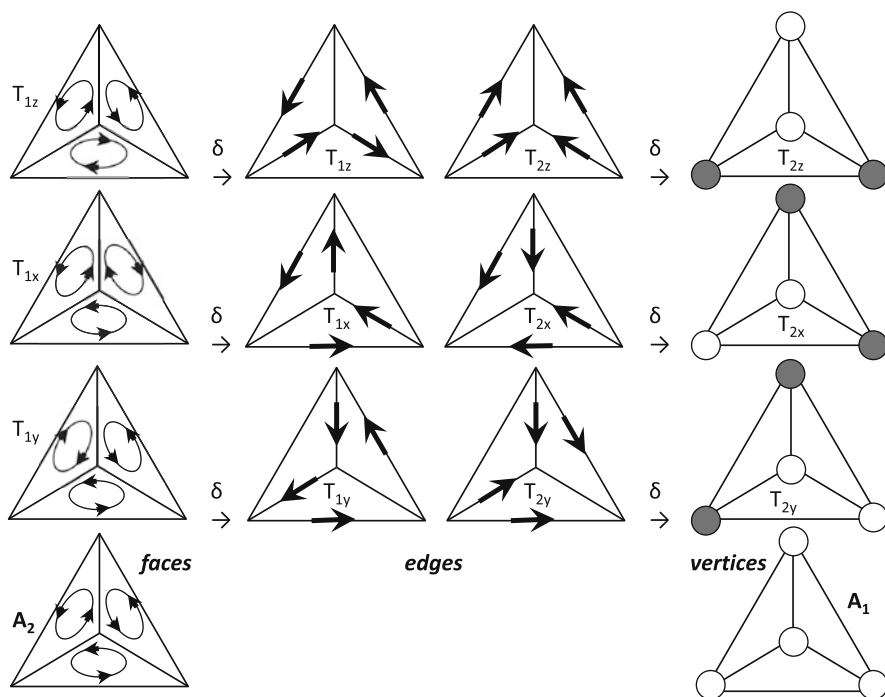
Fig. 6.8 Face, edge and vertex SALCs for a tetrahedron. The δ symbol denotes taking the boundary, from faces to edges, and from edges to vertices (see text). The two topological invariants are the A_2 face term and the A_1 vertex term

- The edges are one-dimensional lines. They form a set of ordered pairs, $\{\langle u, v \rangle\}$. Each of these can be thought of as an arrow, directed along the edge. The symmetry operations will interchange these arrows, but may also change their sense. The corresponding representation is labelled as $\Gamma_{\parallel}(e)$. This symbol indicates that the basic objects on the edge sites are not symmetric points but directed arrows. The site group through the centre of an edge has maximal symmetry C_{2v} and in this site group the arrows transform as the b_1 irrep, which is symmetric under reflection in a plane containing the edge and antisymmetric under the symmetry plane perpendicular to the edge. For a tetrahedron there are six edge vectors, transforming as $T_1 + T_2$.

$$\Gamma_{\parallel}(e) = \Gamma(b_1 C_{2v} \uparrow T_d) = T_1 + T_2 \tag{6.130}$$

- The faces may be represented as closed chains of nodes, which are bordering a polyhedral face, $\{\langle u, v, w, \ldots \rangle\}$. The sequence forms a circulation around the face, in a particular sense (going from $\langle u \rangle$ to $\langle w \rangle$ over $\langle v \rangle$, etc.). The set of face rotations forms the basis for the face representation, which is denoted as $\Gamma_{\circlearrowleft}(f)$. In a polyhedron the maximal site group of a face is C_{nv}, and in this site group the face rotation transforms as the rotation around the $\hat{C}_n$ axis, i.e. it is symmetric

under the axis and antisymmetric with respect to the vertical $\hat{\sigma}_v$ planes, which invert the sense of rotation. For the tetrahedron, the face circulations transform as $A_2 + T_2$, as shown in Fig. 6.8.

$$\Gamma_{\circlearrowleft} = \Gamma(a_2 C_{3v} \uparrow T_d) = A_2 + T_1 \tag{6.131}$$

The following theorem [22] applies:

Theorem 16 *The alternating sum of induced representations of the vertex nodes, edge arrows, and face rotations, is equal to the sum of the totally-symmetric representation, Γ_0, and the pseudo-scalar representation, Γ_ϵ. The latter representation is symmetric under proper symmetry elements and antisymmetric under improper symmetry elements.*

$$\Gamma_\sigma(v) - \Gamma_{\parallel}(e) + \Gamma_{\circlearrowleft}(f) = \Gamma_0 + \Gamma_\epsilon \tag{6.132}$$

The Euler theorem may be considered as the dimensional form of this theorem, which states that the alternating sum of the characters of the induced representations under the unit element, $\hat{E}$, is equal to 2, but the present theorem extends this character equality to all the operations of the group. The theorem silently implies that irreps can be added and subtracted. In the example of the tetrahedron, the theorem is expressed as:

$$\Gamma_\sigma(v) - \Gamma_{\parallel}(e) + \Gamma_{\circlearrowleft}(f) = (A_1 + T_2) - (T_1 + T_2) + (A_2 + T_2) = A_1 + A_2 \tag{6.133}$$

A straightforward interpretation of the theorem is possible in terms of fluid flow on the surface of a polyhedron.[10] Suppose observers are positioned on the vertices, edge centres and face centres, and register the local fluid flow. When the incoming and outgoing currents at a node are not in balance, the observers located on these nodes will report piling up or depletion of the local fluid level. This is the scalar property represented by the vertex term. The corresponding connection between edge flow and vertex density is expressed by the *boundary operation*, indicated by δ in Fig. 6.8. Taking the boundary of an edge arrow means replacing the arrow by the difference of two vertex-localized scalars: a positive one (indicated by a white circle in the figure) at the node to which the arrow's head is pointing, and a negative one (indicated by a black circle) at the node facing the arrow's tail. This projection from edge to vertex will not change the symmetry. Hence, in this way, the boundary of the T_2 edge irrep is the T_2 vertex SALC, as illustrated in the figure. Similarly, observers in face centres will notice the net current that is circulating around the face. Such a circular current through the edges does not give rise to changes at the nodes (indeed the incoming flow at a node is also leaving again), but is observable from the centre of the face around which the current is circulating. The boundaries

---

[10]This flow description provides a simple pictorial illustration of the abstract homology theory. The standard reference is: [23].

of circular currents around face centres are thus chains of arrows on the edges, which again conserve the symmetry. In Fig. 6.8 the boundary of the T_1 face term is thus the T_1 edge term. Clearly, the sum of the vertex and face observations should account for all currents going through the edges, except for two additional terms which escape edge observations. These are the two Euler invariants: the totally-symmetric Γ_0 component corresponds to a uniform change of fluid amplitude at all vertex basins. This does not give rise to edge currents, since it creates no gradients over the edges. The other is the Γ_ϵ component. It corresponds to a simultaneous rotation around all faces in the same sense. Again, such rotor flows do not create net flows through the edges, because two opposite currents are flowing through every edge. The Euler invariant thus points to two invariant characteristic modes of the sphere. They are not boundaries of a mode at a higher level, nor are they bounded by a mode at a lower level. The phenomena, that these two terms describe, might also be referred to in a topological context as the electric and magnetic *monopoles*.

Because of this connection to density and current, this theorem may be applied in various ways to describe chemical bonding, frontier orbital structure, and vibrational properties. The applications of this theorem can be greatly extended by introducing fibre representations, as is shown below.

Taking the Dual   To take the dual of a polyhedron is to replace vertices by faces and vice-versa, as was already mentioned in Sect. 3.7 in relation to the Platonic solids. The dual has the same number of edges as the original, but every edge is rotated $90°$. Hence the relations between v^D, e^D, f^D for the dual and v, e, f for the original are:

$$v^D = f$$
$$e^D = e \tag{6.134}$$
$$f^D = v$$

As a result the Euler formula is invariant under the dual operation.

$$v - e + f = v^D - e^D + f^D = 2 \tag{6.135}$$

A similar invariance holds for the symmetry extension, but in this case "to take the dual" corresponds to multiplying all terms by the pseudo-scalar irrep Γ_ϵ. The terms are then changed as follows:

$$\Gamma_\sigma(v) \times \Gamma_\epsilon = \Gamma_\circlearrowleft(v) = \Gamma_\circlearrowleft(f^D)$$
$$\Gamma_\parallel(e) \times \Gamma_\epsilon = \Gamma_\perp(e) = \Gamma_\parallel(e^D)$$
$$\Gamma_\circlearrowleft(f) \times \Gamma_\epsilon = \Gamma_\sigma(f) = \Gamma_\sigma(v^D) \tag{6.136}$$
$$(\Gamma_0 + \Gamma_\epsilon) \times \Gamma_\epsilon = \Gamma_0 + \Gamma_\epsilon$$

Hence, if the theorem holds for the original, it also holds for the dual.

$$\left(\Gamma_\sigma(v) - \Gamma_\parallel(e) + \Gamma_\circlearrowleft(f)\right) \times \Gamma_\epsilon = \Gamma_\sigma(v^D) - \Gamma_\parallel(e^D) + \Gamma_\circlearrowleft(f^D) = \Gamma_0 + \Gamma_\epsilon \tag{6.137}$$

Note especially the fibre modification of the edge term. The maximal local symmetry of an edge is C_{2v}. The arrow along the edge transforms as b_1, while the pseudo-scalar irrep in C_{2v} is a_2. The product $b_1 \times a_2$ produces b_2, which is precisely the symmetry of an arrow, tangent to the surface of the polyhedron, but directed perpendicular to the edge. Multiplication with the pseudo-scalar irrep thus has the effect of rotating the edges through $90°$. In Eq. (6.136) the resulting representation is denoted as $\Gamma_\perp(e)$.

Deltahedra Deltahedra are polyhedra that consist entirely of triangular faces. Three of the Platonic solids are deltahedra: the tetrahedron, the octahedron and the icosahedron. In a convex deltahedron the bond stretches (i.e. stretchings of the edges) span precisely the representation of the internal vibrations. In other words, a convex deltahedron cannot vibrate if it is made of rigid rods. This is the Cauchy theorem:

Theorem 17 *Convex polyhedra in three dimensions with congruent corresponding faces must be congruent to each other. In consequence, if a polyhedron is made up of triangles with rigid rods, the angles between the triangular faces are fixed.*

This result can be cast in the language of induced representations. The stretchings of the edges correspond to scalar changes of edge lengths and transform as σ-type objects, and hence will correspond to $\Gamma_\sigma(e)$. On the other hand, the internal vibrations span the mechanical representation, which can be written as a bundle of the translation, minus the spurious modes of translation and rotation. The symmetries of these will be denoted as Γ_T and Γ_R, respectively. One thus has:

$$\text{Deltahedron:} \quad \Gamma_\sigma(v) \times \Gamma_T - \Gamma_T - \Gamma_R = \Gamma_\sigma(e) \tag{6.138}$$

Trivalent Polyhedra The dual of a deltahedron is a trivalent polyhedron, meaning that every vertex is connected to three nearest neighbours. The fullerene networks of carbon are usually trivalent polyhedra. This reflects the sp^2 hybridization of carbon, which can form three σ-bonds. Also in this case several specialized forms of the Euler symmetry theorem can be formulated. We may start from Eq. (6.138) and replace vertices by faces. The edge terms remain the same since they are totally symmetric under the local symmetries of the edges. Rotations of the edges by $90°$ will thus not affect these terms.

$$\text{Trivalent:} \quad \Gamma_\sigma(f) \times \Gamma_T - \Gamma_T - \Gamma_R = \Gamma_\sigma(e) \tag{6.139}$$

Furthermore, by multiplying the vertices in a trivalent polyhedron by three, we have accounted for all the edges twice, since each edge is linked to two vertices, hence:

$$\text{Trivalent:} \quad 3v = 2e \tag{6.140}$$

The $3v$ in this formula suggests once again taking the fibre representation $\Gamma_\sigma(v) \times \Gamma_T$. In doing so we have considered on each vertex one σ and two π
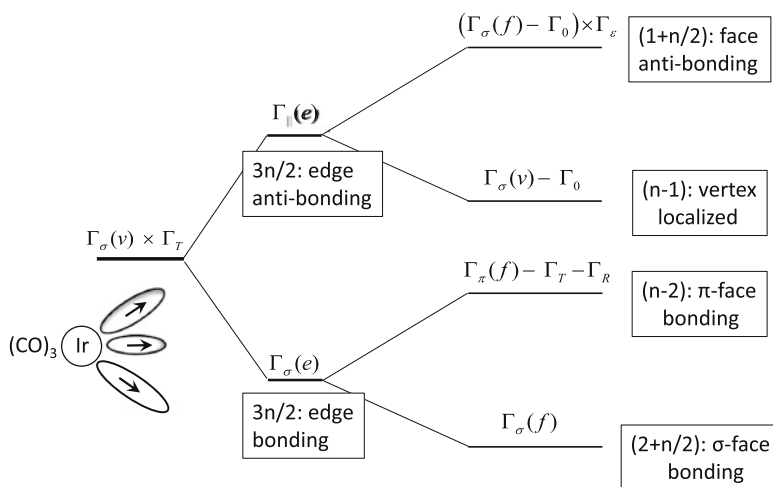
Fig. 6.9 Edge bonding in electron-precise trivalent cages. The valence shell splits into an occupied set of localized edge-bonds, and a matching virtual set of edge-anti-bonds. The sets may be further differentiated by use of the symmetry theorems

objects. Hence, this is not only the mechanical representation with three displacements on each vertex, but it is equally well the symmetry of a set of sp^2 hybrids on every vertex, directed along the three edges. Along each edge the hybrids at either end can be combined in a local bonding and anti-bonding combination. The corresponding induced representations are respectively: $\Gamma_\sigma(e)$ and $\Gamma_\|(e)$; hence, the symmetry extension of Eq. (6.140) reads:

$$\text{Trivalent:}\quad \Gamma_\sigma(v) \times \Gamma_T = \Gamma_\sigma(e) + \Gamma_\|(e) \tag{6.141}$$

Edge Bonding in Trivalent Polyhedra

The understanding of the bonding schemes in polyhedra is based on the correct identification of the local hybridization scheme on the constituent fragments. Trivalent polyhedra are often *electron-precise*: this means that the fragment has three electrons in three orbitals, which are available for cluster bonding and give rise to edge-localized σ-bonds. Such is the case for the methyne fragment, CH, forming *polyhedranes*, but equally well for the *isolobal* [24] organo-transition-metal fragments such as $M(CO)_3$, where M is a d^9 metal such as Co, Rh or Ir. Figure 6.9 shows the bonding pattern based on such electron-precise fragments. As indicated before, the orbital basis corresponds to the fibre representation $\Gamma_\sigma(v) \times \Gamma_T$, and contains $3n$ orbitals. Local interactions along the edges will split this orbital basis into an occupied σ-bonding half and a virtual σ-anti-bonding counterpart, transforming as $\Gamma_\sigma(e)$ and $\Gamma_\|(e)$, respectively. This is precisely the result of Eq. (6.141). Now,

for each half, a more detailed pattern can be discerned [25]. For the anti-bonding orbitals, the general theorem, Eq. (6.132), can be applied directly. The result is illustrated in Fig. 6.9. By this theorem, the $3n/2$ edge anti-bonds are split into two subsets containing $(1 + n/2)$ and $(n - 1)$ orbitals. The former, higher lying, subset transforms as $\Gamma_\circlearrowleft - \Gamma_\epsilon$. These terms correspond to circulations around the faces, which means that these levels will be highly anti-bonding. In fact, they are always at the top of the skeletal spectrum. Note that the pseudo-scalar term, Γ_ϵ, does not take part. This is because a uniform circulation around all faces in the same sense has no contribution on the edges. Below this is a subset of weakly anti-bonding orbitals, transforming as $\Gamma_\sigma(v) - \Gamma_0$. These orbitals are more localized on the vertices. The Γ_0 term is not included since this is the totally-symmetric molecular orbital which is completely bonding, and thus will appear in the lower half of the diagram.

Furthermore, the edge-bonding half can be analysed with the help of Eq. (6.139). The $3n/2$ edge bonds split into two subsets of dimension $(n - 2)$ and $(2 + n/2)$. This analysis involves the fibre representation $\Gamma_\sigma(f) \times \Gamma_T$, which can be decomposed into a radial σ- and tangential π-part. The σ-part corresponds to cylindrically-symmetric bonds around the faces, and will thus be strongly bonding. For the π-part the face terms contain a nodal plane through the faces, and thus will be less bonding.

Frontier Orbitals in Leapfrog Fullerenes

Fullerenes are trivalent polyhedra of carbon, consisting of hexagons and pentagons. The following relations hold:

$$
\begin{aligned}
v - e + f &= 2 \\
3v &= 2e \\
f_5 + f_6 &= f \\
5f_5 + 6f_6 &= 3v
\end{aligned}
\tag{6.142}
$$

The first two relationships are from Eqs. (6.128) and (6.140). The third expresses that the total number of the faces is the sum of the number of pentagons (f_5), and hexagons (f_6). The final equation indicates that by counting the hexagons six times, and the pentagons five times, we have counted all vertices three times, since every vertex is at the junction of three faces. Even though there are fewer equations, here, than unknowns, it can easily be seen by manipulation of Eq. (6.142) that the only value that the number of pentagons, f_5, can take on is 12. Hence, the smallest fullerene is the dodecahedron C_{20}, which only consists of pentagons. Also note that the number of atoms in a fullerene must be even, since $3v$ must be divisible by 2, as e is an integer. Taking the *leapfrog*, L, of a primitive fullerene, P, is an operation of cage expansion, which yields a fullerene with three times as many atoms [26]. This procedure is described by the following rule:

$$
L = \text{Dual}(\text{Omnicap} P)
\tag{6.143}
$$

Fig. 6.10 The leapfrog extension consists of two operations: first, place an extra atom in the centres of all the polygons (*middle panel*), then, take the dual. The result is indicated by *the solid lines* in *the right panel*
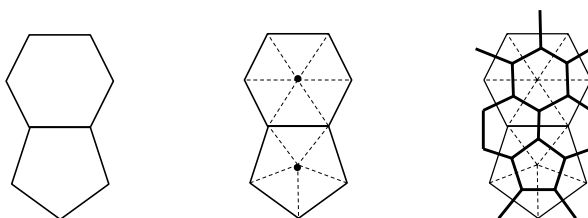
$$P \rightarrow omnicap \rightarrow O(P) \rightarrow dualize \rightarrow L$$

It involves two operations, which are carried out consecutively, as illustrated in Fig. 6.10. One first places an extra *capping* atom on all pentagons and hexagons. This leads to a cage which consists only of triangles, and this is a deltahedron. By taking the dual one restores a trivalent cage. As can be seen, all vertices of the primitive have been turned into hexagons, while the original pentagons and hexagons are recovered, but in a rotational stagger. The edges of the primitive are also recovered, but rotated 90°. In summary, the leapfrog operation inserts 6 vertices in the hexagons of P, and 5 vertices in the pentagons, which, according to the final expression in Eq. (6.142), multiplies the number of atoms by 3. The first and best known leapfrog is Buckminsterfullerene, C_{60}, which is the leapfrog of the dodecahedron itself. Each carbon atom contributes, besides the sp^2 orbitals, which build the σ-frame, one radial p_r-orbital. These orbitals form π-bonds which control the frontier orbitals of fullerenes. In the case of the leapfrog, this frontier MO region is always characterized by six low-lying almost non-bonding orbitals, which, moreover, always transform as $\Gamma_T + \Gamma_R$. This can be explained with the help of the Euler rules [27].

As in the case of C_{60}, all leapfrogs can be considered to be truncations of the primitive fullerenes, in the sense that all the faces of the primitive have become isolated *islands*, surrounded by rings of hexagons. With every bond of the primitive is associated a perpendicular bond, which always forms a *bridge* between these islands. Based on this neat bond separation, two canonical valence-bond frames can be constructed for the leapfrog, which in a sense are the extremes of a correlation diagram, with the actual bonding somewhere in between. These bond schemes are known as the Fries and the Clar structures. The Fries structure is an extreme case where all *bridges* are isolated π-bonds. The induced representation for these bonds corresponds to $\Gamma_\sigma(e^P)$. On the other hand, in the Clar structures the bonding is completely redistributed to aromatic sextets on the hexagonal and pentagonal islands. The corresponding representation is the fibre bundle $\Gamma_\sigma(f^P) \times \Gamma_T$. We now compare the representations of both bonding schemes, using the symmetry theorems. We start with the main theorem, applied to the primitive P, and multiply left and right with Γ_R.

$$\Gamma_\sigma\big(v^P\big) \times \Gamma_R - \Gamma_\parallel\big(e^P\big) \times \Gamma_R + \Gamma_\circlearrowleft\big(f^P\big) \times \Gamma_R = \Gamma_T + \Gamma_R \qquad (6.144)$$
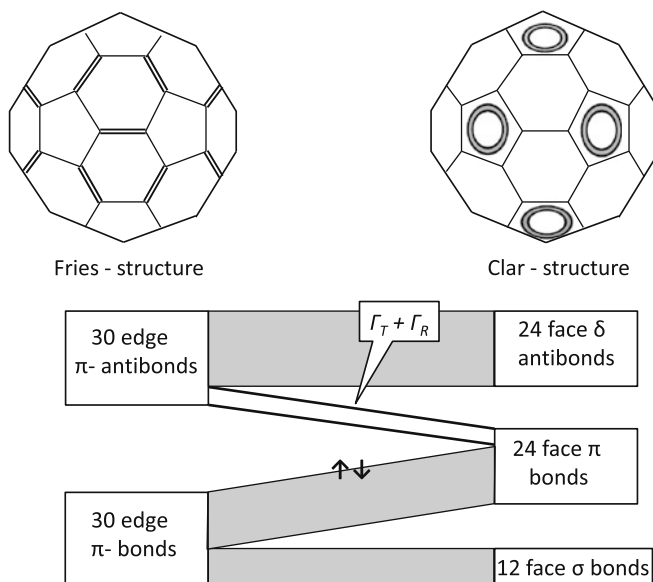
Fig. 6.11 Correlation diagram for C_{60}. The Fries and Clar structures are bonding extremes, where double bonds are either localized on the 30 bonds between the pentagons (Fries), or form isolated aromatic sextets on the twelve pentagons. The true conjugation scheme is found in between, and is characterized by six unoccupied levels, which are anti-bonding in the Fries structure and bonding in the Clar structure, and which transform as rotations and translations. Buckminsterfullerene has low-lying LUMO and LUMO+1 levels of $t_{1u}(\Gamma_T)$ and $t_{1g}(\Gamma_R)$ symmetry

Since $\Gamma_R = \Gamma_T \times \Gamma_\epsilon$, we could already simplify the face term to a form which precisely corresponds to the Clar representation:

$$\Gamma_\circlearrowleft(f^P) \times \Gamma_R = \Gamma_\sigma(f^P) \times \Gamma_T = \Gamma_{\text{Clar}} \tag{6.145}$$

The vertex term can be expressed with the help of Eq. (6.141):

Trivalent: $$\Gamma_\sigma(v^P) \times \Gamma_R = \Gamma_\sigma(e^P) \times \Gamma_\epsilon + \Gamma_\parallel(e^P) \times \Gamma_\epsilon = \Gamma_\circlearrowleft(e^P) + \Gamma_\perp(e^P) \tag{6.146}$$

where the pseudo-scalar irrep turns a σ-object into a circular current, and rotates the parallel edge current over 90°. Note that this is applied in the primitive cage, to the edges of P only. To complete the derivation one final fibre bundle is needed, which applies to all convex polyhedra:

$$\Gamma_\sigma(e) \times \Gamma_T = \Gamma_\sigma(e) + \Gamma_\parallel(e) + \Gamma_\perp(e) \tag{6.147}$$

This result is based on the C_{2v} site-symmetry of an edge. The translation in this site has a radial σ-component of a_1 symmetry, and two tangential π-components of $b_1 + b_2$ symmetry. The fibre bundle will thus correspond to the induction of

$a_1 + b_1 + b_2$, which is precisely the meaning of the three terms on the right-hand side of Eq. (6.147). This expression may be transformed in two steps to the term which is required in the derivation. One first changes the substrate of the fibre from $\Gamma_\sigma(e)$ to $\Gamma_\parallel(e)$. This associates the edges with b_1 objects, and combination with $a_1 + b_1 + b_2$ will thus yield $b_1 + a_1 + a_2$, or:

$$\Gamma_\parallel(e) \times \Gamma_T = \Gamma_\parallel(e) + \Gamma_\sigma(e) + \Gamma_\circlearrowleft(e) \tag{6.148}$$

Finally, multiply this result by Γ_ϵ:

$$\Gamma_\parallel(e) \times \Gamma_R = \Gamma_\perp(e) + \Gamma_\circlearrowleft(e) + \Gamma_\sigma(e) \tag{6.149}$$

We now combine Eqs. (6.146) and (6.149), and find:

$$\text{Trivalent:}\quad \Gamma_\parallel\left(e^P\right) \times \Gamma_R - \Gamma_\sigma\left(v^P\right) \times \Gamma_R = \Gamma_\sigma\left(e^P\right) = \Gamma_{\text{Fries}} \tag{6.150}$$

This is precisely the representation of the Fries bonds. We can thus compare the Fries and Clar structures in a general leapfrog, and find from Eq. (6.144):

$$\Gamma_{\text{Clar}} - \Gamma_{\text{Fries}} = \Gamma_T + \Gamma_R \tag{6.151}$$

The Clar structure thus has six extra bonding orbitals as compared with the Fries structure. When both bonding schemes are correlated, as illustrated in Fig. 6.11, this sextet must correlate with the anti-bonding half of the Fries structure. It will thus be placed on top of the Clar band, and actually be nearly non-bonding, forming six low-lying virtual orbitals, which explains the electron deficiency of the leapfrog fullerenes. Moreover, as the derivation shows, they transform exactly as rotations and translations.

6.11 Problems

6.1 A three-electron wavefunction in an octahedron is given by:

$$\Psi = \left|(t_{1u}x\alpha)(t_{1u}y\alpha)(t_{1u}z\alpha)\right| \tag{6.152}$$

The vertical bars denote a Slater determinant. Determine the symmetry of this function, starting from parent two-electron coupled states, to which the third electron is coupled. Make use of the coupling coefficients in Appendix F.

6.2 Write the Jahn-Teller matrix for a threefold degenerate T_{1u} level in an icosahedral molecule. How many reduced matrix elements are needed?

6.3 Do you expect octahedral e_g orbitals to show a magnetic dipole moment?

6.4 Binaphthyl consists of two linked naphthalene molecules. The dihedral angle between the two naphthyl planes is around 70°, and can be stabilized by bulky substituents on the naphthyl units, as indicated below for the case of 2, 2′-di-biphenylphosphine-1, 1′-binaphthyl. A circular dichroism signal is detected in

the UV region, corresponding to the long-axis polarized transitions of the naphthyl units (indicated by the arrows in the figure). Construct the appropriate exciton states and determine the CD profile of the two enantiomers of binaphthyl.
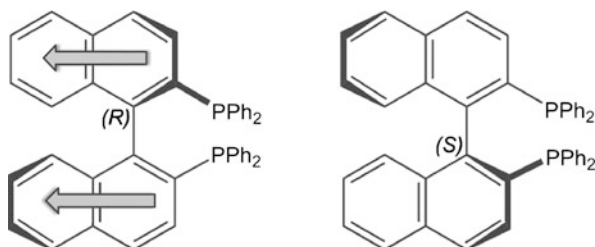
6.5 A diradical is a molecule with two *open* orbitals, each containing one electron. Consider as an example twisted ethylene (D_{2d} symmetry, see Fig. 3.9). The HOMO is a degenerate *e*-orbital, occupied by two electrons. Construct the e^2 diradical states for this molecule, and determine their symmetries.

6.6 Planar trimethylenemethane (TMM), C_4H_6, is a diradical with trigonal symmetry. Determine the Hückel spectrum for the four carbon p_z-orbitals perpendicular to the plane of the molecule. The HOMO in D_{3h} has e'' symmetry and is also occupied by two electrons. Determine the corresponding diradical states, and compare with the results for twisted ethylene. How would you describe the valence bond structure of this molecule?
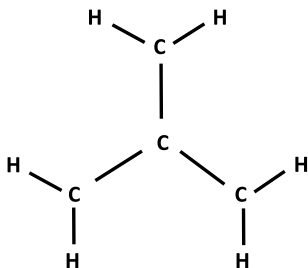
References

1. Wigner, E.P.: Group Theory. Academic Press, New York (1959)
2. Griffith, J.S.: The Irreducible Tensor Method for Molecular Symmetry Groups. Prentice Hall, Englewood-Cliffs (1962)
3. Butler, P.H.: Point Group Symmetry Applications, Methods and Tables. Plenum Press, New York (1981)
4. Ceulemans, A., Beyens, D.: Monomial representations of point-group symmetries. Phys. Rev. A **27**, 621 (1983)
5. Lijnen, E., Ceulemans, A.: The permutational symmetry of the icosahedral orbital quintuplet and its implication for vibronic interactions. Europhys. Lett. **80**, 67006 (2007)

6. Jahn, H.A., Teller, E.: Stability of polyatomic molecules in degenerate electronic states. I. Orbital degeneracy. Proc. R. Soc. A **161**, 220 (1937)

7. Bersuker, I.B.: The Jahn–Teller Effect. Cambridge University Press, Cambridge (2006)

8. Domcke, W., Yarkony, D.R., Köppel, H.: Conical Intersections, Electronic Structure, Dynamics and Spectroscopy. Advanced Series in Physical Chemistry, vol. 15. World Scientific, Singapore (2004)

9. Shapere, A., Wilczek, F.: Geometric Phases in Physics. Advanced Series in Mathematical Physics, vol. 5. World Scientific, Singapore (1989)

10. Judd, B.R.: The theory of the Jahn–Teller effect. In: Flint, C.D. (ed.) Vibronic Processes in Inorganic Chemistry. NATO Advanced Study Institutes Series, vol. C288, p. 79. Kluwer, Dordrecht (1988)

11. Bersuker, I.B., Balabanov, N.B., Pekker, D., Boggs, J.E.: Pseudo Jahn–Teller origin of instability of molecular high-symmetry configurations: novel numerical method and results. J. Chem. Phys. **117**, 10478 (2002)

12. Hoffmann, R., Woodward, R.B.: Orbital symmetry control of chemical reactions. Science **167**, 825 (1970)

13. Halevi, E.A.: Orbital symmetry and reaction mechanism, the OCAMS view. Springer, Berlin (1992)

14. Rodger, A., Nordén, B.: Circular Dichroism and Linear Dichroism. Oxford Chemistry Masters. Oxford University Press, Oxford (1997)

15. Orgel, L.E.: Double bonding in chelated metal complexes. J. Chem. Soc. 3683 (1961). doi:10.1039/JR9610003683

16. Ceulemans, A., Vanquickenborne, L.G.: On the charge-transfer spectra of iron(II)- and ruthenium(II)-tris(2, 2′-bipyridyl) complexes. J. Am. Chem. Soc. **103**, 2238 (1981)

17. Day, P., Sanders, N.: Spectra of complexes of conjugated ligands. 2. Charge-transfer in substituted phenantroline complexes: intensities. J. Chem. Soc. A **10**, 1536 (1967)

18. Yersin, H., Braun, D.: Localization in excited states of molecules. Application to $Ru(bipy)_3^{2+}$. Coord. Chem. Rev. **111**, 39 (1991)

19. Melvin, M.A.: Simplification in finding symmetry-adapted eigenfunctions. Rev. Mod. Phys. **28**, 18 (1956)

20. Ceulemans, A.: The construction of symmetric orbitals for molecular clusters. Mol. Phys. **54**, 161 (1985)

21. Biel, J., Chatterjee, R., Lulek, T.: Fiber structure of space of molecular-orbitals within LCAO method. J. Chem. Phys. **86**, 4531 (1987)

22. Ceulemans, A., Fowler, P.W.: Extension of Euler theorem to the symmetry properties of polyhedra. Nature **353**, 52 (1991)

23. Hilton, P.J., Wylie, S.: Homology Theory. Cambridge University Press, Cambridge (1967)

24. Hoffmann, R.: Building bridges between inorganic and organic chemistry (Nobel lecture). Angew. Chem., Int. Ed. Engl. **21**, 711 (1982)

25. Mingos, D.M.P., Wales, D.J.: Introduction to Cluster Chemistry. Prentice Hall, Englewood-Cliffs (1990)

26. Fowler, P.W., Manolopoulos, D.E.: An Atlas of Fullerenes. Clarendon, Oxford (1995)

27. Fowler, P.W., Ceulemans, A.: Electron deficiency of the fullerenes. J. Phys. Chem. A **99**, 508 (1995)

Chapter 7
Spherical Symmetry and Spins

Abstract A brief excursion is made into the concept of continuous groups, with an example of the rotation groups. The purpose is to familiarize the reader with the concept of electron spin. The coupling of spins is discussed. Applications are taken from Crystal-Field Theory and Electron Spin Resonance.

Contents

7.1 The Spherical-Symmetry Group

Consider the row vector of coordinate functions $(|x\rangle\ |y\rangle\ |z\rangle)$ in 3D space. A rotation must conserve the norm of this function space. As we have seen in Chap. 2, this can be realized by a unitary matrix transformation. For real functions, the unitary transformation is reduced to an orthogonal one. A matrix is orthogonal if the following condition is fulfilled (where T denotes transposition):

$$\mathbb{D}^T \mathbb{D} = \mathbb{I} = \mathbb{D}\mathbb{D}^T \tag{7.1}$$

The set of all ortho-gonal 3×3 matrices forms a group, which is called the orthogonal group in three dimensions, $O(3)$. The order of this group is infinite. It can be shown that this group is isomorphic with the complete group of all proper and improper rotations in three dimensions. The structure that embodies this symmetry is the sphere. Hence, $O(3)$ is the symmetry group of the sphere. The determinants of the matrices must be real with modulus one, which means that they can

represents an axis of rotation
at an angle θ from the
positive z-axis and an angle ϕ
in the (x, y)-plane, measured
counterclockwise from the
positive x-direction
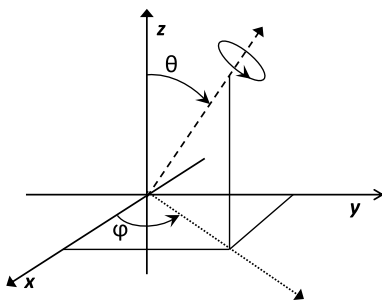
only be ± 1. Improper symmetry elements are represented by matrices with deter-
minant -1, while the proper symmetry elements have determinant $+1$. The latter
matrices form a halving subgroup, which is called the *special orthogonal group* in
three dimensions, $SO(3)$. This subgroup describes the rotational subgroup of the
sphere. A convenient representation of an arbitrary rotation is described by four pa-
rameters: the rotation angle, α, and three direction cosines, n_x, n_y, n_z, indicating
the orientation of the pole of the rotation axis in the Cartesian frame. The latter are
normalized as $n_x^2 + n_y^2 + n_z^2 = 1$. This means that only three angles are required
to describe a rotation: the rotational angle α and two angular coordinates of the
rotational pole (see Fig. 7.1), a result which was obtained by Euler [1]:

$$
\begin{aligned}
n_x &= \sin\theta \cos\phi \\
n_y &= \sin\theta \sin\phi \\
n_z &= \cos\theta
\end{aligned}
\tag{7.2}
$$

This $SO(3)$ matrix for the row vector $(|x\rangle|y\rangle|z\rangle)$ under a rotation $\hat{R}(\alpha, n_x, n_y, n_z)$
reads:

$$
\mathbb{O}(R) = \begin{pmatrix}
1 - 2(n_y^2 + n_z^2)\gamma & -n_z \sin\alpha + 2n_x n_y \gamma & n_y \sin\alpha + 2n_z n_x \gamma \\
n_z \sin\alpha + 2n_x n_y \gamma & 1 - 2(n_z^2 + n_x^2)\gamma & -n_x \sin\alpha + 2n_y n_z \gamma \\
-n_y \sin\alpha + 2n_z n_x \gamma & n_x \sin\alpha + 2n_y n_z \gamma & 1 - 2(n_x^2 + n_y^2)\gamma
\end{pmatrix}
\tag{7.3}
$$

with $\gamma = \sin^2(\alpha/2)$.

The determinant of this matrix is $+1$, as expected. In (n_x, n_y, n_z) space any rota-
tion $\hat{R} \in G$ has two poles. These are the points on the unit sphere that are invariant
under the rotation. These points are at $\pm\mathbf{n}$ and thus are mutual antipodes. We recall
that a rotation over a positive angle is viewed from the pole as counterclockwise. In
the antipodal pole this rotation is observed as clockwise. Rotations about antipodal
poles and over opposite angles thus produce the same effect. Hence, a sign change
of all parameters leaves the matrix invariant. Moreover, since a rotation through an
angle of 2π is equivalent to the unit element, the rotation angle can also be specified
as $\alpha - 2\pi$. In total in the range $[-2\pi, +2\pi]$, there are thus four equivalent sets of

parameters that give rise to the same matrix $\mathbb{O}(R)$:

$$\hat{R}(\alpha, n_x, n_y, n_z)$$
$$\hat{R}(-\alpha, -n_x, -n_y, -n_z)$$
$$\hat{R}(-2\pi + \alpha, n_x, n_y, n_z)$$
$$\hat{R}(2\pi - \alpha, -n_x, -n_y, -n_z)$$

(7.4)

The transformations of the standard vector form the fundamental irrep of spherical symmetry. All other irreps can be constructed by taking direct products of this vector. In particular, the *spherical harmonic functions* can be constructed by taking fully symmetrized powers of the vector. The symmetrized direct square of the p-functions yields a six-dimensional function space with components: $\{z^2, x^2, y^2, yz, xz, xy\}$. This space is not orthonormal: the components are not normalized, and the first three components do overlap. In fact, the space is reducible since the sum of the squares $z^2 + x^2 + y^2$ is a radial function, which is totally symmetric under rotations. Taking out this root leaves five components, which are irreducible and correspond to the five d orbitals, shown in Table 7.1. This result parallels the cubic $[T_{1u}]^2 = A_{1g} + E_g + T_{2g}$ coupling [2].

   When extending these results to the nth power of the p-irrep, symmetrization will be governed by the irreducible representations of the corresponding S_n permutation group. The f-orbitals may be generated by the third power of the p-irrep. Full symmetrization of the three components generates 10 functions, $\{z^3, x^3, y^3, z^2x, z^2y, x^2z, x^2y, y^2z, y^2x, xyz\}$, which in cubic symmetry transform as $A_{2u} + 2T_{1u} + T_{2u}$. Again, this space is reducible and contains a p- and an f-subspace. The reduction is based on the removal of the totally symmetric trace. Indeed, the combination $z(x^2 + y^2 + z^2)$ and its cyclic permutations reduce to the fundamental p-vector. The remainder of the space is irreducible and corresponds to the seven f-functions listed in Table 7.1. Further explorations of the spherical symmetry group opens the book of angular momentum arithmetic and the underlying theory of Lie groups.[1] This is outside the present scope. We shall restrict the treatment to indicating the subduction rules, which describe the decomposition of the spherical irreps in point-group symmetries. To obtain these rules, we have to derive the character of function space of the spherical harmonics, $\{Y_{\ell m_\ell}\}$, for $m_\ell = -\ell, -\ell+1, \ldots, \ell-1, \ell$, under the proper and improper rotations of the point group. We shall start by considering the proper ones first. It is sufficient to limit the treatment to rotations around the z-axis since on a sphere all directions are equivalent. Rotations around z will affect only the angular coordinate, ϕ, in the equatorial plane and leave the azimuthal coordinate, θ, unchanged. The ϕ-dependence of the

---

[1] See, e.g., [3, 4].

Table 7.1 Complex and cubic real forms of the spherical harmonics for $\ell = 0, 1, 2, 3$. The constants N_ℓ are the common normalizing factors over the θ and ϕ coordinates

ℓ	N_ℓ	$\|LM\rangle$	$\|\Gamma\gamma\rangle$
s	$\sqrt{\frac{1}{4\pi}}$	$\|00\rangle = 1$	$\|A_{1g}\rangle = 1$
p	$\sqrt{\frac{3}{4\pi}}r^{-1}$	$\|1+1\rangle = -\frac{1}{\sqrt{2}}(x+iy)$	$\|T_{1u}x\rangle = x$
		$\|1-1\rangle = \frac{1}{\sqrt{2}}(x-iy)$	$\|T_{1u}y\rangle = y$
		$\|10\rangle = z$	$\|T_{1u}z\rangle = z$
d	$\sqrt{\frac{15}{8\pi}}r^{-2}$	$\|2+2\rangle = \frac{1}{2}(x+iy)^2$	$\|E_g\theta\rangle = \frac{1}{\sqrt{6}}(3z^2-r^2)$
		$\|2-2\rangle = \frac{1}{2}(x-iy)^2$	$\|E_g\epsilon\rangle = \frac{1}{\sqrt{2}}(x^2-y^2)$
		$\|2+1\rangle = -(x+iy)z$	$\|T_{2g}\xi\rangle = \sqrt{2}yz$
		$\|2-1\rangle = (x-iy)z$	$\|T_{2g}\eta\rangle = \sqrt{2}xz$
		$\|20\rangle = \frac{1}{\sqrt{6}}(3z^2-r^2)$	$\|T_{2g}\zeta\rangle = \sqrt{2}xy$
f	$\sqrt{\frac{35}{8\pi}}r^{-3}$	$\|3+3\rangle = -\frac{1}{2\sqrt{2}}(x+iy)^3$	$\|A_{2u}\rangle = \sqrt{\frac{3}{2}}xyz$
		$\|3-3\rangle = \frac{1}{2\sqrt{2}}(x-iy)^3$	$\|T_{1u}x\rangle = \frac{1}{\sqrt{10}}x(5x^2-3r^2)$
		$\|3+2\rangle = \frac{\sqrt{3}}{2}z(x+iy)^2$	$\|T_{1u}y\rangle = \frac{1}{\sqrt{10}}y(5y^2-3r^2)$
		$\|3-2\rangle = \frac{\sqrt{3}}{2}z(x-iy)^2$	$\|T_{1u}z\rangle = \frac{1}{\sqrt{10}}z(5z^2-3r^2)$
		$\|3+1\rangle = -\frac{\sqrt{3}}{2\sqrt{10}}(x+iy)(5z^2-3r^2)$	$\|T_{2u}\xi\rangle = \sqrt{\frac{3}{2}}x(z^2-y^2)$
		$\|3-1\rangle = \frac{\sqrt{3}}{2\sqrt{10}}(x-iy)(5z^2-3r^2)$	$\|T_{2u}\eta\rangle = \sqrt{\frac{3}{2}}y(x^2-z^2)$
		$\|30\rangle = \frac{1}{\sqrt{10}}z(5z^2-3r^2)$	$\|T_{2u}\zeta\rangle = \sqrt{\frac{3}{2}}z(y^2-x^2)$

spherical harmonics is given by

$$\Phi_{m_\ell}(\phi) = \frac{1}{\sqrt{2\pi}}\exp(im_\ell\phi) \tag{7.5}$$

A rotation $\hat{C}_\alpha$ about the z-direction affects this function in the following way:

$$\hat{C}_\alpha\Phi_{m_\ell}(\phi) = \Phi_{m_\ell}(\phi - \alpha) = \exp(-im_\ell\alpha)\Phi_{m_\ell}(\phi) \tag{7.6}$$

The trace over the entire function space is then given by

$$\chi^\ell(C_\alpha) = \sum_{m_\ell=-\ell}^{\ell}\exp(-im_\ell\alpha) = \frac{\sin(\ell+1/2)\alpha}{\sin(\alpha/2)} \tag{7.7}$$

To obtain this result, the following sum-rule was used, which is obtained by carrying out a straightforward division:

$$\sum_{n=0}^{N} r^n = \frac{1 - r^N}{1 - r} \tag{7.8}$$

As an example, for $\ell = 1$, the rotation matrix corresponds to the matrix $\mathbb{O}(R)$ in Eq. (7.3). Its trace is given by

$$\chi^p(C_\alpha) = 3 - 4\sin^2(\alpha/2) = \frac{\sin(3\alpha/2)}{\sin(\alpha/2)} \tag{7.9}$$

Improper rotations can always be written as the products of a proper rotation and the inversion operation. The resulting character is then given by the product of the rotational character in Eq. (7.7), times the parity of the spherical harmonics, which is given by

$$\hat{\imath} Y_{\ell m_\ell} = (-1)^\ell Y_{\ell m_\ell} \tag{7.10}$$

Finally, we also remind that the definition of the spherical harmonics in the standard phase convention implies complex conjugation, as

$$\bar{Y}_{\ell m_\ell} = (-1)^{m_\ell} Y_{\ell -m_\ell} \tag{7.11}$$

In Sect. A.2 the character tables for the groups $O(3)$ and $SO(3)$ are given. The subduction relations are listed in Sect. C.1.

7.2 Application: Crystal-Field Potentials

Model treatments of transition-metal and lanthanide complexes are essentially based on the d^n or f^n open-shell states of the central metal atom, which are perturbed by the electrostatic field of the surrounding ligating groups:

$$\mathcal{V}_{CF} = \sum_L \frac{e^2 Z_L}{4\pi\epsilon_0 |\mathbf{R}_L - \mathbf{r}|} \tag{7.12}$$

This term describes the electrostatic repulsion between an electron residing in the metal orbital at a position $\mathbf{r}$ and a negatively charged ligand, with charge $-eZ_L$ at a position $\mathbf{R}_L$. In crystal-field theory the electrostatic field of the surroundings is written as an expansion in spherical harmonic operators, as these elements will be evaluated in the d or f function space of the central metal atom. Series expansion for distances $r < R_L$ yields

$$\mathcal{V}_{CF} = \sum_L \frac{e^2 Z_L}{4\pi\epsilon_0} \sum_{\ell=0}^{\infty} \sum_{m_\ell=-\ell}^{m_\ell=+\ell} \frac{4\pi}{2\ell+1} \frac{r^\ell}{R^{\ell+1}} Y_{\ell m_\ell}(\theta, \phi) \bar{Y}_{\ell m_\ell}(\theta_L, \phi_L) \tag{7.13}$$

This potential is invariant under the symmetry properties of the metal complex. As a result, the operator part reduces to the totally symmetric components of the spherical harmonics. Moreover, interactions with d electrons imply that ℓ must be limited to four, and to six for f electrons. In the case of an octahedral field, the subduction relations for spherical harmonics (see Sect. C.1) indicate that a totally symmetric A_{1g} component can be subduced only from $\ell = 4$ and $\ell = 6$. Filling in the angular positions of the ligands in an octahedron then yields

$$\mathcal{V}_{O_h} = \frac{6e^2 Z_L}{\sqrt{4\pi\epsilon_0 R_L}} Y_{00} + \frac{e^2 Z_L r^4}{\sqrt{4\pi\epsilon_0 R_L^5}} \frac{\sqrt{35}}{6\sqrt{2}} \left(Y_{44} + Y_{4-4} + \frac{\sqrt{14}}{\sqrt{5}} Y_{40} \right) \qquad (7.14)$$

This is the famous crystal-field operator for an octahedron, which splits the d-shell into e_g and t_{2g} subshells. The crystal-field interaction is usually parameterized by the crystal-field parameter, $10Dq$, which corresponds to the splitting of the e_g and t_{2g} orbitals. The term in brackets here is the octahedral invariant of rank 4. In the multipole expansion this corresponds to a *hexadecapole* operator. In normalized form it reads

$$|4A_{1g}| = \frac{1}{2\sqrt{3}} \left(\frac{\sqrt{5}}{\sqrt{2}} (Y_{44} + Y_{4-4}) + \sqrt{7} Y_{40} \right) \qquad (7.15)$$

Here the notation between vertical bars indicates that this is an operator. We shall now derive this expression with the aid of the coupling coefficients. Since the d orbitals transform as $e_g + t_{2g}$, the squares of the d-orbitals yield two totally symmetric results, which may be abbreviated as follows:

$$\left| A_{1g}(e \times e) \right| = \frac{1}{\sqrt{2}} \left(\theta^2 + \epsilon^2 \right)$$

$$\left| A_{1g}(t_2 \times t_2) \right| = \frac{1}{\sqrt{3}} \left(\xi^2 + \eta^2 + \zeta^2 \right) \qquad (7.16)$$

These two invariants are at the origin of two spherical operators: one corresponds to the constant scalar $|0A_{1g}|$, and the other to $|4A_{1g}|$. The former invariant may be obtained by taking the norm of the entire d-manifold, which can be expressed in the A_{1g} functions of Eq. (7.16) as follows:

$$|0A_{1g}| = \frac{1}{\sqrt{5}} \left(\theta^2 + \epsilon^2 + \xi^2 + \eta^2 + \zeta^2 \right)$$

$$= \frac{1}{\sqrt{5}} \left(\sqrt{2} \left| A_{1g}(e \times e) \right| + \sqrt{3} \left| A_{1g}(t_2 \times t_2) \right| \right) \qquad (7.17)$$

The $|4A_{1g}|$ invariant must be orthonormal to this result and thus will be given by

$$|4A_{1g}| = \frac{1}{\sqrt{5}} \left(\sqrt{3} \left| A_{1g}(e \times e) \right| - \sqrt{2} \left| A_{1g}(t_2 \times t_2) \right| \right) \qquad (7.18)$$

Fig. 7.2 The octahedral crystal-field potential corresponding to the $|4A_1|$ hexadecapole. *Grey* and *black* refer to positive and negative values, respectively
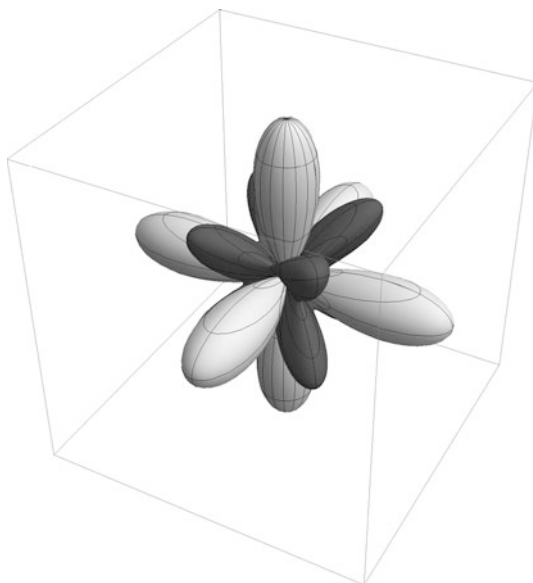
We can use this result to write the functional form of the hexadecapolar invariant by combining the squares of the d-functions:

$$|4A_{1g}| = \frac{1}{\sqrt{5}}\left[\frac{\sqrt{3}}{\sqrt{2}}(\theta^2 + \epsilon^2) - \frac{\sqrt{2}}{\sqrt{3}}(\xi^2 + \eta^2 + \zeta^2)\right]$$
$$\sim \left[z^4 + x^4 + y^4 - 3(x^2y^2 + x^2z^2 + y^2z^2)\right] \tag{7.19}$$

This function corresponds precisely to the crystal-field operator of Eq. (7.14). Figure 7.2 shows this invariant. It is clearly a function that mimics the octahedral symmetry. Moreover, it reflects the multipole character of the crystal-field potential. The potential is repulsive along the coordinate axes where the ligands are and of opposite sign along the threefold directions, in between the ligands, corresponding to the vertices of the cube. In fact, Eq. (7.19) provides a direct route to the crystal-field splitting. The coefficient in front of θ^2 and ϵ^2 in this equation is proportional to the interaction of these e_g-orbitals with the crystal-field operator, and similarly for the coefficient in front of the t_{2g} orbitals. The ratio of these coefficients can be reduced to

$$\frac{\frac{\sqrt{3}}{\sqrt{2}}}{-\frac{\sqrt{2}}{\sqrt{3}}} = \frac{3}{-2} \tag{7.20}$$

which reflects the crystal-field splitting of the d-shell, where the e_g level is raised by $6Dq$, while the t_{2g} level is lowered by $4Dq$, so that the barycentre is conserved and that the total splitting remains $10Dq$.

Typically, the first invariant multipole corresponds to the charge distribution of the Platonic solids of the given symmetry: hence, the $L = 4$ term describes the octahedron, and its dual the cube, while the next invariant, belonging to the $L = 6$ multipoles, represents the dominant term for the charge distribution in the 12-vertex Archimedean solid, known as the cuboctahedron, with a ligand in every edge of the octahedron. Entirely similar relations exist for the icosahedral group. The first icosahedral invariant, with $L = 6$, is the dominant term for the icosahedron and its dual dodecahedron. The next term, with $L = 10$, is the leading multipole for the truncated dodecahedron, alias the "buckyball" [5, 6].

7.3 Interactions of a Two-Component Spinor

The standard vector space in spherical symmetry has three components. We now explore the possibility of a function space with only two components. Such a space will correspond to a spinor. The strategy is to set up a general Hamiltonian matrix in a space with two components and verify that it has spherical symmetry. In order to describe the general interaction Hamiltonian in a space of only two components, a 2×2 Hermitian matrix, $\mathbb{H}$, is required. We can take this matrix to be traceless since the trace will not introduce an interaction inside the spin space but will simply shift the barycentre of the two levels with respect to an external reference. In its most general form, such a traceless Hermitian matrix will thus contain three independent real parameters, which we shall label as x, y, z:

$$\mathbb{H} = \begin{pmatrix} z & x - iy \\ x + iy & -z \end{pmatrix} \tag{7.21}$$

We have purposely chosen the Cartesian labels for the three independent parameters since, later on, a connection will be established between the 2D complex interaction space and the real 3D vector space. An example of such a Hamiltonian is the Zeeman interaction of an isolated spin in a magnetic field:

$$\mathcal{H} = 2.0023 \frac{\mu_B}{\hbar} \mathbf{B} \cdot \mathbf{S} \tag{7.22}$$

Here, $\mathbf{S}$ is the operator for the spin momentum, expressed in units of $\hbar$. The x, y, z parameters in this case are proportional to the magnitude of the magnetic field, $\mathbf{B}$, in the three Cartesian directions.

However, for now, we shall not yet make use of this spatial connotation and just continue to consider x, y, z as the general variables of the Hamiltonian matrix. The two components of the space will be denoted as the spin functions $|\alpha\rangle, |\beta\rangle$, which together form a spinor. The corresponding interaction operator can then be expressed as

$$\begin{aligned} \mathcal{H} = {} & z\big(|\alpha\rangle\langle\alpha| - |\beta\rangle\langle\beta|\big) + x\big(|\alpha\rangle\langle\beta| + |\beta\rangle\langle\alpha|\big) \\ & - iy\big(|\alpha\rangle\langle\beta| - |\beta\rangle\langle\alpha|\big) \end{aligned} \tag{7.23}$$

This result can also be recast in matrix form as

$$\mathcal{H} = \begin{pmatrix} |\alpha\rangle & |\beta\rangle \end{pmatrix} \mathbb{H} \begin{pmatrix} \langle\alpha| \\ \langle\beta| \end{pmatrix} \tag{7.24}$$

or, inversely, as

$$\mathbb{H} = \begin{pmatrix} \langle\alpha| \\ \langle\beta| \end{pmatrix} \mathcal{H} \begin{pmatrix} |\alpha\rangle & |\beta\rangle \end{pmatrix} \tag{7.25}$$

To establish the connection between the spinor and the vector, we now need to verify how transformations in the spinor are manifested as transformations in the vector. Consider a finite unitary transformation of the spinor. The transformation belongs to the unitary group, $U(2)$, and, as we have seen, the determinant of this matrix is unimodular. We consider the special case, however, where the determinant is $+1$. Such matrices form the special unitary group, $SU(2)$. The most general form of an $SU(2)$ matrix involves two complex parameters, say a and b, subject to the condition that their squared norm, $|a|^2 + |b|^2$, equals unity. These parameters are also known as the Cayley–Klein parameters. (Cf. Problem 2.1.) One has

$$\mathbb{U} = \begin{pmatrix} a & b \\ -\bar{b} & \bar{a} \end{pmatrix} \tag{7.26}$$

The operation $\hat{R}$ transforms the spinor as follows:

$$\begin{pmatrix} |\alpha'\rangle & |\beta'\rangle \end{pmatrix} = \hat{R} \begin{pmatrix} |\alpha\rangle & |\beta\rangle \end{pmatrix} = \begin{pmatrix} |\alpha\rangle & |\beta\rangle \end{pmatrix} \mathbb{U}(R) \tag{7.27}$$

In order to apply the transformation to the interaction operator, we must also consider the effect of $\hat{R}$ on the column of bra-functions. This simply requires the inverse of the matrix, which, for a unitary matrix, is nothing but its complex conjugate transposed:

$$\begin{pmatrix} \langle\alpha'| \\ \langle\beta'| \end{pmatrix} = \hat{R} \begin{pmatrix} \langle\alpha| \\ \langle\beta| \end{pmatrix} = \bar{\mathbb{U}}^T(R) \begin{pmatrix} \langle\alpha| \\ \langle\beta| \end{pmatrix} \tag{7.28}$$

The transformation of the spinor thus changes the interaction matrix as follows:

$$\begin{aligned} \mathbb{H}' &= \begin{pmatrix} \langle\alpha'| \\ \langle\beta'| \end{pmatrix} \mathcal{H} \begin{pmatrix} |\alpha'\rangle & |\beta'\rangle \end{pmatrix} \\ &= \bar{\mathbb{U}}^T \begin{pmatrix} \langle\alpha| \\ \langle\beta| \end{pmatrix} \mathcal{H} \begin{pmatrix} |\alpha\rangle & |\beta\rangle \end{pmatrix} \mathbb{U} \\ &= \bar{\mathbb{U}}^T \times \mathbb{H} \times \mathbb{U} \end{aligned} \tag{7.29}$$

The transformed Hamiltonian matrix is defined by a new set of parameters (x', y', z'):

$$\mathbb{H}' = \begin{pmatrix} z' & x' - iy' \\ x' + iy' & -z' \end{pmatrix} \tag{7.30}$$

In this way, the transformation of the spinor $(|\alpha\rangle \, |\beta\rangle) \rightarrow (|\alpha'\rangle \, |\beta'\rangle)$ *induces* a transformation of the vector $(x \ y \ z) \rightarrow (x' \ y' \ z')$. In the vector space this transformation is described by a matrix $\mathbb{O}(R)$. This matrix may easily be constructed by combining the previous two equations. One has

$$\left(x' \quad y' \quad z'\right) = \hat{R}(x \quad y \quad z) = (x \quad y \quad z)\mathbb{O}(R) \tag{7.31}$$

where the transformation matrix is given by

$$\mathbb{O}(R) = \begin{pmatrix} \frac{1}{2}(a^2 + \bar{a}^2 - b^2 - \bar{b}^2) & -\frac{i}{2}(a^2 - \bar{a}^2 + b^2 - \bar{b}^2) & -ab - \overline{ab} \\ \frac{i}{2}(a^2 - \bar{a}^2 - b^2 + \bar{b}^2) & \frac{1}{2}(a^2 + \bar{a}^2 + b^2 + \bar{b}^2) & -i(ab - \overline{ab}) \\ a\bar{b} + \bar{a}b & -i(a\bar{b} - \bar{a}b) & |a|^2 - |b|^2 \end{pmatrix} \tag{7.32}$$

It can easily be shown that this matrix is an orthogonal transformation with determinant equal to unity. Hence, it belongs to the $SO(3)$ group. As a result, it will leave the squared length of the vector invariant:

$$x^2 + y^2 + z^2 = x'^2 + y'^2 + z'^2 \tag{7.33}$$

This conservation of length is the property that confirms the previous identification of the interaction matrix elements with a 3-vector and relates it to ordinary space. In fact, by identifying the rotation matrices in Eqs. (7.3) and (7.32), we may determine the Cayley–Klein parameters. Two solutions with opposite signs are possible:

$$a = \left(\cos\frac{\alpha}{2} - in_z \sin\frac{\alpha}{2}\right)$$
$$b = \left(-n_y \sin\frac{\alpha}{2} - in_x \sin\frac{\alpha}{2}\right) \tag{7.34}$$

or

$$a = -\left(\cos\frac{\alpha}{2} - in_z \sin\frac{\alpha}{2}\right)$$
$$b = -\left(-n_y \sin\frac{\alpha}{2} - in_x \sin\frac{\alpha}{2}\right) \tag{7.35}$$

As this equation shows, the mapping $\mathbb{O}(R)$ is not an isomorphism but a homomorphism (see Fig. 7.3). Indeed, the elements of the matrix $\mathbb{O}$ are bilinear in the a and b parameters; hence, an overall sign change of the two Cayley–Klein parameters will give the same rotational matrix. The mapping between $SU(2)$ and $SO(3)$ is a two-to-one mapping. Each element of the rotation group in 3D space is the image of two elements in $SU(2)$. For this reason, $SU(2)$ is also called a covering group of $SO(3)$. The unit element in $SO(3)$ is the image of the identity matrix in $SU(2)$ and minus the identity matrix. This homomorphism also appears when we check the parameter list of Eq. (7.4), which leaves the rotation matrix of the vector unchanged. The overall sign change of the rotation angle and the directional cosines to

Fig. 7.3 Homomorphism between $SU(2)$ and $SO(3)$
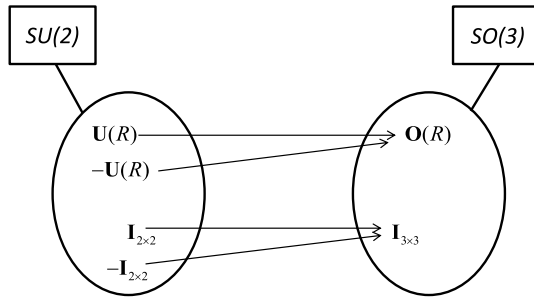
$\hat{R}(-\alpha, -\mathbf{n})$ leaves the Cayley–Klein parameters unchanged. By contrast, the combinations $\hat{R}(2\pi - \alpha, -\mathbf{n})$ and $\hat{R}(-2\pi + \alpha, \mathbf{n})$ change the signs of both Cayley–Klein parameters.

7.4 The Coupling of Spins

The entries in the Hamiltonian provide us with coupling coefficients between vector and spinor. Applying the Wigner–Eckart theorem to the matrix elements of the Zeeman spin Hamiltonian and separating out the constant parameters for the magnetic field yield the following nonzero coupling coefficients in the spin operator **S**, where K is the reduced matrix element:

$$\langle \alpha | \hat{S}_z | \alpha \rangle = K \langle \alpha | z\alpha \rangle = 1/2$$
$$\langle \beta | \hat{S}_z | \beta \rangle = K \langle \beta | z\beta \rangle = -1/2$$
$$\langle \alpha | \hat{S}_x | \beta \rangle = K \langle \alpha | x\beta \rangle = 1/2$$
$$\langle \beta | \hat{S}_x | \alpha \rangle = K \langle \beta | x\alpha \rangle = 1/2 \qquad (7.36)$$
$$\langle \alpha | \hat{S}_y | \beta \rangle = K \langle \alpha | y\beta \rangle = -i/2$$
$$\langle \beta | \hat{S}_y | \alpha \rangle = K \langle \beta | z\alpha \rangle = i/2$$

These coefficients can also be reversed to describe the coupling between two spinors to yield a vector. This requires that the ket spin in the coefficients is relocated to the bra part. In Sect. 6.3 we indicated that, for real functions, such a shift does not change the coupling, except for a renormalization factor. The transposition of the spin functions is more delicate since the bra functions transform as the complex conjugate of the ket functions, as indicated in Eq. (7.28). In order to establish the equivalences between transformations of bra and ket spins, one must identify the basis transformation that turns the matrix $\mathbb{U}$ into its complex conjugate. This transformation is readily achieved by replacing $|\alpha\rangle$ by $|\beta\rangle$, and $|\beta\rangle$ by $-|\alpha\rangle$. The

Table 7.2 The coupling coefficients for the direct product of two spins

	$S=0$	$S=1$					
		$|+1\rangle$	$|0\rangle$	$|-1\rangle$	$|x\rangle$	$|y\rangle$	$|z\rangle$
$|\alpha\rangle|\alpha\rangle$	0	1	0	0	$-1/\sqrt{2}$	$i/\sqrt{2}$	0
$|\alpha\rangle|\beta\rangle$	$1/\sqrt{2}$	0	$1/\sqrt{2}$	0	0	0	$1/\sqrt{2}$
$|\beta\rangle|\alpha\rangle$	$-1/\sqrt{2}$	0	$1/\sqrt{2}$	0	0	0	$1/\sqrt{2}$
$|\beta\rangle|\beta\rangle$	0	0	0	1	$1/\sqrt{2}$	$i/\sqrt{2}$	0

interchange corresponds to the following matrix transformation:

$$
\begin{pmatrix} |\alpha\rangle & |\beta\rangle \end{pmatrix} \begin{pmatrix} 0 & -1 \\ 1 & 0 \end{pmatrix} \tag{7.37}
$$

This matrix gives rise to the mapping of $\mathbb{U}$ onto its complex conjugate:

$$
\begin{pmatrix} 0 & -1 \\ 1 & 0 \end{pmatrix} \begin{pmatrix} a & b \\ -\bar{b} & \bar{a} \end{pmatrix} \begin{pmatrix} 0 & 1 \\ -1 & 0 \end{pmatrix} = \begin{pmatrix} \bar{a} & \bar{b} \\ -b & a \end{pmatrix} \tag{7.38}
$$

For this reason, the matrix in Eq. (7.37) is also called the *conjugating matrix*. The conjugating matrix is defined up to an arbitrary phase. We have taken here the standard phase choice. The conjugating relationships between the two spins can now be used to transfer the spin functions in the coupling coefficients from the ket to the bra part. An α spin in the ket part becomes a β spin in the bra part, while a β spin in the ket becomes a $-\alpha$ spin in the bra part.

The corresponding coupling coefficients are summarized in Table 7.2. They indicate how two spins can be coupled to a vector. Here, we also express the vector in complex form, as

$$
\begin{aligned}
|+1\rangle &= -\frac{1}{\sqrt{2}} \left(|x\rangle + i|y\rangle \right) \\
|0\rangle &= |z\rangle \\
|-1\rangle &= \frac{1}{\sqrt{2}} \left(|x\rangle - i|y\rangle \right)
\end{aligned} \tag{7.39}
$$

This transformation is in accordance with the Condon–Shortley phase conventions for the spherical basis functions [7]. In fact, our initial Hamiltonian matrix in Eq. (7.21) was constructed in this way. The resulting vector corresponds to the triplet spin functions, which we used in Sect. 6.4. The total spinor product space has dimension 4. The remainder after extraction of the three triplet functions corresponds to the spin singlet, which is invariant and transforms as a scalar. Spinors are thus the fundamental building blocks of 3D space. Their transformation properties were known to Rodrigues as early as 1840. It was some ninety years before Pauli realized that elementary particles, such as electrons, had properties that could be described

as internal spin states. In spin-orbit coupling the internal spin degrees of the electron are coupled to its external momentum, and this can be based on the embedding of $SO(3)$ in $SU(2)$.

7.5 Double Groups

The spinor basis enables us to obtain a two-dimensional matrix representation of the point-group operations. Let us first limit ourselves to the relationships for the proper rotations. The counterclockwise rotation of the vector over an angle α with the pole at the positive z-axis is given by the matrix:

$$\hat{R}\left(\begin{array}{ccc}|x\rangle & |y\rangle & |z\rangle\end{array}\right) = \left(\begin{array}{ccc}|x\rangle & |y\rangle & |z\rangle\end{array}\right)\begin{pmatrix} \cos\alpha & -\sin\alpha & 0 \\ \sin\alpha & \cos\alpha & 0 \\ 0 & 0 & 1 \end{pmatrix} \tag{7.40}$$

According to Eqs. (7.34) and (7.35), the corresponding rotation matrix in the spinor basis is determined up to a sign by

$$\hat{R}\left(\begin{array}{cc}|\alpha\rangle & |\beta\rangle\end{array}\right) = \pm\left(\begin{array}{cc}|\alpha\rangle & |\beta\rangle\end{array}\right)\begin{pmatrix} \exp(\frac{-i\alpha}{2}) & 0 \\ 0 & \exp(\frac{i\alpha}{2}) \end{pmatrix} \tag{7.41}$$

How does one deal with this ambiguity of sign? A plausible way is to use a continuity argument [8]. If we approach the neighborhood of the unit element for both spinor and vector by letting α decrease to zero, we should converge to the unit matrix and, hence, take the $+$ sign in Eq. (7.41) with $\alpha = 0$. Now let the rotation angle increase continuously from 0 to 2π. While the matrix $\mathbb{O}(R)$ is periodic in α and passes again to the unit matrix, the spinor matrix becomes minus the unit matrix. Continuing the path in parameter space and increasing the angle to 4π drive the vector rotation once again over the same interval, while the spinor rotation finally completes its path and reaches the unit element again. So, the difference between $\mathbb{U}$ and $-\mathbb{U}$ can be interpreted as a rotation over a full angle of 2π. From the topological point of view, the path that we have described corresponds to a full circle in the 4-parameter space of $SU(2)$, and the rotation over 2π connects a point in this space to its antipode. In this space the $SO(3)$ operations may be identified as the set of straight lines connecting antipodal points.

Our real interest at present is molecular Hamiltonians that are characterized by a point group G. However, as compared with the Hamiltonian considered in Chap. 5, we should also include *spin-orbit coupling* operators. These will be invariant only under concerted transformations of the orbital and spin parts. The homomorphism between $SO(3)$ and $SU(2)$ provides a straightforward *algebraic* way to construct the spinor group associated with the point group. For each operation, $\hat{R} \in G$, a matrix $\mathbb{O}(R)$ is defined, which offers a faithful representation of G and, in turn, gives rise to two spinor matrices, $\pm\mathbb{U}(R)$, which describe the spinor transformation. The set of these matrices forms a group, which contains twice as many elements as G and thus

Table 7.3 Representation matrices for the spinor basis in D_2^*

$$\mathbb{D}(E) = \begin{pmatrix} 1 & 0 \\ 0 & 1 \end{pmatrix} \qquad \mathbb{D}(\aleph) = \begin{pmatrix} -1 & 0 \\ 0 & -1 \end{pmatrix}$$

$$\mathbb{D}(C_2^x) = \begin{pmatrix} 0 & -i \\ -i & 0 \end{pmatrix} \qquad \mathbb{D}(\aleph C_2^x) = \begin{pmatrix} 0 & i \\ i & 0 \end{pmatrix}$$

$$\mathbb{D}(C_2^y) = \begin{pmatrix} 0 & -1 \\ 1 & 0 \end{pmatrix} \qquad \mathbb{D}(\aleph C_2^y) = \begin{pmatrix} 0 & 1 \\ -1 & 0 \end{pmatrix}$$

$$\mathbb{D}(C_2^z) = \begin{pmatrix} -i & 0 \\ 0 & i \end{pmatrix} \qquad \mathbb{D}(\aleph C_2^z) = \begin{pmatrix} i & 0 \\ 0 & -i \end{pmatrix}$$

is called the *double group*, denoted by G^*. While this construction is algebraic, the definition of a *geometrical* link between both groups is much less straightforward and unavoidably involves the introduction of phase conventions. Bethe introduced a formal symmetry operation, R, which corresponds to a rotation over 2π. Subsequently, we shall replace this by the symbol $\aleph$, in order to avoid confusion. This operation is fictitious to the extent that the poles of this rotation are left undefined. It can be multiplied with every operator in the group and thus leads to an actual doubling of the number of symmetry elements. Nonetheless, the double group is not the direct product of G with the group $\{\hat{E}, \aleph\}$. The reason is that G is not a subgroup of G^* because it is no longer closed. Indeed, applying a $\hat{C}_n$ axis in G n times will not lead to the unit element but to $\aleph$.

For the actual construction of the double group as a group of operators, we need a convention to connect the spatial operators to the spinor matrices. As we have seen in Sect. 7.2, the four possible parametric descriptions of a given rotation yield two different choices for the Cayley–Klein parameters. Hence, our convention should define how to characterize unequivocally the parameters of a rotation. It will consist of two criteria: the rotation angle must be positive, and the pole from which the rotation is seen as counterclockwise must belong to the *positive hemisphere* in the n_x, n_y, n_z parameter space. This is the hemisphere above the equatorial plane, i.e., with $n_z > 0$. In the (n_x, n_y)-plane, we include the half-circle of points with positive n_x-value, i.e., with $n_z = 0, n_x > 0$, and also the point with $n_y = 1, n_x = 0$, and $n_z = 0$. The rotational parameters $(\alpha, \mathbf{n})$ are thus chosen in such a way that α is positive, i.e., counterclockwise, and that the vector $\mathbf{n}$ points to the positive hemisphere. This eliminates three of the four equivalent parameter choices of Eq. (7.4). The only remaining description is then inserted into Eq. (7.34) to determine the Cayley–Klein parameters.

As a straightforward example, we take the double group of D_2. The standard drawing puts the twofold rotational axes in the positive hemisphere, and the corresponding spinor matrices are easily obtained from Eq. (7.34). The results are given in Table 7.3. For each operation of G, there are two operations in the double group, $\hat{R}$ and $\aleph\hat{R}$. Note that the Bethe operation, $\aleph$, commutes with every element of the group. Armed with this set of matrices, one can easily construct the multiplication

Table 7.4 Character table for the double group D_2^*

	$\hat{E}$	$\aleph$	$\begin{pmatrix} \hat{C}_2^z \\ \aleph\hat{C}_2^z \end{pmatrix}$	$\begin{pmatrix} \hat{C}_2^y \\ \aleph\hat{C}_2^y \end{pmatrix}$	$\begin{pmatrix} \hat{C}_2^x \\ \aleph\hat{C}_2^x \end{pmatrix}$
A	1	1	1	1	1
B_1	1	1	1	-1	-1
B_2	1	1	-1	1	-1
B_3	1	1	-1	-1	1
$E_{1/2}$	2	-2	0	0	0

Fig. 7.4 D_3 trischelate complex: orientation of the twofold axes on the positive hemicircle in the (x', y') plane
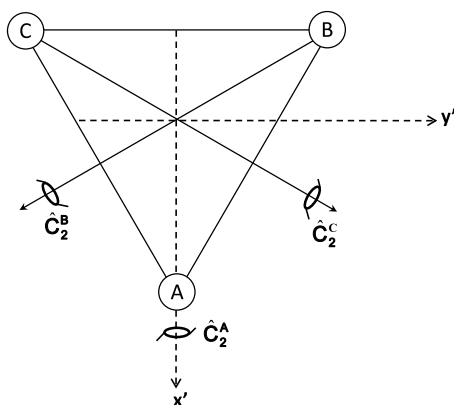
table; as an example,

$$\mathbb{D}(C_{2x}) \times \mathbb{D}(C_{2y}) = \mathbb{D}(\aleph C_{2z}) \tag{7.42}$$

From the multiplication table one can obtain the conjugacy classes. The double group, D_2^*, has five classes; hence, it will contain one extra irrep, as compared with the parent group. The character table is shown in Table 7.4. The irreps are of two different kinds. The *orbital* irreps are not changed under $\aleph$ and thus retain the characters of the single group. The other kind is the *spin* irreps, which are anti-symmetric under $\aleph$. Direct product tables may also be constructed. Note that the totally symmetric component in this case belongs to the anti-symmetrized part of the direct square of the spinor irreps. Relevant tabular information concerning the double groups and spinor irreps is gathered in Appendix G.

As a further example, in the D_3 symmetry group, the three $\hat{C}_2$ operators, which bisect the chelating ligand (cf. Fig. 6.5), all lie in the (x', y') plane. In order to obey the conventions, we have to take the poles of these axes in the positive semicircle with $x' > 0$ (see Fig. 7.4). The $(\alpha, n_{x'}, n_{y'}, n_{z'})$ labeling in the primed coordinate

Table 7.5 Representation matrices for the spinor basis in D_3^*. $\omega = \exp\frac{i\pi}{6}$

$$\mathbb{D}(E) = \begin{pmatrix} 1 & 0 \\ 0 & 1 \end{pmatrix} \qquad\qquad \mathbb{D}(C_2^A) = \begin{pmatrix} 0 & -i \\ -i & 0 \end{pmatrix}$$

$$\mathbb{D}(C_3) = \begin{pmatrix} \bar{\omega}^2 & 0 \\ 0 & \omega^2 \end{pmatrix} \qquad\qquad \mathbb{D}(C_2^B) = \begin{pmatrix} 0 & \bar{\omega} \\ -\omega & 0 \end{pmatrix}$$

$$\mathbb{D}(C_3^2) = \begin{pmatrix} -\omega^2 & 0 \\ 0 & -\bar{\omega}^2 \end{pmatrix} \qquad\qquad \mathbb{D}(C_2^C) = \begin{pmatrix} 0 & -\omega \\ \bar{\omega} & 0 \end{pmatrix}$$

Table 7.6 Character table for the double group D_3^*

	$\hat{E}$	$\aleph$	$\begin{pmatrix}\hat{C}_3\\ \aleph\hat{C}_3^2\end{pmatrix}$	$\begin{pmatrix}\aleph\hat{C}_3\\ \hat{C}_3^2\end{pmatrix}$	$\begin{pmatrix}\hat{C}_2^A\\ \aleph\hat{C}_2^B\\ \aleph\hat{C}_2^C\end{pmatrix}$	$\begin{pmatrix}\aleph\hat{C}_2^A\\ \hat{C}_2^B\\ \hat{C}_2^C\end{pmatrix}$
$E_{1/2}$	2	-2	1	-1	0	0
$E_{3/2}$ $\{\rho_1$	1	-1	-1	1	i	$-i$
$\phantom{E_{3/2}}\{\rho_2$	1	-1	-1	1	$-i$	i

system is thus as follows:

$$\begin{aligned}
\hat{C}_2^A &\quad (180°, \quad 1, \quad 0, \quad 0) \\
\hat{C}_2^B &\quad \left(180°, \ \frac{1}{2}, \ -\frac{\sqrt{3}}{2}, \ 0\right) \\
\hat{C}_2^C &\quad \left(180°, \ \frac{1}{2}, \ \frac{\sqrt{3}}{2}, \ 0\right)
\end{aligned} \tag{7.43}$$

The corresponding Cayley–Klein parameters are then determined as

$$\begin{aligned}
\hat{C}_2^A &\quad (a = 0, b = -i) \\
\hat{C}_2^B &\quad \left(a = 0, b = \frac{\sqrt{3}}{2} - \frac{i}{2}\right) \\
\hat{C}_2^C &\quad \left(a = 0, b = -\frac{\sqrt{3}}{2} - \frac{i}{2}\right)
\end{aligned} \tag{7.44}$$

In Tables 7.5 and 7.6 we provide the corresponding matrices and the character table. The ρ designations in the latter table refer to Kramers doublets and will be explained in the subsequent section. The class structure of the double group in connection to the point group is determined by the Opechowski theorem [9].

Theorem 17 *If a set of proper rotations, $\hat{C}_n$, forms a class in the single group G, then it gives rise to two separate classes in the double group, corresponding to conjugacy classes $\{\hat{C}_n\}$ and $\{\aleph\hat{C}_n\}$. The case of $n = 2$ is exceptional: when $n = 2$*

and there is another twofold axis in G perpendicular to this $\hat{C}_2$, both this $\hat{C}_2$ and $\aleph\hat{C}_2$ belong to the same class.

The theorem can easily be demonstrated in an algebraic way. If a symmetry element $\hat{A}$ is conjugate to $\hat{B}$, then element $\aleph\hat{A}$ is conjugate to $\aleph\hat{B}$, since the Bethe operation commutes with all symmetry elements:

$$\hat{A} = \hat{X}\hat{B}\hat{X}^{-1} \rightarrow \aleph\hat{A} = \hat{X}\aleph\hat{B}\hat{X}^{-1} \tag{7.45}$$

Since multiplication by $\aleph$ corresponds to multiplication by $-\mathbb{I}$, a symmetry element $\hat{A}$ and its double-group partner $\aleph\hat{A}$ have characters that differ by sign. Unless their characters are zero, they cannot belong to the same class since symmetry elements in the same class must have the same character. This explains the first rule of the theorem.[2]

Exceptions can exist when the character is zero. The character of the spinor irrep is given by

$$\chi^{\mathrm{spin}} = a + \bar{a} = \pm 2\cos\frac{\alpha}{2} \tag{7.46}$$

This character can be zero only for $\alpha = \pm\pi$ and, hence, for binary rotations with $n = 2$. To examine whether or not the matrix for a binary rotation can be class-conjugated to minus itself, we may limit ourselves to the study of one orientation of the rotation axis, say $\hat{C}_2^z$. Indeed, in $SU(2)$ any orientation can always be transformed backward to this standard choice by a unitary transformation. The problem thus reduces to finding a spinor operation $\hat{X}$ represented by a matrix $\mathbb{X}$ with Cayley–Klein parameters a_x, b_x, which transforms $\mathbb{D}(C_2^z)$ into minus itself:

$$\hat{X}\hat{C}_2^z\hat{X}^{-1} = \aleph\hat{C}_2^z \tag{7.47}$$

or, in terms of the spinor matrices,

$$\begin{pmatrix} a_x & b_x \\ -\bar{b}_x & \bar{a}_x \end{pmatrix} \begin{pmatrix} -i & 0 \\ 0 & i \end{pmatrix} \begin{pmatrix} \bar{a}_x & -b_x \\ \bar{b}_x & a_x \end{pmatrix} = \begin{pmatrix} i & 0 \\ 0 & -i \end{pmatrix} \tag{7.48}$$

This expression reduces to a set of two equations:

$$|a_x|^2 - |b_x|^2 = -1$$
$$a_x b_x = 0 \tag{7.49}$$

These equations can be solved only when a_x is equal to zero. This implies that both the real and complex parts of this parameter must be equal to zero; hence,

$$\alpha = \pi \quad \mathrm{mod}\ 2\pi$$
$$n_z = 0 \tag{7.50}$$

---

[2]Note that not all elements in the same class will be oriented in the positive hemisphere, as is clear from Tables 7.4 and 7.6.

This result identifies the $\hat{X}$ operator as a twofold rotation in a plane perpendicular to the z-direction. Hence, a twofold rotation axis, $\hat{C}_2$, and its double group extension $\aleph\hat{C}_2$ belong to the same class only if the group contains additional binary elements in a plane perpendicular to this axis. Otherwise, the first rule will apply. The exception referred to in this theorem is illustrated by the D_2^* class structure as shown in Table 7.4.

So far, we have been concerned only with proper rotations because in the spinor basis improper rotations are not defined. Since the electron spin is associated with an internal "spinning" of the electron around its axis, the electron spin is assigned an intrinsic positive parity. As we have seen before in Sect. 3.8, every improper rotation can be written as the product of a proper rotation and an inversion; therefore, whenever an improper rotation acts on a spinor, we simply take the matrix representation for the proper factor in this improper rotation.

7.6 Kramers Degeneracy

In 1930, Kramers showed that in the presence of an arbitrary electrostatic field all states with an odd number of spins must still have even degeneracy.[3]

Theorem 18 *The energy levels of a system that contains an odd number of spin-$\frac{1}{2}$ particles are at least doubly degenerate in the absence of an external magnetic field.*

This theorem reflects the influence of time-reversal symmetry. Already in Chap. 2, we showed that the time-reversal operator is an anti-linear operator. It will turn any spatial wavefunction into its complex conjugate. Applying it twice in succession will return the original wavefunction, and, hence, we may write for spatial functions:

$$\text{vectors}: \quad \vartheta^2 = +1 \tag{7.51}$$

However, the time-reversal properties of a spinor are different. Here we can use the same argument as in Sect. 7.4, viz. in Eq. (7.38), by requiring that the time reversal of the spinor components would lead to complex conjugation of their transformation properties. This implies that time reversal must turn $|\alpha\rangle$ into $|\beta\rangle$, and vice versa, but with a sign difference:

$$\begin{aligned} \vartheta\,|\alpha\rangle &= |\beta\rangle \\ \vartheta\,|\beta\rangle &= -|\alpha\rangle \end{aligned} \tag{7.52}$$

Hence, for spinors, applying time reversal twice leads to a sign change:

$$\text{spinors}: \quad \vartheta^2 = -1 \tag{7.53}$$

---

[3] Adapted from [10].

Note that the action of time reversal on the spin functions precisely corresponds to the $\hat{C}_2^y$ operator and thus is represented by $\mathbb{D}(C_2^y)$. This result may be generalized, in the sense that time reversal can be represented as the product of complex conjugation, denoted as K, and a unitary operator acting on the components of a function space, which we shall denote by the unitary matrix $\mathbb{U}$. We thus write $\vartheta = \mathbb{U}K$. When this operator is applied twice, it must return the same state, except possibly for a phase factor, say $\exp(i\kappa)$. Following Wigner, we now show that the two cases $\vartheta^2 = \pm 1$ are in fact the only possibilities. Hence, the phase factor can be only either $+1$ (time-even state) or -1 (time-odd state) [11, Chap. 26]. Taking time reversal twice, we have

$$\vartheta^2 = \mathbb{U}K\mathbb{U}K = \mathbb{U} \times \bar{\mathbb{U}} = \exp(i\kappa)\mathbb{I} \tag{7.54}$$

Since $\mathbb{U}$ is unitary, we have $\mathbb{U} \times \bar{\mathbb{U}}^T = \mathbb{I}$. Comparing this result with the previous expression, it follows that

$$\bar{\mathbb{U}} = \exp(i\kappa)\bar{\mathbb{U}}^T \tag{7.55}$$

Taking the transpose of both matrices in this equation will not affect the phase factor:

$$\bar{\mathbb{U}}^T = \exp(i\kappa)\bar{\mathbb{U}} \tag{7.56}$$

Combining Eqs. (7.55) and (7.56) yields

$$\bar{\mathbb{U}} = \exp(2i\kappa)\bar{\mathbb{U}} \tag{7.57}$$

which implies that $\exp(i\kappa) = \pm 1$.

We shall now examine the effects of these two kinds of time-reversal symmetry on quantum systems under time-even Hamiltonians, i.e., in the absence of external magnetic fields.

- $\vartheta^2 = +1$. In the case of a positive sign, it is always possible to write states that are time invariant. Consider a state that is described by a complex wavefunction, $|\Psi\rangle$, which is an eigenfunction of a time-even Hamiltonian. The time-reversed function, $\vartheta|\Psi\rangle$, will thus also be an eigenfunction with the same eigenenergy. The two functions will either coincide or be linearly independent. The latter case leads to a state that is at least twofold-degenerate. Both components of this degeneracy may transform as the complex-conjugate irreps of point groups such as the cyclic groups or the T_h group. When $\vartheta^2 = +1$, it is always possible to recombine these two degenerate states into two linear combinations that are invariant under time reversal. It is indeed sufficient to project the real and imaginary parts of these functions:

$$|\phi\rangle = \frac{1}{\sqrt{2}}\big(|\Psi\rangle + \vartheta|\Psi\rangle\big)$$

$$|\chi\rangle = \frac{-i}{\sqrt{2}}\big(|\Psi\rangle - \vartheta|\Psi\rangle\big) \tag{7.58}$$

It can easily be demonstrated that the Hamiltonian in this new basis is real:

$$\langle \phi | \mathcal{H} | \chi \rangle = \overline{\langle \vartheta \phi | \vartheta (\mathcal{H} \chi) \rangle} = \overline{\langle \vartheta \phi | \vartheta \mathcal{H} \vartheta | \vartheta \chi \rangle} = \overline{\langle \phi | \mathcal{H} | \chi \rangle} \qquad (7.59)$$

Hence, in this case, it is always possible to rewrite the basis in such a way that the Hamiltonian matrix is completely real, and the states behave in all respects as a real twofold-degenerate irrep, which can be split by symmetry-lowering electrostatic fields. In particular, such states will be subject to Jahn–Teller distortions.

- $\vartheta^2 = -1$. In the case of a negative sign, it is impossible to obtain states that are time invariant. This can be shown as follows. We start again with two states that are each other's time inverse ($|\Psi\rangle$ and $\vartheta|\Psi\rangle$) and first show that these states must be linearly independent:

$$\langle \Psi | \vartheta \Psi \rangle = \overline{\langle \vartheta \Psi | \vartheta^2 \Psi \rangle} = -\overline{\langle \vartheta \Psi | \Psi \rangle} = -\langle \Psi | \vartheta \Psi \rangle = 0 \qquad (7.60)$$

In contrast to the previous case, all attempts to construct a linear combination of these basis states that is invariant under time reversal, fail. Indeed, suppose that $|X\rangle$ is a linear combination with coefficients a and b, such that $\vartheta|X\rangle = |X\rangle$. Then we have:

$$|X\rangle = a|\Psi\rangle + b\vartheta|\Psi\rangle$$
$$\vartheta|X\rangle = \bar{a}\vartheta|\Psi\rangle - \bar{b}|\Psi\rangle \equiv a|\Psi\rangle + b\vartheta|\Psi\rangle \qquad (7.61)$$

Since the two kets are linearly independent, their respective coefficients must coincide, and this is possible only for $a = b = 0$. Hence, it is not possible to remove the degeneracy by time-even external fields. In particular, these states will not be subject to the JT effect.

Time-Reversal Selection Rules

The argument used in Eq. (7.59) can be generalized to describe selection rules that depend on time reversal [12]. We first introduce two parities, τ and η, which describe the time-dependence of the state and of the Hamiltonian:

$$\vartheta^2 = (-1)^\tau \hat{E}$$
$$\vartheta \mathcal{H} \vartheta^{-1} = (-1)^\eta \mathcal{H} \qquad (7.62)$$

The first label, τ, indicates the parity of the state functions, as we have just introduced in this section. The second label, η, indicates whether the Hamiltonian is time-even or time-odd. Time-even interactions are typically interactions associated with the electrostatic potential, such as the Jahn–Teller and Stark effects. Time-odd interactions are electrodynamic in nature, the most common one being the Zeeman interaction. We shall now study a function space that is invariant under time reversal

and transforms according to a degenerate irrep Γ with all characters real. As we have seen, this can be either an orbital or a spinor irrep. If $|\phi\rangle$ is an element of this space, so is $\vartheta|\phi\rangle$. Now, instead of considering matrix elements of type $\langle\phi|\mathcal{H}|\chi\rangle$, we shall replace the bra-functions by their time-reversed partners. The interaction element will then be of type $\langle\vartheta\phi|\mathcal{H}|\chi\rangle$. This may seem awkward, but in fact it does not lead to inconsistencies. In the case of orbital irreps, basis functions will either be real or may be arranged in complex-conjugate pairs, which are mutually time inverses. For spinor irreps, we can always write the basis functions in time-reversal pairs, such as the α and β spins.

The Hamiltonian for physical interactions must be Hermitian; hence, the bracket will be equal to the complex-conjugate inverted bracket:

$$\langle\vartheta\phi|\mathcal{H}|\chi\rangle = \overline{\langle\chi|\mathcal{H}|\vartheta\phi\rangle} \tag{7.63}$$

Complex conjugation of the bracket can also be achieved by time reversal. But, as an operator, time reversal can also enter into the bracket and operate on the components:

$$\overline{\langle\chi|\mathcal{H}|\vartheta\phi\rangle} = \langle\vartheta\chi|\vartheta(\mathcal{H}\vartheta\phi)\rangle = \langle\vartheta\chi|\vartheta\mathcal{H}\vartheta^{-1}|\vartheta^2\phi\rangle = (-1)^{\tau+\eta}\langle\vartheta\chi|\mathcal{H}|\phi\rangle \quad (7.64)$$

By combining these results we may thus write

$$\langle\vartheta\phi|\mathcal{H}|\chi\rangle = \frac{1}{2}\left[\langle\vartheta\phi|\mathcal{H}|\chi\rangle + (-1)^{\tau+\eta}\langle\vartheta\chi|\mathcal{H}|\phi\rangle\right] \tag{7.65}$$

The transformations of a time-reversed bra, $\langle\vartheta f_i|$, and its original ket, $|f_i\rangle$, are described by exactly the same matrices because complex conjugation is applied twice:

$$\hat{R}\langle\vartheta f_i| = \sum_j D_{ji}^{\Gamma}(R)\langle\vartheta f_j|$$
$$\hat{R}|f_i\rangle = \sum_j D_{ji}^{\Gamma}(R)f_j\rangle \tag{7.66}$$

This implies that the matrix elements in Eq. (7.65) are described by CG coupling coefficients, which are symmetric with respect to exchange of the bra and ket parts. This result leads to the following selection rules:

1. If the Hamiltonian and the system have the same parity under time reversal, interaction can take place only with the symmetrized square of the irrep, $[\Gamma]^2$.
2. If the Hamiltonian and the system have opposite parity under time reversal, the only allowed interaction elements must belong to the anti-symmetrized square of the irrep, $\{\Gamma\}^2$.

As a case in point, the JT Hamiltonian for orbital systems is limited to the symmetrized square, whereas the Zeeman Hamiltonian only arises if the anti-symmetrized square contains the symmetries of an axial field. For systems with an odd number of electrons, which therefore transform according to spinor representations, the selection rules are exactly opposite.

7.7 Application: Spin Hamiltonian for the Octahedral Quartet State

The octahedral double group contains a four-dimensional spin representation, which is commonly denoted as the Γ_8 quartet, or U' in Griffith's notation. The direct square of this irrep is given by

$$\Gamma_8 \times \Gamma_8 = [A_2 + 2T_1 + T_2] + \{A_1 + E + T_2\} \qquad (7.67)$$

According to the time-reversal selection rules, time-odd interactions with a magnetic field will be based on the symmetrized square. The spin-operator of the Zeeman Hamiltonian transforms as T_{1g}, which is indeed included in the symmetrized square. The present case is, however, special since the T_{1g} irrep occurs twice in the product. The multiplicity separation cannot be achieved on the basis of symmetrization since both T_{1g} irreps appear in the symmetrized part. One way to distinguish the two products is through the subduction process from spherical symmetry. The addition rules of angular momenta give rise to

$$3/2 \times 3/2 = [p + f] + \{s + d\} \qquad (7.68)$$

On these grounds the two T_{1g} interactions can be distinguished on the basis of a different spherical parentage corresponding to p or f coupling. We shall return to this point in a moment. For a systematic treatment of this problem, we start by setting up a suitable function space. The spherical $S = 3/2$ spin-quartet level subduces directly the octahedral Γ_8. We can thus use the quartet spin functions as symmetry bases. The components of $S = 3/2$ can be obtained by a fully symmetrized product of the basic spinor:

$$
\begin{aligned}
|3/2 + 3/2\rangle &= \alpha_1\alpha_2\alpha_3 \\
|3/2 + 1/2\rangle &= \frac{1}{\sqrt{3}}(\alpha_1\alpha_2\beta_3 + \alpha_1\beta_2\alpha_3 + \beta_1\alpha_2\alpha_3) \\
|3/2 - 1/2\rangle &= \frac{1}{\sqrt{3}}(\alpha_1\beta_2\beta_3 + \beta_1\alpha_2\beta_3 + \beta_1\beta_2\alpha_3) \\
|3/2 - 3/2\rangle &= \beta_1\beta_2\beta_3
\end{aligned}
\qquad (7.69)
$$

In this expression the fundamental $\{|\alpha\rangle, |\beta\rangle\}$ spinor resembles a quark state: three quarks are coupled together to form the quartet result. The use of the quartet spin bases does not mean that our Γ_8 really corresponds to a quartet spin. It only means that we can introduce a fictitious spin operator, $\tilde{S}$, which acts on the Γ_8 components in the same way as the real spin momentum would act on the components of a spin quartet. The transformations of the Γ_8 spinor under the elements of the group O^* may be obtained by combining the transformation matrices for the fundamental $(|\alpha\rangle|\beta\rangle)$ spins with the quartet coupling scheme in Eq. (7.69). In the group O^*, this irrep is denoted as Γ_6. In Table 7.7 the results are shown for two generators of the octahedral group. These matrices can be taken as the canonical basis relationships

Table 7.7 Representation matrices for the spinor basis in O^*

$$\mathbb{D}^{\Gamma_6}(C_4^z) = \frac{1}{\sqrt{2}} \begin{pmatrix} 1-i & 0 \\ 0 & 1+i \end{pmatrix} \quad \mathbb{D}^{\Gamma_6}(C_3^{xyz}) = \frac{1}{2} \begin{pmatrix} 1-i & -1-i \\ 1-i & 1+i \end{pmatrix}$$

$$\mathbb{D}^{\Gamma_8}(\hat{C}_4^z) = \frac{1}{\sqrt{2}} \begin{pmatrix} -1-i & 0 & 0 & 0 \\ 0 & 1-i & 0 & 0 \\ 0 & 0 & 1+i & 0 \\ 0 & 0 & 0 & -1+i \end{pmatrix}$$

$$\mathbb{D}^{\Gamma_8}(\hat{C}_3^{xyz}) = \frac{1}{4} \begin{pmatrix} -1-i & \sqrt{3}(-1+i) & \sqrt{3}(1+i) & 1-i \\ \sqrt{3}(-1-i) & -1+i & -1-i & \sqrt{3}(-1+i) \\ \sqrt{3}(-1-i) & 1-i & -1-i & \sqrt{3}(1-i) \\ -1-i & \sqrt{3}(1-i) & \sqrt{3}(1+i) & -1+i \end{pmatrix}$$

that define the components of the Γ_8. In Griffith's notation, these four components are defined in the following way:

$$
\begin{aligned}
|U'\kappa\rangle &\sim \left|\frac{3}{2} + \frac{3}{2}\right\rangle \\
|U'\lambda\rangle &\sim \left|\frac{3}{2} + \frac{1}{2}\right\rangle \\
|U'\mu\rangle &\sim \left|\frac{3}{2} - \frac{1}{2}\right\rangle \\
|U'\nu\rangle &\sim \left|\frac{3}{2} - \frac{3}{2}\right\rangle
\end{aligned}
\tag{7.70}
$$

Knowing the symmetries of the components, we can now turn to the coupling coefficients that describe their interactions. The coupling coefficients that we need are determined by the Zeeman Hamiltonian, which can be written as

$$\mathcal{H}_{Ze} = \frac{\mu_B}{\hbar} \mathbf{B} \cdot (\mathbf{L} + 2.0023\mathbf{S}) \tag{7.71}$$

The electronic part of this operator contains the orbital angular momentum and the spin operator. In octahedral symmetry the overall electronic operator transforms as T_{1g}. Applying the Wigner–Eckart theorem to the interaction elements in this operator yields

$$
\frac{\mu_B}{\hbar} \langle \Gamma_8 i | (\mathbf{L} + 2.0023\mathbf{S}) | \Gamma_8 j \rangle = \langle \Gamma_8 || T_1 || \Gamma_8 \rangle_a \langle \Gamma_8 i | T_1 j \Gamma_8 k \rangle_a
$$
$$
+ \langle \Gamma_8 || T_1 || \Gamma_8 \rangle_b \langle \Gamma_8 i | T_1 j \Gamma_8 k \rangle_b \tag{7.72}
$$

Here, we have introduced the extra labels a and b in order to distinguish that there are two coupling channels. The coupling coefficients that are required are of type $\langle \Gamma_{8k} | \Gamma_{8i} T_{1j} \rangle$, while the coefficients, as given in Appendix G, are of type

$\langle \Gamma_{8i} T_{1j} | \Gamma_{8k} \rangle$ and describe the spin-orbit coupling coefficients for the spin-orbit lev-
els of a $^4T_1$ state. However, since all coefficients in the table are real, turning them
around does not make any difference. Hence, we can directly use the spin-orbit
tables to obtain the Zeeman matrix. Only one of the coupling channels is seen to
link the κ and ν levels. In spherical symmetry this requires a jump of 3 spin units,
which can be bridged only by an $\ell = 3$ operator. The coupling coefficients of this
channel are thus of spherical octupole parentage ($\ell = 3$), while the other set is of
dipole parentage ($\ell = 1$). We shall parameterize the corresponding reduced matrix
elements as J_f and J_p, respectively. The constant $\mu_B/\hbar$, as well as a common fac-
tor of $1/\sqrt{15}$, is also absorbed into these parameters. The electronic operator will
be represented as $|T_i|$, and the Zeeman Hamiltonian is then recast in complex form
as

$$
\begin{aligned}
\mathcal{H}_{Ze} &= B_x |T_x| + B_y |T_y| + B_z |T_z| \\
&= B_z |T_0| - \frac{1}{\sqrt{2}} (B_x - i B_y) |T_{+1}| + \frac{1}{\sqrt{2}} (B_x + i B_y) |T_{-1}| \quad (7.73)
\end{aligned}
$$

This expression follows the convention of Eq. (7.39). The operator part is defined
by

$$
\begin{aligned}
|T_0| &= |T_z| \\
|T_{+1}| &= -\frac{1}{\sqrt{2}} \big(|T_x| + i |T_y| \big) \quad (7.74) \\
|T_{-1}| &= \frac{1}{\sqrt{2}} \big(|T_x| - i |T_y| \big)
\end{aligned}
$$

The elements of the interaction matrix are then given by

$$
\begin{aligned}
H_{ij} = {}& B_z \big(J_p \langle \Gamma_8 i | T_0 \Gamma_8 j \rangle_p + J_f \langle \Gamma_8 i | T_0 \Gamma_8 j \rangle_f \big) \\
& - \frac{1}{\sqrt{2}} (B_x - i B_y) \big(J_p \langle \Gamma_8 i | T_{+1} \Gamma_8 j \rangle_p + J_f \langle \Gamma_8 i | T_{+1} \Gamma_8 j \rangle_f \big) \\
& + \frac{1}{\sqrt{2}} (B_x + i B_y) \big(J_p \langle \Gamma_8 i | T_{-1} \Gamma_8 j \rangle_p + J_f \langle \Gamma_8 i | T_{-1} \Gamma_8 j \rangle_f \big) \quad (7.75)
\end{aligned}
$$

The resulting interaction matrix is given in Table 7.8. Since the Zeeman inter-
action leads to a splitting of the levels that conserves the barycentre, the secular
equation does not contain odd powers in the energy:

$$
a E^4 + b E^2 + c = 0 \quad (7.76)
$$

Table 7.8 Spin Hamiltonian matrix for the octahedral quartet irrep. A common factor of $1/\sqrt{15}$ is absorbed into the J-parameters

B_z	$\lvert\Gamma_8\kappa\rangle$	$\lvert\Gamma_8\lambda\rangle$	$\lvert\Gamma_8\mu\rangle$	$\lvert\Gamma_8\nu\rangle$
$\langle\Gamma_8\kappa\rvert$	$(3J_p - J_f)$			
$\langle\Gamma_8\lambda\rvert$		$(J_p + 3J_f)$		
$\langle\Gamma_8\mu\rvert$			$-(J_p + 3J_f)$	
$\langle\Gamma_8\nu\rvert$				$-(3J_p - J_f)$
$B_x - iB_y$	$\lvert\Gamma_8\kappa\rangle$	$\lvert\Gamma_8\lambda\rangle$	$\lvert\Gamma_8\mu\rangle$	$\lvert\Gamma_8\nu\rangle$
$\langle\Gamma_8\kappa\rvert$		$\sqrt{3}(J_p + \tfrac{1}{2}J_f)$		
$\langle\Gamma_8\lambda\rvert$			$(2J_p - \tfrac{3}{2}J_f)$	
$\langle\Gamma_8\mu\rvert$				$\sqrt{3}(J_p + \tfrac{1}{2}J_f)$
$\langle\Gamma_8\nu\rvert$	$-\tfrac{5}{2}J_f$			
$B_x + iB_y$	$\lvert\Gamma_8\kappa\rangle$	$\lvert\Gamma_8\lambda\rangle$	$\lvert\Gamma_8\mu\rangle$	$\lvert\Gamma_8\nu\rangle$
$\langle\Gamma_8\kappa\rvert$				$-\tfrac{5}{2}J_f$
$\langle\Gamma_8\lambda\rvert$	$\sqrt{3}(J_p + \tfrac{1}{2}J_f)$			
$\langle\Gamma_8\mu\rvert$		$(2J_p - \tfrac{3}{2}J_f)$		
$\langle\Gamma_8\nu\rvert$			$\sqrt{3}(J_p + \tfrac{1}{2}J_f)$	

The parameters are identified as

$$a = 1$$

$$b = -10\big(B_x^2 + B_y^2 + B_z^2\big)\big(J_p^2 + J_f^2\big)$$

$$c = \big(B_x^4 + B_y^4 + B_z^4\big)\big(9J_p^4 + 48J_p^3 J_f + 46J_p^2 J_f^2 - 48J_p J_f^3 + 9J_f^4\big) \quad (7.77)$$

$$+ \big(B_x^2 B_y^2 + B_x^2 B_z^2 + B_y^2 B_z^2\big)$$

$$\times \big(18J_p^4 - 144J_p^3 J_f + 32J_p^2 J_f^2 + 24J_p J_f^3 + 63J_f^4\big)$$

The parameter b in this expression is isotropic, i.e., it does not depend on the orientation of the magnetic field in the octahedron. On the other hand, the parameter c contains an anisotropic contribution. It depends on the orientation of the magnetic field in the octahedron, but symmetry-equivalent orientations must, of course, yield the same splitting. This means that c is certainly an octahedral invariant and may thus be written as the sum of the familiar scalar $L = 0$ and hexadecapolar $L = 4$ cubic invariants that we derived in Sect. 7.2. We thus write

$$c = c_1\big(B_x^2 + B_y^2 + B_z^2\big)^2$$

$$+ c_2\big(B_x^4 + B_y^4 + B_z^4 - 3B_x^2 B_y^2 - 3B_x^2 B_z^2 - 3B_y^2 B_z^2\big) \quad (7.78)$$
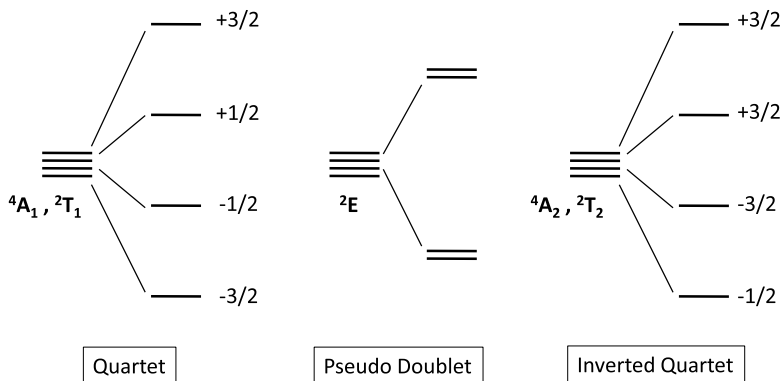
Fig. 7.5 Possible isotropic Zeeman splittings of the octahedral Γ_8 spinor irrep

The coefficients in this equation are identified as

$$
\begin{aligned}
c_1 &= 9J_p^4 + 34J_p^2 J_f^2 - 24J_p J_f^3 + 18J_f^4 \\
c_2 &= J_f(4J_p + 2J_f)^2(3J_p - 9/4J_f)
\end{aligned}
\tag{7.79}
$$

The c_2 coefficient is of special interest since it controls the only octahedral term in the linear Zeeman effect. If this coefficient vanishes, the splitting will be completely isotropic and does not depend on the orientation of the magnetic field in the octahedron. There are three possible isotropies [13].

- For $J_f = 0$, the spin operator is strictly dipolar, and the Zeeman Hamiltonian will induce a regular splitting of the quartet level, which is proportional to the spin quantum number, M_S. This case is illustrated in the left-hand panel of Fig. 7.5. Such cases will arise for an octahedral $^4A_1$ state and also for the quartet spin-orbit level of a $^2T_1$ state.
- For $4J_p + 2J_f = 0$, the matrix splits into two separate 2×2 blocks, which have the same eigenvalues. The splitting pattern is thus as in the central panel of Fig. 7.5. Such a case can occur for a ^2E state. The orbital part of this state has no angular momentum, since the corresponding operator is not included in the direct square: $T_1 \notin E \times E$. As a result, the magnetic moment of such a state is due only to the doublet spin part. Such a state behaves as a *pseudo-doublet*.
- Finally, for $3J_p - 9/4J_f = 0$, the splitting again resembles the Zeeman splitting of a regular spherical quartet, but the spin labels are interchanged, as compared with the standard quartet splitting: the $\pm 3/2$ levels become the inner levels of the split manifold, while the $\pm 1/2$ levels form the outer levels. This *inverted quartet* behavior is observed for $^2A_2$ and $^2T_2$ states. The orbital part in these states reverses the assignment of the fictitious spin levels, as can be seen, for instance, from the $A_2 \times \Gamma_8$ coupling table in Appendix G.

To conclude, we present the eigenenergies in the notation of Satten [14], who used parameters g_1 and g_2. The reduced matrix elements are expressed as

$$J_p = \frac{\mu_B}{2\hbar} \frac{g_1 + 9g_2}{10}$$

$$J_f = \frac{\mu_B}{2\hbar} \frac{3(g_1 - g_2)}{10} \tag{7.80}$$

Furthermore, the magnetic field is represented by directional cosines as $B_z = Bn_z$, $B_x = Bn_x$, $B_y = Bn_y$. The four eigenvalues then become

$$E = \pm \frac{\mu_B}{2\hbar} B \left[\frac{1}{2}(g_1^2 + 9g_2^2) \pm \frac{1}{4\sqrt{2}}(g_1 + 3g_2)\big(9(g_1 - 9g_2)(g_1 - g_2)\mathcal{F} \right.$$

$$\left. - (g_1^2 - 42g_1g_2 + 9g_2^2))^{1/2} \right]^{1/2} \tag{7.81}$$

The three isotropic cases are reflected by the zeroes of the three factors preceding the function $\mathcal{F} = (n_x^4 + n_y^4 + n_z^4)$.

7.8 Problems

7.1 Find a relationship between the crystal-field potentials of an octahedron and a cube.

7.2 The product of two rotations is a rotation. Obtain an expression for the Cayley–Klein parameters of the product as a function of the parameters of its factors. Is the product commutative? The $SU(2)$ matrices may also be identified as normalized *quaternions*.

7.3 Work out the group multiplication table for the D_3^* double group and derive the class structure.

7.4 Consider a set of three eigenlevels transforming as $A_1 + E$ in D_3 symmetry. A general matrix for the interaction between the states can be written as

$\mathcal{H}$	$|A_1\rangle$	$|E_x\rangle$	$|E_y\rangle$
$\langle A_1|$	-2Δ	$a + ib$	$c + id$
$\langle E_x|$	$a - ib$	Δ	$e - if$
$\langle E_y|$	$c - id$	$e + if$	Δ

Introduce a fictitious spin operator $\tilde{\mathbf{S}}$ that recognizes these states as the components of a triplet spin, $\tilde{S} = 1$, and consider the spin Hamiltonian

$$\mathcal{H}_{Ze} = \frac{\mu_B}{\hbar}\left[g_\parallel B_z \tilde{S}_z + g_\perp (B_x \tilde{S}_x + B_y \tilde{S}_y)\right] \tag{7.82}$$

Express the $a, \dots, f$ parameters as functions of the two g-parameters.

7.5 In octahedral symmetry the fictitious $\tilde{\mathbf{S}}$ operator follows the T_1 irrep. Its third symmetrized power transforms as the components of the f-harmonics and also subduces a T_1 irrep, as indicated in Table 7.1. Rewrite the p- and f-parts of the $|T_i|$ operators for the Γ_8 quartet state as a spin Hamiltonian of the fictitious spin.

References

1. Altmann, S.L.: Rotations, Quaternions, and Double Groups. Clarendon Press, Oxford (1986)
2. Butler, P.H.: Point Group Symmetry Applications, Methods and Tables. Plenum Press, New York (1981)
3. Edmonds, A.R.: Angular Momentum in Quantum Mechanics, 4th edn. Princeton University Press, Princeton (1996)
4. Gilmore, R.: Lie Groups, Physics, and Geometry: An Introduction for Physicists, Engineers and Chemists. Cambridge University Press, Cambridge (2008)
5. Ceulemans, A., Compernolle, S., Lijnen, E.: Hiatus in the spherical shell model of fullerenes. Phys. Chem. Chem. Phys. **6**, 238 (2004)
6. Troullier, N., Martins, J.L.: Structural and electronic properties of C_{60}. Phys. Rev. B **46**, 1754 (1992)
7. Condon, E.U., Odabaşi, H.: Atomic Structure. Cambridge University Press, Cambridge (1980)
8. Griffith, J.S.: The Theory of Transition-Metal Ions. Cambridge University Press, Cambridge (1961)
9. Opechowski, W.: Sur les groupes cristallographiques "doubles". Physica **7**, 552 (1940)
10. Haake, F.: Quantum Signatures of Chaos, 3rd edn. Springer Series in Synergetics. Springer, Berlin (2010)
11. Wigner, E.P.: Group Theory. Academic Press, New York (1959)
12. Abragam, A., Bleaney, B.: Electron Paramagnetic Resonance of Transition Ions p. 656. Clarendon Press, Oxford (1970)
13. Ceulemans, A., Mys, G., Walçerz, S.: Symmetries of time-odd electron–phonon coupling in the cubic Γ_8 system. New J. Chem. **17**, 131 (1993)
14. Satten, R.A.: Vibronic splitting and Zeeman effect in octahedral molecules: odd-electron systems. Phys. Rev. A **3**, 1246 (1971)

Appendix A
Character Tables

Contents

Character tables were introduced to chemistry through the pioneering work of Robert Mulliken [1]. The book on "Chemical Applications of Group Theory" by F. Albert Cotton has been instrumental in disseminating their use in chemistry [2]. Atkins, Child, and Phillips [3] produced a handy pamphlet of the point group character tables.[1]

---

[1]In the tables the columns on the right list representative coordinate functions that transform according to the corresponding irrep. The symbols R_x, R_y, R_z stand for rotations about the Cartesian directions.

A.1 Finite Point Groups

C_1 and the Binary Groups C_s, C_i, C_2

C_1	$\hat{E}$			
A	1			

C_s	$\hat{E}$	$\hat{\sigma}_h$		
A'	1	1	x, y, R_z	x^2, y^2, z^2, xy
A''	1	-1	z, R_x, R_y	yz, xz

C_i	$\hat{E}$	$\hat{\imath}$		
A_g	1	1	R_x, R_y, R_z	$x^2, y^2, z^2, yz, xz, xy$
A_u	1	-1	x, y, z	

C_2	$\hat{E}$	$\hat{C}_2^z$		
A	1	1	z, R_z	x^2, y^2, z^2, xy
B	1	-1	x, y, R_x, R_y	yz, xz

The Cyclic Groups C_n ($n = 3, 4, 5, 6, 7, 8$)

C_3	$\hat{E}$	$\hat{C}_3$	$\hat{C}_3^2$	$\epsilon = \exp(2\pi i/3)$	
A	1	1	1	z, R_z	$x^2 + y^2, z^2$
E $\big\{$	1	ϵ	$\bar{\epsilon}$	$(x, y)(R_x, R_y)$	$(x^2 - y^2, xy)(yz, xz)$
	1	$\bar{\epsilon}$	ϵ		

C_4	$\hat{E}$	$\hat{C}_4$	$\hat{C}_2$	$\hat{C}_4^3$		
A	1	1	1	1	z, R_z	$x^2 + y^2, z^2$
B	1	-1	1	-1		$x^2 - y^2, xy$
E $\big\{$	1	i	-1	$-i$	$(x, y)(R_x, R_y)$	(yz, xz)
	1	$-i$	-1	i		

C_5	$\hat{E}$	$\hat{C}_5$	$\hat{C}_5^2$	$\hat{C}_5^3$	$\hat{C}_5^4$	$\epsilon = \exp(2\pi i/5)$	
A	1	1	1	1	1	z, R_z	x^2+y^2, z^2
$E_1\left\{\vphantom{\begin{matrix}1\\1\end{matrix}}\right.$	1	ϵ	ϵ^2	$\bar{\epsilon}^2$	$\bar{\epsilon}$	$(x,y)(R_x,R_y)$	(yz,xz)
	1	$\bar{\epsilon}$	$\bar{\epsilon}^2$	ϵ^2	ϵ		
$E_2\left\{\vphantom{\begin{matrix}1\\1\end{matrix}}\right.$	1	ϵ^2	$\bar{\epsilon}$	ϵ	$\bar{\epsilon}^2$		(x^2-y^2, xy)
	1	$\bar{\epsilon}^2$	ϵ	$\bar{\epsilon}$	ϵ^2		

C_6	$\hat{E}$	$\hat{C}_6$	$\hat{C}_3$	$\hat{C}_2$	$\hat{C}_3^2$	$\hat{C}_6^5$	$\epsilon = \exp(2\pi i/6)$	
A	1	1	1	1	1	1	z, R_z	x^2+y^2, z^2
B	1	-1	1	-1	1	-1		
$E_1\left\{\vphantom{\begin{matrix}1\\1\end{matrix}}\right.$	1	ϵ	$-\bar{\epsilon}$	-1	$-\epsilon$	$\bar{\epsilon}$	$(x,y)(R_x,R_y)$	(yz,xz)
	1	$\bar{\epsilon}$	$-\epsilon$	-1	$-\bar{\epsilon}$	ϵ		
$E_2\left\{\vphantom{\begin{matrix}1\\1\end{matrix}}\right.$	1	$-\bar{\epsilon}$	$-\epsilon$	1	$-\bar{\epsilon}$	$-\epsilon$		(x^2-y^2, xy)
	1	$-\epsilon$	$-\bar{\epsilon}$	1	$-\epsilon$	$-\bar{\epsilon}$		

C_7	$\hat{E}$	$\hat{C}_7$	$\hat{C}_7^2$	$\hat{C}_7^3$	$\hat{C}_7^4$	$\hat{C}_7^5$	$\hat{C}_7^6$	$\epsilon = \exp(2\pi i/7)$	
A	1	1	1	1	1	1	1	z, R_z	x^2+y^2, z^2
$E_1\left\{\vphantom{\begin{matrix}1\\1\end{matrix}}\right.$	1	ϵ	ϵ^2	ϵ^3	$\bar{\epsilon}^3$	$\bar{\epsilon}^2$	$\bar{\epsilon}$	$(x,y)(R_x,R_y)$	(yz,xz)
	1	$\bar{\epsilon}$	$\bar{\epsilon}^2$	$\bar{\epsilon}^3$	ϵ^3	ϵ^2	ϵ		
$E_2\left\{\vphantom{\begin{matrix}1\\1\end{matrix}}\right.$	1	ϵ^2	$\bar{\epsilon}^3$	$\bar{\epsilon}$	ϵ	ϵ^3	$\bar{\epsilon}^2$		(x^2-y^2, xy)
	1	$\bar{\epsilon}^2$	ϵ^3	ϵ	$\bar{\epsilon}$	$\bar{\epsilon}^3$	ϵ^2		
$E_3\left\{\vphantom{\begin{matrix}1\\1\end{matrix}}\right.$	1	ϵ^3	$\bar{\epsilon}$	ϵ^2	$\bar{\epsilon}^2$	ϵ	$\bar{\epsilon}^3$		$[x(x^2-3y^2),$
	1	$\bar{\epsilon}^3$	ϵ	$\bar{\epsilon}^2$	ϵ^2	$\bar{\epsilon}$	ϵ^3		$y(3x^2-y^2)]$

C_8	$\hat{E}$	$\hat{C}_8$	$\hat{C}_4$	$\hat{C}_2$	$\hat{C}_4^3$	$\hat{C}_8^3$	$\hat{C}_8^5$	$\hat{C}_8^7$	$\epsilon = \exp(2\pi i/8)$	
A	1	1	1	1	1	1	1	1	z, R_z	x^2+y^2, z^2
B	1	-1	1	1	1	-1	-1	-1		
$E_1\left\{\vphantom{\begin{matrix}1\\1\end{matrix}}\right.$	1	ϵ	i	-1	$-i$	$-\bar{\epsilon}$	$-\epsilon$	$\bar{\epsilon}$	$(x,y)(R_x,R_y)$	(yz,xz)
	1	$\bar{\epsilon}$	$-i$	-1	i	$-\epsilon$	$-\bar{\epsilon}$	ϵ		
$E_2\left\{\vphantom{\begin{matrix}1\\1\end{matrix}}\right.$	1	i	-1	1	-1	$-i$	i	$-i$		(x^2-y^2, xy)
	1	$-i$	-1	1	-1	i	$-i$	i		
$E_3\left\{\vphantom{\begin{matrix}1\\1\end{matrix}}\right.$	1	$-\epsilon$	i	-1	$-i$	$\bar{\epsilon}$	ϵ	$-\bar{\epsilon}$		$[x(x^2-3y^2),$
	1	$-\bar{\epsilon}$	$-i$	-1	i	ϵ	$\bar{\epsilon}$	$-\epsilon$		$y(3x^2-y^2)]$

The Dihedral Groups D_n (n = 2, 3, 4, 5, 6)

D_2	$\hat{E}$	$\hat{C}_2^z$	$\hat{C}_2^y$	$\hat{C}_2^x$		
A	1	1	1	1		x^2, y^2, z^2
B_1	1	1	-1	-1	z, R_z	xy
B_2	1	-1	1	-1	y, R_y	xz
B_3	1	-1	-1	1	x, R_x	yz

D_3	$\hat{E}$	$2\hat{C}_3$	$3\hat{C}_2$		
A_1	1	1	1		$x^2 + y^2, z^2$
A_2	1	1	-1	z, R_z	
E	2	-1	0	$(x, y)(R_x, R_y)$	$(xz, yz)(x^2 - y^2, xy)$

D_4	$\hat{E}$	$2\hat{C}_4$	$\hat{C}_2 (= \hat{C}_4^2)$	$2\hat{C}_2'$	$2\hat{C}_2''$		
A_1	1	1	1	1	1		$x^2 + y^2, z^2$
A_2	1	1	1	-1	-1	z, R_z	
B_1	1	-1	1	1	-1		$x^2 - y^2$
B_2	1	-1	1	-1	1		xy
E	2	0	-2	0	0	$(x, y)(R_x, R_y)$	(xz, yz)

D_5	$\hat{E}$	$2\hat{C}_5$	$2\hat{C}_5^2$	$5\hat{C}_2'$		
A_1	1	1	1	1		$x^2 + y^2, z^2$
A_2	1	1	1	-1	z, R_z	
E_1	2	$2\cos(2\pi/5)$	$2\cos(4\pi/5)$	0	$(x, y)(R_x, R_y)$	(xz, yz)
E_2	2	$2\cos(4\pi/5)$	$2\cos(2\pi/5)$	0		$(x^2 - y^2, xy)$

D_6	$\hat{E}$	$2\hat{C}_6$	$2\hat{C}_3$	$\hat{C}_2$	$3\hat{C}_2'$	$3\hat{C}_2''$		
A_1	1	1	1	1	1	1		$x^2 + y^2, z^2$
A_2	1	1	1	1	-1	-1	z, R_z	
B_1	1	-1	1	-1	1	-1		$x(x^2 - 3y^2)$
B_2	1	-1	1	-1	-1	1		$y(3x^2 - y^2)$
E_1	2	1	-1	-2	0	0	$(x, y)(R_x, R_y)$	(xz, yz)
E_2	2	-1	-1	2	0	0		$(x^2 - y^2, xy)$

The Conical Groups C_{nv} ($n = 2, 3, 4, 5, 6$)

C_{2v}	$\hat{E}$	$\hat{C}_2^z$	$\hat{\sigma}_v^{xz}$	$\hat{\sigma}_v^{yz}$		
A_1	1	1	1	1	z	x^2, y^2, z^2
A_2	1	1	-1	-1	R_z	xy
B_1	1	-1	1	-1	x, R_y	xz
B_2	1	-1	-1	1	y, R_x	yz

C_{3v}	$\hat{E}$	$2\hat{C}_3$	$3\hat{\sigma}_v$		
A_1	1	1	1	z	$x^2 + y^2, z^2$
A_2	1	1	-1	R_z	
E	2	-1	0	$(x, y)(R_x, R_y)$	$(x^2 - y^2, xy)(xz, yz)$

C_{4v}	$\hat{E}$	$2\hat{C}_4$	$\hat{C}_2$	$2\hat{\sigma}_v$	$2\hat{\sigma}_d$		
A_1	1	1	1	1	1	z	$x^2 + y^2, z^2$
A_2	1	1	1	-1	-1	R_z	
B_1	1	-1	1	1	-1		$x^2 - y^2$
B_2	1	-1	1	-1	1		xy
E	2	0	-2	0	0	$(x, y)(R_x, R_y)$	(xz, yz)

C_{5v}	$\hat{E}$	$2\hat{C}_5$	$2\hat{C}_5^2$	$5\hat{\sigma}_v$		
A_1	1	1	1	1	z	$x^2 + y^2, z^2$
A_2	1	1	1	-1	R_z	
E_1	2	$2\cos(2\pi/5)$	$2\cos(4\pi/5)$	0	$(x, y)(R_x, R_y)$	(xz, yz)
E_2	2	$2\cos(4\pi/5)$	$2\cos(2\pi/5)$	0		$(x^2 - y^2, xy)$

C_{6v}	$\hat{E}$	$2\hat{C}_6$	$2\hat{C}_3$	$\hat{C}_2$	$3\hat{\sigma}_v$	$3\hat{\sigma}_d$		
A_1	1	1	1	1	1	1	z	$x^2 + y^2, z^2$
A_2	1	1	1	1	-1	-1	R_z	
B_1	1	-1	1	-1	1	-1		$x(x^2 - 3y^2)$
B_2	1	-1	1	-1	-1	1		$y(3x^2 - y^2)$
E_1	2	1	-1	-2	0	0	$(x, y)(R_x, R_y)$	(xz, yz)
E_2	2	-1	-1	2	0	0		$(x^2 - y^2, xy)$

The C_{nh} Groups ($n = 2, 3, 4, 5, 6$)

C_{2h}	$\hat{E}$	$\hat{C}_2^z$	$\hat{\imath}$	$\hat{\sigma}_h$		
A_g	1	1	1	1	R_z	x^2, y^2, z^2, xy
B_g	1	-1	1	-1	R_x, R_y	xz, yz
A_u	1	1	-1	-1	z	
B_u	1	-1	-1	1	x, y	

C_{3h}	$\hat{E}$	$\hat{C}_3$	$\hat{C}_3^2$	$\hat{\sigma}_h$	$\hat{S}_3$	$\hat{S}_3^2$	$\epsilon = \exp(2\pi i/3)$	
A'	1	1	1	1	1	1	R_z	$x^2 + y^2, z^2$
E' $\Big\{$	1	ϵ	$\bar{\epsilon}$	1	ϵ	$\bar{\epsilon}$	(x, y)	$(x^2 - y^2, xy)$
	1	$\bar{\epsilon}$	ϵ	1	$\bar{\epsilon}$	ϵ		
A''	1	1	1	-1	-1	-1	z	
E'' $\Big\{$	1	ϵ	$\bar{\epsilon}$	-1	$-\epsilon$	$-\bar{\epsilon}$	(R_x, R_y)	(xz, yz)
	1	$\bar{\epsilon}$	ϵ	-1	$-\bar{\epsilon}$	$-\epsilon$		

C_{4h}	$\hat{E}$	$\hat{C}_4$	$\hat{C}_2$	$\hat{C}_4^3$	$\hat{\imath}$	$\hat{S}_4^3$	$\hat{\sigma}_h$	$\hat{S}_4$		
A_g	1	1	1	1	1	1	1	1	R_z	$x^2 + y^2, z^2$
B_g	1	-1	1	-1	1	-1	1	-1		$x^2 - y^2, xy$
E_g $\Big\{$	1	i	-1	$-i$	1	i	-1	$-i$	(R_x, R_y)	(yz, xz)
	1	$-i$	-1	i	1	$-i$	-1	i		
A_u	1	1	1	1	-1	-1	-1	-1	z	
B_u	1	-1	1	-1	-1	1	-1	1		
E_u $\Big\{$	1	i	-1	$-i$	-1	$-i$	1	i	(x, y)	
	1	$-i$	-1	i	-1	i	1	$-i$		

C_{5h}	$\hat{E}$	$\hat{C}_5$	$\hat{C}_5^2$	$\hat{C}_5^3$	$\hat{C}_5^4$	$\hat{\sigma}_h$	$\hat{S}_5$	$\hat{S}_5^7$	$\hat{S}_5^3$	$\hat{S}_5^9$	$\epsilon = \exp(2\pi i/5)$	
A'	1	1	1	1	1	1	1	1	1	1	R_z	$x^2 + y^2, z^2$
E_1' $\Big\{$	1	ϵ	ϵ^2	$\bar{\epsilon}^2$	$\bar{\epsilon}$	1	ϵ	ϵ^2	$\bar{\epsilon}^2$	$\bar{\epsilon}$	(x, y)	
	1	$\bar{\epsilon}$	$\bar{\epsilon}^2$	ϵ^2	ϵ	1	$\bar{\epsilon}$	$\bar{\epsilon}^2$	ϵ^2	ϵ		
E_2' $\Big\{$	1	ϵ^2	$\bar{\epsilon}$	ϵ	$\bar{\epsilon}^2$	1	ϵ^2	$\bar{\epsilon}$	ϵ	$\bar{\epsilon}^2$		$(x^2 - y^2, xy)$
	1	$\bar{\epsilon}^2$	ϵ	$\bar{\epsilon}$	ϵ^2	1	$\bar{\epsilon}^2$	ϵ	$\bar{\epsilon}$	ϵ^2		
A''	1	1	1	1	1	-1	-1	-1	-1	-1	z	
E_1'' $\Big\{$	1	ϵ	ϵ^2	$\bar{\epsilon}^2$	$\bar{\epsilon}$	-1	$-\epsilon$	$-\epsilon^2$	$-\bar{\epsilon}^2$	$-\bar{\epsilon}$	(R_x, R_y)	(xz, yz)
	1	$\bar{\epsilon}$	$\bar{\epsilon}^2$	ϵ^2	ϵ	-1	$-\bar{\epsilon}$	$-\bar{\epsilon}^2$	$-\epsilon^2$	$-\epsilon$		
E_2'' $\Big\{$	1	ϵ^2	$\bar{\epsilon}$	ϵ	$\bar{\epsilon}^2$	-1	$-\epsilon^2$	$-\bar{\epsilon}$	$-\epsilon$	$-\bar{\epsilon}^2$		
	1	$\bar{\epsilon}^2$	ϵ	$\bar{\epsilon}$	ϵ^2	-1	$-\bar{\epsilon}^2$	$-\epsilon$	$-\bar{\epsilon}$	$-\epsilon^2$		

C_{6h}	$\hat{E}$	$\hat{C}_6$	$\hat{C}_3$	$\hat{C}_2$	$\hat{C}_3^2$	$\hat{C}_6^5$	$\hat{i}$	$\hat{S}_3^5$	$\hat{S}_6^5$	$\hat{\sigma}_h$	$\hat{S}_6$	$\hat{S}_3$	$\epsilon = \exp(2\pi i/6)$	
A_g	1	1	1	1	1	1	1	1	1	1	1	1	R_z	x^2+y^2, z^2
B_g	1	-1	1	-1	1	-1	1	-1	1	-1	1	-1		
E_{1g}	1	ϵ	$-\bar\epsilon$	-1	$-\epsilon$	$\bar\epsilon$	1	ϵ	$-\bar\epsilon$	-1	$-\epsilon$	$\bar\epsilon$	(R_x, R_y)	(yz, xz)
	1	$\bar\epsilon$	$-\epsilon$	-1	$-\bar\epsilon$	ϵ	1	$\bar\epsilon$	$-\epsilon$	-1	$-\bar\epsilon$	ϵ		
E_{2g}	1	$-\bar\epsilon$	$-\epsilon$	1	$-\bar\epsilon$	$-\epsilon$	1	$-\bar\epsilon$	$-\epsilon$	1	$-\bar\epsilon$	$-\epsilon$		
	1	$-\epsilon$	$-\bar\epsilon$	1	$-\epsilon$	$-\bar\epsilon$	1	$-\epsilon$	$-\bar\epsilon$	1	$-\epsilon$	$-\bar\epsilon$		
A_u	1	1	1	1	1	1	-1	-1	-1	-1	-1	-1	z	x^2+y^2, z^2
B_u	1	-1	1	-1	1	-1	-1	1	-1	1	-1	1		
E_{1u}	1	ϵ	$-\bar\epsilon$	-1	$-\epsilon$	$\bar\epsilon$	-1	$-\epsilon$	$\bar\epsilon$	1	ϵ	$-\bar\epsilon$	(x, y)	
	1	$\bar\epsilon$	$-\epsilon$	-1	$-\bar\epsilon$	ϵ	-1	$-\bar\epsilon$	ϵ	1	$\bar\epsilon$	$-\epsilon$		
E_{2u}	1	$-\bar\epsilon$	$-\epsilon$	1	$-\bar\epsilon$	$-\epsilon$	-1	$\bar\epsilon$	ϵ	-1	$\bar\epsilon$	ϵ		
	1	$-\epsilon$	$-\bar\epsilon$	1	$-\epsilon$	$-\bar\epsilon$	-1	ϵ	$\bar\epsilon$	-1	ϵ	$\bar\epsilon$		

The Rotation–Reflection Groups S_{2n} ($n = 2, 3, 4$)

S_4	$\hat{E}$	$\hat{S}_4$	$\hat{C}_2$	$\hat{S}_4^3$		
A	1	1	1	1	R_z	x^2+y^2, z^2
B	1	-1	1	-1	z	x^2-y^2, xy
E	1	i	-1	$-i$	$(x, y)(R_x, R_y)$	(xz, yz)
	1	$-i$	-1	i		

S_6	$\hat{E}$	$\hat{C}_3$	$\hat{C}_3^2$	$\hat{i}$	$\hat{S}_6^5$	$\hat{S}_6$	$\epsilon = \exp(2\pi i/3)$	
A_g	1	1	1	1	1	1	R_z	x^2+y^2, z^2
E_g	1	ϵ	$\bar\epsilon$	1	ϵ	$\bar\epsilon$	(R_x, R_y)	$(x^2-y^2, xy)(yz, xz)$
	1	$\bar\epsilon$	ϵ	1	$\bar\epsilon$	ϵ		
A_u	1	1	1	-1	-1	-1	z	
E_u	1	ϵ	$\bar\epsilon$	-1	$-\epsilon$	$-\bar\epsilon$	(x, y)	
	1	$\bar\epsilon$	ϵ	-1	$-\bar\epsilon$	$-\epsilon$		

S_8	$\hat{E}$	$\hat{S}_8$	$\hat{C}_4$	$\hat{S}_8^3$	$\hat{C}_2$	$\hat{S}_8^5$	$\hat{C}_4^3$	$\hat{S}_8^7$	$\epsilon = \exp(2\pi i/8)$	
A	1	1	1	1	1	1	1	1	R_z	x^2+y^2, z^2
B	1	-1	1	-1	1	-1	1	-1	z	
E_1	1	ϵ	i	$-\bar\epsilon$	-1	$-\epsilon$	$-i$	$\bar\epsilon$	$(x, y)(R_x, R_y)$	
	1	$\bar\epsilon$	$-i$	$-\epsilon$	-1	$-\bar\epsilon$	i	ϵ		
E_2	1	i	-1	$-i$	1	i	-1	$-i$		(x^2-y^2, xy)
	1	$-i$	-1	i	1	$-i$	-1	i		
E_3	1	$-\bar\epsilon$	$-i$	ϵ	-1	$\bar\epsilon$	i	$-\epsilon$		(xz, yz)
	1	$-\epsilon$	i	$\bar\epsilon$	-1	ϵ	$-i$	$-\bar\epsilon$		

The Prismatic Groups D_{nh} (n = 2, 3, 4, 5, 6, 8)

D_{2h}	$\hat{E}$	$\hat{C}_2^z$	$\hat{C}_2^y$	$\hat{C}_2^x$	$\hat{i}$	$\hat{\sigma}_{xy}$	$\hat{\sigma}_{xz}$	$\hat{\sigma}_{yz}$		
A_g	1	1	1	1	1	1	1	1		x^2, y^2, z^2
B_{1g}	1	1	-1	-1	1	1	-1	-1	R_z	xy
B_{2g}	1	-1	1	-1	1	-1	1	-1	R_y	xz
B_{3g}	1	-1	-1	1	1	-1	-1	1	R_x	yz
A_u	1	1	1	1	-1	-1	-1	-1		xyz
B_{1u}	1	1	-1	-1	-1	-1	1	1	z	
B_{2u}	1	-1	1	-1	-1	1	-1	1	y	
B_{3u}	1	-1	-1	1	-1	1	1	-1	x	

D_{3h}	$\hat{E}$	$2\hat{C}_3$	$3\hat{C}_2$	$\hat{\sigma}_h$	$2\hat{S}_3$	$3\hat{\sigma}_v$		
A_1'	1	1	1	1	1	1		$x^2 + y^2, z^2$
A_2'	1	1	-1	1	1	-1	R_z	
E'	2	-1	0	2	-1	0	(x, y)	$(x^2 - y^2, xy)$
A_1''	1	1	1	-1	-1	-1		
A_2''	1	1	-1	-1	-1	1	z	
E''	2	-1	0	-2	1	0	(R_x, R_y)	(xz, yz)

D_{4h}	$\hat{E}$	$2\hat{C}_4$	$\hat{C}_2$	$2\hat{C}_2'$	$2\hat{C}_2''$	$\hat{i}$	$2\hat{S}_4$	$\hat{\sigma}_h$	$2\hat{\sigma}_v$	$2\hat{\sigma}_d$		
A_{1g}	1	1	1	1	1	1	1	1	1	1		$x^2 + y^2, z^2$
A_{2g}	1	1	1	-1	-1	1	1	1	-1	-1	R_z	
B_{1g}	1	-1	1	1	-1	1	-1	1	1	-1		$x^2 - y^2$
B_{2g}	1	-1	1	-1	1	1	-1	1	-1	1		xy
E_g	2	0	-2	0	0	2	0	-2	0	0	(R_x, R_y)	(xz, yz)
A_{1u}	1	1	1	1	1	-1	-1	-1	-1	-1		
A_{2u}	1	1	1	-1	-1	-1	-1	-1	1	1	z	
B_{1u}	1	-1	1	1	-1	-1	1	-1	-1	1		
B_{2u}	1	-1	1	-1	1	-1	1	-1	1	-1		
E_u	2	0	-2	0	0	-2	0	2	0	0	(x, y)	

D_{5h}	$\hat{E}$	$2\hat{C}_5$	$2\hat{C}_5^2$	$5\hat{C}_2$	$\hat{\sigma}_h$	$2\hat{S}_5$	$2\hat{S}_5^3$	$5\hat{\sigma}_v$	$\alpha = \cos(2\pi/5)$	$\beta = \cos(4\pi/5)$
A_1'	1	1	1	1	1	1	1	1		$x^2 + y^2, z^2$
A_2'	1	1	1	-1	1	1	1	-1	R_z	
E_1'	2	2α	2β	0	2	2α	2β	0	(x, y)	
E_2'	2	2β	2α	0	2	2β	2α	0		$(x^2 - y^2, xy)$
A_1''	1	1	1	1	-1	-1	-1	-1		
A_2''	1	1	1	-1	-1	-1	-1	1	z	
E_1''	2	2α	2β	0	-2	-2α	-2β	0	(R_x, R_y)	
E_2''	2	2β	2α	0	-2	-2β	-2α	0		(xz, yz)

D_{6h}	$\hat{E}$	$2\hat{C}_6$	$2\hat{C}_3$	$\hat{C}_2$	$3\hat{C}_2'$	$3\hat{C}_2''$	$\hat{\imath}$	$2\hat{S}_3$	$2\hat{S}_6$	$\hat{\sigma}_h$	$3\hat{\sigma}_d$	$3\hat{\sigma}_v$	
A_{1g}	1	1	1	1	1	1	1	1	1	1	1	1	x^2+y^2, z^2
A_{2g}	1	1	1	1	-1	-1	1	1	1	1	-1	-1	R_z
B_{1g}	1	-1	1	-1	1	-1	1	-1	1	-1	1	-1	
B_{2g}	1	-1	1	-1	-1	1	1	-1	1	-1	-1	1	
E_{1g}	2	1	-1	-2	0	0	2	1	-1	-2	0	0	$(R_x, R_y)(xz, yz)$
E_{2g}	2	-1	-1	2	0	0	2	-1	-1	2	0	0	(x^2-y^2, xy)
A_{1u}	1	1	1	1	1	1	-1	-1	-1	-1	-1	-1	
A_{2u}	1	1	1	1	-1	-1	-1	-1	-1	-1	1	1	z
B_{1u}	1	-1	1	-1	1	-1	-1	1	-1	1	-1	1	$x(x^2-3y^2)$
B_{2u}	1	-1	1	-1	-1	1	-1	1	-1	1	1	-1	$y(3x^2-y^2)$
E_{1u}	2	1	-1	-2	0	0	-2	-1	1	2	0	0	(x, y)
E_{2u}	2	-1	-1	2	0	0	-2	1	1	-2	0	0	

D_{8h}	$\hat{E}$	$2\hat{C}_8$	$2\hat{C}_8^3$	$2\hat{C}_4$	$\hat{C}_2$	$4\hat{C}_2'$	$4\hat{C}_2''$	$\hat{\imath}$	$2\hat{S}_8^3$	$2\hat{S}_8$	$2\hat{S}_4$	$\hat{\sigma}_h$	$4\hat{\sigma}_v$	$4\hat{\sigma}_d$
A_{1g}	1	1	1	1	1	1	1	1	1	1	1	1	1	1
A_{2g}	1	1	1	1	1	-1	-1	1	1	1	1	1	-1	-1
B_{1g}	1	-1	-1	1	1	1	-1	1	-1	-1	1	1	1	-1
B_{2g}	1	-1	-1	1	1	-1	1	1	-1	-1	1	1	-1	1
E_{1g}	2	$\sqrt{2}$	$-\sqrt{2}$	0	-2	0	0	2	$\sqrt{2}$	$-\sqrt{2}$	0	-2	0	0
E_{2g}	2	0	0	-2	2	0	0	2	0	0	-2	2	0	0
E_{3g}	2	$-\sqrt{2}$	$\sqrt{2}$	0	-2	0	0	2	$-\sqrt{2}$	$\sqrt{2}$	0	-2	0	0
A_{1u}	1	1	1	1	1	1	1	-1	-1	-1	-1	-1	-1	-1
A_{2u}	1	1	1	1	1	-1	-1	-1	-1	-1	-1	-1	1	1
B_{1u}	1	-1	-1	1	1	1	-1	-1	1	1	-1	-1	-1	1
B_{2u}	1	-1	-1	1	1	-1	1	-1	1	1	-1	-1	1	-1
E_{1u}	2	$\sqrt{2}$	$-\sqrt{2}$	0	-2	0	0	-2	$-\sqrt{2}$	$\sqrt{2}$	0	2	0	0
E_{2u}	2	0	0	-2	2	0	0	-2	0	0	2	-2	0	0
E_{3u}	2	$-\sqrt{2}$	$\sqrt{2}$	0	-2	0	0	-2	$\sqrt{2}$	$-\sqrt{2}$	0	2	0	0

The Antiprismatic Groups D_{nd} ($n = 2, 3, 4, 5, 6$)

D_{2d}	$\hat{E}$	$2\hat{S}_4$	$\hat{C}_2$	$2\hat{C}_2'$	$2\hat{\sigma}_d$		
A_1	1	1	1	1	1		x^2+y^2, z^2
A_2	1	1	1	-1	-1	R_z	
B_1	1	-1	1	1	-1		x^2-y^2
B_2	1	-1	1	-1	1	z	xy
E	2	0	-2	0	0	$(x, y)(R_x, R_y)$	(xz, yz)

D_{3d}	$\hat{E}$	$2\hat{C}_3$	$3\hat{C}_2$	$\hat{\imath}$	$2\hat{S}_6$	$3\hat{\sigma}_d$		
A_{1g}	1	1	1	1	1	1		x^2+y^2, z^2
A_{2g}	1	1	-1	1	1	-1	R_z	
E_g	2	-1	0	2	-1	0	(R_x, R_y)	$(x^2-y^2, xy)(xz, yz)$
A_{1u}	1	1	1	-1	-1	-1		
A_{2u}	1	1	-1	-1	-1	1	z	
E_u	2	-1	0	-2	1	0	(x, y)	

D_{4d}	$\hat{E}$	$2\hat{S}_8$	$2\hat{C}_4$	$2\hat{S}_8^3$	$\hat{C}_2$	$4\hat{C}_2'$	$4\hat{\sigma}_d$		
A_1	1	1	1	1	1	1	1		x^2+y^2, z^2
A_2	1	1	1	1	1	-1	-1	R_z	
B_1	1	-1	1	-1	1	1	-1		
B_2	1	-1	1	-1	1	-1	1	z	
E_1	2	$\sqrt{2}$	0	$-\sqrt{2}$	-2	0	0	(x, y)	
E_2	2	0	-2	0	2	0	0		(x^2-y^2, xy)
E_3	2	$-\sqrt{2}$	0	$\sqrt{2}$	-2	0	0	(R_x, R_y)	(xz, yz)

D_{5d}	$\hat{E}$	$2\hat{C}_5$	$2\hat{C}_5^2$	$5\hat{C}_2$	$\hat{\imath}$	$2\hat{S}_{10}^3$	$2\hat{S}_{10}$	$5\hat{\sigma}_d$	$\alpha=\cos(2\pi/5)$	$\beta=\cos(4\pi/5)$
A_{1g}	1	1	1	1	1	1	1	1		x^2+y^2, z^2
A_{2g}	1	1	1	-1	1	1	1	-1	R_z	
E_{1g}	2	2α	2β	0	2	2α	2β	0	(R_x, R_y)	(xz, yz)
E_{2g}	2	2β	2α	0	2	2β	2α	0		(x^2-y^2, xy)
A_{1u}	1	1	1	1	-1	-1	-1	-1		
A_{2u}	1	1	1	-1	-1	-1	-1	1	z	
E_{1u}	2	2α	2β	0	-2	-2α	-2β	0	(x, y)	
E_{2u}	2	2β	2α	0	-2	-2β	-2α	0		

D_{6d}	$\hat{E}$	$2\hat{S}_{12}$	$2\hat{C}_6$	$2\hat{S}_4$	$2\hat{C}_3$	$2\hat{S}_{12}^5$	$\hat{C}_2$	$6\hat{C}_2'$	$6\hat{\sigma}_d$		
A_1	1	1	1	1	1	1	1	1	1		x^2+y^2, z^2
A_2	1	1	1	1	1	1	1	-1	-1	R_z	
B_1	1	-1	1	-1	1	-1	1	1	-1		
B_2	1	-1	1	-1	1	-1	1	-1	1	z	
E_1	2	$\sqrt{3}$	1	0	-1	$-\sqrt{3}$	-2	0	0	(x, y)	
E_2	2	1	-1	-2	-1	1	2	0	0		(x^2-y^2, xy)
E_3	2	0	-2	0	2	0	-2	0	0		
E_4	2	-1	-1	2	-1	-1	2	0	0		
E_5	2	$-\sqrt{3}$	1	0	-1	$\sqrt{3}$	-2	0	0	(R_x, R_y)	(xz, yz)

The Tetrahedral and Cubic Groups

T	$\hat{E}$	$4\hat{C}_3$	$4\hat{C}_3^2$	$3\hat{C}_2$	$\epsilon = \exp(2\pi i/3)$	
A	1	1	1	1		$x^2 + y^2 + z^2$
$E \left\{ \begin{array}{c} \\ \\ \end{array} \right.$	1	ϵ	$\bar{\epsilon}$	1		$(2z^2 - x^2 - y^2, x^2 - y^2)$
	1	$\bar{\epsilon}$	ϵ	1		
T	3	0	0	-1	$(R_x, R_y, R_z)(x, y, z)$	(xz, yx, xy)

T_d	$\hat{E}$	$8\hat{C}_3$	$3\hat{C}_2$	$6\hat{S}_4$	$6\hat{\sigma}_d$		
A_1	1	1	1	1	1		$x^2 + y^2 + z^2$
A_2	1	1	1	-1	-1		
E	2	-1	2	0	0		$(2z^2 - x^2 - y^2, x^2 - y^2)$
T_1	3	0	-1	1	-1	(R_x, R_y, R_z)	
T_2	3	0	-1	-1	1	(x, y, z)	(xz, yz, xy)

T_h	$\hat{E}$	$4\hat{C}_3$	$4\hat{C}_3^2$	$3\hat{C}_2$	$\hat{i}$	$4\hat{S}_6^5$	$4\hat{S}_6$	$3\hat{\sigma}_h$	$\epsilon = \exp(2\pi i/3)$	
A_g	1	1	1	1	1	1	1	1		$x^2 + y^2 + z^2$
A_u	1	1	1	1	-1	-1	-1	-1		
$E_g \left\{ \begin{array}{c} \\ \\ \end{array} \right.$	1	ϵ	$\bar{\epsilon}$	1	1	ϵ	$\bar{\epsilon}$	1		$(2z^2 - x^2 - y^2,$
	1	$\bar{\epsilon}$	ϵ	1	1	$\bar{\epsilon}$	ϵ	1		$x^2 - y^2)$
$E_u \left\{ \begin{array}{c} \\ \\ \end{array} \right.$	1	ϵ	$\bar{\epsilon}$	1	-1	$-\epsilon$	$-\bar{\epsilon}$	-1		
	1	$\bar{\epsilon}$	ϵ	1	-1	$-\bar{\epsilon}$	$-\epsilon$	-1		
T_g	3	0	0	-1	3	0	0	-1	(R_x, R_y, R_z)	(xz, yz, xy)
T_u	3	0	0	-1	-3	0	0	1	(x, y, z)	

O	$\hat{E}$	$6\hat{C}_4$	$3\hat{C}_2 (= \hat{C}_4^2)$	$8\hat{C}_3$	$6\hat{C}_2$		
A_1	1	1	1	1	1		$x^2 + y^2 + z^2$
A_2	1	-1	1	1	-1		
E	2	0	2	-1	0		$(2z^2 - x^2 - y^2,$
							$x^2 - y^2)$
T_1	3	1	-1	0	-1	$(R_x, R_y, R_z)(x, y, z)$	
T_2	3	-1	-1	0	1		(xz, yz, xy)

O_h	$\hat{E}$	$8\hat{C}_3$	$6\hat{C}_2$	$6\hat{C}_4$	$3\hat{C}_2$	$\hat{\imath}$	$6\hat{S}_4$	$8\hat{S}_6$	$3\hat{\sigma}_h$	$6\hat{\sigma}_d$	
A_{1g}	1	1	1	1	1	1	1	1	1	1	$x^2+y^2+z^2$
A_{2g}	1	1	-1	-1	1	1	-1	1	1	-1	
E_g	2	-1	0	0	2	2	0	-1	2	0	$(2z^2-x^2-y^2,$ $x^2-y^2)$
T_{1g}	3	0	-1	1	-1	3	1	0	-1	-1	(R_x, R_y, R_z)
T_{2g}	3	0	1	-1	-1	3	-1	0	-1	1	(xz, yz, xy)
A_{1u}	1	1	1	1	1	-1	-1	-1	-1	-1	
A_{2u}	1	1	-1	-1	1	-1	1	-1	-1	1	
E_u	2	-1	0	0	2	-2	0	1	-2	0	
T_{1u}	3	0	-1	1	-1	-3	-1	0	1	1	(x, y, z)
T_{2u}	3	0	1	-1	-1	-3	1	0	1	-1	

The Icosahedral Groups

I	$\hat{E}$	$12\hat{C}_5$	$12\hat{C}_5^2$	$20\hat{C}_3$	$15\hat{C}_2$	$\phi=(1+\sqrt{5})/2$	
A	1	1	1	1	1		$x^2+y^2+z^2$
T_1	3	ϕ	$-\phi^{-1}$	0	-1	$(R_x, R_y, R_z)(x, y, z)$	
T_2	3	$-\phi^{-1}$	ϕ	0	-1		
G	4	-1	-1	1	0		
H	5	0	0	-1	1		$(2z^2-x^2-y^2,$ $x^2-y^2,$ (xz, yz, xy)

I_h	$\hat{E}$	$12\hat{C}_5$	$12\hat{C}_5^2$	$20\hat{C}_3$	$15\hat{C}_2$	$\hat{\imath}$	$12\hat{S}_{10}$	$12\hat{S}_{10}^3$	$20\hat{S}_6$	$15\hat{\sigma}$	$\phi=(1+\sqrt{5})/2$
A_g	1	1	1	1	1	1	1	1	1	1	$x^2+y^2+z^2$
T_{1g}	3	ϕ	$-\phi^{-1}$	0	-1	3	$-\phi^{-1}$	ϕ	0	-1	(R_x, R_y, R_z)
T_{2g}	3	$-\phi^{-1}$	ϕ	0	-1	3	ϕ	$-\phi^{-1}$	0	-1	
G_g	4	-1	-1	1	0	4	-1	-1	1	0	
H_g	5	0	0	-1	1	5	0	0	-1	1	$(2z^2-x^2-y^2,$ $x^2-y^2,$ $xz, yz, xy)$
A_u	1	1	1	1	1	-1	-1	-1	-1	-1	
T_{1u}	3	ϕ	$-\phi^{-1}$	0	-1	-3	ϕ^{-1}	$-\phi$	0	1	(x, y, z)
T_{2u}	3	$-\phi^{-1}$	ϕ	0	-1	-3	$-\phi$	ϕ^{-1}	0	1	
G_u	4	-1	-1	1	0	-4	1	1	-1	0	
H_u	5	0	0	-1	1	-5	0	0	1	-1	

A.2 Infinite Groups

Cylindrical Symmetry

C_∞	$\hat{E}$	$\hat{C}_2$	$\hat{C}_\phi$		
Σ	1	1	1	z	$x^2 + y^2, z^2$
$\Pi\ \{$	1	-1	$\exp(i\phi)$	(x, y)	(xz, yz)
	1	-1	$\exp(-i\phi)$		
$\Delta\ \{$	1	1	$\exp(2i\phi)$		$(x^2 - y^2, xy)$
	1	1	$\exp(-2i\phi)$		
$\Phi\ \{$	1	-1	$\exp(3i\phi)$		$[x(x^2 - 3y^2), y(3x^2 - y^2)]$
	1	-1	$\exp(-3i\phi)$		

$C_{\infty v}$	$\hat{E}$	$\hat{C}_2$	$2\hat{C}_\phi$	$\infty\hat{\sigma}_v$		
Σ^+	1	1	1	1	z	$x^2 + y^2, z^2$
Σ^-	1	1	1	-1	R_z	
Π	2	-2	$2\cos(\phi)$	0	$(x, y)(R_x, R_y)$	(xz, yz)
Δ	2	2	$2\cos(2\phi)$	0		$(x^2 - y^2, xy)$
Φ	2	-2	$2\cos(3\phi)$	0		

$C_{\infty h}$	$\hat{E}$	$\hat{C}_2$	$\hat{C}_\phi$	$\hat{i}$	$\hat{S}_\phi$	$\hat{\sigma}_h$		
Σ_g	1	1	1	1	1	1		$x^2 + y^2, z^2$
$\Pi_g\ \{$	1	-1	$\exp(i\phi)$	1	$-\exp(i\phi)$	-1		(xz, yz)
	1	-1	$\exp(-i\phi)$	1	$-\exp(-i\phi)$	-1		
$\Delta_g\ \{$	1	1	$\exp(2i\phi)$	1	$\exp(2i\phi)$	1		$(x^2 - y^2, xy)$
	1	1	$\exp(-2i\phi)$	1	$\exp(-2i\phi)$	1		
$\Phi_g\ \{$	1	-1	$\exp(3i\phi)$	1	$-\exp(3i\phi)$	-1		
	1	-1	$\exp(-3i\phi)$	1	$-\exp(-3i\phi)$	-1		
Σ_u	1	1	1	-1	-1	-1	z	z^3
$\Pi_u\ \{$	1	-1	$\exp(i\phi)$	-1	$\exp(i\phi)$	1	(x, y)	(xz^2, yz^2)
	1	-1	$\exp(-i\phi)$	-1	$\exp(-i\phi)$	1		
$\Delta_u\ \{$	1	1	$\exp(2i\phi)$	-1	$-\exp(2i\phi)$	-1		$((x^2 - y^2)z,$
	1	1	$\exp(-2i\phi)$	-1	$-\exp(-2i\phi)$	-1		$xyz)$
$\Phi_u\ \{$	1	-1	$\exp(3i\phi)$	-1	$\exp(3i\phi)$	1		
	1	-1	$\exp(-3i\phi)$	-1	$\exp(-3i\phi)$	1		

$D_{\infty h}$	$\hat{E}$	$\hat{C}_2^z$	$2\hat{C}_\phi$	$\infty\hat{\sigma}_v$	$\hat{\imath}$	$2\hat{S}_\phi$	$\infty\hat{C}_2^\perp$		
Σ_g^+	1	1	1	1	1	1	1		x^2+y^2, z^2
Σ_g^-	1	1	1	-1	1	1	-1	R_z	
Π_g	2	-2	$2\cos(\phi)$	0	2	$-2\cos(\phi)$	0	(R_x, R_y)	(xz, yz)
Δ_g	2	2	$2\cos(2\phi)$	0	2	$2\cos(2\phi)$	0		(x^2-y^2, xy)
Φ_g	2	-2	$2\cos(3\phi)$	0	2	$-2\cos(3\phi)$	0		
$\cdots$									
Σ_u^+	1	1	1	1	-1	-1	-1	z	
Σ_u^-	1	1	1	-1	-1	-1	1		
Π_u	2	-2	$2\cos(\phi)$	0	-2	$2\cos(\phi)$	0	(x, y)	
Δ_u	2	2	$2\cos(2\phi)$	0	-2	$-2\cos(2\phi)$	0		
Φ_u	2	-2	$2\cos(3\phi)$	0	-2	$2\cos(3\phi)$	0		

Spherical Symmetry

$SO(3)$	$\hat{E}$	$\infty\hat{C}_\alpha^{\phi\theta}$		
S	1	1		$x^2+y^2+z^2$
P	3	$1+2\cos\alpha$	$(x, y, z)(R_x, R_y, R_z)$	
D	5	$1+2\cos\alpha+2\cos 2\alpha$		$(2z^2-x^2-y^2,$ $x^2-y^2, xz, yz, xy)$
$\cdots$				
L	$2L+1$	$\dfrac{\sin(L+\frac{1}{2})\alpha}{\sin\frac{1}{2}\alpha}$		

$O(3)$	$\hat{E}$	$\infty\hat{C}_\alpha^{\phi\theta}$	$\hat{\imath}$	$\infty\hat{\sigma}$	$\infty\hat{S}_\alpha^{\theta,\phi}$	
S_g	1	1	1	1	1	$x^2+y^2+z^2$
P_g	3	$1+2\cos\alpha$	3	-1	$1-2\cos\alpha$	(R_x, R_y, R_z)
D_g	5	$1+2\cos\alpha$ $+2\cos 2\alpha$	5	1	$1-2\cos\alpha$ $+2\cos 2\alpha$	d-orbitals
L_g	$2L+1$	$\dfrac{\sin(L+\frac{1}{2})\alpha}{\sin\frac{1}{2}\alpha}$	$2L+1$	$(-1)^L$	$\dfrac{(-1)^L\cos(L+\frac{1}{2})\alpha}{\cos\frac{1}{2}\alpha}$	
$\cdots$						
S_u	1	1	-1	-1	-1	
P_u	3	$1+2\cos\alpha$	-3	1	$-1+2\cos\alpha$	p-orbitals
D_u	5	$1+2\cos\alpha$ $+2\cos 2\alpha$	-5	-1	$-1+2\cos\alpha$ $-2\cos 2\alpha$	
L_u	$2L+1$	$\dfrac{\sin(L+\frac{1}{2})\alpha}{\sin\frac{1}{2}\alpha}$	$-(2L+1)$	$(-1)^{L+1}$	$\dfrac{(-1)^{L+1}\cos(L+\frac{1}{2})\alpha}{\cos\frac{1}{2}\alpha}$	

Appendix B
Symmetry Breaking by Uniform Linear Electric and Magnetic Fields

Contents

B.1 Spherical Groups

G	B	E
T	C_3, C_2, C_1	C_3, C_2, C_1
T_d	S_4, C_3, C_2, C_s, C_1	C_{3v}, C_{2v}, C_s, C_1
T_h	S_6, C_{2h}, C_i	C_3, C_2, C_s, C_1
O	C_4, C_3, C_2, C_1	C_4, C_3, C_2, C_1
O_h	C_{4h}, S_6, C_{2h}, C_i	$C_{4v}, C_{3v}, C_{2v}, C_s, C_1$
I	C_5, C_3, C_2, C_1	C_5, C_3, C_2, C_1
I_h	S_{10}, S_6, C_{2h}, C_i	$C_{5v}, C_{3v}, C_{2v}, C_s, C_1$

B.2 Binary and Cylindrical Groups

The $\parallel$ notation refers to a field oriented along the principal cylindrical axis; in the $\perp$ direction several symmetry breakings are possible: C_2 symmetry implies that the field coincides with the $\hat{C}_2$ axis; a magnetic field perpendicular to a symmetry plane or an electric field in a symmetry plane will conserve at least C_s symmetry.

G	B		E	
	$\parallel$	$\perp$	$\parallel$	$\perp$
C_i	C_i		C_1	
C_s	C_1	C_s	C_s	C_1
C_2	C_2	C_1	C_2	C_1
C_n	C_n	C_1	C_n	C_1
D_n	C_n	C_2, C_1	C_n	C_2, C_1
C_{nv}	C_n	C_s, C_1	C_{nv}	C_s, C_1
C_{2nh}	C_{2nh}	C_i	C_{2n}	C_s
$C_{(2n+1)h}$	$C_{(2n+1)h}$	C_1	C_{2n+1}	C_s
S_{4n}	S_{4n}	C_1	C_{2n}	C_1
S_{4n+2}	S_{4n+2}	C_i	C_{2n+1}	C_1
D_{2nh}	C_{2nh}	C_{2h}, C_i	C_{2nv}	C_{2v}, C_s
$D_{(2n+1)h}$	$C_{(2n+1)h}$	C_2, C_s, C_1	$C_{(2n+1)v}$	C_2, C_s
D_{2nd}	S_{4n}	C_2, C_s, C_1	C_{2nv}	C_2, C_s, C_1
$D_{(2n+1)d}$	S_{4n+2}	C_{2h}, C_i	$C_{(2n+1)v}$	C_2, C_s, C_1

Appendix C
Subduction and Induction

Contents

C.1   Subduction $G \downarrow H$

C_{6v}	C_6	C_{3v}^{v} $2\hat{C}_3, 3\hat{\sigma}_v$	C_{3v}^{d} $2\hat{C}_3, 3\hat{\sigma}_d$	C_{2v}
A_1	A	A_1	A_1	A_1
A_2	A	A_2	A_2	A_2
B_1	B	A_1	A_2	B_1
B_2	B	A_2	A_1	B_2
E_1	E_1	E	E	$B_1 + B_2$
E_2	E_2	E	E	$A_1 + A_2$

D_{4h}	D_{2d}	C_{4h}	C_{2v}^{zv}	C_{2v}^{zd}	C_{2v}'	C_{2v}''
	$\hat{C}_2^z, 2\hat{C}_2', 2\hat{\sigma}_d$		$\hat{C}_2^z, 2\hat{\sigma}_v$	$\hat{C}_2^z, 2\hat{\sigma}_d$	$\hat{C}_2', \hat{\sigma}_h, \hat{\sigma}_v$	$\hat{C}_2'', \hat{\sigma}_h, \hat{\sigma}_d$
A_{1g}	A_1	A_g	A_1	A_1	A_1	A_1
A_{2g}	A_2	A_g	A_2	A_2	B_1	B_1
B_{1g}	B_1	B_g	A_1	A_2	A_1	B_1
B_{2g}	B_2	B_g	A_2	A_1	B_1	A_1
E_g	E	E	$B_1 + B_2$	$B_1 + B_2$	$A_2 + B_2$	$A_2 + B_2$
A_{1u}	B_1	A_u	A_2	A_2	A_2	A_2
A_{2u}	B_2	A_u	A_1	A_1	B_2	B_2
B_{1u}	A_1	B_u	A_2	A_1	A_2	B_2
B_{2u}	A_2	B_u	A_1	A_2	B_2	A_2
E_u	E	E	$B_1 + B_2$	$B_1 + B_2$	$A_1 + B_1$	$A_1 + B_1$

D_{3d}		S_6		C_{3v}		C_{2h}
A_{1g}		A_g		A_1		A_g
A_{2g}		A_g		A_2		B_g
E_g		E_g		E		$A_g + B_g$
A_{1u}		A_u		A_2		A_u
A_{2u}		A_u		A_1		B_u
E_u		E_u		E		$A_u + B_u$

T_d	D_{2d}	C_{3v}	D_2	C_{2v}	S_4
A_1	A_1	A_1	A	A_1	A
A_2	B_1	A_2	A	A_2	B
E	$A_1 + B_1$	E	$2A$	$A_1 + A_2$	$A + B$
T_1	$A_2 + E$	$A_2 + E$	$B_1 + B_2 + B_3$	$A_2 + B_1 + B_2$	$A + E$
T_2	$B_2 + E$	$A_1 + E$	$B_1 + B_2 + B_3$	$A_1 + B_1 + B_2$	$B + E$

T_h	D_{2h}		S_6	C_{2v}		C_{2h}
A_g	A_g		A_g	A_1		A_g
A_u	A_u		A_u	A_2		A_u
E_g	$2A_g$		E_g	$2A_1$		$2A_g$
E_u	$2A_u$		E_u	$2A_2$		$2A_u$
T_g	$B_{1g} + B_{2g} + B_{3g}$		$A_g + E_g$	$A_2 + B_1 + B_2$		$A_g + 2B_g$
T_u	$B_{1u} + B_{2u} + B_{3u}$		$A_u + E_u$	$A_1 + B_1 + B_2$		$A_u + 2B_u$

O_h	T_d	D_{4h}	D_{3d}	T_h	D_{2h}^z	D'_{2h}
A_{1g}	A_1	A_{1g}	A_{1g}	A_g	A_g	A_g
A_{2g}	A_2	B_{1g}	A_{2g}	A_g	A_g	B_{1g}
E_g	E	$A_{1g}+B_{1g}$	E_g	E_g	$2A_g$	A_g+B_{1g}
T_{1g}	T_1	$A_{2g}+E_g$	$A_{2g}+E_g$	T_g	$B_{1g}+B_{2g}+B_{3g}$	$B_{1g}+B_{2g}+B_{3g}$
T_{2g}	T_2	$B_{2g}+E_g$	$A_{1g}+E_g$	T_g	$B_{1g}+B_{2g}+B_{3g}$	$A_g+B_{2g}+B_{3g}$
A_{1u}	A_2	A_{1u}	A_{1u}	A_u	A_u	A_u
A_{2u}	A_1	B_{1u}	A_{2u}	A_u	A_u	B_{1u}
E_u	E	$A_{1u}+B_{1u}$	E_u	E_u	$2A_u$	A_u+B_{1u}
T_{1u}	T_2	$A_{2u}+E_u$	$A_{2u}+E_u$	T_u	$B_{1u}+B_{2u}+B_{3u}$	$B_{1u}+B_{2u}+B_{3u}$
T_{2u}	T_1	$B_{2u}+E_u$	$A_{1u}+E_u$	T_u	$B_{1u}+B_{2u}+B_{3u}$	$A_u+B_{2u}+B_{3u}$

I_h	T_h	D_{5d}	D_{3d}	D_{2h}	C_{2v}
A_g	A_g	A_{1g}	A_{1g}	A_g	A_1
T_{1g}	T_g	$A_{2g}+E_{1g}$	$A_{2g}+E_g$	$B_{1g}+B_{2g}+B_{3g}$	$A_2+B_1+B_2$
T_{2g}	T_g	$A_{2g}+E_{2g}$	$A_{2g}+E_g$	$B_{1g}+B_{2g}+B_{3g}$	$A_2+B_1+B_2$
G_g	A_g+T_g	$E_{1g}+E_{2g}$	$A_{1g}+A_{2g}+E_g$	$A_g+B_{1g}+B_{2g}+B_{3g}$	$A_1+A_2+B_1+B_2$
H_g	E_g+T_g	$A_{1g}+E_{1g}+E_{2g}$	$A_{1g}+2E_g$	$2A_g+B_{1g}+B_{2g}+B_{3g}$	$2A_1+A_2+B_1+B_2$
A_u	A_u	A_{1u}	A_{1u}	A_u	A_2
T_{1u}	T_u	$A_{2u}+E_{1u}$	$A_{2u}+E_u$	$B_{1u}+B_{2u}+B_{3u}$	$A_1+B_1+B_2$
T_{2u}	T_u	$A_{2u}+E_{2u}$	$A_{2u}+E_u$	$B_{1u}+B_{2u}+B_{3u}$	$A_1+B_1+B_2$
G_u	A_u+T_u	$E_{1u}+E_{2u}$	$A_{1u}+A_{2u}+E_u$	$A_u+B_{1u}+B_{2u}+B_{3u}$	$A_1+A_2+B_1+B_2$
H_u	E_u+T_u	$A_{1u}+E_{1u}+E_{2u}$	$A_{1u}+2E_u$	$2A_u+B_{1u}+B_{2u}+B_{3u}$	$A_1+2A_2+B_1+B_2$

$SO(3)$	I	O
ℓ		
0 (S)	A	A_1
1 (P)	T_1	T_1
2 (D)	H	$E + T_2$
3 (F)	$T_2 + G$	$A_2 + T_1 + T_2$
4 (G)	$G + H$	$A_1 + E + T_1 + T_2$
5	$T_1 + T_2 + H$	$E + 2T_1 + T_2$
6	$A + T_1 + G + H$	$A_1 + A_2 + E + T_1 + 2T_2$
7	$T_1 + T_2 + G + H$	$A_2 + E + 2T_1 + 2T_2$
8	$T_2 + G + 2H$	$A_1 + 2E + 2T_1 + 2T_2$
9	$T_1 + T_2 + 2G + H$	$A_1 + A_2 + E + 3T_1 + 2T_2$
10	$A + T_1 + T_2 + G + 2H$	$A_1 + A_2 + 2E + 2T_1 + 3T_2$
11	$2T_1 + T_2 + G + 2H$	$A_2 + 2E + 3T_1 + 3T_2$
12	$A + T_1 + T_2 + 2G + 2H$	$A_1 + \Gamma_{reg}$

C.2 Induction: $H \uparrow G$

Ascent in symmetry tables have been provided by Boyle [4]. Fowler and Quinn have listed the irreps that are induced by σ-, π-, and δ-type orbitals on molecular sites [5]. These tables are reproduced below. They are useful for the construction of cluster orbitals. Γ_{reg} always denotes the regular representation. Γ_{σ} corresponds to the positional representation. The mechanical representation is the sum $\Gamma_{\sigma} + \Gamma_{\pi}$.

G	H	$\frac{G}{H}$	Γ_{σ}	Γ_{π}	Γ_{δ}
D_2	C_2^z	2	$A + B_1$	$2B_2 + 2B_3$	$2\Gamma_{\sigma}$
D_3	C_2	3	$A_1 + E$	$2A_2 + 2E$	$2\Gamma_{\sigma}$
D_4	C_4	2	$A_1 + A_2$	$2E$	$2B_1 + 2B_2$
	C_2'	4	$A_1 + B_1 + E$	$2A_2 + 2B_2 + 2E$	$2\Gamma_{\sigma}$
	C_2''	4	$A_2 + B_2 + E$	$2A_2 + 2B_1 + 2E$	$2\Gamma_{\sigma}$
D_5	C_5	2	$A_1 + A_2$	$2E_1$	$2E_2$
	C_2	4	$A_1 + E_1 + E_2$	$2A_2 + 2E_1 + 2E_2$	$2\Gamma_{\sigma}$
D_6	C_6	6	$A_1 + A_2$	$2E_1$	$2E_2$
	C_2'	4	$A_1 + B_1 + E_1 + E_2$	$2A_2 + 2B_2 + 2E_1 + 2E_2$	$2\Gamma_{\sigma}$
	C_2''	4	$A_1 + B_2 + E_1 + E_2$	$2A_2 + 2B_1 + 2E_1 + 2E_2$	$2\Gamma_{\sigma}$
C_{2v}	C_s^{xz}	2	$A_1 + B_1$	Γ_{reg}	Γ_{reg}
C_{3v}	C_s	3	$A_1 + E$	Γ_{reg}	Γ_{reg}
C_{4v}	C_s^v	4	$A_1 + B_1 + E$	Γ_{reg}	Γ_{reg}
	C_s^d	4	$A_1 + B_2 + E$	Γ_{reg}	Γ_{reg}
C_{5v}	C_s	5	$A_1 + E_1 + E_2$	Γ_{reg}	Γ_{reg}
C_{6v}	C_s^v	6	$A_1 + B_1 + E_1 + E_2$	Γ_{reg}	Γ_{reg}
	C_s^d	6	$A_1 + B_2 + E_1 + E_2$	Γ_{reg}	Γ_{reg}
C_{2h}	C_2	2	$A_g + A_u$	$2B_g + 2B_u$	$2\Gamma_{\sigma}$
	C_s	2	$A_g + B_u$	Γ_{reg}	Γ_{reg}
C_{3h}	C_3	2	$A' + A''$	$E' + E''$	$E' + E''$
	C_s	3	$A' + E'$	Γ_{reg}	Γ_{reg}
C_{4h}	C_4	2	$A_g + A_u$	$E_g + E_u$	$2B_g + 2B_u$
	C_s	4	$A_g + B_g + E_u$	Γ_{reg}	Γ_{reg}
C_{5h}	C_5	2	$A' + A''$	$E_1' + E_1''$	$E_2' + E_2''$
	C_s	5	$A' + E_1' + E_2'$	Γ_{reg}	Γ_{reg}
C_{6h}	C_6	2	$A_g + A_u$	$E_{1g} + E_{1u}$	$E_{2g} + E_{2u}$
	C_s	6	$A_g + B_u + E_{2g} + E_{1u}$	Γ_{reg}	Γ_{reg}
S_4	C_2	2	$A + B$	$2E$	$2\Gamma_{\sigma}$
S_6	C_3	2	$A_g + A_u$	$E_g + E_u$	$E_g + E_u$

G	H	$\frac{\lvert G\rvert}{\lvert H\rvert}$	Γ_σ	Γ_π	Γ_δ
D_{2h}	C_{2v}^{z}	2	$A_g + B_{1u}$	$B_{2g} + B_{2u} + B_{3g}$ $+ B_{3u}$	$A_g + A_u + B_{1g}$ $+ B_{1u}$
	C_s^{xy}	4	$A_g + B_{1g} + B_{2u}$ $+ B_{3u}$	Γ_{reg}	Γ_{reg}
D_{3h}	C_{3v}	2	$A_1' + A_2''$	$E' + E''$	$E' + E''$
	C_{2v}	3	$A_1' + E'$	$A_1' + A_2'' + E' + E''$	$A_1' + A_1'' + E' + E''$
	C_s^{v}	6	$A_1' + A_2'' + E' + E''$	Γ_{reg}	Γ_{reg}
D_{4h}	C_{4v}	2	$A_{1g} + A_{2u}$	$E_g + E_u$	$B_{1g} + B_{1u} + B_{2g}$ $+ B_{2u}$
	C_{2v}'	4	$A_{1g} + B_{1g} + E_u$	$A_{2g} + A_{2u} + B_{2g}$ $+ B_{2u} + E_g + E_u$	$A_{1g} + A_{1u} + B_{1g}$ $+ B_{1u} + E_g + E_u$
	C_{2v}''	4	$A_{1g} + B_{2g} + E_u$	$A_{2g} + A_{2u} + B_{1g}$ $+ B_{1u} + E_g + E_u$	$A_{1g} + A_{1u} + B_{2g}$ $+ B_{2u} + E_g + E_u$
	C_s^{h}	8	$A_{1g} + A_{2g} + B_{1g}$ $+ B_{2g} + 2E_u$	Γ_{reg}	Γ_{reg}
	C_s^{v}	8	$A_{1g} + A_{2u} + B_{1g}$ $+ B_{2u} + E_g + E_u$	Γ_{reg}	Γ_{reg}
	C_s^{d}	8	$A_{1g} + A_{2u} + B_{1u}$ $+ B_{2g} + E_g + E_u$	Γ_{reg}	Γ_{reg}
D_{5h}	C_{5v}	2	$A_1' + A_2''$	$E_1' + E_1''$	$E_2' + E_2''$
	C_{2v}	5	$A_1' + E_1' + E_2'$	$A_2' + A_2'' + E_1' + E_1''$ $+ E_2' + E_2''$	$A_1' + A_1'' + E_1' + E_1''$ $+ E_2' + E_2''$
	C_s^{h}	10	$A_1' + A_2' + 2E_1' + 2E_2'$	Γ_{reg}	Γ_{reg}
	C_s^{v}	10	$A_1' + A_2'' + E_1' + E_1''$ $+ E_2' + E_2''$	Γ_{reg}	Γ_{reg}
D_{6h}	C_{6v}	2	$A_{1g} + A_{2u}$	$E_{1g} + E_{1u}$	$E_{2g} + E_{2u}$
	C_{2v}'	6	$A_{1g} + B_{1u} + E_{1u}$ $+ E_{2g}$	$A_{2g} + A_{2u} + B_{2g}$ $+ B_{2u} + E_{1g} + E_{1u}$ $+ E_{2g} + E_{2u}$	$A_{1g} + A_{1u} + B_{1g}$ $+ B_{1u} + E_{1g}$ $+ E_{1u} + E_{2g} + E_{2u}$
	C_{2v}''	6	$A_{1g} + B_{2u} + E_{1u}$ $+ E_{2g}$	$A_{2g} + A_{2u} + B_{1g}$ $+ B_{1u} + E_{1g} + E_{1u}$ $+ E_{2g} + E_{2u}$	$A_{1g} + A_{1u} + B_{2g}$ $+ B_{2u} + E_{1g}$ $+ E_{1u} + E_{2g} + E_{2u}$
	C_s^{h}	12	$A_{1g} + A_{2g} + B_{1u}$ $+ B_{2u} + 2E_{1u} + 2E_{2g}$	Γ_{reg}	Γ_{reg}
	C_s^{v}	12	$A_{1g} + A_{2u} + B_{1g}$ $+ B_{2u} + E_{1g} + E_{1u}$ $+ E_{2g} + E_{2u}$	Γ_{reg}	Γ_{reg}
	C_s^{d}	12	$A_{1g} + A_{2u} + B_{1g}$ $+ B_{2u} + E_{1g} + E_{1u}$ $+ E_{2g} + E_{2u}$	Γ_{reg}	Γ_{reg}

G	H	$\frac{|G|}{|H|}$	Γ_σ	Γ_π	Γ_δ
D_{2d}	C_{2v}^z	2	$A_1 + B_2$	$2E$	$A_1 + A_2 + B_1 + B_2$
	C_2'	4	$A_1 + B_1 + E$	$2A_2 + 2B_2 + 2E$	$2\Gamma_\sigma$
	C_s	4	$A_1 + B_2 + E$	Γ_{reg}	Γ_{reg}
D_{3d}	C_{3v}	2	$A_{1g} + A_{2u}$	$E_g + E_u$	$E_g + E_u$
	C_2	6	$A_{1g} + A_{1u} + E_g + E_u$	$2A_{2g} + 2A_{2u}$ $+ 2E_g + 2E_u$	$2\Gamma_\sigma$
	C_s	6	$A_{1g} + A_{2u} + E_g + E_u$	Γ_{reg}	Γ_{reg}
D_{4d}	C_{4v}	2	$A_1 + B_2$	$E_1 + E_3$	$2E_2$
	C_2'	8	$A_1 + B_1 + E_1 + E_2$ $+ E_3$	$2A_2 + 2B_2 + 2E_1$ $+ 2E_2 + 2E_3$	$2\Gamma_\sigma$
	C_s	8	$A_1 + B_2 + E_1 + E_2$ $+ E_3$	Γ_{reg}	Γ_{reg}
D_{5d}	C_{5v}	2	$A_{1g} + A_{2u}$	$E_{1g} + E_{1u}$	$E_{2g} + E_{2u}$
	C_2	10	$A_{1g} + A_{1u} + E_{1g}$ $+ E_{1u} + E_{2g} + E_{2u}$	$2A_{2g} + 2A_{2u} + 2E_{1g}$ $+ 2E_{1u} + 2E_{2g}$ $+ 2E_{2u}$	$2\Gamma_\sigma$
	C_s	10	$A_{1g} + A_{2u} + E_{1g}$ $+ E_{1u} + E_{2g} + E_{2u}$	Γ_{reg}	Γ_{reg}
D_{6d}	C_{6v}	2	$A_1 + B_2$	$E_1 + E_5$	$E_2 + E_4$
	C_2'	12	$A_1 + B_1 + E_1 + E_2$ $+ E_3 + E_4 + E_5$	$2A_2 + 2B_2 + 2E_1$ $+ 2E_2 + 2E_3$ $+ 2E_4 + 2E_5$	$2\Gamma_\sigma$
	C_s	12	$A_1 + B_2 + E_1 + E_2$ $+ E_3 + E_4 + E_5$	Γ_{reg}	Γ_{reg}
T	C_3	4	$A + T$	$E + 2T$	Γ_π
	C_2	6	$A + E + T$	$4T$	$2\Gamma_\sigma$
T_d	C_{3v}	4	$A_1 + T_2$	$E + T_1 + T_2$	Γ_π
	C_{2v}	6	$A_1 + E + T_2$	$2T_1 + 2T_2$	$A_1 + A_2 + 2E$ $+ T_1 + T_2$
	C_s	12	$A_1 + E + T_1 + 2T_2$	Γ_{reg}	Γ_{reg}
T_h	C_3	8	$A_g + A_u + T_g + T_u$	$E_g + E_u + 2T_g + 2T_u$	Γ_π
	C_{2v}	6	$A_g + E_g + T_u$	$2T_g + 2T_u$	$A_g + A_u + E_g$ $+ E_u + T_g + T_u$
	C_s	12	$A_g + E_g + T_g + 2T_u$	Γ_{reg}	Γ_{reg}
O	C_4	6	$A_1 + E + T_1$	$2T_1 + 2T_2$	$2A_2 + 2E + 2T_2$
	C_3	8	$A_1 + A_2 + T_1 + T_2$	$2E + 2T_1 + 2T_2$	Γ_π
	C_2	12	$A_1 + E + T_1 + 2T_2$	$2A_2 + 2E + 4T_1 + 2T_2$	$2\Gamma_\sigma$

G	H	$\frac{\lvert G\rvert}{\lvert H\rvert}$	Γ_σ	Γ_π	Γ_δ
O_h	C_{4v}	6	$A_{1g} + E_g + T_{1u}$	$T_{1g} + T_{1u} + T_{2g} + T_{2u}$	$A_{2g} + A_{2u} + E_g$ $+ E_u + T_{2g} + T_{2u}$
	C_{3v}	8	$A_{1g} + A_{2u} + T_{1u}$ $+ T_{2g}$	$E_g + E_u + T_{1g} + T_{1u}$ $+ T_{2g} + T_{2u}$	Γ_π
	C_{2v}	12	$A_{1g} + E_g + T_{1u}$ $+ T_{2g} + T_{2u}$	$A_{2g} + A_{2u} + E_g + E_u$ $+ 2T_{1g} + 2T_{1u}$ $+ T_{2g} + T_{2u}$	$A_{1g} + A_{1u} + E_g$ $+ E_u + T_{1g} + T_{1u}$ $+ 2T_{2g} + 2T_{2u}$
	C_s^h	24	$A_{1g} + A_{2g} + 2E_g$ $+ T_{1g} + 2T_{1u} + T_{2g}$ $+ 2T_{2u}$	Γ_{reg}	Γ_{reg}
	C_s^d	24	$A_{1g} + A_{2u} + E_g$ $+ E_u + T_{1g} + 2T_{1u}$ $+ 2T_{2g} + T_{2u}$	Γ_{reg}	Γ_{reg}
I	C_5	12	$A + T_1 + T_2 + H$	$2T_1 + 2G + 2H$	$2T_2 + 2G + 2H$
	C_3	20	$A + T_1 + T_2$ $+ 2G + H$	$2T_1 + 2T_2 + 2G$ $+ 4H$	Γ_π
	C_2	30	$A + T_1 + T_2$ $+ 2G + 3H$	$4T_1 + 4T_2 + 4G$ $+ 4H$	$2\Gamma_\sigma$
I_h	C_{5v}	12	$A_g + T_{1u} + T_{2u} + H_g$	$T_{1g} + T_{1u} + G_g$ $+ G_u + H_g + H_u$	$T_{2g} + T_{2u} + G_g$ $+ G_u + H_g + H_u$
	C_{3v}	20	$A_g + T_{1u} + T_{2u}$ $+ G_g + G_u + H_g$	$T_{1g} + T_{1u} + T_{2g}$ $+ T_{2u} + G_g + G_u$ $+ 2H_g + 2H_u$	Γ_π
	C_{2v}	30	$A_g + T_{1u} + T_{2u} + G_g$ $+ G_u + 2H_g + H_u$	$2T_{1g} + 2T_{1u} + 2T_{2g}$ $+ 2T_{2u} + 2G_g$ $+ 2G_u + 2H_g$ $+ 2H_u$	$A_g + A_u + T_{1g} + T_{1u}$ $+ T_{2g} + T_{2u} + 2G_g$ $+ 2G_u + 3H_g + 3H_u$
	C_s	60	$A_g + T_{1g} + 2T_{1u}$ $+ T_{2g} + 2T_{2u} + 2G_g$ $+ 2G_u + 3H_g + 2H_u$	Γ_{reg}	Γ_{reg}

Appendix D
Canonical-Basis Relationships

The importance of canonical-basis relationships was demonstrated by Griffith in his monumental work on the theory of transition-metal ions [6]. The icosahedral basis sets were defined by Boyle and Parker [7].

| D_3	$\mathbb{D}(C_3^z)$	$\mathbb{D}(C_2^x)$
$\lvert E_x\rangle, \lvert E_y\rangle$	$\begin{pmatrix} -\frac{1}{2} & -\frac{\sqrt{3}}{2} \\ +\frac{\sqrt{3}}{2} & -\frac{1}{2} \end{pmatrix}$	$\begin{pmatrix} 1 & 0 \\ 0 & -1 \end{pmatrix}$

D_4	$\mathbb{D}(C_4^z)$	$\mathbb{D}(C_2^x)$
$\lvert E_x\rangle, \lvert E_y\rangle$	$\begin{pmatrix} 0 & -1 \\ 1 & 0 \end{pmatrix}$	$\begin{pmatrix} 1 & 0 \\ 0 & -1 \end{pmatrix}$

D_5	$\mathbb{D}(C_5^z)$	$\mathbb{D}(C_2^x)$
$\lvert E_{1x}\rangle, \lvert E_{1y}\rangle$	$\begin{pmatrix} \cos(2\pi/5) & -\sin(2\pi/5) \\ \sin(2\pi/5) & \cos(2\pi/5) \end{pmatrix}$	$\begin{pmatrix} 1 & 0 \\ 0 & -1 \end{pmatrix}$
$\lvert E_{2x}\rangle, \lvert E_{2y}\rangle$	$\begin{pmatrix} \cos(4\pi/5) & -\sin(4\pi/5) \\ \sin(4\pi/5) & \cos(4\pi/5) \end{pmatrix}$	$\begin{pmatrix} 1 & 0 \\ 0 & -1 \end{pmatrix}$

D_6	$\mathbb{D}(C_6^z)$	$\mathbb{D}(C_2^x)$
$\lvert E_{1x}\rangle, \lvert E_{1y}\rangle$	$\begin{pmatrix} \frac{1}{2} & -\frac{\sqrt{3}}{2} \\ +\frac{\sqrt{3}}{2} & \frac{1}{2} \end{pmatrix}$	$\begin{pmatrix} 1 & 0 \\ 0 & -1 \end{pmatrix}$
$\lvert E_{2x}\rangle, \lvert E_{2y}\rangle$	$\begin{pmatrix} -\frac{1}{2} & -\frac{\sqrt{3}}{2} \\ +\frac{\sqrt{3}}{2} & -\frac{1}{2} \end{pmatrix}$	$\begin{pmatrix} 1 & 0 \\ 0 & -1 \end{pmatrix}$
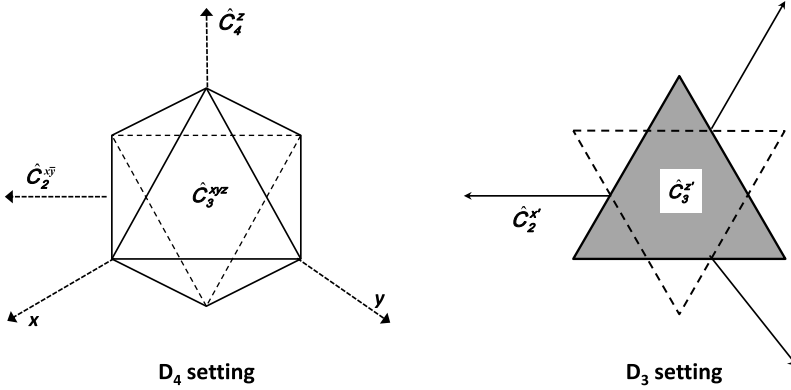
Fig. D.1 Octahedron with x, y, z coordinates in D_4 and D_3 setting

O (D_4 basis)	$\mathbb{D}(C_4^z)$	$\mathbb{D}(C_3^{xyz})$
$\lvert E_\theta\rangle, \lvert E_\epsilon\rangle$	$\begin{pmatrix} 1 & 0 \\ 0 & -1 \end{pmatrix}$	$\begin{pmatrix} -\frac{1}{2} & -\frac{\sqrt{3}}{2} \\ +\frac{\sqrt{3}}{2} & -\frac{1}{2} \end{pmatrix}$
$\lvert T_{1x}\rangle, \lvert T_{1y}\rangle, \lvert T_{1z}\rangle$	$\begin{pmatrix} 0 & -1 & 0 \\ 1 & 0 & 0 \\ 0 & 0 & 1 \end{pmatrix}$	$\begin{pmatrix} 0 & 0 & 1 \\ 1 & 0 & 0 \\ 0 & 1 & 0 \end{pmatrix}$
$\lvert T_{2\xi}\rangle, \lvert T_{2\eta}\rangle, \lvert T_{2\zeta}\rangle$	$\begin{pmatrix} 0 & 1 & 0 \\ -1 & 0 & 0 \\ 0 & 0 & -1 \end{pmatrix}$	$\begin{pmatrix} 0 & 0 & 1 \\ 1 & 0 & 0 \\ 0 & 1 & 0 \end{pmatrix}$

(See Fig. D.1.) Transformation to trigonal basis set:

$$\lvert E_\theta\rangle = d_{z^2} = \frac{1}{\sqrt{3}}(-d_{x'^2-y'^2} - \sqrt{2}d_{y'z'})$$

$$\lvert E_\epsilon\rangle = d_{x^2-y^2} = \frac{1}{\sqrt{3}}(d_{x'y'} + \sqrt{2}d_{x'z'})$$

$$\lvert T_{1a}\rangle = \frac{1}{\sqrt{3}}\big(\lvert T_{1x}\rangle + \lvert T_{1y}\rangle + \lvert T_{1z}\rangle\big) = p_{z'}$$

$$\lvert T_{1\theta}\rangle = \frac{1}{\sqrt{2}}\big(\lvert T_{1x}\rangle - \lvert T_{1y}\rangle\big) = p_{x'}$$

$$\lvert T_{1\epsilon}\rangle = \frac{1}{\sqrt{6}}\big(\lvert T_{1x}\rangle + \lvert T_{1y}\rangle - 2\lvert T_{1z}\rangle\big) = p_{y'}$$

Fig. D.2 Icosahedron with x, y, z coordinates in D_2 setting
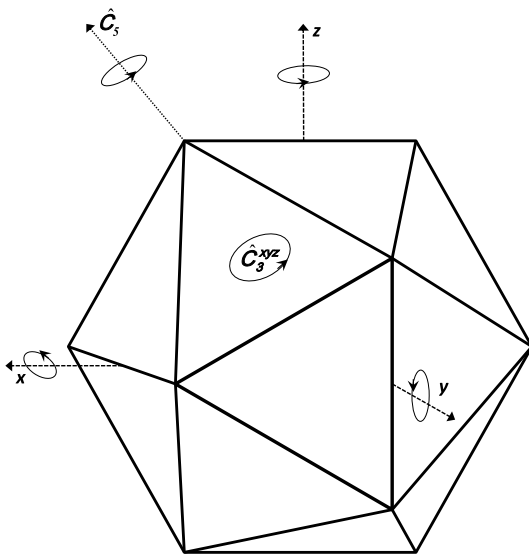
$$|T_{2a}\rangle = \frac{1}{\sqrt{3}}\left(|T_{2\xi}\rangle + |T_{2\eta}\rangle + |T_{2\zeta}\rangle\right) = d_{z'^2}$$

$$|T_{2\theta}\rangle = \frac{1}{\sqrt{6}}\left(|T_{2\xi}\rangle + |T_{2\eta}\rangle - 2|T_{2\zeta}\rangle\right) = \frac{1}{\sqrt{3}}(\sqrt{2}d_{x'^2-y'^2} - d_{y'z'})$$

$$|T_{2\epsilon}\rangle = \frac{1}{\sqrt{2}}\left(|T_{2\eta}\rangle - |T_{2\xi}\rangle\right) = \frac{1}{\sqrt{3}}(-\sqrt{2}d_{x'y'} + d_{x'z'})$$

O (D_3 basis)	$\mathbb{D}(C_3^{z'})$	$\mathbb{D}(C_2^{x'})$
$|E_\theta\rangle, |E_\epsilon\rangle$	$\begin{pmatrix} -\frac{1}{2} & -\frac{\sqrt{3}}{2} \\ +\frac{\sqrt{3}}{2} & -\frac{1}{2} \end{pmatrix}$	$\begin{pmatrix} 1 & 0 \\ 0 & -1 \end{pmatrix}$
$|T_{1a}\rangle, |T_{1\theta}\rangle, |T_{1\epsilon}\rangle$	$\begin{pmatrix} 1 & 0 & 0 \\ 0 & -\frac{1}{2} & -\frac{\sqrt{3}}{2} \\ 0 & +\frac{\sqrt{3}}{2} & -\frac{1}{2} \end{pmatrix}$	$\begin{pmatrix} -1 & 0 & 0 \\ 0 & 1 & 0 \\ 0 & 0 & -1 \end{pmatrix}$
$|T_{2a}\rangle, |T_{2\theta}\rangle, |T_{2\epsilon}\rangle$	$\begin{pmatrix} 1 & 0 & 0 \\ 0 & -\frac{1}{2} & -\frac{\sqrt{3}}{2} \\ 0 & +\frac{\sqrt{3}}{2} & -\frac{1}{2} \end{pmatrix}$	$\begin{pmatrix} 1 & 0 & 0 \\ 0 & 1 & 0 \\ 0 & 0 & -1 \end{pmatrix}$

I (D_2 basis, Fig. D.2)	$\mathbb{D}(C_5)$	$\mathbb{D}(C_3^{xyz})$	$\mathbb{D}(C_2^z)$
$\lvert T_{1x}\rangle, \lvert T_{1y}\rangle, \lvert T_{1z}\rangle$	$\frac{1}{2}\begin{pmatrix} 1 & -\phi & \phi^{-1} \\ \phi & \phi^{-1} & -1 \\ \phi^{-1} & 1 & \phi \end{pmatrix}$	$\begin{pmatrix} 0 & 0 & 1 \\ 1 & 0 & 0 \\ 0 & 1 & 0 \end{pmatrix}$	$\begin{pmatrix} -1 & 0 & 0 \\ 0 & -1 & 0 \\ 0 & 0 & 1 \end{pmatrix}$
$\lvert T_{2x}\rangle, \lvert T_{2y}\rangle, \lvert T_{2z}\rangle$	$\frac{1}{2}\begin{pmatrix} 1 & \phi^{-1} & -\phi \\ -\phi^{-1} & -\phi & -1 \\ -\phi & 1 & -\phi^{-1} \end{pmatrix}$	$\begin{pmatrix} 0 & 0 & 1 \\ 1 & 0 & 0 \\ 0 & 1 & 0 \end{pmatrix}$	$\begin{pmatrix} -1 & 0 & 0 \\ 0 & -1 & 0 \\ 0 & 0 & 1 \end{pmatrix}$
$\lvert G_a\rangle, \lvert G_x\rangle, \lvert G_y\rangle,$ $\lvert G_z\rangle$	$\frac{1}{4}\begin{pmatrix} -1 & -\sqrt{5} & \sqrt{5} & \sqrt{5} \\ \sqrt{5} & -3 & -1 & -1 \\ \sqrt{5} & 1 & -1 & 3 \\ -\sqrt{5} & -1 & -3 & 1 \end{pmatrix}$	$\begin{pmatrix} 1 & 0 & 0 & 0 \\ 0 & 0 & 0 & 1 \\ 0 & 1 & 0 & 0 \\ 0 & 0 & 0 & 1 \end{pmatrix}$	$\begin{pmatrix} 1 & 0 & 0 & 0 \\ 0 & -1 & 0 & 0 \\ 0 & 0 & -1 & 0 \\ 0 & 0 & 0 & 1 \end{pmatrix}$

I	$\lvert H\theta\rangle, \lvert H\epsilon\rangle, \lvert H\xi\rangle, \lvert H\eta\rangle, \lvert H\zeta\rangle$

$$\mathbb{D}(C_5) = \begin{pmatrix} -\frac{1}{4} & -\frac{\sqrt{3}}{4} & \frac{1}{\sqrt{8}} & \frac{1}{\sqrt{2}} & -\frac{1}{\sqrt{8}} \\ -\frac{\sqrt{3}}{4} & \frac{1}{4} & -\frac{\sqrt{3}}{\sqrt{8}} & 0 & -\frac{\sqrt{3}}{\sqrt{8}} \\ -\frac{1}{\sqrt{8}} & \frac{\sqrt{3}}{\sqrt{8}} & 0 & \frac{1}{2} & \frac{1}{2} \\ \frac{1}{\sqrt{2}} & 0 & -\frac{1}{2} & \frac{1}{2} & 0 \\ \frac{1}{\sqrt{8}} & \frac{\sqrt{3}}{\sqrt{8}} & \frac{1}{2} & 0 & -\frac{1}{2} \end{pmatrix}$$

$$\mathbb{D}(C_3^{xyz}) = \begin{pmatrix} -\frac{1}{2} & -\frac{\sqrt{3}}{2} & 0 & 0 & 0 \\ \frac{\sqrt{3}}{2} & -\frac{1}{2} & 0 & 0 & 0 \\ 0 & 0 & 0 & 0 & 1 \\ 0 & 0 & 1 & 0 & 0 \\ 0 & 0 & 0 & 1 & 0 \end{pmatrix}$$

$$\mathbb{D}(C_2^z) = \begin{pmatrix} 1 & 0 & 0 & 0 & 0 \\ 0 & 1 & 0 & 0 & 0 \\ 0 & 0 & -1 & 0 & 0 \\ 0 & 0 & 0 & -1 & 0 \\ 0 & 0 & 0 & 0 & 1 \end{pmatrix}$$

It is important to note that in the Boyle and Parker basis the $\lvert H\theta\rangle$ and $\lvert H\epsilon\rangle$ components do not denote components that transform like the functions d_{z^2} and $d_{x^2-y^2}$, but refer to linear combinations of these:

$$\lvert H\theta\rangle = \sqrt{\frac{3}{8}}d_{z^2} + \sqrt{\frac{5}{8}}d_{x^2-y^2}$$

$$\lvert H\epsilon\rangle = -\sqrt{\frac{5}{8}}d_{z^2} + \sqrt{\frac{3}{8}}d_{x^2-y^2}$$

Griffith has presented the subduction of spherical $\lvert JM\rangle$ states to point-group canonical bases for the case of the octahedral group. Similar tables for subduction to the icosahedral canonical basis have been published by Qiu and Ceulemans [8]. Extensive tables of bases in terms of spherical harmonics for several branching schemes are also provided by Butler [9].

Appendix E
Direct-Product Tables

Extensive direct-product tables are provided by Herzberg [10]. Antisymmetrized and symmetrized parts of direct squares are indicated by braces and brackets, respectively.

D_3		A_1		A_2		E
A_1		A_1		A_2		E
A_2		A_2		A_1		E
E		E		E		$[A_1 + E] + \{A_2\}$

D_4	A_1	A_2	B_1	B_2	E
A_1	A_1	A_2	B_1	B_2	E
A_2	A_2	A_1	B_2	B_1	E
B_1	B_1	B_2	A_1	A_2	E
B_2	B_2	B_1	A_2	A_1	E
E	E	E	E	E	$[A_1 + B_1 + B_2] + \{A_2\}$

D_5		A_1		A_2		E_1		E_2
A_1		A_1		A_2		E_1		E_2
A_2		A_2		A_1		E_1		E_2
E_1		E_1		E_1		$[A_1 + E_2] + \{A_2\}$		$E_1 + E_2$
E_2		E_2		E_2		$E_1 + E_2$		$[A_1 + E_1] + \{A_2\}$

D_6	A_1	A_2	B_1	B_2	E_1		E_2
A_1	A_1	A_2	B_1	B_2	E_1		E_2
A_2	A_2	A_1	B_2	B_1	E_1		E_2
B_1	B_1	B_2	A_1	A_2	E_2		E_1
B_2	B_2	B_1	A_2	A_1	E_2		E_1
E_1	E_1	E_1	E_2	E_2	$[A_1 + E_2] + \{A_2\}$		$B_1 + B_2 + E_1$
E_2	E_2	E_2	E_1	E_1	$B_1 + B_2 + E_1$		$[A_1 + E_2] + \{A_2\}$

T_d	A_1	A_2	E	T_1	T_2
A_1	A_1	A_2	E	T_1	T_2
A_2	A_2	A_1	E	T_2	T_1
E	E	E	$[A_1 + E] + \{A_2\}$	$T_1 + T_2$	$T_1 + T_2$
T_1	T_1	T_2	$T_1 + T_2$	$[A_1 + E + T_2] + \{T_1\}$	$A_2 + E + T_1 + T_2$
T_2	T_2	T_1	$T_1 + T_2$	$A_2 + E + T_1 + T_2$	$[A_1 + E + T_2] + \{T_1\}$

O	A_1	A_2	E	T_1	T_2
A_1	A_1	A_2	E	T_1	T_2
A_2	A_2	A_1	E	T_2	T_1
E	E	E	$[A_1 + E] + \{A_2\}$	$T_1 + T_2$	$T_1 + T_2$
T_1	T_1	T_2	$T_1 + T_2$	$[A_1 + E + T_2] + \{T_1\}$	$A_2 + E + T_1 + T_2$
T_2	T_2	T_1	$T_1 + T_2$	$A_2 + E + T_1 + T_2$	$[A_1 + E + T_2] + \{T_1\}$

I	A	T_1	T_2	G	H
A	A	T_1	T_2	G	H
T_1	T_1	$[A + H] + \{T_1\}$	$G + H$	$T_2 + G + H$	$T_1 + T_2 + G + H$
T_2	T_2	$G + H$	$[A + H] + \{T_2\}$	$T_1 + G + H$	$T_1 + T_2 + G + H$
G	G	$T_2 + G + H$	$T_1 + G + H$	$[A + G + H] + \{T_1 + T_2\}$	$T_1 + T_2 + G + 2H$
H	H	$T_1 + T_2 + G + H$	$T_1 + T_2 + G + H$	$T_1 + T_2 + G + 2H$	$[A + G + 2H] + \{T_1 + T_2 + G\}$

Appendix F
Coupling Coefficients

Coupling coefficients are denoted as 3Γ symbols: $\langle \Gamma_a \gamma_a \Gamma_b \gamma_b | \Gamma \gamma \rangle$. Their symmetry properties were given in Sect. 6.3. Octahedral coefficients have been listed by Griffith. Icosahedral coefficients are taken from the work of Fowler and Ceulemans [11].

D_3		
$A_2 \times E$		E
	x	y
a_2 x	0	-1
a_2 y	1	0

D_3				
$E \times E$	A_1	A_2		E
	a_1	a_2	x	y
x x	$\frac{1}{\sqrt{2}}$	0	$-\frac{1}{\sqrt{2}}$	0
y y	$\frac{1}{\sqrt{2}}$	0	$\frac{1}{\sqrt{2}}$	0
x y	0	$\frac{1}{\sqrt{2}}$	0	$\frac{1}{\sqrt{2}}$
y x	0	$-\frac{1}{\sqrt{2}}$	0	$\frac{1}{\sqrt{2}}$

D_4				
$E \times E$	A_1	A_2	B_1	B_2
	a_1	a_2	b_1	b_2
x x	$\frac{1}{\sqrt{2}}$	0	$-\frac{1}{\sqrt{2}}$	0
y y	$\frac{1}{\sqrt{2}}$	0	$\frac{1}{\sqrt{2}}$	0
x y	0	$\frac{1}{\sqrt{2}}$	0	$\frac{1}{\sqrt{2}}$
y x	0	$-\frac{1}{\sqrt{2}}$	0	$\frac{1}{\sqrt{2}}$

D_5

$E_1 \times E_1$	A_1	A_2	E_2	
	a_1	a_2	c	s
$x\ x$	$\frac{1}{\sqrt{2}}$	0	$\frac{1}{\sqrt{2}}$	0
$y\ y$	$\frac{1}{\sqrt{2}}$	0	$-\frac{1}{\sqrt{2}}$	0
$x\ y$	0	$\frac{1}{\sqrt{2}}$	0	$\frac{1}{\sqrt{2}}$
$y\ x$	0	$-\frac{1}{\sqrt{2}}$	0	$\frac{1}{\sqrt{2}}$

D_5

$E_2 \times E_2$	A_1	A_2	E_1	
	a_1	a_2	x	y
$c\ c$	$\frac{1}{\sqrt{2}}$	0	$-\frac{1}{\sqrt{2}}$	0
$s\ s$	$\frac{1}{\sqrt{2}}$	0	$\frac{1}{\sqrt{2}}$	0
$c\ s$	0	$\frac{1}{\sqrt{2}}$	0	$\frac{1}{\sqrt{2}}$
$s\ c$	0	$-\frac{1}{\sqrt{2}}$	0	$\frac{1}{\sqrt{2}}$

D_5

$E_1 \times E_2$	E_1		E_2	
	x	y	c	s
$x\ c$	$\frac{1}{\sqrt{2}}$	0	$-\frac{1}{\sqrt{2}}$	0
$y\ s$	$\frac{1}{\sqrt{2}}$	0	$\frac{1}{\sqrt{2}}$	0
$x\ s$	0	$\frac{1}{\sqrt{2}}$	0	$\frac{1}{\sqrt{2}}$
$y\ c$	0	$-\frac{1}{\sqrt{2}}$	0	$\frac{1}{\sqrt{2}}$

D_6

$E_1 \times E_1$	A_1	A_2	E_2	
	a_1	a_2	c	s
$x\ x$	$\frac{1}{\sqrt{2}}$	0	$\frac{1}{\sqrt{2}}$	0
$y\ y$	$\frac{1}{\sqrt{2}}$	0	$-\frac{1}{\sqrt{2}}$	0
$x\ y$	0	$\frac{1}{\sqrt{2}}$	0	$\frac{1}{\sqrt{2}}$
$y\ x$	0	$-\frac{1}{\sqrt{2}}$	0	$\frac{1}{\sqrt{2}}$

D_6

$E_2 \times E_2$	A_1	A_2	E_1	
	a_1	a_2	x	y
$c\ c$	$\frac{1}{\sqrt{2}}$	0	$-\frac{1}{\sqrt{2}}$	0
$s\ s$	$\frac{1}{\sqrt{2}}$	0	$\frac{1}{\sqrt{2}}$	0
$c\ s$	0	$\frac{1}{\sqrt{2}}$	0	$\frac{1}{\sqrt{2}}$
$s\ c$	0	$-\frac{1}{\sqrt{2}}$	0	$\frac{1}{\sqrt{2}}$

D_6

$E_1 \times E_2$	B_1	B_2	E_1	
	b_1	b_2	x	y
$x\ c$	$\frac{1}{\sqrt{2}}$	0	$\frac{1}{\sqrt{2}}$	0
$y\ s$	$-\frac{1}{\sqrt{2}}$	0	$\frac{1}{\sqrt{2}}$	0
$x\ s$	0	$\frac{1}{\sqrt{2}}$	0	$\frac{1}{\sqrt{2}}$
$y\ c$	0	$\frac{1}{\sqrt{2}}$	0	$-\frac{1}{\sqrt{2}}$

O

$A_2 \times E$	E	
	θ	ϵ
$a_2\ \theta$	0	-1
$a_2\ \epsilon$	1	0

O

$A_2 \times T_1$	T_2		
	ξ	η	ζ
$a_2\ x$	1	0	0
$a_2\ y$	0	1	0
$a_2\ z$	0	0	1

O

$A_2 \times T_2$	T_1		
	x	y	z
$a_2\ \xi$	1	0	0
$a_2\ \eta$	0	1	0
$a_2\ \zeta$	0	0	1

O

$E \times E$	A_1	A_2	E	
	a_1	a_2	θ	ϵ
$\theta\ \theta$	$\frac{1}{\sqrt{2}}$	0	$-\frac{1}{\sqrt{2}}$	0
$\epsilon\ \epsilon$	$\frac{1}{\sqrt{2}}$	0	$\frac{1}{\sqrt{2}}$	0
$\theta\ \epsilon$	0	$\frac{1}{\sqrt{2}}$	0	$\frac{1}{\sqrt{2}}$
$\epsilon\ \theta$	0	$-\frac{1}{\sqrt{2}}$	0	$\frac{1}{\sqrt{2}}$

O

$E \times T_1$		T_1			T_2		
		x	y	z	ξ	η	ζ
$\theta\ x$		$-\frac{1}{2}$	0	0	$-\frac{\sqrt{3}}{2}$	0	0
$\theta\ y$		0	$-\frac{1}{2}$	0	0	$\frac{\sqrt{3}}{2}$	0
$\theta\ z$		0	0	1	0	0	0
$\epsilon\ x$		$\frac{\sqrt{3}}{2}$	0	0	$-\frac{1}{2}$	0	0
$\epsilon\ y$		0	$-\frac{\sqrt{3}}{2}$	0	0	$-\frac{1}{2}$	0
$\epsilon\ z$		0	0	0	0	0	1

O

$E \times T_2$		T_1			T_2		
		x	y	z	ξ	η	ζ
$\theta\ \xi$		$\frac{-\sqrt{3}}{2}$	0	0	$-\frac{1}{2}$	0	0
$\theta\ \eta$		0	$\frac{\sqrt{3}}{2}$	0	0	$-\frac{1}{2}$	0
$\theta\ \zeta$		0	0	0	0	0	1
$\epsilon\ \xi$		$-\frac{1}{2}$	0	0	$\frac{\sqrt{3}}{2}$	0	0
$\epsilon\ \eta$		0	$-\frac{1}{2}$	0	0	$-\frac{\sqrt{3}}{2}$	0
$\epsilon\ \zeta$		0	0	1	0	0	0

O

$T_1 \times T_1$ or $T_2 \times T_2$		A_1 a_1	E θ	ϵ
$x\ x$	$\xi\ \xi$	$\frac{1}{\sqrt{3}}$	$\frac{1}{\sqrt{6}}$	$-\frac{1}{\sqrt{2}}$
$y\ y$	$\eta\ \eta$	$\frac{1}{\sqrt{3}}$	$\frac{1}{\sqrt{6}}$	$\frac{1}{\sqrt{2}}$
$z\ z$	$\zeta\ \zeta$	$\frac{1}{\sqrt{3}}$	$-\frac{2}{\sqrt{6}}$	0

O

$T_1 \times T_2$	A_2 a_2	E θ	ϵ
$x\ \xi$	$\frac{1}{\sqrt{3}}$	$-\frac{1}{\sqrt{2}}$	$-\frac{1}{\sqrt{6}}$
$y\ \eta$	$\frac{1}{\sqrt{3}}$	$\frac{1}{\sqrt{2}}$	$-\frac{1}{\sqrt{6}}$
$z\ \zeta$	$\frac{1}{\sqrt{3}}$	0	$\frac{2}{\sqrt{6}}$

O

$T_1 \times T_1$ or $T_2 \times T_2$		T_1			T_2		
		x	y	z	ξ	η	ζ
$x\ y$	$\xi\ \eta$	0	0	$-\frac{1}{\sqrt{2}}$	0	0	$-\frac{1}{\sqrt{2}}$
$x\ z$	$\xi\ \zeta$	0	$\frac{1}{\sqrt{2}}$	0	0	$-\frac{1}{\sqrt{2}}$	0
$y\ x$	$\eta\ \xi$	0	0	$\frac{1}{\sqrt{2}}$	0	0	$-\frac{1}{\sqrt{2}}$
$y\ z$	$\eta\ \zeta$	$-\frac{1}{\sqrt{2}}$	0	0	$-\frac{1}{\sqrt{2}}$	0	0
$z\ x$	$\zeta\ \xi$	0	$-\frac{1}{\sqrt{2}}$	0	0	$-\frac{1}{\sqrt{2}}$	0
$z\ y$	$\zeta\ \eta$	$\frac{1}{\sqrt{2}}$	0	0	$-\frac{1}{\sqrt{2}}$	0	0

O

$T_1 \times T_2$	T_1			T_2		
	x	y	z	ξ	η	ζ
$x\ \eta$	0	0	$-\frac{1}{\sqrt{2}}$	0	0	$-\frac{1}{\sqrt{2}}$
$x\ \zeta$	0	$-\frac{1}{\sqrt{2}}$	0	0	$\frac{1}{\sqrt{2}}$	0
$y\ \xi$	0	0	$-\frac{1}{\sqrt{2}}$	0	0	$\frac{1}{\sqrt{2}}$
$y\ \zeta$	$-\frac{1}{\sqrt{2}}$	0	0	$-\frac{1}{\sqrt{2}}$	0	0
$z\ \xi$	0	$-\frac{1}{\sqrt{2}}$	0	0	$-\frac{1}{\sqrt{2}}$	0
$z\ \eta$	$-\frac{1}{\sqrt{2}}$	0	0	$\frac{1}{\sqrt{2}}$	0	0

In the icosahedral tables, ϕ denotes the golden number $(1 + \sqrt{5})/2$, and $\alpha = 3\phi - 1$, $\beta = 3\phi^{-1} + 1$.

I

$T_1 \times T_1$	A	T_1			H				
		x	y	z	θ	ϵ	ξ	η	θ
$x\ x$	$\frac{1}{\sqrt{3}}$	0	0	0	$\frac{\phi^{-1}}{2}$	$\frac{\phi^2}{2\sqrt{3}}$	0	0	0
$x\ y$	0	0	0	$\frac{1}{\sqrt{2}}$	0	0	0	0	$\frac{1}{\sqrt{2}}$
$x\ z$	0	0	$-\frac{1}{\sqrt{2}}$	0	0	0	0	$\frac{1}{\sqrt{2}}$	0
$y\ x$	0	0	0	$-\frac{1}{\sqrt{2}}$	0	0	0	0	$\frac{1}{\sqrt{2}}$
$y\ y$	$\frac{1}{\sqrt{3}}$	0	0	0	$-\frac{\phi}{2}$	$-\frac{\phi^{-2}}{2\sqrt{3}}$	0	0	0
$y\ z$	0	$\frac{1}{\sqrt{2}}$	0	0	0	0	$\frac{1}{\sqrt{2}}$	0	0
$z\ x$	0	0	$\frac{1}{\sqrt{2}}$	0	0	0	0	$\frac{1}{\sqrt{2}}$	0
$z\ y$	0	$-\frac{1}{\sqrt{2}}$	0	0	0	0	$\frac{1}{\sqrt{2}}$	0	0
$z\ z$	$\frac{1}{\sqrt{3}}$	0	0	0	$\frac{1}{2}$	$-\frac{\sqrt{5}}{2\sqrt{3}}$	0	0	0

I									
$T_1 \times T_2$		G				H			
	a	x	y	z	θ	ϵ	ξ	η	ζ
$x\ x$	$\frac{1}{\sqrt{3}}$	0	0	0	$\frac{1}{\sqrt{6}}$	$-\frac{1}{\sqrt{2}}$	0	0	0
$x\ y$	0	0	0	$-\frac{\phi^{-1}}{\sqrt{3}}$	0	0	0	0	$\frac{\phi}{\sqrt{3}}$
$x\ z$	0	0	$-\frac{\phi}{\sqrt{3}}$	0	0	0	0	$-\frac{\phi^{-1}}{\sqrt{3}}$	0
$y\ x$	0	0	0	$-\frac{\phi}{\sqrt{3}}$	0	0	0	0	$-\frac{\phi^{-1}}{\sqrt{3}}$
$y\ y$	$\frac{1}{\sqrt{3}}$	0	0	0	$\frac{1}{\sqrt{6}}$	$\frac{1}{\sqrt{2}}$	0	0	0
$y\ z$	0	$-\frac{\phi^{-1}}{\sqrt{3}}$	0	0	0	0	$\frac{\phi}{\sqrt{3}}$	0	0
$z\ x$	0	0	$-\frac{\phi^{-1}}{\sqrt{3}}$	0	0	0	0	$\frac{\phi}{\sqrt{3}}$	0
$z\ y$	0	$-\frac{\phi}{\sqrt{3}}$	0	0	0	0	$-\frac{\phi^{-1}}{\sqrt{3}}$	0	0
$z\ z$	$\frac{1}{\sqrt{3}}$	0	0	0	$-\frac{\sqrt{2}}{\sqrt{3}}$	0	0	0	0

I												
$T_1 \times G$		T_2			G				H				
	x	y	z	a	x	y	z	θ	ϵ	ξ	η	ζ
$x\ a$	$\frac{1}{2}$	0	0	0	$\frac{1}{\sqrt{3}}$	0	0	0	0	$\frac{\sqrt{5}}{2\sqrt{3}}$	0	0
$x\ x$	0	0	0	$-\frac{1}{\sqrt{3}}$	0	0	0	$-\frac{\beta}{2\sqrt{6}}$	$-\frac{\phi}{2\sqrt{2}}$	0	0	0
$x\ y$	0	0	$-\frac{\phi}{2}$	0	0	0	$\frac{1}{\sqrt{3}}$	0	0	0	0	$\frac{\phi^{-2}}{2\sqrt{3}}$
$x\ z$	0	$-\frac{\phi^{-1}}{2}$	0	0	0	$-\frac{1}{\sqrt{3}}$	0	0	0	0	$\frac{\phi^{2}}{2\sqrt{3}}$	0
$y\ a$	0	$\frac{1}{2}$	0	0	0	$\frac{1}{\sqrt{3}}$	0	0	0	0	$\frac{\sqrt{5}}{2\sqrt{3}}$	0
$y\ x$	0	0	$-\frac{\phi^{-1}}{2}$	0	0	0	$-\frac{1}{\sqrt{3}}$	0	0	0	0	$\frac{\phi^{2}}{2\sqrt{3}}$
$y\ y$	0	0	0	$-\frac{1}{\sqrt{3}}$	0	0	0	$\frac{\alpha}{2\sqrt{6}}$	$-\frac{\phi^{-1}}{2\sqrt{2}}$	0	0	0
$y\ z$	$-\frac{\phi}{2}$	0	0	0	$\frac{1}{\sqrt{3}}$	0	0	0	0	$\frac{\phi^{-2}}{2\sqrt{3}}$	0	0
$z\ a$	0	0	$\frac{1}{2}$	0	0	0	$\frac{1}{\sqrt{3}}$	0	0	0	0	$\frac{\sqrt{5}}{2\sqrt{3}}$
$z\ x$	0	$-\frac{\phi}{2}$	0	0	0	$\frac{1}{\sqrt{3}}$	0	0	0	0	0	$\frac{\phi^{-2}}{2\sqrt{3}}$
$z\ y$	$-\frac{\phi^{-1}}{2}$	0	0	0	$-\frac{1}{\sqrt{3}}$	0	0	0	0	$\frac{\phi^{2}}{2\sqrt{3}}$	0	0
$z\ z$	0	0	0	$-\frac{1}{\sqrt{3}}$	0	0	0	$-\frac{1}{2\sqrt{6}}$	$\frac{\sqrt{5}}{2\sqrt{2}}$	0	0	0

I

$T_2 \times G$	T_1			G				H				
	x	y	z	a	x	y	z	θ	ϵ	ξ	η	ζ
$x\ a$	$\frac{1}{2}$	0	0	0	$\frac{1}{\sqrt{3}}$	0	0	0	0	$\frac{\sqrt{5}}{2\sqrt{3}}$	0	0
$x\ x$	0	0	0	$-\frac{1}{\sqrt{3}}$	0	0	0	$\frac{\alpha}{2\sqrt{6}}$	$\frac{\phi^{-1}}{2\sqrt{2}}$	0	0	0
$x\ y$	0	0	$-\frac{\phi^{-1}}{2}$	0	0	0	$-\frac{1}{\sqrt{3}}$	0	0	0	0	$\frac{\phi^{2}}{2\sqrt{3}}$
$x\ z$	0	$-\frac{\phi}{2}$	0	0	0	$\frac{1}{\sqrt{3}}$	0	0	0	0	$\frac{\phi^{-2}}{2\sqrt{3}}$	0
$y\ a$	0	$\frac{1}{2}$	0	0	0	$\frac{1}{\sqrt{3}}$	0	0	0	0	$\frac{\sqrt{5}}{2\sqrt{3}}$	0
$y\ x$	0	0	$-\frac{\phi}{2}$	0	0	0	$\frac{1}{\sqrt{3}}$	0	0	0	0	$\frac{\phi^{-2}}{2\sqrt{3}}$
$y\ y$	0	0	0	$-\frac{1}{\sqrt{3}}$	0	0	0	$-\frac{\beta}{2\sqrt{6}}$	$\frac{\phi}{2\sqrt{2}}$	0	0	0
$y\ z$	$-\frac{\phi^{-1}}{2}$	0	0	0	$-\frac{1}{\sqrt{3}}$	0	0	0	0	$\frac{\phi^{2}}{2\sqrt{3}}$	0	0
$z\ a$	0	0	$\frac{1}{2}$	0	0	0	$\frac{1}{\sqrt{3}}$	0	0	0	0	$\frac{\sqrt{5}}{2\sqrt{3}}$
$z\ x$	0	$-\frac{\phi^{-1}}{2}$	0	0	0	$-\frac{1}{\sqrt{3}}$	0	0	0	0	0	$\frac{\phi^{2}}{2\sqrt{3}}$
$z\ y$	$-\frac{\phi}{2}$	0	0	0	$\frac{1}{\sqrt{3}}$	0	0	0	0	$\frac{\phi^{-2}}{2\sqrt{3}}$	0	0
$z\ z$	0	0	0	$-\frac{1}{\sqrt{3}}$	0	0	0	$-\frac{1}{2\sqrt{6}}$	$-\frac{\sqrt{5}}{2\sqrt{2}}$	0	0	0

I

$T_1 \times H$	T_1			T_2			G			
	x	y	z	x	y	z	a	x	y	z
$x\ \theta$	$\frac{\phi^{-1}\sqrt{3}}{2\sqrt{5}}$	0	0	$\frac{1}{\sqrt{10}}$	0	0	0	$\frac{\beta}{\sqrt{30}}$	0	0
$x\ \epsilon$	$\frac{\phi^{2}}{2\sqrt{5}}$	0	0	$-\frac{3}{\sqrt{10}}$	0	0	0	$\frac{\phi}{\sqrt{10}}$	0	0
$x\ \xi$	0	0	0	0	0	0	$-\frac{1}{\sqrt{3}}$	0	0	0
$x\ \eta$	0	0	$\frac{\sqrt{3}}{\sqrt{10}}$	0	0	$-\frac{\phi^{-1}}{\sqrt{5}}$	0	0	0	$-\frac{\phi^{2}}{\sqrt{15}}$
$x\ \zeta$	0	$\frac{\sqrt{3}}{\sqrt{10}}$	0	0	$\frac{\phi}{\sqrt{5}}$	0	0	0	$-\frac{\phi^{-2}}{\sqrt{15}}$	0
$y\ \theta$	0	$-\frac{\phi\sqrt{3}}{2\sqrt{5}}$	0	0	$\frac{1}{\sqrt{10}}$	0	0	0	$-\frac{\alpha}{\sqrt{30}}$	0
$y\ \epsilon$	0	$-\frac{\phi^{-2}}{2\sqrt{5}}$	0	0	$\frac{3}{\sqrt{10}}$	0	0	0	$\frac{\phi^{-1}}{\sqrt{10}}$	0
$y\ \xi$	0	0	$\frac{\sqrt{3}}{\sqrt{10}}$	0	0	$\frac{\phi}{\sqrt{5}}$	0	0	0	$-\frac{\phi^{-2}}{\sqrt{15}}$
$y\ \eta$	0	0	0	0	0	0	$-\frac{1}{\sqrt{3}}$	0	0	0
$y\ \zeta$	$\frac{\sqrt{3}}{\sqrt{10}}$	0	0	$-\frac{\phi^{-1}}{\sqrt{5}}$	0	0	0	$-\frac{\phi^{2}}{\sqrt{15}}$	0	0
$z\ \theta$	0	0	$\frac{\sqrt{3}}{2\sqrt{5}}$	0	0	$-\frac{\sqrt{2}}{\sqrt{5}}$	0	0	0	$\frac{1}{\sqrt{30}}$
$z\ \epsilon$	0	0	$-\frac{1}{2}$	0	0	0	0	0	0	$-\frac{1}{\sqrt{2}}$
$z\ \xi$	0	$\frac{\sqrt{3}}{\sqrt{10}}$	0	0	$-\frac{\phi^{-1}}{\sqrt{5}}$	0	0	0	$-\frac{\phi^{2}}{\sqrt{15}}$	0
$z\ \eta$	$\frac{\sqrt{3}}{\sqrt{10}}$	0	0	$\frac{\phi}{\sqrt{5}}$	0	0	0	$-\frac{\phi^{-2}}{\sqrt{15}}$	0	0
$z\ \zeta$	0	0	0	0	0	0	$-\frac{1}{\sqrt{3}}$	0	0	0

I

$T_2 \times T_2$	A	T_2			H				
		x	y	z	θ	ϵ	x	y	z
$x\ x$	$\frac{1}{\sqrt{3}}$	0	0	0	$\frac{\phi}{2}$	$-\frac{\phi^{-2}}{2\sqrt{3}}$	0	0	0
$x\ y$	0	0	0	$\frac{1}{\sqrt{2}}$	0	0	0	0	$-\frac{1}{\sqrt{2}}$
$x\ z$	0	0	$-\frac{1}{\sqrt{2}}$	0	0	0	0	$-\frac{1}{\sqrt{2}}$	0
$y\ x$	0	0	0	$-\frac{1}{\sqrt{2}}$	0	0	0	0	$-\frac{1}{\sqrt{2}}$
$y\ y$	$\frac{1}{\sqrt{3}}$	0	0	0	$-\frac{\phi^{-1}}{2}$	$\frac{\phi^{2}}{2\sqrt{3}}$	0	0	0
$y\ z$	0	$\frac{1}{\sqrt{2}}$	0	0	0	0	$-\frac{1}{\sqrt{2}}$	0	0
$z\ x$	0	0	$\frac{1}{\sqrt{2}}$	0	0	0	0	$-\frac{1}{\sqrt{2}}$	0
$z\ y$	0	$-\frac{1}{\sqrt{2}}$	0	0	0	0	$-\frac{1}{\sqrt{2}}$	0	0
$z\ z$	$\frac{1}{\sqrt{3}}$	0	0	0	$-\frac{1}{2}$	$-\frac{\sqrt{5}}{2\sqrt{3}}$	0	0	0

I

$T_2 \times H$	T_1			T_2			G			
	x	y	z	x	y	z	a	x	y	z
$x\ \theta$	$\frac{1}{\sqrt{10}}$	0	0	$\frac{\phi\sqrt{3}}{2\sqrt{5}}$	0	0	0	$\frac{\alpha}{\sqrt{30}}$	0	0
$x\ \epsilon$	$-\frac{3}{\sqrt{10}}$	0	0	$-\frac{\phi^{-2}}{2\sqrt{5}}$	0	0	0	$\frac{\phi^{-1}}{\sqrt{10}}$	0	0
$x\ \xi$	0	0	0	0	0	0	$\frac{1}{\sqrt{3}}$	0	0	0
$x\ \eta$	0	0	$\frac{\phi}{\sqrt{5}}$	0	0	$-\frac{\sqrt{3}}{\sqrt{10}}$	0	0	0	$\frac{\phi^{-2}}{\sqrt{15}}$
$x\ \zeta$	0	$-\frac{\phi^{-1}}{\sqrt{5}}$	0	0	$-\frac{\sqrt{3}}{\sqrt{10}}$	0	0	0	$\frac{\phi^{2}}{\sqrt{15}}$	0
$y\ \theta$	0	$\frac{1}{\sqrt{10}}$	0	0	$-\frac{\phi^{-1}\sqrt{3}}{2\sqrt{5}}$	0	0	0	$-\frac{\beta}{\sqrt{30}}$	0
$y\ \epsilon$	0	$\frac{3}{\sqrt{10}}$	0	0	$\frac{\phi^{2}}{2\sqrt{5}}$	0	0	0	$\frac{\phi}{\sqrt{10}}$	0
$y\ \xi$	0	0	$-\frac{\phi^{-1}}{\sqrt{5}}$	0	0	$-\frac{\sqrt{3}}{\sqrt{10}}$	0	0	0	$\frac{\phi^{2}}{\sqrt{15}}$
$y\ \eta$	0	0	0	0	0	0	$\frac{1}{\sqrt{3}}$	0	0	0
$y\ \zeta$	$\frac{\phi}{\sqrt{5}}$	0	0	$-\frac{\sqrt{3}}{\sqrt{10}}$	0	0	0	$\frac{\phi^{-2}}{\sqrt{15}}$	0	0
$z\ \theta$	0	0	$-\frac{\sqrt{2}}{\sqrt{5}}$	0	0	$-\frac{\sqrt{3}}{2\sqrt{5}}$	0	0	0	$-\frac{1}{\sqrt{30}}$
$z\ \epsilon$	0	0	0	0	0	$-\frac{1}{2}$	0	0	0	$-\frac{1}{\sqrt{2}}$
$z\ \xi$	0	$\frac{\phi}{\sqrt{5}}$	0	0	$-\frac{\sqrt{3}}{\sqrt{10}}$	0	0	0	$\frac{\phi^{-2}}{\sqrt{15}}$	0
$z\ \eta$	$-\frac{\phi^{-1}}{\sqrt{5}}$	0	0	$-\frac{\sqrt{3}}{\sqrt{10}}$	0	0	0	$\frac{\phi^{2}}{\sqrt{15}}$	0	0
$z\ \zeta$	0	0	0	0	0	0	$\frac{1}{\sqrt{3}}$	0	0	0

I $T_1 \times H$	H					I $T_2 \times H$	H				
	θ	ϵ	ξ	η	ζ		θ	ϵ	ξ	η	ζ
$x\ \theta$	0	0	$\frac{\phi^2}{2\sqrt{3}}$	0	0	$x\ \theta$	0	0	$\frac{\phi^{-2}}{2\sqrt{3}}$	0	0
$x\ \epsilon$	0	0	$-\frac{\phi^{-1}}{2}$	0	0	$x\ \epsilon$	0	0	$\frac{\phi}{2}$	0	0
$x\ \xi$	$-\frac{\phi^2}{2\sqrt{3}}$	$\frac{\phi^{-1}}{2}$	0	0	0	$x\ \xi$	$-\frac{\phi^{-2}}{2\sqrt{3}}$	$-\frac{\phi}{2}$	0	0	0
$x\ \eta$	0	0	0	0	$\frac{1}{\sqrt{6}}$	$x\ \eta$	0	0	0	0	$\frac{1}{\sqrt{6}}$
$x\ \zeta$	0	0	0	$-\frac{1}{\sqrt{6}}$	0	$x\ \zeta$	0	0	0	$-\frac{1}{\sqrt{6}}$	0
$y\ \theta$	0	0	0	$-\frac{\phi^{-2}}{2\sqrt{3}}$	0	$y\ \theta$	0	0	0	$-\frac{\phi^2}{2\sqrt{3}}$	0
$y\ \epsilon$	0	0	0	$\frac{\phi}{2}$	0	$y\ \epsilon$	0	0	0	$-\frac{\phi^{-1}}{2}$	0
$y\ \xi$	0	0	0	0	$-\frac{1}{\sqrt{6}}$	$y\ \xi$	0	0	0	0	$-\frac{1}{\sqrt{6}}$
$y\ \eta$	$\frac{\phi^{-2}}{2\sqrt{3}}$	$-\frac{\phi}{2}$	0	0	0	$y\ \eta$	$\frac{\phi^2}{2\sqrt{3}}$	$\frac{\phi^{-1}}{2}$	0	0	0
$y\ \zeta$	0	0	$\frac{1}{\sqrt{6}}$	0	0	$y\ \zeta$	0	0	$\frac{1}{\sqrt{6}}$	0	0
$z\ \theta$	0	0	0	0	$-\frac{\sqrt{5}}{2\sqrt{3}}$	$z\ \theta$	0	0	0	0	$\frac{\sqrt{5}}{2\sqrt{3}}$
$z\ \epsilon$	0	0	0	0	$-\frac{1}{2}$	$z\ \epsilon$	0	0	0	0	$-\frac{1}{2}$
$z\ \xi$	0	0	0	$\frac{1}{\sqrt{6}}$	0	$z\ \xi$	0	0	0	$\frac{1}{\sqrt{6}}$	0
$z\ \eta$	0	0	$-\frac{1}{\sqrt{6}}$	0	0	$z\ \eta$	0	0	$-\frac{1}{\sqrt{6}}$	0	0
$z\ \zeta$	$\frac{\sqrt{5}}{2\sqrt{3}}$	$\frac{1}{2}$	0	0	0	$z\ \zeta$	$-\frac{\sqrt{5}}{2\sqrt{3}}$	$\frac{1}{2}$	0	0	0

I						
$G \times G$	A	T_1			T_2		

$G \times G$	A	x	y	z	x	y	z
$a\ a$	$\frac{1}{2}$	0	0	0	0	0	0
$a\ x$	0	$\frac{1}{2}$	0	0	$\frac{1}{2}$	0	0
$a\ y$	0	0	$\frac{1}{2}$	0	0	$\frac{1}{2}$	0
$a\ z$	0	0	0	$\frac{1}{2}$	0	0	$\frac{1}{2}$
$x\ a$	0	$-\frac{1}{2}$	0	0	$-\frac{1}{2}$	0	0
$x\ x$	$\frac{1}{2}$	0	0	0	0	0	0
$x\ y$	0	0	0	$\frac{1}{2}$	0	0	$-\frac{1}{2}$
$x\ z$	0	0	$-\frac{1}{2}$	0	0	$\frac{1}{2}$	0
$y\ a$	0	0	$-\frac{1}{2}$	0	0	$-\frac{1}{2}$	0
$y\ x$	0	0	0	$-\frac{1}{2}$	0	0	$\frac{1}{2}$
$y\ y$	$\frac{1}{2}$	0	0	0	0	0	0
$y\ z$	0	$\frac{1}{2}$	0	0	$-\frac{1}{2}$	0	0
$z\ a$	0	0	0	$-\frac{1}{2}$	0	0	$-\frac{1}{2}$
$z\ x$	0	0	$\frac{1}{2}$	0	0	$-\frac{1}{2}$	0
$z\ y$	0	$-\frac{1}{2}$	0	0	$\frac{1}{2}$	0	0
$z\ z$	$\frac{1}{2}$	0	0	0	0	0	0

I

$G \times G$	G				H				
	a	x	y	z	θ	ϵ	ξ	η	ζ
$a\ a$	$\frac{1}{2\sqrt{3}}$	0	0	0	0	0	0	0	0
$a\ x$	0	$-\frac{1}{2\sqrt{3}}$	0	0	0	0	$\frac{\sqrt{5}}{2\sqrt{3}}$	0	0
$a\ y$	0	0	$-\frac{1}{2\sqrt{3}}$	0	0	0	0	$\frac{\sqrt{5}}{2\sqrt{3}}$	0
$a\ z$	0	0	0	$-\frac{1}{2\sqrt{3}}$	0	0	0	0	$\frac{\sqrt{5}}{2\sqrt{3}}$
$x\ a$	0	$-\frac{1}{2\sqrt{3}}$	0	0	0	0	$\frac{\sqrt{5}}{2\sqrt{3}}$	0	0
$x\ x$	$-\frac{1}{2\sqrt{3}}$	0	0	0	$-\frac{1}{\sqrt{6}}$	$\frac{1}{\sqrt{2}}$	0	0	0
$x\ y$	0	0	0	$-\frac{\sqrt{5}}{2\sqrt{3}}$	0	0	0	0	$-\frac{1}{2\sqrt{3}}$
$x\ z$	0	0	$-\frac{\sqrt{5}}{2\sqrt{3}}$	0	0	0	0	$-\frac{1}{2\sqrt{3}}$	0
$y\ a$	0	0	$-\frac{1}{2\sqrt{3}}$	0	0	0	0	$\frac{\sqrt{5}}{2\sqrt{3}}$	0
$y\ x$	0	0	0	$-\frac{\sqrt{5}}{2\sqrt{3}}$	0	0	0	0	$-\frac{1}{2\sqrt{3}}$
$y\ y$	$-\frac{1}{2\sqrt{3}}$	0	0	0	$-\frac{1}{\sqrt{6}}$	$-\frac{1}{\sqrt{2}}$	0	0	0
$y\ z$	0	$-\frac{\sqrt{5}}{2\sqrt{3}}$	0	0	0	0	$-\frac{1}{2\sqrt{3}}$	0	0
$z\ a$	0	0	0	$-\frac{1}{2\sqrt{3}}$	0	0	0	0	$\frac{\sqrt{5}}{2\sqrt{3}}$
$z\ x$	0	0	$-\frac{\sqrt{5}}{2\sqrt{3}}$	0	0	0	0	$-\frac{1}{2\sqrt{3}}$	0
$z\ y$	0	$-\frac{\sqrt{5}}{2\sqrt{3}}$	0	0	0	0	$-\frac{1}{2\sqrt{3}}$	0	0
$z\ z$	$-\frac{1}{2\sqrt{3}}$	0	0	0	$\frac{\sqrt{2}}{\sqrt{3}}$	0	0	0	0

I						
$H \times H$	A	T_1			T_2		

$H \times H$	A	x	y	z	x	y	z
$\theta\ \theta$	$\frac{1}{\sqrt{5}}$	0	0	0	0	0	0
$\theta\ \epsilon$	0	0	0	0	0	0	0
$\theta\ \xi$	0	$\frac{\phi^2}{2\sqrt{5}}$	0	0	$\frac{\phi^{-2}}{2\sqrt{5}}$	0	0
$\theta\ \eta$	0	0	$-\frac{\phi^{-2}}{2\sqrt{5}}$	0	0	$-\frac{\phi^2}{2\sqrt{5}}$	0
$\theta\ \zeta$	0	0	0	$-\frac{1}{2}$	0	0	$\frac{1}{2}$
$\epsilon\ \theta$	0	0	0	0	0	0	0
$\epsilon\ \epsilon$	$\frac{1}{\sqrt{5}}$	0	0	0	0	0	0
$\epsilon\ \xi$	0	$-\frac{\phi^{-1}\sqrt{3}}{2\sqrt{5}}$	0	0	$\frac{\phi\sqrt{3}}{2\sqrt{5}}$	0	0
$\epsilon\ \eta$	0	0	$\frac{\phi\sqrt{3}}{2\sqrt{5}}$	0	0	$-\frac{\phi^{-1}\sqrt{3}}{2\sqrt{5}}$	0
$\epsilon\ \zeta$	0	0	0	$-\frac{\sqrt{3}}{2\sqrt{5}}$	0	0	$-\frac{\sqrt{3}}{2\sqrt{5}}$
$\xi\ \theta$	0	$-\frac{\phi^2}{2\sqrt{5}}$	0	0	$-\frac{\phi^{-2}}{2\sqrt{5}}$	0	0
$\xi\ \epsilon$	0	$\frac{\phi^{-1}\sqrt{3}}{2\sqrt{5}}$	0	0	$-\frac{\phi\sqrt{3}}{2\sqrt{5}}$	0	0
$\xi\ \xi$	$\frac{1}{\sqrt{5}}$	0	0	0	0	0	0
$\xi\ \eta$	0	0	0	$\frac{1}{\sqrt{10}}$	0	0	$\frac{1}{\sqrt{10}}$
$\xi\ \zeta$	0	0	$-\frac{1}{\sqrt{10}}$	0	0	$-\frac{1}{\sqrt{10}}$	0
$\eta\ \theta$	0	0	$\frac{\phi^{-2}}{2\sqrt{5}}$	0	0	$\frac{\phi^2}{2\sqrt{5}}$	0
$\eta\ \epsilon$	0	0	$-\frac{\phi\sqrt{3}}{2\sqrt{5}}$	0	0	$\frac{\phi^{-1}\sqrt{3}}{2\sqrt{5}}$	0
$\eta\ \xi$	0	0	0	$-\frac{1}{\sqrt{10}}$	0	0	$-\frac{1}{\sqrt{10}}$
$\eta\ \eta$	$\frac{1}{\sqrt{5}}$	0	0	0	0	0	0
$\eta\ \zeta$	0	$\frac{1}{\sqrt{10}}$	0	0	$\frac{1}{\sqrt{10}}$	0	0
$\zeta\ \theta$	0	0	0	$\frac{1}{2}$	0	0	$-\frac{1}{2}$
$\zeta\ \epsilon$	0	0	0	$\frac{\sqrt{3}}{2\sqrt{5}}$	0	0	$\frac{\sqrt{3}}{2\sqrt{5}}$
$\zeta\ \xi$	0	0	$\frac{1}{\sqrt{10}}$	0	0	$\frac{1}{\sqrt{10}}$	0
$\zeta\ \eta$	0	$-\frac{1}{\sqrt{10}}$	0	0	$-\frac{1}{\sqrt{10}}$	0	0
$\zeta\ \zeta$	$\frac{1}{\sqrt{5}}$	0	0	0	0	0	0

I								
$H \times H$	[G]				{G}			
	a	x	y	z	a	x	y	z
$\theta\ \theta$	$\frac{\sqrt{3}}{\sqrt{10}}$	0	0	0	0	0	0	0
$\theta\ \epsilon$	0	0	0	0	$-\frac{1}{\sqrt{2}}$	0	0	0
$\theta\ \xi$	0	$-\frac{1}{2\sqrt{3}}$	0	0	0	$\frac{\sqrt{3}}{2\sqrt{5}}$	0	0
$\theta\ \eta$	0	0	$-\frac{1}{2\sqrt{3}}$	0	0	0	$-\frac{\sqrt{3}}{2\sqrt{5}}$	0
$\theta\ \zeta$	0	0	0	$\frac{1}{\sqrt{3}}$	0	0	0	0
$\epsilon\ \theta$	0	0	0	0	$\frac{1}{\sqrt{2}}$	0	0	0
$\epsilon\ \epsilon$	$\frac{\sqrt{3}}{\sqrt{10}}$	0	0	0	0	0	0	0
$\epsilon\ \xi$	0	$\frac{1}{2}$	0	0	0	$\frac{1}{2\sqrt{5}}$	0	0
$\epsilon\ \eta$	0	0	$-\frac{1}{2}$	0	0	0	$\frac{1}{2\sqrt{5}}$	0
$\epsilon\ \zeta$	0	0	0	0	0	0	0	$-\frac{1}{\sqrt{5}}$
$\xi\ \theta$	0	$-\frac{1}{2\sqrt{3}}$	0	0	0	$-\frac{\sqrt{3}}{2\sqrt{5}}$	0	0
$\xi\ \epsilon$	0	$\frac{1}{2}$	0	0	0	$-\frac{1}{2\sqrt{5}}$	0	0
$\xi\ \xi$	$-\frac{\sqrt{2}}{\sqrt{15}}$	0	0	0	0	0	0	0
$\xi\ \eta$	0	0	0	$\frac{1}{\sqrt{6}}$	0	0	0	$-\frac{\sqrt{3}}{\sqrt{10}}$
$\xi\ \zeta$	0	0	$\frac{1}{\sqrt{6}}$	0	0	0	$\frac{\sqrt{3}}{\sqrt{10}}$	0
$\eta\ \theta$	0	0	$-\frac{1}{2\sqrt{3}}$	0	0	0	$\frac{\sqrt{3}}{2\sqrt{5}}$	0
$\eta\ \epsilon$	0	0	$-\frac{1}{2}$	0	0	0	$-\frac{1}{2\sqrt{5}}$	0
$\eta\ \xi$	0	0	0	$\frac{1}{\sqrt{6}}$	0	0	0	$\frac{\sqrt{3}}{\sqrt{10}}$
$\eta\ \eta$	$-\frac{\sqrt{2}}{\sqrt{15}}$	0	0	0	0	0	0	0
$\eta\ \zeta$	0	$\frac{1}{\sqrt{6}}$	0	0	0	$-\frac{\sqrt{3}}{\sqrt{10}}$	0	0
$\zeta\ \theta$	0	0	0	$\frac{1}{\sqrt{3}}$	0	0	0	0
$\zeta\ \epsilon$	0	0	0	0	0	0	0	$\frac{1}{\sqrt{5}}$
$\zeta\ \xi$	0	0	$\frac{1}{\sqrt{6}}$	0	0	0	$-\frac{\sqrt{3}}{\sqrt{10}}$	0
$\zeta\ \eta$	0	$\frac{1}{\sqrt{6}}$	0	0	0	$\frac{\sqrt{3}}{\sqrt{10}}$	0	0
$\zeta\ \zeta$	$-\frac{\sqrt{2}}{\sqrt{15}}$	0	0	0	0	0	0	0

I

$H \times H$	H_a					H_b				
	θ	ϵ	ξ	η	ζ	θ	ϵ	ξ	η	ζ
$\theta\ \theta$	$\frac{\sqrt{3}}{2\sqrt{2}}$	0	0	0	0	0	$\frac{1}{2\sqrt{2}}$	0	0	0
$\theta\ \epsilon$	0	$-\frac{\sqrt{3}}{2\sqrt{2}}$	0	0	0	$\frac{1}{2\sqrt{2}}$	0	0	0	0
$\theta\ \xi$	0	0	$-\frac{1}{2\sqrt{6}}$	0	0	0	0	$\frac{\sqrt{3}}{2\sqrt{2}}$	0	0
$\theta\ \eta$	0	0	0	$-\frac{1}{2\sqrt{6}}$	0	0	0	0	$-\frac{\sqrt{3}}{2\sqrt{2}}$	0
$\theta\ \zeta$	0	0	0	0	$\frac{1}{\sqrt{6}}$	0	0	0	0	0
$\epsilon\ \theta$	0	$-\frac{\sqrt{3}}{2\sqrt{2}}$	0	0	0	$\frac{1}{2\sqrt{2}}$	0	0	0	0
$\epsilon\ \epsilon$	$-\frac{\sqrt{3}}{2\sqrt{2}}$	0	0	0	0	0	$-\frac{1}{2\sqrt{2}}$	0	0	0
$\epsilon\ \xi$	0	0	$\frac{1}{2\sqrt{2}}$	0	0	0	0	$\frac{1}{2\sqrt{2}}$	0	0
$\epsilon\ \eta$	0	0	0	$-\frac{1}{2\sqrt{2}}$	0	0	0	0	$\frac{1}{2\sqrt{2}}$	0
$\epsilon\ \zeta$	0	0	0	0	0	0	0	0	0	$-\frac{1}{\sqrt{2}}$
$\xi\ \theta$	0	0	$-\frac{1}{2\sqrt{6}}$	0	0	0	0	$\frac{\sqrt{3}}{2\sqrt{2}}$	0	0
$\xi\ \epsilon$	0	0	$\frac{1}{2\sqrt{2}}$	0	0	0	0	$\frac{1}{2\sqrt{2}}$	0	0
$\xi\ \xi$	$-\frac{1}{2\sqrt{6}}$	$\frac{1}{2\sqrt{2}}$	0	0	0	$\frac{\sqrt{3}}{2\sqrt{2}}$	$\frac{1}{2\sqrt{2}}$	0	0	0
$\xi\ \eta$	0	0	0	0	$-\frac{1}{\sqrt{3}}$	0	0	0	0	0
$\xi\ \zeta$	0	0	0	$-\frac{1}{\sqrt{3}}$	0	0	0	0	0	0
$\eta\ \theta$	0	0	0	$-\frac{1}{2\sqrt{6}}$	0	0	0	0	$-\frac{\sqrt{3}}{2\sqrt{2}}$	0
$\eta\ \epsilon$	0	0	0	$-\frac{1}{2\sqrt{2}}$	0	0	0	0	$\frac{\sqrt{1}}{2\sqrt{2}}$	0
$\eta\ \xi$	0	0	0	0	$-\frac{1}{\sqrt{3}}$	0	0	0	0	0
$\eta\ \eta$	$-\frac{1}{2\sqrt{6}}$	$-\frac{1}{2\sqrt{2}}$	0	0	0	$-\frac{\sqrt{3}}{2\sqrt{2}}$	$\frac{1}{2\sqrt{2}}$	0	0	0
$\eta\ \zeta$	0	0	$-\frac{1}{\sqrt{3}}$	0	0	0	0	0	0	0
$\zeta\ \theta$	0	0	0	0	$\frac{1}{\sqrt{6}}$	0	0	0	0	0
$\zeta\ \epsilon$	0	0	0	0	0	0	0	0	0	$-\frac{1}{\sqrt{2}}$
$\zeta\ \xi$	0	0	0	$-\frac{1}{\sqrt{3}}$	0	0	0	0	0	0
$\zeta\ \eta$	0	0	$-\frac{1}{\sqrt{3}}$	0	0	0	0	0	0	0
$\zeta\ \zeta$	$\frac{1}{\sqrt{6}}$	0	0	0	0	0	$-\frac{1}{\sqrt{2}}$	0	0	0

Appendix G
Spinor Representations

Contents

Extensive character tables for double groups were provided by Herzberg. The $\aleph$ symbol in the present table corresponds to the Bethe rotation through an angle of 2π. Spin-orbit coupling coefficients for the icosahedral double group have been listed by Fowler and Ceulemans [12]. The notation ρ_1, ρ_2 for conjugate components follows Griffith. The single-valued irreps in Appendix A also represent the double groups. The rotation through 2π leaves these irreps invariant. Their characters under $\hat{R}$ and $\aleph\hat{R}$ are thus the same.

G.1 Character Tables

D_2^*	$\hat{E}$	$\hat{\aleph}$	$2\hat{C}_2^z$	$2\hat{C}_2^y$	$2\hat{C}_2^x$
$E_{1/2}(\Gamma_5)$	2	-2	0	0	0

D_3^*		$\hat{E}$	$\hat{\aleph}$	$2\hat{C}_3$	$2\aleph\hat{C}_3$	$3\hat{C}_2$	$3\aleph\hat{C}_2$
$E_{1/2}(\Gamma_4)$		2	-2	1	-1	0	0
$E_{3/2}$	ρ_1	1	-1	-1	1	i	$-i$
	ρ_2	1	-1	-1	1	$-i$	i

D_4^*	$\hat{E}$	$\hat{\aleph}$	$2\hat{C}_4$	$2\hat{\aleph}\hat{C}_4$	$2\hat{C}_2\,(=\hat{C}_4^2)$	$4\hat{C}_2'$	$4\hat{C}_2''$
$E_{1/2}(\Gamma_6)$	2	-2	$\sqrt{2}$	$-\sqrt{2}$	0	0	0
$E_{3/2}(\Gamma_7)$	2	-2	$-\sqrt{2}$	$\sqrt{2}$	0	0	0

D_5^*	$\hat{E}$	$\hat{\aleph}$	$2\hat{C}_5$	$2\hat{\aleph}\hat{C}_5$	$2\hat{C}_5^2$	$2\hat{\aleph}\hat{C}_5^2$	$5\hat{C}_2'$	$5\hat{\aleph}\hat{C}_2'$
$E_{1/2}$		2	-2	ϕ	$-\phi$	ϕ^{-1}	$-\phi^{-1}$	0	0
$E_{3/2}$		2	-2	$-\phi^{-1}$	ϕ^{-1}	$-\phi$	ϕ	0	0
$E_{5/2}$ $\{\ \rho_1$		1	-1	-1	1	1	-1	i	$-i$
ρ_2		1	-1	-1	1	1	-1	$-i$	i

D_6^*	$\hat{E}$	$\hat{\aleph}$	$2\hat{C}_6$	$2\hat{\aleph}\hat{C}_6$	$2\hat{C}_3$	$2\hat{\aleph}\hat{C}_3$	$2\hat{C}_2$	$6\hat{C}_2'$	$6\hat{C}_2''$
$E_{1/2}(\Gamma_7)$	2	-2	$\sqrt{3}$	$-\sqrt{3}$	1	-1	0	0	0
$E_{5/2}(\Gamma_8)$	2	-2	$-\sqrt{3}$	$\sqrt{3}$	1	-1	0	0	0
$E_{3/2}(\Gamma_9)$	2	-2	0	0	-2	2	0	0	0

T^*	$\hat{E}$	$\hat{\aleph}$	$4\hat{C}_3$	$4\hat{\aleph}\hat{C}_3$	$4\hat{C}_3^2$	$4\hat{\aleph}\hat{C}_3^2$	$6\hat{C}_2$	$\epsilon = \exp(2\pi i/3)$
$E_{1/2}$		2	-2	1	-1	-1	1	0	
$G_{3/2}$ $\{\ E''$		2	-2	ϵ	$-\epsilon$	$-\bar{\epsilon}$	$\bar{\epsilon}$	0	
E'''		2	-2	$\bar{\epsilon}$	$-\bar{\epsilon}$	$-\epsilon$	ϵ	0	

T_d^*	$\hat{E}$	$\hat{\aleph}$	$8\hat{C}_3$	$8\hat{\aleph}\hat{C}_3$	$6\hat{C}_2$	$6\hat{S}_4$	$6\hat{\aleph}\hat{S}_4$	$12\hat{\sigma}_d$
O^*	$\hat{E}$	$\hat{\aleph}$	$8\hat{C}_3$	$8\hat{\aleph}\hat{C}_3$	$6\hat{C}_2$	$6\hat{C}_4$	$6\hat{\aleph}\hat{C}_4$	$12\hat{C}_2'$
$E_{1/2}(\Gamma_6)$	2	-2	1	-1	0	$\sqrt{2}$	$-\sqrt{2}$	0
$E_{5/2}(\Gamma_7)$	2	-2	1	-1	0	$-\sqrt{2}$	$\sqrt{2}$	0
$G_{3/2}(\Gamma_8)$	4	-4	-1	1	0	0	0	0

I^*	$\hat{E}$	$\hat{\aleph}$	$12\hat{C}_5$	$12\hat{\aleph}\hat{C}_5$	$12\hat{C}_5^2$	$12\hat{\aleph}\hat{C}_5^2$	$20\hat{C}_3$	$20\hat{\aleph}\hat{C}_3$	$30\hat{C}_2$
$E_{1/2}(\Gamma_6)$	2	-2	ϕ	$-\phi$	ϕ^{-1}	$-\phi^{-1}$	1	-1	0
$E_{7/2}(\Gamma_7)$	2	-2	$-\phi^{-1}$	ϕ^{-1}	$-\phi$	ϕ	1	-1	0
$G_{3/2}(\Gamma_8)$	4	-4	1	-1	-1	1	-1	1	0
$I_{5/2}(\Gamma_9)$	6	-6	-1	1	1	-1	0	0	0

G.2 Subduction

$SO(3)$	I	O
j		
1/2	$E_{1/2}$	$E_{1/2}$
3/2	$G_{3/2}$	$G_{3/2}$
5/2	$I_{5/2}$	$E_{5/2} + G_{3/2}$
7/2	$E_{7/2} + I_{5/2}$	$E_{1/2} + E_{5/2} + G_{3/2}$
9/2	$G_{3/2} + I_{5/2}$	$E_{1/2} + 2G_{3/2}$
11/2	$E_{1/2} + G_{3/2} + I_{5/2}$	$E_{1/2} + E_{5/2} + 2G_{3/2}$
13/2	$E_{1/2} + E_{7/2} + G_{3/2} + I_{5/2}$	$E_{1/2} + 2E_{5/2} + 2G_{3/2}$
15/2	$G_{3/2} + 2I_{5/2}$	$E_{1/2} + E_{5/2} + 3G_{3/2}$
17/2	$E_{7/2} + G_{3/2} + 2I_{5/2}$	$2E_{1/2} + E_{5/2} + 3G_{3/2}$
19/2	$E_{1/2} + E_{7/2} + G_{3/2} + 2I_{5/2}$	$2E_{1/2} + 2E_{5/2} + 3G_{3/2}$

G.3 Canonical-Basis Relationships

D_3^*	$\mathbb{D}(C_3^z)$	$\mathbb{D}(C_2^x)$
$\lvert E_{1/2}\alpha\rangle, \lvert E_{1/2}\beta\rangle$	$\begin{pmatrix} \frac{1-i\sqrt{3}}{2} & 0 \\ 0 & \frac{1+i\sqrt{3}}{2} \end{pmatrix}$	$\begin{pmatrix} 0 & -i \\ -i & 0 \end{pmatrix}$
$\lvert E_{3/2}\rho_1\rangle$	(-1)	(i)
$\lvert E_{3/2}\rho_2\rangle$	(-1)	$(-i)$

D_4^*	$\mathbb{D}(C_4^z)$	$\mathbb{D}(C_2^x)$
$\lvert E_{1/2}\alpha\rangle, \lvert E_{1/2}\beta\rangle$	$\begin{pmatrix} \frac{1-i}{\sqrt{2}} & 0 \\ 0 & \frac{1+i}{\sqrt{2}} \end{pmatrix}$	$\begin{pmatrix} 0 & -i \\ -i & 0 \end{pmatrix}$
$\lvert E_{3/2}\alpha'\rangle, \lvert E_{3/2}\beta'\rangle$	$\begin{pmatrix} \frac{-1+i}{\sqrt{2}} & 0 \\ 0 & \frac{-1-i}{\sqrt{2}} \end{pmatrix}$	$\begin{pmatrix} 0 & -i \\ -i & 0 \end{pmatrix}$

The components of the fourfold-degenerate $G_{3/2}$ irrep in O^* and I^* are labeled as $\kappa, \lambda, \mu,$ and ν. For a quartet spin, these labels correspond to $M_S = +3/2, +1/2, -1/2,$ and $-3/2$, respectively.

O^*	$\mathbb{D}(C_4^z)$	$\mathbb{D}(C_3^{xyz})$
$\lvert E_{1/2}\alpha\rangle, \lvert E_{1/2}\beta\rangle$	$\frac{1}{\sqrt{2}}\begin{pmatrix} 1-i & 0 \\ 0 & 1+i \end{pmatrix}$	$\begin{pmatrix} \frac{1-i}{2} & \frac{-1-i}{2} \\ \frac{1-i}{2} & \frac{1+i}{2} \end{pmatrix}$
$\lvert E_{5/2}\alpha'\rangle, \lvert E_{5/2}\beta'\rangle$	$\frac{1}{\sqrt{2}}\begin{pmatrix} -1+i & 0 \\ 0 & -1-i \end{pmatrix}$	$\begin{pmatrix} \frac{1-i}{2} & \frac{-1-i}{2} \\ \frac{1-i}{2} & \frac{1+i}{2} \end{pmatrix}$

O^*	$|G_{3/2}\kappa\rangle, |G_{3/2}\lambda\rangle|G_{3/2}\mu\rangle, |G_{3/2}\nu\rangle$

$\mathbb{D}(C_4^z)$

$$\frac{1}{\sqrt{2}}\begin{pmatrix} -1-i & 0 & 0 & 0 \\ 0 & 1-i & 0 & 0 \\ 0 & 0 & 1+i & 0 \\ 0 & 0 & 0 & -1+i \end{pmatrix}$$

$\mathbb{D}(C_3^{xyz})$

$$\frac{1}{4}\begin{pmatrix} -1-i & \sqrt{3}(-1+i) & \sqrt{3}(1+i) & 1-i \\ \sqrt{3}(-1-i) & -1+i & -1-i & \sqrt{3}(-1+i) \\ \sqrt{3}(-1-i) & 1-i & -1-i & \sqrt{3}(1-i) \\ -1-i & \sqrt{3}(1-i) & \sqrt{3}(1+i) & -1+i \end{pmatrix}$$

I^*	$\mathbb{D}(C_5)$	$\mathbb{D}(C_3^{x,y,z})$
$|E_{1/2}\alpha\rangle, |E_{1/2}\beta\rangle$	$\frac{1}{2}\begin{pmatrix} \phi-i & -i\phi^{-1} \\ -i\phi^{-1} & \phi+i \end{pmatrix}$	$\frac{1}{2}\begin{pmatrix} 1-i & -1-i \\ 1-i & 1+i \end{pmatrix}$
$|E_{7/2}\alpha'\rangle, |E_{7/2}\beta'\rangle$	$\frac{1}{2}\begin{pmatrix} -\phi^{-1}-i & i\phi \\ i\phi & -\phi^{-1}+i \end{pmatrix}$	$\frac{1}{2}\begin{pmatrix} 1-i & -1-i \\ 1-i & 1+i \end{pmatrix}$

I^*	$|G_{3/2}\kappa\rangle, |G_{3/2}\lambda\rangle|G_{3/2}\mu\rangle, |G_{3/2}\nu\rangle$

$\mathbb{D}(C_5)$

$$\frac{1}{8}\begin{pmatrix} -\phi^{-1}-i\phi^4 & -\sqrt{3}(2+i) & -\sqrt{3}(\phi^{-1}-i\phi^{-2}) & i\phi^{-3} \\ -\sqrt{3}(2+i) & 3+\phi+i(3-\phi^{-4}) & -i(4+\phi^{-3}) & -\sqrt{3}(\phi^{-1}+i\phi^{-2}) \\ -\sqrt{3}(\phi^{-1}-i\phi^{-2}) & -i(4+\phi^{-3}) & 3+\phi+i(3-\phi^{-4}) & \sqrt{3}(2-i) \\ i\phi^{-3} & -\sqrt{3}(\phi^{-1}+i\phi^{-2}) & \sqrt{3}(2-i) & -\phi^{-1}+i\phi^4 \end{pmatrix}$$

$\mathbb{D}(C_3^{x,y,z})$

$$\frac{1}{4}\begin{pmatrix} -1-i & \sqrt{3}(-1+i) & \sqrt{3}(1+i) & 1-i \\ \sqrt{3}(-1-i) & -1+i & -1-i & \sqrt{3}(-1+i) \\ \sqrt{3}(-1-i) & 1-i & -1-i & \sqrt{3}(1-i) \\ -1-i & \sqrt{3}(1-i) & \sqrt{3}(1+i) & -1+i \end{pmatrix}$$

$I^*I_{5/2}: |5/2\rangle, |3/2\rangle|1/2\rangle, |-1/2\rangle, |-3/2\rangle, |-5/2\rangle$

$\mathbb{D}(C_5)$

$$\frac{1}{32}\begin{pmatrix}
-7-i-\phi(10+5i) & -\sqrt{5}\phi(4-3i) & \sqrt{10}(\phi^{-3}+i\phi^2) \\
-\sqrt{5}\phi(4-3i) & -5-3i+6\phi^{-1}-7i\phi & -\sqrt{2}(2+i)(5\phi-2) \\
\sqrt{10}(\phi^{-3}+i\phi^2) & -\sqrt{2}(2+i)(5\phi-2) & 2\phi^3-2i\phi^2 \\
\sqrt{10}\phi^{-2}(2+i) & -\sqrt{2}(3+2\phi+i-3i\phi) & -2i(8+\phi) \\
\sqrt{5}(\phi^{-3}-i\phi^{-4}) & i(-8+7\phi) & -\sqrt{2}(3+2\phi-i+3i\phi) \\
-i\phi^{-5} & \sqrt{5}(\phi^{-3}+i\phi^{-4}) & -\sqrt{10}\phi^{-2}(2-i)
\end{pmatrix}$$

$$\begin{pmatrix}
\sqrt{10}\phi^{-2}(2+i) & \sqrt{5}(\phi^{-3}-i\phi^{-4}) & -i\phi^{-5} \\
-\sqrt{2}(3+2\phi+i-3i\phi) & i(-8+7\phi) & \sqrt{5}(\phi^{-3}+i\phi^{-4}) \\
-2i(8+\phi) & -\sqrt{2}(3+2\phi-i+3i\phi) & -\sqrt{10}\phi^{-2}(2-i) \\
2\phi^3+2i\phi^2 & \sqrt{2}(2-i)(5\phi-2) & \sqrt{10}(\phi^{-3}-i\phi^2) \\
\sqrt{2}(2-i)(5\phi-2) & -5+3i+6\phi^{-1}+7i\phi & \sqrt{5}\phi(4+3i) \\
\sqrt{10}(\phi^{-3}-i\phi^2) & \sqrt{5}\phi(4+3i) & -7+i-\phi(10-5i)
\end{pmatrix}$$

$\mathbb{D}(C_3^{x,y,z})$

$$\frac{1}{8}\begin{pmatrix}
-1+i & \sqrt{5}(1+i) & \sqrt{10}(1-i) & -\sqrt{10}(1+i) \\
-\sqrt{5}(1-i) & 3(1+i) & \sqrt{2}(1-i) & \sqrt{2}(1+i) \\
-\sqrt{10}(1-i) & \sqrt{2}(1+i) & 2(-1+i) & 2(1+i) \\
-\sqrt{10}(1-i) & -\sqrt{2}(1+i) & 2(-1+i) & -2(1+i) \\
-\sqrt{5}(1-i) & -3(1+i) & \sqrt{2}(1-i) & -\sqrt{2}(1+i) \\
-1+i & -\sqrt{5}(1+i) & \sqrt{10}(1-i) & \sqrt{10}(1+i)
\end{pmatrix}$$

$$\begin{pmatrix}
-\sqrt{5}(1-i) & 1+i \\
3(1-i) & -\sqrt{5}(1+i) \\
-\sqrt{2}(1-i) & \sqrt{10}(1+i) \\
-\sqrt{2}(1-i) & -\sqrt{10}(1+i) \\
3(1-i) & \sqrt{5}(1+i) \\
-\sqrt{5}(1-i) & -1-i
\end{pmatrix}$$

G.4 Direct-Product Tables

D_3^*	$E_{1/2}$	ρ_1	ρ_2
A_1	$E_{1/2}$	ρ_1	ρ_2
A_2	$E_{1/2}$	ρ_2	ρ_1
E	$E_{1/2} + E_{3/2}$	$E_{1/2}$	$E_{1/2}$
$E_{1/2}$	$[A_2 + E] + \{A_1\}$	E	E
ρ_1	E	A_2	A_1
ρ_2	E	A_1	A_2

D_4^*	$E_{1/2}$	$E_{3/2}$
A_1	$E_{1/2}$	$E_{3/2}$
A_2	$E_{1/2}$	$E_{3/2}$
B_1	$E_{3/2}$	$E_{1/2}$
B_2	$E_{3/2}$	$E_{1/2}$
E	$E_{1/2} + E_{3/2}$	$E_{1/2} + E_{3/2}$
$E_{1/2}$	$[A_2 + E] + \{A_1\}$	$B_1 + B_2 + E$
$E_{3/2}$	$B_1 + B_2 + E$	$[A_2 + E] + \{A_1\}$

D_5^*	$E_{1/2}$	$E_{3/2}$	ρ_1	ρ_2
A_1	$E_{1/2}$	$E_{3/2}$	ρ_1	ρ_2
A_2	$E_{1/2}$	$E_{3/2}$	ρ_2	ρ_1
E_1	$E_{1/2} + E_{3/2}$	$E_{1/2} + E_{5/2}$	$E_{3/2}$	$E_{3/2}$
E_2	$E_{3/2} + E_{5/2}$	$E_{1/2} + E_{3/2}$	$E_{1/2}$	$E_{1/2}$
$E_{1/2}$	$[A_2 + E_1] + \{A_1\}$	$E_1 + E_2$	E_2	E_2
$E_{3/2}$	$E_1 + E_2$	$[A_2 + E_2] + \{A_1\}$	E_1	E_1
ρ_1	E_2	E_1	A_2	A_1
ρ_2	E_2	E_1	A_1	A_2

D_6^*	$E_{1/2}(\Gamma_7)$	$E_{5/2}(\Gamma_8)$	$E_{3/2}(\Gamma_9)$
A_1	$E_{1/2}$	$E_{5/2}$	$E_{3/2}$
A_2	$E_{1/2}$	$E_{5/2}$	$E_{3/2}$
B_1	$E_{5/2}$	$E_{1/2}$	$E_{3/2}$
B_2	$E_{5/2}$	$E_{1/2}$	$E_{3/2}$
E_1	$E_{1/2} + E_{3/2}$	$E_{5/2} + E_{3/2}$	$E_{1/2} + E_{5/2}$
E_2	$E_{5/2} + E_{3/2}$	$E_{1/2} + E_{3/2}$	$E_{1/2} + E_{5/2}$
$E_{1/2}$	$[A_2 + E_1] + \{A_1\}$	$B_1 + B_2 + E_2$	$E_1 + E_2$
$E_{5/2}$	$B_1 + B_2 + E_2$	$[A_2 + E_1] + \{A_1\}$	$E_1 + E_2$
$E_{3/2}$	$E_1 + E_2$	$E_1 + E_2$	$[A_2 + B_1 + B_2] + \{A_1\}$

O^*	$E_{1/2}$	$E_{5/2}$	$G_{3/2}$
A_1	$E_{1/2}$	$E_{5/2}$	$G_{3/2}$
A_2	$E_{5/2}$	$E_{1/2}$	$G_{3/2}$
E	$G_{3/2}$	$G_{3/2}$	$E_{1/2} + E_{5/2} + G_{3/2}$
T_1	$E_{1/2} + G_{3/2}$	$E_{5/2} + G_{3/2}$	$E_{1/2} + E_{5/2} + 2G_{3/2}$
T_2	$E_{5/2} + G_{3/2}$	$E_{1/2} + G_{3/2}$	$E_{1/2} + E_{5/2} + 2G_{3/2}$
$E_{1/2}$	$[T_1] + \{A_1\}$	$A_2 + T_2$	$E + T_1 + T_2$
$E_{5/2}$	$A_2 + T_2$	$[T_1] + \{A_1\}$	$E + T_1 + T_2$
$G_{3/2}$	$E + T_1 + T_2$	$E + T_1 + T_2$	$[A_2 + 2T_1 + T_2] + \{A_1 + E + T_2\}$

I^*	$E_{1/2}$	$E_{7/2}$	$G_{3/2}$	$I_{5/2}$
A	$E_{1/2}$	$E_{7/2}$	$G_{3/2}$	$I_{5/2}$
T_1	$E_{1/2} + G_{3/2}$	$I_{5/2}$	$E_{1/2} + G_{3/2} + I_{5/2}$	$E_{7/2} + G_{3/2} + 2I_{5/2}$
T_2	$I_{5/2}$	$E_{7/2} + G_{3/2}$	$E_{7/2} + G_{3/2} + I_{5/2}$	$E_{1/2} + G_{3/2} + 2I_{5/2}$
G	$E_{7/2} + I_{5/2}$	$E_{1/2} + I_{5/2}$	$G_{3/2} + 2I_{5/2}$	$E_{1/2} + E_{7/2} + 2G_{3/2} + 2I_{5/2}$
H	$G_{3/2} + I_{5/2}$	$G_{3/2} + I_{5/2}$	$E_{1/2} + E_{7/2} + G_{3/2} + 2I_{5/2}$	$E_{1/2} + E_{7/2} + 2G_{3/2} + 3I_{5/2}$
$E_{1/2}$	$[T_1] + \{A\}$	G	$T_1 + H$	$T_2 + G + H$
$E_{7/2}$	G	$[T_2] + \{A\}$	$T_2 + H$	$T_1 + G + H$
$G_{3/2}$	$T_1 + H$	$T_2 + H$	$[T_1 + T_2 + G] + \{A + H\}$	$T_1 + T_2 + 2G + 2H$
$I_{5/2}$	$T_2 + G + H$	$T_1 + G + H$	$T_1 + T_2 + 2G + 2H$	$[2T_1 + 2T_2 + G + H] + \{A + G + 2H\}$

G.5 Coupling Coefficients

O^* $A_2 \times G_{3/2}$	$G_{3/2}$			
	κ	λ	μ	ν
$a_2\ \kappa$	0	0	1	0
$a_2\ \lambda$	0	0	0	-1
$a_2\ \mu$	-1	0	0	0
$a_2\ \nu$	0	1	0	0

O^* $E \times E_{1/2}$	$G_{3/2}$			
	κ	λ	μ	ν
$\theta\ \alpha$	0	-1	0	0
$\theta\ \beta$	0	0	1	0
$\epsilon\ \alpha$	0	0	0	-1
$\epsilon\ \beta$	1	0	0	0

O^*

$E \times E_{5/2}$	$G_{3/2}$			
	κ	λ	μ	ν
$\theta\ \alpha'$	0	0	0	-1
$\theta\ \beta'$	1	0	0	0
$\epsilon\ \alpha'$	0	1	0	0
$\epsilon\ \beta'$	0	0	-1	0

O^*

$E \times G_{3/2}$	$E_{1/2}$		$E_{5/2}$		$G_{3/2}$			
	α	β	α'	β'	κ	λ	μ	ν
$\theta\ \kappa$	0	0	0	$\frac{1}{\sqrt{2}}$	$\frac{1}{\sqrt{2}}$	0	0	0
$\theta\ \lambda$	$\frac{1}{\sqrt{2}}$	0	0	0	0	$-\frac{1}{\sqrt{2}}$	0	0
$\theta\ \mu$	0	$-\frac{1}{\sqrt{2}}$	0	0	0	0	$-\frac{1}{\sqrt{2}}$	0
$\theta\ \nu$	0	0	$-\frac{1}{\sqrt{2}}$	0	0	0	0	$\frac{1}{\sqrt{2}}$
$\epsilon\ \kappa$	0	$-\frac{1}{\sqrt{2}}$	0	0	0	0	$\frac{1}{\sqrt{2}}$	0
$\epsilon\ \lambda$	0	0	$\frac{1}{\sqrt{2}}$	0	0	0	0	$\frac{1}{\sqrt{2}}$
$\epsilon\ \mu$	0	0	0	$-\frac{1}{\sqrt{2}}$	$\frac{1}{\sqrt{2}}$	0	0	0
$\epsilon\ \nu$	$\frac{1}{\sqrt{2}}$	0	0	0	0	$\frac{1}{\sqrt{2}}$	0	0

Canonical complex T_1 and T_2 basis functions:

$$T_1: \quad |1\rangle = \frac{1}{\sqrt{2}}\left[-|T_{1x}\rangle - i|T_{1y}\rangle\right]$$

$$|0\rangle = |T_{1z}\rangle$$

$$|-1\rangle = \frac{1}{\sqrt{2}}\left[|T_{1x}\rangle - i|T_{1y}\rangle\right]$$

$$T_2: \quad |1\rangle = \frac{1}{\sqrt{2}}\left[-|T_{2x}\rangle - i|T_{2y}\rangle\right]$$

$$|0\rangle = |T_{2z}\rangle$$

$$|-1\rangle = \frac{1}{\sqrt{2}}\left[|T_{2x}\rangle - i|T_{2y}\rangle\right]$$

O^* $T_1 \times E_{1/2}$	$E_{1/2}$ α	β	$G_{3/2}$ κ	λ	μ	ν
$1\ \alpha$	0	0	1	0	0	0
$0\ \alpha$	$\frac{1}{\sqrt{3}}$	0	0	$\frac{\sqrt{2}}{\sqrt{3}}$	0	0
$-1\ \alpha$	0	$\frac{\sqrt{2}}{\sqrt{3}}$	0	0	$\frac{1}{\sqrt{3}}$	0
$1\ \beta$	$-\frac{\sqrt{2}}{\sqrt{3}}$	0	0	$\frac{1}{\sqrt{3}}$	0	0
$0\ \beta$	0	$-\frac{1}{\sqrt{3}}$	0	0	$\frac{\sqrt{2}}{\sqrt{3}}$	0
$-1\ \beta$	0	0	0	0	0	1

O^* $T_2 \times E_{1/2}$	$E_{5/2}$ α'	β'	$G_{3/2}$ κ	λ	μ	ν
$1\ \alpha'$	0	0	0	0	1	0
$0\ \alpha'$	$\frac{1}{\sqrt{3}}$	0	0	0	0	$-\frac{\sqrt{2}}{\sqrt{3}}$
$-1\ \alpha'$	0	$\frac{\sqrt{2}}{\sqrt{3}}$	$-\frac{1}{\sqrt{3}}$	0	0	0
$1\ \beta'$	$-\frac{\sqrt{2}}{\sqrt{3}}$	0	0	0	0	$-\frac{1}{\sqrt{3}}$
$0\ \beta'$	0	$-\frac{1}{\sqrt{3}}$	$-\frac{\sqrt{2}}{\sqrt{3}}$	0	0	0
$-1\ \beta'$	0	0	0	1	0	0

O^* — $T_1 \times G_{3/2}$

	$E_{1/2}$ α	β	$E_{5/2}$ α'	β'	$G_{3/2}$ κ	λ	μ	ν	$G_{3/2}$ κ	λ	μ	ν
$1\ \kappa$	0	0	$\frac{1}{\sqrt{6}}$	0	0	0	0	0	0	0	0	$\frac{\sqrt{5}}{\sqrt{6}}$
$0\ \kappa$	0	0	0	$-\frac{1}{\sqrt{3}}$	$\frac{\sqrt{3}}{\sqrt{5}}$	0	0	0	$-\frac{1}{\sqrt{15}}$	0	0	0
$-1\ \kappa$	$\frac{1}{\sqrt{2}}$	0	0	0	0	$\frac{\sqrt{2}}{\sqrt{5}}$	0	0	0	$\frac{1}{\sqrt{10}}$	0	0
$1\ \lambda$	0	0	0	$-\frac{1}{\sqrt{2}}$	$-\frac{\sqrt{2}}{\sqrt{5}}$	0	0	0	$-\frac{1}{\sqrt{10}}$	0	0	0
$0\ \lambda$	$-\frac{1}{\sqrt{3}}$	0	0	0	0	$\frac{1}{\sqrt{15}}$	0	0	0	$\frac{\sqrt{3}}{\sqrt{5}}$	0	0
$-1\ \lambda$	0	$\frac{1}{\sqrt{6}}$	0	0	0	0	$\frac{2\sqrt{2}}{\sqrt{15}}$	0	0	0	$-\frac{\sqrt{3}}{\sqrt{10}}$	0
$1\ \mu$	$\frac{1}{\sqrt{6}}$	0	0	0	0	$-\frac{2\sqrt{2}}{\sqrt{15}}$	0	0	0	$\frac{\sqrt{3}}{\sqrt{10}}$	0	0
$0\ \mu$	0	$-\frac{1}{\sqrt{3}}$	0	0	0	0	$-\frac{1}{\sqrt{15}}$	0	0	0	$-\frac{\sqrt{3}}{\sqrt{5}}$	0
$-1\ \mu$	0	0	$-\frac{1}{\sqrt{2}}$	0	0	0	0	$\frac{\sqrt{2}}{\sqrt{5}}$	0	0	0	$\frac{1}{\sqrt{10}}$
$1\ \nu$	0	$\frac{1}{\sqrt{2}}$	0	0	0	0	$-\frac{\sqrt{2}}{\sqrt{5}}$	0	0	0	$-\frac{1}{\sqrt{10}}$	0
$0\ \nu$	0	0	$-\frac{1}{\sqrt{3}}$	0	0	0	0	$-\frac{\sqrt{3}}{\sqrt{5}}$	0	0	0	$\frac{1}{\sqrt{15}}$
$-1\ \nu$	0	0	0	$\frac{1}{\sqrt{6}}$	0	0	0	0	$-\frac{\sqrt{5}}{\sqrt{6}}$	0	0	0

I^* — $T_1 \times E_{1/2}$

	$E_{1/2}$ α	β	$G_{3/2}$ κ	λ	μ	ν
$1\ \alpha$	0	0	1	0	0	0
$0\ \alpha$	$\frac{1}{\sqrt{3}}$	0	0	$\frac{\sqrt{2}}{\sqrt{3}}$	0	0
$-1\ \alpha$	0	$\frac{\sqrt{2}}{\sqrt{3}}$	0	0	$\frac{1}{\sqrt{3}}$	0
$1\ \beta$	$-\frac{\sqrt{2}}{\sqrt{3}}$	0	0	$\frac{1}{\sqrt{3}}$	0	0
$0\ \beta$	0	$-\frac{1}{\sqrt{3}}$	0	0	$\frac{\sqrt{2}}{\sqrt{3}}$	0
$-1\ \beta$	0	0	0	0	0	1

I^* — $T_2 \times E_{1/2}$

	$I_{5/2}$ $\frac{5}{2}$	$\frac{3}{2}$	$\frac{1}{2}$	$-\frac{1}{2}$	$-\frac{3}{2}$	$-\frac{5}{2}$
$1\ \alpha'$	0	$-\frac{1}{4}$	0	$\frac{\sqrt{5}}{2\sqrt{2}}$	0	$-\frac{\sqrt{5}}{4}$
$0\ \alpha'$	$\frac{1}{2\sqrt{2}}$	0	$\frac{1}{2}$	0	$\frac{\sqrt{5}}{2\sqrt{2}}$	0
$-1\ \alpha'$	0	$\frac{\sqrt{5}}{4}$	0	$-\frac{1}{2\sqrt{2}}$	0	$-\frac{3}{4}$
$1\ \beta'$	$\frac{3}{4}$	0	$\frac{1}{2\sqrt{2}}$	0	$-\frac{\sqrt{5}}{4}$	0
$0\ \beta'$	0	$-\frac{\sqrt{5}}{2\sqrt{2}}$	0	$-\frac{1}{2}$	0	$-\frac{1}{2\sqrt{2}}$
$-1\ \beta'$	$\frac{\sqrt{5}}{4}$	0	$-\frac{\sqrt{5}}{2\sqrt{2}}$	0	$\frac{1}{4}$	0

I^*	$T_1 \times G_{3/2}$											
	$E_{1/2}$		$G_{3/2}$				$I_{5/2}$					
	α	β	κ	λ	μ	ν	$\frac{5}{2}$	$\frac{3}{2}$	$\frac{1}{2}$	$-\frac{1}{2}$	$-\frac{3}{2}$	$-\frac{5}{2}$
$1\ \kappa$	0	0	0	0	0	0	1	0	0	0	0	0
$0\ \kappa$	0	0	$\frac{\sqrt{3}}{\sqrt{5}}$	0	0	0	0	$\frac{\sqrt{2}}{\sqrt{5}}$	0	0	0	0
$-1\ \kappa$	$-\frac{1}{\sqrt{2}}$	0	0	$\frac{\sqrt{2}}{\sqrt{5}}$	0	0	0	0	$\frac{1}{\sqrt{10}}$	0	0	0
$1\ \lambda$	0	0	$-\frac{\sqrt{2}}{\sqrt{5}}$	0	0	0	0	$\frac{\sqrt{3}}{\sqrt{5}}$	0	0	0	0
$0\ \lambda$	$\frac{1}{\sqrt{3}}$	0	0	$\frac{1}{\sqrt{15}}$	0	0	0	0	$\frac{\sqrt{3}}{\sqrt{5}}$	0	0	0
$-1\ \lambda$	0	$-\frac{1}{\sqrt{6}}$	0	0	$\frac{2\sqrt{2}}{\sqrt{15}}$	0	0	0	0	$\frac{\sqrt{3}}{\sqrt{10}}$	0	0
$1\ \mu$	$-\frac{1}{\sqrt{6}}$	0	0	$-\frac{2\sqrt{2}}{\sqrt{15}}$	0	0	0	0	$\frac{\sqrt{3}}{\sqrt{10}}$	0	0	0
$0\ \mu$	0	$\frac{1}{\sqrt{3}}$	0	0	$-\frac{1}{\sqrt{15}}$	0	0	0	0	$\frac{\sqrt{3}}{\sqrt{5}}$	0	0
$-1\ \mu$	0	0	0	0	0	$\frac{\sqrt{2}}{\sqrt{5}}$	0	0	0	0	$\frac{\sqrt{3}}{\sqrt{5}}$	0
$1\ \nu$	0	$-\frac{1}{\sqrt{2}}$	0	0	$-\frac{\sqrt{2}}{\sqrt{5}}$	0	0	0	0	$\frac{1}{\sqrt{10}}$	0	0
$0\ \nu$	0	0	0	0	0	$-\frac{\sqrt{3}}{\sqrt{5}}$	0	0	0	0	$\frac{\sqrt{2}}{\sqrt{5}}$	0
$-1\ \nu$	0	0	0	0	0	0	0	0	0	0	0	1

Solutions to Problems

1.1 The diagram for the product $\hat{C}_2^z\,\hat{\imath}$ is the same as in Fig. 1.1, except for the intermediate point P_2, which should be denoted by a circle instead of a cross, since it is now below the gray disc. However, the end point P_3 remains the same, irrespective of the order of the operators. This implies that their commutator vanishes.

1.2 Represent the rotation of the coordinates by the rotational matrix $\mathbb{D}$ as given by

$$\begin{pmatrix} x_2 \\ y_2 \end{pmatrix} = \mathbb{D} \begin{pmatrix} x_1 \\ y_1 \end{pmatrix} = \begin{pmatrix} \cos\alpha & -\sin\alpha \\ \sin\alpha & \cos\alpha \end{pmatrix} \begin{pmatrix} x_1 \\ y_1 \end{pmatrix}$$

$$\begin{pmatrix} x_2 & y_2 \end{pmatrix} = \begin{pmatrix} x_1 & y_1 \end{pmatrix} \mathbb{D}^T = \begin{pmatrix} x_1 & y_1 \end{pmatrix} \begin{pmatrix} \cos\alpha & \sin\alpha \\ -\sin\alpha & \cos\alpha \end{pmatrix}$$

Express the sum $x_2^2 + y_2^2$ as the scalar product of the coordinate row with the coordinate column and verify that this scalar product remains invariant under the matrix transformation.

1.3 In general, the radius does not change if $\mathbb{D}$ is orthogonal, i.e., if

$$\mathbb{D}^T \times \mathbb{D} = \mathbb{I}$$

1.4 Apply the general rule that a displacement of the function corresponds to an opposite coordinate displacement. As a result of the transformation, the function acquires an additional phase factor:

$$\mathcal{T}_a\, e^{ikx} = e^{ik(x-a)} = e^{-ika} e^{ikx}$$

1.5 The action of a rotation about the z-axis can be expressed by a differential operator as

$$\hat{O}(\alpha) = \cos\alpha \left(x\frac{\partial}{\partial x} + y\frac{\partial}{\partial y} \right) + \sin\alpha \left(y\frac{\partial}{\partial x} - x\frac{\partial}{\partial y} \right)$$

The unit element corresponds to $\alpha = 0$, and hence,

$$\hat{E} = \hat{O}(0) = \left(x\frac{\partial}{\partial x} + y\frac{\partial}{\partial y} \right)$$

The angular momentum operator is given by

$$
\begin{aligned}
\mathcal{L}_z &= x p_y - y p_x \\
&= \frac{\hbar}{i} \left(x \frac{\partial}{\partial y} - y \frac{\partial}{\partial x} \right) \\
&= -\frac{\hbar}{i} \lim_{\alpha \to 0} \frac{\hat{O}(\alpha) - \hat{E}}{\alpha}
\end{aligned}
$$

The angular momentum operator thus is proportional to an infinitesimal rotation in the neighborhood of the unit element.

2.1 The condition that $\mathbb{C}$ be unitary gives rise to six equations:

$$
\begin{aligned}
1 &= |a|^2 + |b|^2 \\
1 &= |a|^2 + |c|^2 \\
1 &= |b|^2 + |d|^2 \\
1 &= |c|^2 + |d|^2 \\
0 &= |ac| e^{i(\alpha - \gamma)} + |bd| e^{i(\beta - \delta)} \\
0 &= |ab| e^{i(\alpha - \beta)} + |cd| e^{i(\gamma - \delta)}
\end{aligned}
$$

From these equations it is clear that $|a| = |d|$ and $|b| = |c|$. The phase relationships may be reduced to

$$
e^{i(\beta + \gamma)} = -e^{i(\alpha + \delta)}
$$

With the help of these results the four matrix entries can be rewritten as

$$
\begin{aligned}
|a| e^{i\alpha} &= |a| e^{i(\alpha + \delta)/2} e^{i(\alpha - \delta)/2} \\
|d| e^{i\delta} &= |a| e^{i(\alpha + \delta)/2} e^{-i(\alpha - \delta)/2} \\
|b| e^{i\beta} &= |b| e^{i(\alpha + \delta)/2} e^{i[\beta - \frac{\alpha + \delta}{2}]} \\
|c| e^{i\gamma} &= -|b| e^{i(\alpha + \delta)/2} e^{i[-\beta + \frac{\alpha + \delta}{2}]}
\end{aligned}
$$

The general $U(2)$ matrix may thus be rewritten as

$$
\mathbb{U} = e^{i(\alpha + \delta)/2} \begin{pmatrix} |a| e^{i(\alpha - \delta)/2} & |b| e^{i[\beta - \frac{\alpha + \delta}{2}]} \\ -|b| e^{i[-\beta + \frac{\alpha + \delta}{2}]} & |a| e^{-i(\alpha - \delta)/2} \end{pmatrix}
$$

with $|a|^2 + |b|^2 = 1$. Note that a general phase factor has been taken out. The remaining matrix has determinant $+1$ and is called a special unitary matrix (see further in Chap. 7).

2.2 The relevant integrals are given by

$$
\int_0^{2\pi} e^{-ik\phi} e^{ik\phi} d\phi = [\phi]_0^{2\pi} = 2\pi
$$

$$
\int_0^{2\pi} e^{\pm 2ik\phi} d\phi = \frac{1}{\pm 2ik} [e^{\pm 2ik\phi}]_0^{2\pi} = 0
$$

The normalized cyclic waves are thus given by

$$| \pm k \rangle = \frac{1}{\sqrt{2\pi}} e^{\pm i k \phi}$$

and these waves are orthogonal: $\langle -k | k \rangle = 0$.

2.3 The combination of transposition and complex conjugation is called the *adjoint* operation, indicated by a dagger. A Hermitian matrix is thus self-adjoint. An eigenfunction of this matrix, operating in a function space, may be expressed as a linear combination

$$|\psi_m\rangle = \sum_k c_k |f_k\rangle$$

We may arrange the expansion coefficients as a column vector $\mathbf{c}$. This is called the eigenvector. Its adjoint, $\mathbf{c}^\dagger$, is then the complex-conjugate row vector. The corresponding eigenvalue is denoted as E_m. Now start by writing the eigenvalue equation and multiply left and right with the adjoint eigenvector:

$$\mathbb{H}\mathbf{c} = E_m \mathbf{c}$$
$$\mathbf{c}^\dagger \mathbb{H}\mathbf{c} = E_m \mathbf{c}^\dagger \mathbf{c}$$

Now take the adjoint and use the self-adjoint property of $\mathbb{H}$:

$$\mathbf{c}^\dagger \mathbb{H}^\dagger \mathbf{c} = \bar{E}_m \mathbf{c}^\dagger \mathbf{c}$$
$$\mathbf{c}^\dagger \mathbb{H}\mathbf{c} = \bar{E}_m \mathbf{c}^\dagger \mathbf{c}$$

A comparison of both results shows that the eigenvalue must be equal to its complex conjugate and hence be real. If $\mathbb{H}$ is skew-symmetric, a similar argument shows that the eigenvalue must be imaginary.

3.1 The table is a valid multiplication table of a group that is isomorphic to D_2. The element C is the unit element. There are six ways to assign the three twofold axes to the letters A, B, D.

3.2 Any nonlinear triatomic molecule with three different atoms has only C_s symmetry, e.g., a water molecule with one hydrogen replaced by deuterium. C_2 symmetry requires a nonplanar tetra-atomic molecule, such as H_2O_2. In the free state the dihedral angle of this molecule is almost a right angle (see the figure). To realize C_i symmetry, one needs at least six atoms. Since three atoms are always coplanar, the smallest molecule with no symmetry at all has at least four atoms.
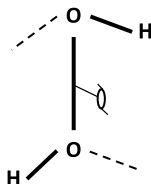
3.3 There are only three regular tesselations of the plane: triangles, squares, and hexagons.

3.4 The rotation generates points that are lying on a circle, perpendicular to the rotation. If the rotational angle is not a rational fraction of a full angle, every time the rotation is repeated, a new point will be generated. To obtain an integer order, the additional requirement is to be added that the original point is retrieved after one full turn.

3.5 Consider a subgroup $H \subset G$ such that $|G|/|H| = 2$. Then the coset expansion of G will be limited to only two cosets:

$$G = H + \hat{g}H$$

Here $\hat{g}$ is a coset generator outside H. The subgroup is normal if the right and left cosets coincide, Since there is only one coset outside H, it is required that

$$\hat{g}H = H\hat{g}$$

Suppose that this equation does not hold. Then this can only mean that there are elements in H such that

$$\hat{h}_x \hat{g} = \hat{h}_y$$

But then the coset generator must be an element of H, which contradicts the staring assumption.

3.6 Soccer ball: I_h. Tennis ball: D_{2d}. Basketball: D_{2h}. Trefoil knot: D_3.

3.7 The figure (from Wikipedia) shows the helix function for $n = 1$. One full turn is realized for $t/a = 2\pi \approx 6.283$. This is a right-handed helix.
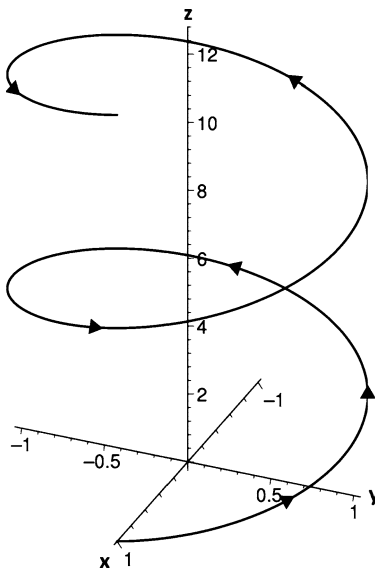
The enantiomeric function reads:

$$x(t) = a \cos\left(\frac{nt}{a}\right)$$

$$y(t) = a \sin\left(-\frac{nt}{a}\right)$$

$$z(t) = t$$

Note that a uniform sign change of t would leave the right-handed helix unchanged. For the discrete helix, the screw symmetry consists of a translation in the z-direction over a distance $2\pi a/m$ in combination with a rotation around the z-axis over an angle $2\pi n/m$. If m is irrational, the helix will not be periodic, and the screw symmetry is lost.

4.1 The site symmetry of a cube is T_h. The cube is an invariant of its site group and transforms as a_g in T_h. The set of five cubes thus spans the induced representation: $aT_h \uparrow I_h$. Applying the Frobenius theorem to the subduction (see Sect. C.1), one obtains

$$aT_h \uparrow I_h = A_g + G_g \tag{1}$$

4.2 The irreps can be obtained from the induction table in Sect. C.2, as $\Gamma_\pi C_{3v} \uparrow T_d$:

$$\Gamma_\pi C_{3v} \uparrow T_d = E + T_1 + T_2 \tag{2}$$

The SALCs shown span the tetrahedral E irrep, the one on the left is the E_θ component, and the one on the right is the E_ϵ component. Note that they transform into each other by rotating all π-orbitals over $90°$ in the same sense [13].

4.3 The 24 carbon atoms of coronene form three orbits: two orbits of six atoms, corresponding to the internal hexagon and to the six atoms on the outer ring that have bonds to the inner ring, and one orbit of the twelve remaining atoms. The elements of the 6-orbit occupy sites of C_{2v}' symmetry, based on $\hat{C}_2', \hat{\sigma}_h, \hat{\sigma}_v$ in D_{6h}. The p_z orbitals on these sites transform as b_1, and hence the induced irreps are as in the case of benzene:

$$b_1 C_{2v} \uparrow D_{6h} = B_{2g} + A_{2u} + E_{1g} + E_{2u} \tag{3}$$

The remaining 12-orbit connects carbon atoms with only C_s site symmetry, the p_z orbitals on these sites transforming as a''. The induced irreps read:

$$a'' C_s \uparrow D_{6h} = B_{1g} + B_{2g} + A_{1u} + A_{2u} + 2E_{1g} + 2E_{2u} \tag{4}$$

The A_{1u} and B_{1g} irreps only appear in the 12-orbit, so we can infer that the molecular orbitals with this symmetry will entirely be localized on the 12-orbit. The SALCs can easily be constructed, as they should be antisymmetric with respect to the $\hat{\sigma}_v$ planes in order not to hybridize with the SALCs based on the 6-orbits.
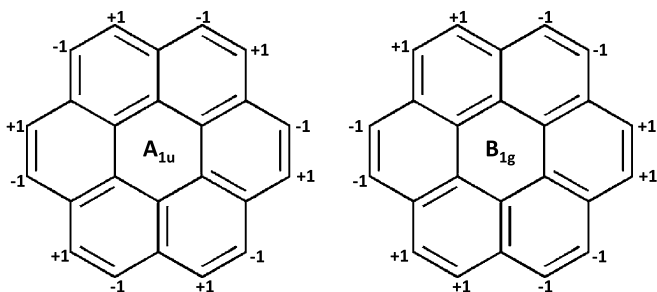
4.4 The tangential π-orbitals transform as Γ_π in the C_{5v} site group of I_h. According to Sect. C.2, one has:

$$\Gamma_\pi \, C_{5v} \uparrow I_h = T_{1g} + T_{1u} + G_g + G_u + H_g + H_u$$

4.5 When the projector that generated the component is characterized as $\hat{P}_{kl}^{\Gamma_i}$, the other components may be found by varying the k index.

4.6 Act with an operator $\hat{S}$ on the projector and carry out the substitution $\hat{R} = \hat{S}^{-1}\hat{T}$:

$$\hat{S}\hat{P}_{11}^{\Gamma_0} = \hat{S}\frac{1}{|G|}\sum_R \hat{R}$$

$$= \frac{1}{|G|}\sum_R \hat{S}\hat{R} = \frac{1}{|G|}\sum_T \hat{T} = \hat{P}_{11}^{\Gamma_0}$$

4.7 Applying the inverse transformation to the SALCs of the hydrogens in ammonia yields

$$\left(|sp_A^2\rangle \quad |sp_B^2\rangle \quad |sp_C^2\rangle\right) = \left(|2s\rangle \quad |2p_x\rangle \quad |2p_y\rangle\right) \begin{pmatrix} \frac{1}{\sqrt{3}} & \frac{1}{\sqrt{3}} & \frac{1}{\sqrt{3}} \\ \frac{2}{\sqrt{6}} & -\frac{1}{\sqrt{6}} & -\frac{1}{\sqrt{6}} \\ 0 & \frac{1}{\sqrt{2}} & -\frac{1}{\sqrt{2}} \end{pmatrix}$$

4.8 This mode transforms as E_y. It can be written as a linear combination of a radial and a tangent mode:

$$Q = \frac{-1}{\sqrt{2}}Q_y^{\text{rad}} + \frac{1}{\sqrt{2}}Q_y^{\text{tan}}$$

with

$$Q_y^{\text{rad}} = \frac{1}{\sqrt{2}}(\Delta R_B - \Delta R_C)$$

$$Q_y^{\text{tan}} = \frac{1}{\sqrt{6}}R(2\Delta\phi_A - \Delta\phi_B - \Delta\phi_C)$$

This mode preserves the center of mass and is a genuine normal mode.

4.9 Since all irreps are one-dimensional, the characters can only consist of a phase factor:

$$\mathbb{D}(C_5) = e^{i\lambda}\mathbb{I} \tag{5}$$

The fifth power of the generator will yield the unit element, and hence,

$$e^{5i\lambda} = 1 \tag{6}$$

This is the Euler equation. Its solutions are the characters in the table of C_5, as given in Appendix A.

4.10 The product of inversion with a $\hat{C}_2$ axis must yield a reflection plane, perpendicular to this axis. As an example, a product of type $\hat{\iota} \cdot \hat{C}_2'$ must yield a reflection plane of $\hat{\sigma}_d$ type, as this is perpendicular to the primed twofold axis. For the one-dimensional irreps of D_{6h}, one thus should have

$$\chi(\iota)\chi(C_2') = \chi(\sigma_d) \tag{7}$$

This is indeed verified to be the case.

4.11 The a_2'' distortion is antisymmetric with respect to $3\hat{C}_2$, $\hat{\sigma}_h$, and $2\hat{S}_3$. As a result, when the mode is launched, all these symmetry elements will be destroyed, and the symmetry reduces to the subgroup C_{3v}. In general, the result of a distortion will always be the maximal subgroup for which the distortion is totally symmetric [14].

4.12 The group of this fullerene is D_{6d}. The 24 atoms separate into two orbits: a 12-orbit containing the top and bottom hexagons and another 12-orbit containing the crown of the 12 atoms, numbered from 7 to 18. In both cases the site group is only C_s, and hence both orbits will span the same irreps:

$$a'C_s \uparrow D_{6d} = A_1 + B_2 + E_1 + E_2 + E_3 + E_4 + E_5$$

Quite remarkably, the Hückel spectrum for this fullerene has a nonbonding level of E_4 symmetry.

5.1 Let $\mathbf{r}_i$ and $\mathbf{r}_j$ denote the position vectors of electrons i and j. The electron repulsion operator contains the distance between both electrons as $|\mathbf{r}_i - \mathbf{r}_j|$. The matrix $\mathbb{D}(R)$ expresses the transformation of the Cartesian coordinates under a rotation. This matrix will also rotate the coordinate *differences*:

$$\hat{R}\begin{pmatrix} x_i - x_j \\ y_i - y_j \\ z_i - z_j \end{pmatrix} = \mathbb{D}(R)\begin{pmatrix} x_i - x_j \\ y_i - y_j \\ z_i - z_j \end{pmatrix} \tag{8}$$

Exactly as in the derivation for Problem 1.2, the square of the distance between the two electrons is then found to be invariant under any orthogonal transformation of the coordinates.

5.2 For the G irrep, it is noted from Sect. C.1 that a tetrahedral splitting field will branch G into $A + T$. It thus acts as a splitting field to isolate the unique Ga component. Symmetry adaptation to $\hat{C}_2^z$ will yield two totally symmetric components, one of which will be the Ga already obtained; the remaining one is

then Gz. The corresponding Gx and Gy may then be found by cyclic permutation under the $\hat{C}_3^{xyz}$ axis.

For the H irrep, one may make use of the $\hat{C}_3^{xyz}$ axis again. It resolves H into $A_1 + 2E$. This unique A_1 component will be the sum $H\xi + H\eta + H\zeta$. We can project the $H\zeta$ component out of this sum by using the $\hat{C}_2^z$ axis. Although the H level subduces three totally symmetric irreps in C_2, there will be no contamination with $H\theta$ and $H\epsilon$ since these were already removed in the first step by projecting out the trigonal A_1.

5.3 The total number of nuclear permutations and permutation-inversions for CH_3BF_2 is 24. This is the product of six permutations of the protons, two permutations of the fluorine nuclei, and the binary group of the spatial inversion. However, as the fluxionality of this molecule is limited to free rotations of the methyl group, the operations should be limited to those permutations or permutation-inversions that lead to structures that can be rotated back to the original frame *or to a rotamer of this frame*. Only half of the operations will comply with this requirement. As an example, the odd permutations of the protons are not allowed since the resulting structure cannot be turned into the original one by outer rotations or by rotations of the methyl group around the C-B bond. The results are given in [15]. The corresponding symmetry group is isomorphic with D_{3h}.

5.4 Ferrocene is a molecule with two identical coaxial rotors. Its nuclear permutation-inversion group consists of 100 elements. It has a halving rotational subgroup of 50 proper permutations: for each of the cyclo-pentadienyl rings, there are 5 cyclic permutation operations, yielding a total of $5^2 = 25$ operations, and this number must be doubled to account for the permutation of the upper and lower rings. In addition, there is a coset of improper permutation-inversions containing the other 50 elements. This coset also contains two kinds of elements. In the table we summarize the structure of the group. The carbon atoms are numbered $1, \ldots, 5$ in the upper ring and $6, \ldots, 10$ in the lower ring.

Nuclear permutation-inversion group for ferrocene (u and l refer to upper and lower rotor)

	$\hat{R}$	#
$C_5^u \times C_5^l$	(12345)	25
(ul)	(16) (2, 10) (39) (48) (57)	25
$5\hat{\sigma}_v^u \times 5\hat{\sigma}_v^l$	(25) (34) (7, 10) (89)*	25
$(ul)^*$	(16) (27) (38) (49) (5, 10)*	25

6.1 The $(t_{1u})^2$ configuration gives rise to 15 states. The direct product decomposes as follows (see Appendix D):

$$T_{1u} \times T_{1u} = [A_{1g} + E_g + T_{2g}] + \{T_{1g}\}$$

The symmetrized part will give rise to six singlet functions, while there are nine triplet substates, forming a $^3T_{1g}$ multiplet. Since the 3-electron Ψ state is a

quartet, the singlet states cannot contribute, and we need to couple the triplet to a $^2T_{1u}$ state, resulting from a $(t_{1u})^1$ configuration. The orbital part of the triplet is obtained from the $T_1 \times T_1 = T_1$ coupling table in Appendix F:

$$|T_{1g}x\rangle = \frac{1}{\sqrt{2}}\left[-y(1)z(2) + z(1)y(2)\right]$$

$$|T_{1g}y\rangle = \frac{1}{\sqrt{2}}\left[x(1)z(2) - z(1)x(2)\right]$$

$$|T_{1g}z\rangle = \frac{1}{\sqrt{2}}\left[-x(1)y(2) + y(1)x(2)\right]$$

The coupling with the third electron can yield A_{1u}, E_u, T_{1u}, and T_{2u} states. Our results is based on the A_{1u} product. This yields

$$A_{1u} = \frac{1}{\sqrt{3}}\left[|T_{1g}x\rangle|x(3)\rangle + |T_{1g}y\rangle|y(3)\rangle + |T_{1g}z\rangle|z(3)\rangle\right]$$

$$= -\frac{1}{\sqrt{6}}\begin{vmatrix} x(1) & y(1) & z(1) \\ x(2) & y(2) & z(2) \\ x(3) & y(3) & z(3) \end{vmatrix}$$

This should be multiplied by the product of the three α-spins, $\alpha_1\alpha_2\alpha_3$, to obtain the $^4A_{1u}$ ground state of the $(t_{1u})^3$ configuration.

6.2 The JT problem is determined by the symmetrized direct product of T_{1u}. As we have seen in the previous problem, this product contains $A_{1g} + E_g + T_{2g}$. Since A_{1g} modes do not break the symmetry, the JT problem is of type $T_1 \times (e+t_2)$. In the linear problem only two force elements are required. The distortion matrix is thus as follows:

$$\mathcal{H}' = \frac{F_E}{\sqrt{6}}\begin{pmatrix} Q_\theta & 0 & 0 \\ 0 & Q_\theta & 0 \\ 0 & 0 & -2Q_\theta \end{pmatrix} + \frac{F_T}{\sqrt{2}}\begin{pmatrix} 0 & -Q_\zeta & -Q_\eta \\ -Q_\zeta & 0 & -Q_\xi \\ -Q_\eta & 0_\xi & 0 \end{pmatrix}$$

6.3 The magnetic dipole operator transforms as T_{1g}, while the direct square of e_g irreps yields $A_{1g} + A_{2g} + E_g$. Since the operator irrep is not contained in the product space, the selection rules will not allow a dipole matrix element between e_g orbitals.

6.4 We first draw a simple diagram representing the R-conformation. The point group is C_2. The twofold-axis is oriented along the y-direction, and the centers of the two chromophores are placed on the positive and negative x-axes. The dipole moments are then oriented as

$$\boldsymbol{\mu}_1 = \mu\left(0, \cos\frac{\alpha}{2}, -\sin\frac{\alpha}{2}\right)$$

$$\boldsymbol{\mu}_2 = \mu\left(0, \cos\frac{\alpha}{2}, \sin\frac{\alpha}{2}\right)$$
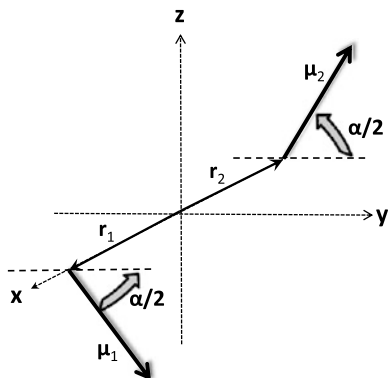
The exciton states on both chromophores are interchanged by the twofold axis and can be recombined to yield a symmetric and an antisymmetric combination, denoted as A and B, respectively. One has:

$$|\Psi_A\rangle = \frac{1}{\sqrt{2}}\big(|\Psi_1\rangle + |\Psi_2\rangle\big)$$
$$|\Psi_B\rangle = \frac{1}{\sqrt{2}}\big(|\Psi_1\rangle - |\Psi_2\rangle\big)$$

The corresponding transition dipoles are oriented along the positive y- and negative z-direction, respectively:

$$\boldsymbol{\mu}_A = \sqrt{2}\mu\left(0, \cos\frac{\alpha}{2}, 0\right)$$
$$\boldsymbol{\mu}_B = \sqrt{2}\mu\left(0, 0, -\sin\frac{\alpha}{2}\right)$$

The dipole-dipole interaction is given by

$$V_{12} = \frac{1}{4\pi\epsilon_0}\frac{\cos\alpha}{R_{12}^3} \tag{9}$$

For $\alpha < \pi/2$, the dipole orientation is repulsive. As a result, the in-phase coupled exciton state $|\Psi_A\rangle$ will be at higher energy than the out-of-phase $|\Psi_B\rangle$ state. Finally, we also calculate the magnetic transition dipoles, using the expressions from Sect. 6.8:

$$\mathbf{m}_A = \frac{i\pi\nu}{\sqrt{2}}(\mathbf{r}_1 \times \boldsymbol{\mu}_1 + \mathbf{r}_2 \times \boldsymbol{\mu}_2) = \frac{i\pi\nu\mu}{\sqrt{2}}R_{12}\sin\frac{\alpha}{2}(0, 1, 0)$$
$$\mathbf{m}_B = \frac{i\pi\nu}{\sqrt{2}}(\mathbf{r}_1 \times \boldsymbol{\mu}_1 - \mathbf{r}_2 \times \boldsymbol{\mu}_2) = \frac{i\pi\nu\mu}{\sqrt{2}}R_{12}\cos\frac{\alpha}{2}(0, 0, 1)$$

These results are now combined in the Rosenfeld equation to yield the rotatory strength of both exciton states:

$$\mathcal{R}_A = \frac{\pi\nu\mu^2}{2}R_{12}\sin\alpha$$

$$\mathcal{R}_B = -\frac{\pi \nu \mu^2}{2} R_{12} \sin \alpha$$

This result predicts a normal CD sign, with a lower negative branch (B-state) and an upper positive branch (A-state) [16]. This is a typical right-handed helix, corresponding to a rotation of the dipoles in the right-handed sense when going from chromophore 1 to chromophore 2 along the inter-chromophore axis. In the S-conformation the sign of α will change, and the CD spectrum will be inverted.

6.5 The direct square of the e-irrep in D_{2d} yields four coupled states:

$$e \times e = A_1 + A_2 + B_1 + B_2 \tag{10}$$

The corresponding coupling coefficients are given in the table below. This table is almost the same as the table for D_4 in Appendix F, but note that B_1 and B_2 are interchanged. Such details are important, and therefore we draw again a simple picture of the molecule in a Cartesian system. Both in D_4 and in D_{2d}, the B_1 and B_2 irreps are distinguished by their symmetry with respect to the $\hat{C}_2'$ axes.

D_{2d} $E \times E$	A_1 a_1	A_2 a_2	B_1 b_1	B_2 b_2
$x\ x$	$\frac{1}{\sqrt{2}}$	0	0	$-\frac{1}{\sqrt{2}}$
$y\ y$	$\frac{1}{\sqrt{2}}$	0	0	$\frac{1}{\sqrt{2}}$
$x\ y$	0	$\frac{1}{\sqrt{2}}$	$\frac{1}{\sqrt{2}}$	0
$y\ x$	0	$-\frac{1}{\sqrt{2}}$	$\frac{1}{\sqrt{2}}$	0

In the orientation of twisted ethylene, as indicated in the figure below, the directions of these axes are along the bisectors of x and y. In contrast, in the standard orientation for D_4 they are *along* the x and y axes, while the bisector directions coincide with the $\hat{C}_2''$ axes, and hence the interchange between B_1 and B_2.
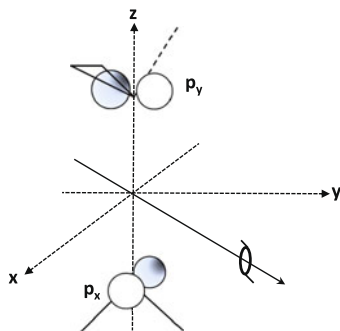
Note that the two-electron states are symmetrized, except the A_2 combination. The symmetrized states will combine with singlet spin states, while the A_2 state will be a triplet. One thus has:

$$^1A_1 = \frac{1}{\sqrt{2}}(x(1)x(2) + y(1)y(2))\frac{1}{\sqrt{2}}(\alpha(1)\beta(2) - \beta(1)\alpha(2))$$

$$= \frac{1}{\sqrt{2}}(|(x\alpha)(x\beta)| + |(y\alpha)(y\beta)|)$$

$$^1B_1 = \frac{1}{\sqrt{2}}(|(x\alpha)(y\beta)| + |(y\alpha)(x\beta)|)$$

$$^1B_2 = \frac{1}{\sqrt{2}}(-|(x\alpha)(x\beta)| + |(y\alpha)(y\beta)|)$$

$$^3A_2 = |(x\alpha)(y\alpha)|$$

The $^1A_1$ and $^1B_2$ states are the *zwitterionic states*, while the $^1B_1$ and $^3A_2$ states are called the *diradical* states. It is clear from the expressions that in both cases the two radical carbon sites are neutral. The zwitterionic states are easily polarizable though.

6.6 The carbon atoms form two orbits. The p_z orbital on the central atom is in the center of the symmetry group and transforms as a_2''. The three methylene orbitals are in C_{2v} sites, transforming as the b_2 irrep of the site group, i.e., they are antisymmetric with respect to $\hat{\sigma}_h$ and symmetric with respect to $\hat{\sigma}_v$. The induced representation is

$$b_2 C_{2v} \uparrow D_{3h} = a_2'' + e'' \tag{11}$$

The SALCs are entirely similar to the hydrogen SALCs in the case of ammonia; this implies, for instance, that the component labeled x is symmetric under the vertical symmetry plane through atom A. It will be antisymmetric for the twofold-axis going through atom A since the relevant orbital is of p_z type:

$$|\Psi_a\rangle = \frac{1}{\sqrt{3}}(|p_A\rangle + |p_B\rangle + |p_C\rangle)$$

$$|\Psi_x\rangle = \frac{1}{\sqrt{6}}(2|p_A\rangle - |p_B\rangle - |p_C\rangle)$$

$$|\Psi_y\rangle = \frac{1}{\sqrt{2}}(|p_B\rangle - |p_C\rangle)$$

The a_2'' orbitals interact to yield bonding and antibonding combinations at $E = \alpha \pm \sqrt{3}\beta$. Since the graph is bipartite, the remaining e'' orbitals are neces-

sarily nonbonding and will be occupied by two electrons. The direct square of this irrep yields symmetrized A'_1 and E' states and an antisymmetrized A'_2 state. The expressions for these states are obtained from the coupling coefficients for D_3 in Appendix F:

$$^1A'_1 = \frac{1}{\sqrt{2}}\big(x(1)x(2) + y(1)y(2)\big)\frac{1}{\sqrt{2}}\big(\alpha(1)\beta(2) - \beta(1)\alpha(2)\big)$$

$$= \frac{1}{\sqrt{2}}\big(\big|(x\alpha)(x\beta)\big| + \big|(y\alpha)(y\beta)\big|\big)$$

$$^1E'_x = \frac{1}{\sqrt{2}}\big(\big|(x\alpha)(y\beta)\big| + \big|(y\alpha)(x\beta)\big|\big)$$

$$^1E'_y = \frac{1}{\sqrt{2}}\big(-\big|(x\alpha)(x\beta)\big| + \big|(y\alpha)(y\beta)\big|\big)$$

$$^3A_2 = \big|(x\alpha)(y\alpha)\big|$$

Note that the distinction between zwitterionic and diradical states does not hold in this case. Formally, TMM can be described as a valence isomer between three configurations in which one of the peripheral atoms has a double bond to the central atom and the other two sites carry an unpaired electron.

7.1 In a cube the d-shell also splits in $e_g + t_{2g}$, but the ordering is reversed. Explicit calculation of the potential shows that the splitting is reduced by a factor 8/9:

$$\Delta_{\text{cube}} = -\frac{8}{9}\Delta_{\text{octahhedron}}$$

7.2 Perform the matrix multiplication and verify that the product matrix is of Cayley–Klein form. The multiplication is not commutative:

$$\begin{pmatrix} a_1 & b_1 \\ -\bar{b}_1 & \bar{a}_1 \end{pmatrix} \times \begin{pmatrix} a_2 & b_2 \\ -\bar{b}_2 & \bar{a}_2 \end{pmatrix} = \begin{pmatrix} a_1a_2 - b_1\bar{b}_2 & a_1b_2 + \bar{a}_2b_1 \\ -\bar{a}_1\bar{b}_2 - a_2\bar{b}_1 & \bar{a}_1\bar{a}_2 - \bar{b}_1b_2 \end{pmatrix} \quad (12)$$

7.3 The double group D_3^* contains 12 elements. In Table 7.5 we have listed the six representation matrices for the elements on the positive hemisphere. The $\hat{C}_2^A$ axis is along the x-direction, $\hat{C}_2^B$ is at $-60°$ and $\hat{C}_2^C$ is at $+60°$. The derivation of the multiplication table and the underlying class structure (see Table 7.6) is based on a straightforward matrix multiplication.

Multiplication table for the double group D_3^*

D_3^*	$\hat{E}$	$\hat{C}_3$	$\hat{C}_3^2$	$\aleph\hat{C}_3$	$\aleph\hat{C}_3^2$	$\aleph$	$\hat{C}_2^A$	$\hat{C}_2^B$	$\hat{C}_2^C$	$\aleph\hat{C}_2^A$	$\aleph\hat{C}_2^B$	$\aleph\hat{C}_2^C$
$\hat{E}$	$\hat{E}$	$\hat{C}_3$	$\hat{C}_3^2$	$\aleph\hat{C}_3$	$\aleph\hat{C}_3^2$	$\aleph$	$\hat{C}_2^A$	$\hat{C}_2^B$	$\hat{C}_2^C$	$\aleph\hat{C}_2^A$	$\aleph\hat{C}_2^B$	$\aleph\hat{C}_2^C$
$\hat{C}_3$	$\hat{C}_3$	$\hat{C}_3^2$	$\aleph$	$\aleph\hat{C}_3^2$	$\hat{E}$	$\aleph\hat{C}_3$	$\hat{C}_2^C$	$\hat{C}_2^A$	$\aleph\hat{C}_2^B$	$\aleph\hat{C}_2^C$	$\aleph\hat{C}_2^A$	$\hat{C}_2^B$
$\hat{C}_3^2$	$\hat{C}_3^2$	$\aleph$	$\aleph\hat{C}_3$	$\hat{E}$	$\hat{C}_3$	$\aleph\hat{C}_3^2$	$\aleph\hat{C}_2^B$	$\hat{C}_2^C$	$\aleph\hat{C}_2^A$	$\hat{C}_2^B$	$\aleph\hat{C}_2^C$	$\hat{C}_2^A$
$\aleph\hat{C}_3$	$\aleph\hat{C}_3$	$\aleph\hat{C}_3^2$	$\hat{E}$	$\hat{C}_3^2$	$\aleph$	$\hat{C}_3$	$\aleph\hat{C}_2^C$	$\aleph\hat{C}_2^A$	$\hat{C}_2^B$	$\hat{C}_2^C$	$\hat{C}_2^A$	$\aleph\hat{C}_2^B$
$\aleph\hat{C}_3^2$	$\aleph\hat{C}_3^2$	$\hat{E}$	$\hat{C}_3$	$\aleph$	$\aleph\hat{C}_3$	$\hat{C}_3^2$	$\hat{C}_2^B$	$\aleph\hat{C}_2^C$	$\hat{C}_2^A$	$\aleph\hat{C}_2^B$	$\hat{C}_2^C$	$\aleph\hat{C}_2^A$
$\aleph$	$\aleph$	$\aleph\hat{C}_3$	$\aleph\hat{C}_3^2$	$\hat{C}_3$	$\hat{C}_3^2$	$\hat{E}$	$\aleph\hat{C}_2^A$	$\aleph\hat{C}_2^B$	$\aleph\hat{C}_2^C$	$\hat{C}_2^A$	$\hat{C}_2^B$	$\hat{C}_2^C$
$\hat{C}_2^A$	$\hat{C}_2^A$	$\hat{C}_2^B$	$\aleph\hat{C}_2^C$	$\aleph\hat{C}_2^B$	$\hat{C}_2^C$	$\aleph\hat{C}_2^A$	$\aleph$	$\aleph\hat{C}_3$	$\hat{C}_3^2$	$\hat{E}$	$\hat{C}_3$	$\aleph\hat{C}_3^2$
$\hat{C}_2^B$	$\hat{C}_2^B$	$\aleph\hat{C}_2^C$	$\aleph\hat{C}_2^A$	$\hat{C}_2^C$	$\hat{C}_2^A$	$\aleph\hat{C}_2^B$	$\hat{C}_3^2$	$\aleph$	$\hat{C}_3$	$\aleph\hat{C}_3^2$	$\hat{E}$	$\aleph\hat{C}_3$
$\hat{C}_2^C$	$\hat{C}_2^C$	$\hat{C}_2^A$	$\hat{C}_2^B$	$\aleph\hat{C}_2^A$	$\aleph\hat{C}_2^B$	$\aleph\hat{C}_2^C$	$\aleph\hat{C}_3$	$\aleph\hat{C}_3^2$	$\aleph$	$\hat{C}_3$	$\hat{C}_3^2$	$\hat{E}$
$\aleph\hat{C}_2^A$	$\aleph\hat{C}_2^A$	$\aleph\hat{C}_2^B$	$\hat{C}_2^C$	$\hat{C}_2^B$	$\aleph\hat{C}_2^C$	$\hat{C}_2^A$	$\hat{E}$	$\hat{C}_3$	$\aleph\hat{C}_3^2$	$\aleph$	$\aleph\hat{C}_3$	$\hat{C}_3^2$
$\aleph\hat{C}_2^B$	$\aleph\hat{C}_2^B$	$\hat{C}_2^C$	$\hat{C}_2^A$	$\aleph\hat{C}_2^C$	$\aleph\hat{C}_2^A$	$\hat{C}_2^B$	$\aleph\hat{C}_3^2$	$\hat{E}$	$\aleph\hat{C}_3$	$\hat{C}_3^2$	$\aleph$	$\hat{C}_3$
$\aleph\hat{C}_2^C$	$\aleph\hat{C}_2^C$	$\aleph\hat{C}_2^A$	$\aleph\hat{C}_2^B$	$\hat{C}_2^A$	$\hat{C}_2^B$	$\hat{C}_2^C$	$\hat{C}_3$	$\hat{C}_3^2$	$\hat{E}$	$\aleph\hat{C}_3$	$\aleph\hat{C}_3^2$	$\aleph$

7.4 The action of the spin operators on the components of a spin-triplet can be found by acting on the coupled states, as summarized in Table 7.2. As an example, where we have added the electron labels 1 and 2 for clarity:

$$S_x|+1\rangle = S_x\big[|\alpha_1\rangle|\alpha_2\rangle\big] = \big[S_x|\alpha_1\rangle\big]|\alpha_2\rangle + |\alpha_1\rangle\big[S_x|\alpha_2\rangle\big]$$

$$= \frac{\hbar}{2}\big[|\beta_1\rangle|\alpha_2\rangle + |\alpha_1\rangle|\beta_2\rangle\big] = \frac{\hbar}{\sqrt{2}}|0\rangle$$

$$S_y|-1\rangle = -\frac{i\hbar}{\sqrt{2}}|0\rangle$$

These results can be generalized as follows:

$$S_z|M_S\rangle = \hbar M_S|M_S\rangle$$

$$(S_x \pm i S_y)|M_S\rangle = \hbar\big[(S \mp M_S)(S \pm M_s + 1)\big]^{\frac{1}{2}}|M_s \pm 1\rangle$$

The action of the spin Hamiltonian in the fictitious spin basis gives then rise to the following Hamiltonian matrix (in units of μ_B):

$\mathcal{H}_{Ze}$	$|0\rangle$	$|+1\rangle$	$|-1\rangle$
$\langle 0|$	0	$g_\perp \frac{1}{\sqrt{2}}(B_x + i B_y)$	$g_\perp \frac{1}{\sqrt{2}}(B_x - i B_y)$
$\langle +1|$	$g_\perp \frac{1}{\sqrt{2}}(B_x - i B_y)$	$g_{\|}B_z$	0
$\langle -1|$	$g_\perp \frac{1}{\sqrt{2}}(B_x + i B_y)$	0	$-g_{\|}B_z$

We can now identify these expressions with the actual matrix elements in the basis of the three D_3 components, keeping in mind the relationship be-

tween the complex and real triplet basis, as given in Eq. (7.39). One obtains:

$$\langle 0|\mathcal{H}_{Ze}|+1\rangle = -\frac{1}{\sqrt{2}}\langle A_1|\mathcal{H}|E_x+iE_y\rangle = \frac{1}{\sqrt{2}}\big[-a+d+i(-b-c)\big]$$

$$\langle 0|\mathcal{H}_{Ze}|-1\rangle = \frac{1}{\sqrt{2}}\langle A_1|\mathcal{H}|E_x-iE_y\rangle = \frac{1}{\sqrt{2}}\big[a+d+i(b-c)\big]$$

$$\langle \pm 1|\mathcal{H}_{Ze}|\pm 1\rangle = \frac{1}{2}\big[\langle x|\mathcal{H}|x\rangle + \langle y|\mathcal{H}|y\rangle \pm i\big(\langle x|\mathcal{H}|y\rangle - \langle y|\mathcal{H}|x\rangle\big)\big] = \pm f$$

From these equations the parameters may be identified as follows:

$$a = 0$$
$$b = -g_\perp B_y$$
$$c = 0$$
$$d = g_\perp B_x$$
$$e = 0$$
$$f = g_{||} B_z$$

The Zeeman Hamiltonian does not include the zero-field splitting between the A_1 and E states. This can be rendered by a second-order spin operator, which transforms as the octahedral $E_g\theta$ quadrupole component:

$$\mathcal{H}_{ZF} = \frac{D}{3\hbar^2}\big(2\tilde{S}_z^2 - \tilde{S}_x^2 - \tilde{S}_y^2\big) = \frac{D}{\hbar^2}\left(\tilde{S}_z^2 - \frac{1}{3}\tilde{S}^2\right)$$

One then obtains

$$D = 3\Delta$$

7.5 The action of the components of the fictitious spin operator on the Γ_8 basis is dictated by the general expressions for the action of the spin operators on the $S = \frac{3}{2}$ basis functions. It is verified that the spin-Hamiltonian that generates the J_p part of the matrix precisely corresponds to

$$\mathcal{H}_p = J_p \mathbf{B} \cdot \tilde{\mathbf{S}}$$

The fictitious spin operator indeed transforms as a T_1 operator and has the tensorial rank of a p-orbital. However, as we have shown, the full Hamiltonian also includes a J_f part, which involves an f-like operator. To mimic this part by a spin Hamiltonian, one thus will need a symmetrized triple product of the fictitious spin, which will embody an f-tensor, transforming in the octahedral symmetry as the T_1 irrep. These f-functions can be found in Table 7.1 and are of type $z(5z^2 - 3r^2)$. But beware! To find the corresponding spin operator, it is not sufficient simply to substitute the Cartesian variables by the corresponding spinor components, i.e., z by $\tilde{S}_z$, etc.; indeed, while products of x, y, and z are commutative, the products of the corresponding operators are not. Hence, when constructing the octupolar product

of the spin components, products of noncommuting operators must be fully symmetrized. For the f_{z^3} function, this is the case for the functions $3zx^2$ and $3xy^2$, which are parts of $3zr^3$. As an example, the operator analogue of $3zx^2$ reads

$$3zx^2 \to \tilde{S}_z \tilde{S}_x \tilde{S}_x + \tilde{S}_x \tilde{S}_z \tilde{S}_x + \tilde{S}_x \tilde{S}_x \tilde{S}_z$$

One then has for the operator equivalent of $3z(x^2 + y^2)$:

$$\tilde{S}_z \tilde{S}_x \tilde{S}_x + \tilde{S}_x \tilde{S}_z \tilde{S}_x + \tilde{S}_x \tilde{S}_x \tilde{S}_z + \tilde{S}_z \tilde{S}_y \tilde{S}_y + \tilde{S}_y \tilde{S}_z \tilde{S}_y + \tilde{S}_y \tilde{S}_y \tilde{S}_z$$
$$= 3\tilde{S}_z (\tilde{S}_x^2 + \tilde{S}_y^2) + i\hbar(\tilde{S}_x \tilde{S}_y - \tilde{S}_y \tilde{S}_x) = 3\tilde{S}_z (\tilde{S}_x^2 + \tilde{S}_y^2) - \hbar^2 \tilde{S}_z$$

where we have used the commutation relation for the spin-operators:

$$S_x S_y - S_y S_x = i\hbar S_z$$

The octupolar spin operator will then be of type

$$\mathcal{H}_f = \frac{\mu_B}{\hbar^3} g_f B_z \left(\tilde{S}_z^3 - \frac{3}{5} \tilde{S}_z \tilde{S}^2 + \frac{1}{5} \hbar^2 \tilde{S}_z \right) + B_x \left(\tilde{S}_x^3 - \frac{3}{5} \tilde{S}_x \tilde{S}^2 + \frac{1}{5} \hbar^2 \tilde{S}_x \right)$$
$$+ B_y \left(\tilde{S}_y^3 - \frac{3}{5} \tilde{S}_y \tilde{S}^2 + \frac{1}{5} \hbar^2 \tilde{S}_y \right)$$

In order to identify the parameter correspondence, let us work out the action of this operator on the quartet functions. As an example for a magnetic field along the z-direction, the matrix is diagonal, and its elements (in units of μ_B) are given by

$$\left\langle \pm\frac{3}{2} \left| \mathcal{H}_f \right| \pm\frac{3}{2} \right\rangle = \pm g_f B_z \frac{3}{2} \left(\frac{9}{4} - \frac{45}{20} + \frac{1}{5} \right) = \pm\frac{3}{10} g_f B_z$$

$$\left\langle \pm\frac{1}{2} \left| \mathcal{H}_f \right| \pm\frac{1}{2} \right\rangle = \mp\frac{9}{10} g_f B_z$$

By comparing these elements to the results in Table 7.8 we can identify the parameter correspondence as

$$J_f = -\frac{3}{10} g_f \tag{13}$$

References

1. Mulliken, R.S., Ramsay, D.A., Hinze, J. (eds.): Selected Papers. University of Chicago Press, Chicago (1975)
2. Cotton, F.A.: Chemical Applications of Group Theory. Wiley, New York (1963)
3. Atkins, P.W., Child, M.S., Phillips, C.S.G.: Tables for Group Theory. Oxford University Press, Oxford (1970)
4. Boyle, L.L.: The method of ascent in symmetry. I. Theory and tables. Acta Cryst. A **28**, 172 (1972)
5. Fowler, P.W., Quinn, C.M.: Theor. Chim. Acta **70**, 333 (1986)
6. Griffith, J.S.: The Theory of Transition-Metal Ions. Cambridge University Press, Cambridge (1961)
7. Boyle, L.L., Parker, Y.M.: Symmetry coordinates and vibration frequencies for an icosahedral cage. Mol. Phys. **39**, 95 (1980)
8. Qiu, Q.C., Ceulemans, A.: Icosahedral symmetry adaptation of $|JM\rangle$ bases. Mol. Phys. **100**, 255 (2002)
9. Butler, P.H.: Point Group Symmetry Applications, Methods and Tables. Plenum Press, New York (1981)
10. Herzberg, G.: Molecular Spectra and Molecular Structure. III. Electronic Spectra and Electronic Structure of Polyatomic Molecules. Van Nostrand, Princeton (1966)
11. Fowler, P.W., Ceulemans, A.: Symmetry relations in the property surfaces of icosahedral molecules. Mol. Phys. **54**, 767 (1985)
12. Fowler, P.W., Ceulemans, A.: Spin-orbit coupling coefficients for icosahedral molecules. Theor. Chim. Acta **86**, 315 (1993)
13. Stone, A.J.: A new approach to bonding in transition-metal clusters. Theory. Mol. Phys. **41**, 1339 (1980)
14. Ceulemans, A., Vanquickenborne, L.G.: The epikernel principle. Structure and Bonding **71**, 125–159 (1989)
15. Longuet-Higgins, H.C.: The symmetry group of non-rigid molecules. Mol. Phys. **6**, 445 (1963)
16. Kobayashi, N., Higashi, R., Titeca, B.C., Lamote, F., Ceulemans, A.: Substituent-induced circular dichroism in phthalocyanines. J. Am. Chem. Soc. **121**, 12018 (1999)

Index